INFORMATION TO USERS

This manuscript has been reproduced from the microfilm master. UMI films the text directly from the original or copy submitted. Thus, some thesis and dissertation copies are in typewriter face, while others may be from any type of computer printer.

The quality of this reproduction is dependent upon the quality of the copy submitted. Broken or indistinct print, colored or poor quality illustrations and photographs, print bleedthrough, substandard margins, and improper alignment can adversely affect reproduction.

In the unlikely event that the author did not send UMI a complete manuscript and there are missing pages, these will be noted. Also, if unauthorized copyright material had to be removed, a note will indicate the deletion.

Oversize materials (e.g., maps, drawings, charts) are reproduced by sectioning the original, beginning at the upper left-hand corner and continuing from left to right in equal sections with small overlaps. Each original is also photographed in one exposure and is included in reduced form at the back of the book.

Photographs included in the original manuscript have been reproduced xerographically in this copy. Higher quality 6" x 9" black and white photographic prints are available for any photographs or illustrations appearing in this copy for an additional charge. Contact UMI directly to order.

UMI

A Bell & Howell Information Company
300 North Zeeb Road, Ann Arbor MI 48106-1346 USA
313/761-4700 800/521-0600

UNIVERSITÉ D'OTTAWA
UNIVERSITY OF OTTAWA

ELEMENT MOBILITY DURING SVECONORWEGIAN METAMORPHISM IN THE MODUM COMPLEX, SOUTH NORWAY

by

Paul Aloysius Marc Waqué

A thesis submitted to the School of Graduate Studies and Research

in partial fulfillment of the requirements

for the degree of M.Sc. in Earth Sciences

OTTAWA-CARLETON GEOSCIENCE CENTRE

AND

UNIVERSITY OF OTTAWA

OTTAWA, CANADA

ABSTRACT

The Modum complex within the Kongsberg sector of southern Norway is dominated by Early- to Mid-Proterozoic quartz-rich metasedimentary rocks that have been metamorphosed to sillimanite grade during the Kongsbergian orogeny (ca. 1500 Ma). At the onset of the Sveconorwegian (Grenvillian) metamorphism, multiple gabbroic units were emplaced at mid-crustal levels (less than 8 kbar) along north-south deformation zones. The Kongsberg sector, including the Modum complex, contains a strong north-south fabric with several mylonitic zones parallel to the fabric. Ubiquitous subsolidous recrystallization of the gabbro produced coronitic metagabbro with uralitic hornblende replacing cumulate olivine, orthopyroxene and clinopyroxene. The metagabbros contain more H_2O and Cl than expected for igneous rocks. Preserved metagabbros have a trace element character that is indicative of a tholeiitic magma derived from a subducted oceanic slab, with little crustal contamination. Similar gabbros (hyperites) in the associaated Bamble sector have been interpreted to have similar petrogenesis. The metagabbros arc extensively hydrothermally altered to amphibolite, these units are locally metasomatized to form albite-rich rock. Alteration of the metagabbros to amphibolite was nonisochemical, with increases in the concentration of Na, Fe, P and high field strength elements (HFSE) (i.e. Ti, rare earth elements (REE), U, Th, Nb), and decreases in the concentration of Al, Mg, and Ca. The consistent and significant increase in HFSE is not observed in other studies of amphibolitization from southwest Scandinavia. The HFSE were either mobile and enriched or alteration to amphibolite was accompanied by a loss of mass in the order of 60%. Hornblende and scapolite in metagabbros and amphibolites contain very high concentrations of Cl (ranging from 0.76 to 2.03 wt. % and 2.85 to 3.34 wt. % for the respective minerals). Moderate to intense albitization of the amphibolites and metagabbros occurs in discrete veins and diffuse zones. Albitization occured during the Sveconorwegian event, post-dating the amphibolites and primarily occuring under greenschist conditions. Accessory minerals in the albitized rocks are typically characteristic of greenschist grade metamorphism, including actinolite and chlorite; locally hornblende is

observed. Albitized rocks range from amphibolites with moderate enrichment of Na_2O, to rocks dominated by albite (albitites). Albitization mainly affects amphibolites or metagabbros, but quartz-rich metasediments may be partially albitized. Unlike the amphibolites, amphiboles or biotite in the albitized rocks do not contain abundant Cl, which may be a result of the ionized character of Cl in fluids at greenschist grade temperatures. Albitites display relative increases in the concentration of major elements Na and Si and decreases in Mg, Fe and Ca. The trace element concentrations are similar to amphibolites, with the exception of Sr and Cl, which occur at lower concentrations in the albitites. Oxide assemblages, sulphide-scapolite associations and REE patterns indicate that the hydrothermal fluids for the significant alteration types had high fO_2 levels; close to the sulphide-sulphate fence. A large exposure of massive hydrothermal calcite is isotopically and geochemically similar to hydrothermal dolomite from the Kragerø region of the Bamble sector.

North-south trending bands of disseminated Fe-sulphides, in the order of ten metres wide, occur within the quartz-rich metasedimentary rocks of the Kongsberg sector; historically known as fahlbands. Values of $\delta^{13}C$ and $\delta^{34}S$ suggest a sedimentary origin for the graphite and pyrite of the fahlbands (the respective averages are -22.9‰ and 20.4‰). The past producing Co-As Skuterud mine occurs marginal to a body of amphibolite, the Co-As-Cu-Ni-U-Au mineralization is interpreted to be a result of reduction of oxidized hydrothermal fluids on intersection with graphitic fahlbands during greenschist and amphibolite (?) facies Sveconorwegian metamorphism.

Metagabbro samples and amphibolite samples contain, on average <1 ppb Au, which is below the worldwide average of 4.1 ppb for mafic rocks. Albitized samples also contain less than 2 ppb Au. Low concentrations of gold in the mafic rocks precede amphibolitization, and may have been removed by an aqueous fluid from the magma or during subsolidous recrystallization. Chemical similarities between the amphibolite and the albitized rocks suggest that one evolving fluid may be responsible for both. Similar hydrothermal products observed in the Bamble sector suggest the involvement of a large homogenous fluid source,

such as the lower crust or upper mantle. The hydrothermal alteration and tectonic setting of the Modum complex is similar to many lode Au deposits, including a predicted source of metals and fluids from depth. A fluid with the following characteristics can account for the amphibolitization and albitization observed in the Modum complex: a high oxygen fugacity (close to the sulphide-sulphate fence); high ε_{Sr} and low ε_{Nd}; an alkaline pH; a high Cl content, probably mainly as NaCl; a high Cl activity during alteration at amphibolite facies and a low Cl activity during albitization at greenschist facies; high concentrations of U, REE, TiO_2

ACKNOWLEDGMENTS

There are many people who along the way have been an important help to me; thank you to everyone. My parents have provided an immeasurable amount of love, patience and support. Dave, Tom and Anne have been great and understanding siblings.

Thanks to my advisor Eion Cameron for initiating the project, insightful input, patience, and particularly the funding. The funding for was provided by an NSERC grant to Eion Cameron. Several members of the faculty of the Ottawa-Carleton Geoscience Centre made helpful comments during the project and at the defense. Ralph Kretz was helpful with the mass balancing portion. André Lalonde is thanked for comments on the thesis and input into description of the albitite samples. Keith Bell also made useful comments on the manuscript.. Thanks to the staff in the stable isotope laboratory, especially Nattalie Morrissette. Peter Jones at the Carleton microprobe was consistently helpful.

The students in the department were a great bunch with many relevant and irrelevant things that we pondered, I will miss them very much; cheers to everyone. Special thanks to Saeed, Dave and Charles, and Matthew for direct thesis input; Mark Mihalasky helped with the Spans procedure. Telmer, Johannes, Peter (Mr. Gesticulation) Duncan, Misha, and The Persian Tea Society were great comrades. Special thanks to Jim Crowley for making me try and catch him on skis or bicycle, and for his hospitality.

TABLE OF CONTENTS

LIST OF FIGURES

LIST OF PLATES

MACRO PHOTOGRAPHS

PHOTOMICROGRAPHS

LIST OF TABLES

CHAPTER 1. INTRODUCTION

The gold-only deposit type, known as "lode gold deposits" occur in metamorphic terranes and have various host rocks. There is usually a spatial association with intrusions and crustal scale shear zones. Many of the deposits are Archean in age, though younger examples occur. Lode gold deposits found the Canadian Shield account for about 70% or more of Canada's total cumulative gold production (Thorpe and Franklin, 1984). Important Canadian gold camps of this group include Timmins, Red Lake, Hemlo, Yellowknife, and Kirkland Lake. For larger Canadian lode gold deposits a typical grade is 7-17 g/tonne with a production of 1-6 million tonnes of ore (Thorpe and Franklin, 1984). For a grade 8 g/tonne, there is a 2000 fold increase Au concentration from unmineralized rocks (4.1 ppb) (Boyle and Jonasson, 1984).

Gold that occurs in these deposits is known to have moved along the associated shear zones from depth (e.g. Robert, 1989; Wyman and Kerrich, 1988; Cameron, 1988). The source of gold and the mineralizing fluid is a matter of much controversy. The hypothesized sources include magmatic derivation (Griffis 1968; Cameron and Hattori, 1987), lateral secretion (Boyle, 1979), exhalative (Fripp, 1976; Ridler, 1976), structurally focused metamorphic outgassing (Fyfe and Henley, 1973; Henley et al., 1976; Kerrich and Fryer, 1979; Kerrich and Fyfe, 1981; Kerrich, 1987; Groves et al., 1987; Kerrich and Wyman, 1990; Goldfarb et al., 1991; Cameron, 1993).

In this thesis the hydrothermal alteration of gabbros emplaced at 5-8 kbar (Munz and Morvik, 1991) is considered as a possible mechanism for liberation of gold and removal by the hydrothermal fluids. Reasons for this choice are briefly outlined in following paragraphs. The Modum complex of the Proterozoic Kongsberg sector in southern Norway contains quartz-rich metasedimentary rocks that were metamorphosed to amphibolite and locally granulite facies metamorphic conditions during the Gothian orogeny (1.75-1.3 Ga). The term Sector refers to an area of rock grouped on geological, chronological and structural

similarities, equivalent to the North American term "province"; the terms Belt is also used in the literature. The Modum complex is a geoiogically distinctive area within the Kongsberg sector. Initiation of the Sveconorwegian orogeny (1.2-0.9 Ga) is coincident with emplacement of mantle derived intrusions. These intrusions occur across southwest Scandinavia and through the related Grenville province. In the Modum complex of the Kongsberg sector this event is represented by intrusion of gabbros at 1224±15 Ma (Munz and Morvik, 1991). In the 10 km by 15 km Modum complex these intrusions occupy about 30% of the area.

Subsequent to the intrusion of the gabbros into metasedimentary rock, hydrothermal fluids substantially modified the metagabbros. As observed in the hyperites of the Bamble sector, subsolidus coronitic alteration was ubiquitous, forming metagabbros (e.g. Bugge, 1943; Munz and Morvik, 1991). In the Modum complex the metagabbros are rarely preserved, as the intrusions have been almost entirely amphibolitized to hornblende and plagioclase with local garnet and scapolite. Conditions for amphibolitization have been estimated as 7-10 kbar and 800-600°C (Munz and Morvik, 1991). Albitization affects all of the intrusive bodies at the margins to varying degrees, as described in subsequent chapters. This occurs at greenschist grade and to a limited extent at amphibolite metamorphic grade. An albitite has been dated at 1080±3 Ma by a U-Pb age on titanite (Munz et al., 1994). A Co-Cu-As deposit (the Skuterud mine) occurs at the margin of an amphibolite mainly within sulphide-rich metasedimentary rocks. The Skuterud mine is the site locality for the mineral skutterudite; note the spelling difference between the mine and the mineral (e.g. Gammon, 1966) Bodies of calcite and magnesite locally occur as well. The hypothesis is that gold, initially in the gabbro, was mobilized from the gabbro by hydrothermal fluids. The setting of the gabbro and alteration can be shown to be similar to favorable conditions for gold mineralization. Studies by Cameron (1989a, 1989b, 1989c) have documented depleted gold concentrations in mafic intrusions of the closely related Bamble sector.

1.1. Assessment of similarities between the Modum complex and crustal environments associated with lode gold deposits

1.1.1. Tectonics

Lode gold deposits tend to occur along major structural breaks such as the Cadillac-Larder Lake structural break, a feature that has been indicated to extend to the mantle (Robert, 1989). North-south shear zones are numerous throughout the Kongsberg sector and Modum complex. One major shear zone. The Kristiansand-Bang shear zone is about 250 km long; it defines the western margin of the Kongsberg and Bamble sectors. Occurring along the south-western margin of the Modum complex is the north-south Hokksund-Solumsmo mylonite zone , shear zones also occur within the Modum complex (Starmer, 1985b; this study). This deformation predates and postdates intrusion of the gabbros in the Modum complex (Jøsang, 1966; Starmer, 1985b; Chapter 3 this study).

1.1.2. Fluids

A major line of evidence supporting a genetic link for gold deposits through a range of metamorphic grades comes from the similarities of ore-fluids from different deposits at various grades (e.g. Groves et al., 1987; Witt, 1992). Based on fluid inclusions and alteration assemblages mineralizing fluids related to the deposits are relatively consistent: H_2O-CO_2 rich ($X(CO_2)$ = 0.1- 0.2), with low salinity, near neutral pH, and with the typical major cation concentrations of Na>>K≥Ca. There is typically an alteration zone around ore zones, the type of alteration is variable, wall rock composition is influential (e.g. Böhlke, 1989). Gold is known to be most soluble as chloride complexes and sulphur complexes, with sulphur being the main complexing agent at temperatures below about 400°C (Fyfe, 1973). Typically these deposits have high Au/Ag ratios and high Au/base metals and often have quartz, carbonate minerals, and feldspar as gangue. Factors such as associated alteration, amount of sulphide minerals, and trace element distribution patterns are highly variable (e.g. Böhlke, 1989; Boyle 1979; Witt, 1992).

Describing the fluids related to the alteration of the gabbro is a major goal of this thesis, this interpretation is made in Chapter 5. Related to the albitites variable salinities up to 23% have been recorded in fluid inclusions (Munz et al., 1994).

1.1.3. Associated alteration

The occurrences of carbonate units in the Modum complex may be comparable to the carbonate of the quartz-carbonate veins that hosts gold mineralization in the deposits. The association between the calcite and magnesite is uncertain and appears to postdate the amphibolitization and albitization

1.1.4. Metamorphic grade and timing

As described in Table 1.1 gold mineralization typically occurs after the peak of metamorphism. In the Modum complex peak metamorphic conditions occur prior to emplacement of the gabbros. The gabbro intrusions provide a source of heat that contributes to the amphibolite grade temperatures during amphibolitization of the gabbros (Munz and Morvik, 1991). As described in this study and elsewhere, greenschist grade assemblages occur in the mineralized metasedimentary rock and many of the albitized rocks are of Sveconorwegian age. Isobaric or near isobaric cooling through amphibolite grade has been described for southern Norway (Touret, 1985) including the Modum complex (Munz, 1990; Munz and Morvik, 1991).

1.1.5. Presence of Albitites

Rocks dominated by albite are considered albitites. Albite-rich rocks are observed proximal to many gold deposits. Wall rock alteration may lead to enrichment of albite as is observed in amphibolites and granites at Alleghany, California (Böhlke, 1989). Mafic alkaline dykes are altered to albitites at the Kerr Addison-Chesterville mines, Ontario (Smith et al., 1991). There is a secondary enrichment of albite along with carbonate minerals and chlorite in some dykes of the McIntyre-Hollinger Au-Cu mines in Timmins (Wood et al.,

1986; Mason and Melnik, 1986). At the Bralorne Au deposit in B.C , veins of hydrothermal origin hosting Au mineralization are synchronous with albitite dykes that may be of magmatic origin (Gallagher, 1940; Leitch, 1990; Leitch et al., 1991). In some of the Kalgoorlie deposits of Western Australia there is hydrothermal (?) albitization of porphyries associated with gold mineralization (Witt, 1992). In these deposits the albitization event appears to be syn-mineralization with some uncertainty. The albitite in the Modum complex appears to be of hydrothermal origin based on replacement textures and mineralogy (Munz et al., 1994; this study).

1.1.6. Relation to intrusion

Intrusive activity occurs throughout greenstone belts but there is a concentration along major shear zones. Shear zones being zones of weakness direct fluids and magma. Known gold deposits usually have spatially-associated intrusions. Hodgson and MacGeehan (1982) estimated that more than 90% of the large gold deposits (greater than one million oz.) in the Superior Province are hosted or are immediately adjacent to felsic intrusions. There are no felsic intrusions of appropriate age exposed in the Modum complex. The gabbroic intrusions, however, may relate to more evolved intrusions emplaced at shallower crustal levels.

1.2. Methods and Contributions

Based on existing literature, the regional geology is described in Chapter 2. In Chapter 3 the petrographic characteristics of the relevant geological units of the Modum complex are described. The geochemical character of the metagabbros, amphibolites, metasedimentary rock, and albitized rocks is described and compared in Chapter 4.

1.2.1. Field work

Field work was conducted in the summer of 1992 by the author (PW). Assistance and guidance in the field was provided in the field by Dr. E. M. Cameron for one week. One day of orientation was provided by Dr. A. Bjørlykke and Dr. I. A. Munz at the beginning of the project.

One hundred and twenty-eight rock samples were collected during field work. The samples were generally about 1 to 2 kg in size. Weathered surfaces were removed, where possible. Veins were avoided in the rocks sampled for whole rock analyses. A minority of samples were collected from within the mine workings of the Skuterud mine.

The most detailed geological map available of the Modum complex (Jøsang, 1966) was used in combination with the generalized map of Munz and Morvik (1991). The map of Jøsang (1966) does not show roads over the mapped area so some of the unit locations were difficult to establish given the time constraints. The geology map did not correlate perfectly with what we found in the field, making the units of interest difficult to find. Significantly metagabbros were not observed at Døvikkollen, at least to the extent described, and metagabbros were found in the Bingås locality. The original map published at approximately 1:20 000 could not show much more detail than it does.

1.2.2. Sample preparation

Rock samples were cut by PW. Half of sample from selected samples were then sand blasted using silica sand by PW. The cleaned portion was then submitted for crushing and powdering at the Geological Survey of Canada (GSC). Between samples the jaw crusher was cleaned with quartz and compressed air. Powdering of the samples was done using a tungsten-carbide ring mill, which was cleaned using alcohol and compressed air between samples. Approximately 25 sample powders were prepared in this manner by PW for subsequent analyses.

1.2.3. Methods for geochemical analyses

Powders were submitted to the GSC Analytical Section for major and selected trace element analyses, the methods used are indicated in Table 1.2. Trace element analyses were carried out at Becquerel Laboratories Inc. by neutron activation analysis. For the elements analyzed by both laboratories the results from the GSC laboratories typically reported one more significant figure and lower detection limits; The results from the two labs were similar and did not suggest any gross systematic errors. Some data on accuracy and precision is included in Appendix 3. The GSC results were used for those elements where duplication existed. To overcome limitations of low level resolution for rare earth and selected other elements ICP-MS analyses were carried out at the GSC for about 12 samples including the metagabbros. The concentration of Au in most samples was below the detection limit of 2 ppb for the neutron activation method. Eighteen samples were analyzed using a specialized method for measuring low Au concentrations. For this method approximately 10 g of sample was decomposed in HF aqua regia; extraction with small amounts of methyl isobutyl ketone (MIBK); and multiple injections of the MIBK into a graphite furnace-atomic absorption spectrometer (GFAAS), permitting a detection limit of 0.1 ppb Au.

1.2.4. Other methods

Polished thin sections were prepared externally using slabs provided by PW. Microprobe analyses were carried out at Carleton University by Peter Jones; see Chapter 4 for methods. Staining of thin sections for K-feldspar was done by PW using the sodium cobaltinitrate method. Mineral formula produced from microprobe results were carried out by PW using existing software. A method for area analysis of raster images (SEM images and photographs) using Spans® GIS software and Corel Photopaint® was developed, but this was used minimally. Stable isotope analyses were done at the University of Ottawa by staff in the stable isotope laboratory.

Table 1.2. Analysis methods used in this study

Element / oxide	SiO_2	TiO_2	Al_2O_3	$Fe_2O_3^*$	FeO	MnO	MgO	CaO	Na_2O	K_2O	P_2O_5	H_2O^{total}	CO_2=	C	CO_2^{total}	S	Cl	LOI
Units of measure	%	%	%	%	%	%	%	%	%	%	%	%	%	%	%	ppm	ppm	%
Analysis Method																		
XRF and/or ICP-MJ1[1]	Yes	Yes	Yes	Yes		Yes	Yes	Yes	Yes	Yes	Yes							
ICP-TR1[1]																		
Chemical					Yes							Yes	Yes	Yes	Yes	Yes	Yes	Yes

Element	Ag	As	Au	Ba	Be	Br	Cd	Co	Cr	Cs	Cu	F	Ga	Hf	In	Ir	Mo	Nb
Units of measure	ppm	ppm	ppb	ppm	ppm	ppm	ppm	ppm	ppm	ppm	ppm	ppm	ppm	ppm	ppm	ppb	ppm	ppm
Analysis Method																		
ICP-TR1[2]				Yes	Yes			Yes	Yes		Yes							Yes
Chemical												Yes						
ICP-MS[1]	Yes									Yes			Yes	Yes	Yes		Yes	Yes
INAA[4]	Yes	Yes	Yes	N.R.		Yes	Yes		N.R.	Yes	N.R.			Yes		Yes	Yes	N.R.
GFAA[5]			Yes															

Element	Ni	Pb	Rb	Sb	Sc	Se	Sn	Sr	Ta	Te	Th	Tl	U	V	W	Y	Zn	Zr
Units of measure	ppm	ppm	ppm	ppm	ppm	ppm	ppm	ppm	ppm	ppm	ppm	ppm	ppm	ppm	ppm	ppm	ppm	ppm
Analysis Method																		
ICP-TR1[2]	Yes		Yes		Yes			Yes						Yes		Yes	Yes	Yes
ICP-MS[3]		Yes	Yes						Yes			Yes	Yes			Yes		Yes
INAA[4]			Yes	Yes	N.R.	Yes	Yes	N.R.	Yes	Yes	Yes		Yes	N.R.	Yes		N.R.	N.R.

Element	La	Ce	Pr	Nd	Sm	Eu	Gd	Tb	Dy	Ho	Er	Tm	Yb	Lu
Units of measure	ppm	ppm	ppm	ppm	ppm	ppm	ppm	ppm	ppm	ppm	ppm	ppm	ppm	ppm
Analysis Method														
ICP-TR1[1]	N.R.												N.R.	
ICP-MS[3]	Yes	Yes	Yes	Yes	Yes	Yes	Yes	Yes	Yes	Yes	Yes	Yes	Yes	Yes
INAA[4]	Yes	Yes			Yes	Yes		Yes					Yes	Yes

[1]ICP-MJ1 data obtained on 0.5 g of sample fused with lithium metaborate dissolved in 5% HNO_3 and diluted to 250 ml

[2]ICP-TR1 data are obtained on 1.0 g of sample (acid +fusion of residue) dissolved in 10% Hcl and diluted to 100ml.

[3]Inductively cooled plasma - mass spectrometry method, applies to samples PWN 42.1, 50, 52, 53, 67, 111, 118.1, 119, 120, 121, and 122

[4]Instrumental neutron activation analyses carried out by Bequerel Laboratories Inc.

[5]These analyses were carried out by XRAL Laboratories; applies to samples PWN 28, 38, 42.1, 50, 51, 52, 53, 65, 98, 100, 102.1, 113, 118.2, 119, 120, 121, 122

N.R. indicates not reported

*Fe_2O_3 is calculated using $Fe_2O_3 = Fe_2O_3^T$ (ICP) - 1.11134 * FeO (volumetric)

1.2.5. Original contribution

The rocks of the Modum complex have been investigated in detail historically including the more recent papers of Bugge. (1943) and Jøsang (1966). Detailed transmitted light petrography of some assemblages. fluid inclusion work and radiogenic isotope studies have been carried out by I. A. Munz and her various coworkers (Munz. 1990: Munz and Morvik. 1991: Munz et al.. 1994: Munz et al., 1995: Andersen and Munz. 1995). The sulphide mineralogy of the Skuterud mine and the fahlbands has been described in the English literature by Gammon (1966. 1967).

The contributions to this thesis include additional petrographic studies. especially of sulphides and oxides: major and trace element geochemistry: and stable isotope geochemistry. A comparison of the geochemistry of metagabbros and amphibolites is made: this has not been done before in the Modum complex. The rocks of the Modum complex have not been investigated as a source of Au in the past. though broadly similar studies have been undertaken for similar and older rocks of the Bamble sector (Cameron. 1989a: Cameron. 1989b: Cameron. 1989c: Cameron. 1993: Cameron et al., 1993). Interpretations made based largely on data in this thesis regard origin of disseminated pyrite bands (fahlbands) petrogenesis of the gabbros. chemical nature of the amphibolitization. albitization. calcite metasomatism. and Skuterud ore mineralization.

CHAPTER 2. GEOLOGY OF THE BALTIC SHIELD AND SOUTHWEST SCANDINAVIA

2.1. Summary of Proterozoic metamorphic and magmatic events in Laurentia and Baltica

The review of literature in this section comes mainly from a review by Gower et al. (1990), more detailed references can be found there. During the Early to Middle Proterozoic the Canadian and Baltic shields evolved as a single mass after amalgamating between 1.98 and 1.83 Ga. The name "Nena" has been proposed for this single cratonic landmass, an acronym for Northern Europe-North America. Continuity of anorthosites and related rocks between the two regions is one of many similarities used for the correlation. Preserved from Nena are Archean cratons with Proterozoic belts accreted to the south. Accretionary tectonics from 2.1 to 1.6 Ga created most of Baltica and some of Eastern North America.

From the period 1.9 to 1.8 Ga both Baltica and Laurentia experienced continental magmatic accretion from the south and orogenesis. Baltica experienced significant growth with the closely spaced Karelian Continental Development Period (2.5-2.1 Ga) and Svecofennian orogeny (2.0-1.75 Ga); this is jointly known as the Svecokarelian (e.g. Veraschure, 1985). Karelian rocks are typically epicontinental metasedimentary and metavolcanic rocks. Svecofennian rocks occurring through much of central Scandinavia are dominantly pelitic and metavolcanic rocks with island arc affinities.

The period from 1.69 to 1.60 Ga marks the last major phase of crustal accretion in Nena except for much later terranes accreted in the southwest Grenville province.

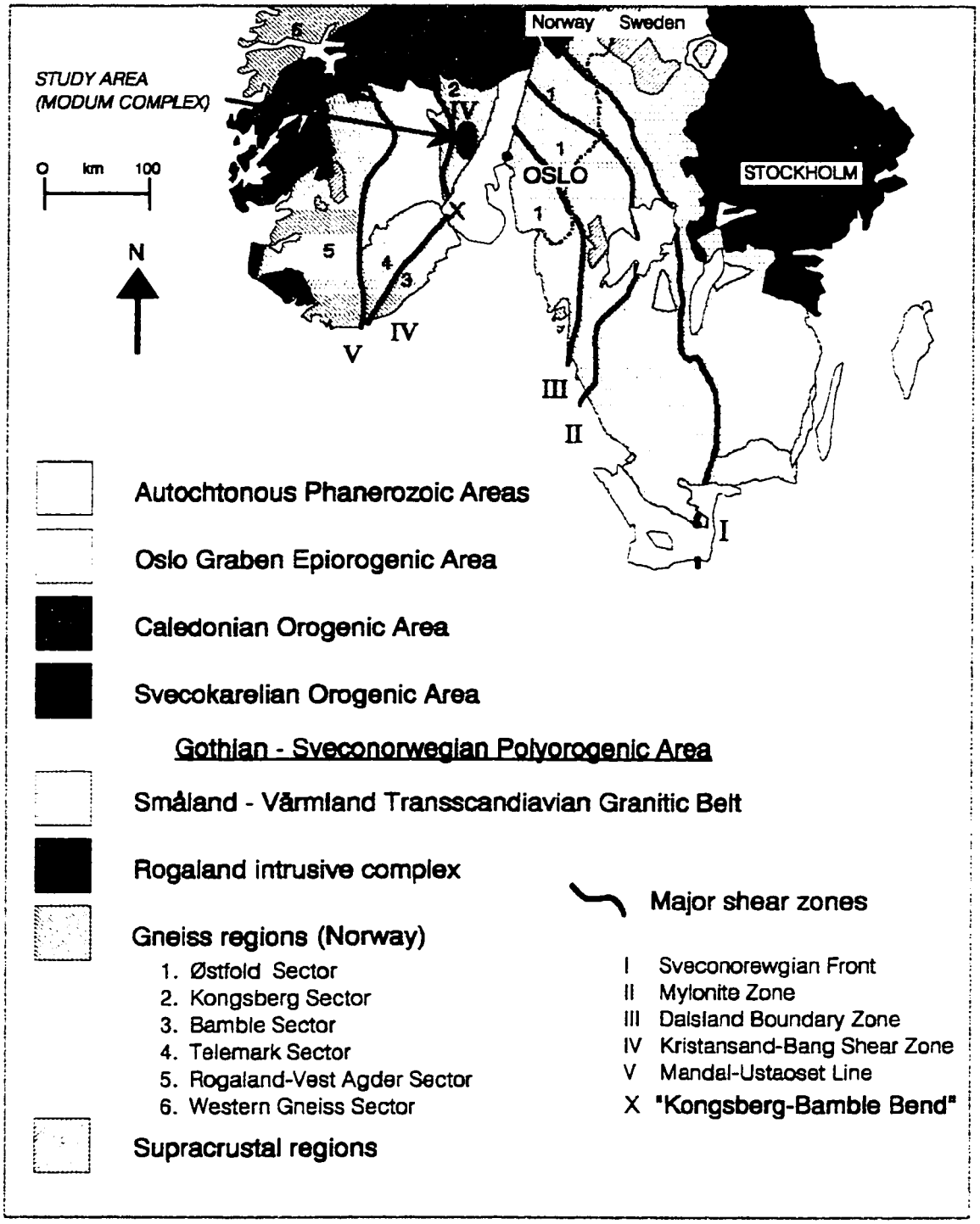

Figure 2.1. Major geologic and structural divisions in southern Scandinavia (after Veraschure, 1985).

TABLE 2.1: SUMMARY OF RELEVANT EVENTS IN SOUTHERN GNEISS REGION AND CENTRAL SCANDINAVIAN DOLERITE GROUP (CSDG).

Event Name	Age	Affected area	Metamorphic grade	Associated features including magmatism	References
Initiation of Deposition	?1.9-1.6 Ga	southwestern Scandinavia		Deposition of shelf sediments overlain by deep water sediments and lesser intermediate to mafic igneous rocks throughout	Starmer, 1985; Veraschure, 1985
Gothian orogeny	1.76-1.50 Ga,	Central and southwestern Scandinavia	Upper amphibolite and local granulite	Subduction of oceanic crust along the margin of the south Western gneiss sector	Gaál and Gorbatschev, 1987, Starmer, 1991
Gothian-Sveconorwegian Interlude	~1.55-~1.25 Ga	southwestern Scandinavia	Amphibolite	Granites; gabbro-diorite-tonalite, CSDG	Starmer, 1985
Sveconorwegian Anorogenic phase	1.25-~1.1 Ga	Bamble and Kongsberg sectors	Amphibolite (to granulite?)	Emplacement of Modum gabbros, scapolization amphibolization, CSDG	de Haas, 1992; Veraschure, 1985; Munz and Morvik, 1991
Scevonorwegian orogenic phase	~1.1-0.9 Ga	Bamble and Kongsberg sectors	Amphibolite to greenschist	albitites, calcite rich units as well as other retrograde units, post orogenic granites	Munz et al., 1993

orogenesis affected The Gothian orogeny of southern Sweden. While the term Gothian orogeny initially referred to the orogeny in Sweden it is often used to describe the orogeny across the southwestern gneiss region. The term Kongsbergian has been used to refer to the same orogeny in southern Norway (e.g. Oftedahl, 1980; Starmer, 1990).

From about 1.55 to 1.25 Ga there was period of relative crustal stability across Nena characterized by anorogenic magmatism, rift related tectonism and deposition of supracrustal rocks. Across southwestern and midwestern U.S.A. there was widespread emplacement of anorogenic granite-rhyolite (± gabbro) (1.51-1.32 Ga), this also occurs in less abundance across the eastern Grenville (Gower et al., 1990). In Scandinavia the "Gothian-Sveconorwegian interlude" (~1.55-1.27 Ga) had similar characteristics. Some hyperites in the Bamble sector are found to be of this age (de Haas et al., 1992b).

The Grenville-Sveconorwegian orogeny (~1.25-0.9 Ga) was a period of magmatism and metamorphic reworking of preexisting rocks in southwestern Scandinavia and across the Grenville structural province of North America. During the early part of the orogeny there is evidence for both granitoid emplacement and an initial extensional phase with associated widespread mafic magmatism associated with rifting. During the early extensional period widespread anorthosite-monzonite-charnokite-granite (AMCG) suites occur throughout the central Grenville province. They were emplaced between 1.16 and 1.12 Ga (Emslie and Hunt, 1990; McLelland and Chiarenzelli, 1990). In the Bamble and Kongsberg sectors mafic intrusions have a subduction affinity (Smalley and Field, 1991; this study), though isobaric cooling or cooling under increasing pressure has been used to invoke crustal extension (Munz and Morvik, 1991; Touret, 1985). Mafic dyke swarms occurred beyond the area affected by orogenies including the Central Scandinavian Dolerite group (1.25 to 1.2 Ga) along the margin of Sveconorwegian metamorphism (Gorbatschev et al., 1979). The Abitibi dyke swarm was emplaced north of the Grenville front at 1.14 Ga (Ernst et al., 1987).

After about 1.10 Ga. to 1.00 Ga a more orogenic nature was characteristic of the Grenville and Sveconorwegian orogens. Emplacement of granitoids is quite common. with examples throughout the Grenville Province. northwest Ireland. and southern Norway. In the Central Metasedimentary belt of the Grenville Province there was widespread fenitization along with intrusions of carbonatite. pegmatite and albite syenite (Lumbers et al.. 1990). In northwest Ireland a period of granitization. metamorphism. and migmatization occurred (van Breemen et al.. 1978). In southern Norway there is metamorphism. albitization. and intrusion of pegmatites. granites. albitites and hydrothermal carbonates especially in the Bamble and Kongsberg sectors (Starmer. 1990; Munz. 1990; Munz et al.. 1994; Munz et al.. 1995; Dahlgren et al.. 1993). Close to 0.9 Ga post tectonic granites and syenites occur in the Grenville province and Scandinavia.

Through much of the Proterozoic. the Baltic shield and Laurentia shared the same southern tectonic margin. Rotation of the Baltic shield during the Sveconorwegian-Grenvillian orogeny subsequent to the formation of the "Central Scandinavian Dolerite Group" (1.25 to 1.2 Ga) has been suggested based on paleomagnetic data and lithologic correlation (Patchett et al.. 1978; Gower and Owen. 1984; Gorbatschev et al.. 1987; Stearn and Piper. 1984). This rotation required Grenville rifting along the current North Atlantic. though the only dykes that could possibly be associated with such rifting occur in the far transported Caledonian nappes (Gorbatschev et al.. 1987). This rotation resulted in oblique orientation of what was previously the same tectonic margin.

2.2. Structural divisions of the southwestern gneiss region

In the Southwestern gneiss region. 5 major north-south trending tectonic zones separate the region into geographical crustal blocks or "sectors" (Figure 2.1). Several names have been used for the zones but the following are the most common names: the

Sveconorwegian Front, the Mylonite Zone, the Dalsland Boundary Thrust, the Kristiansand-Bang Shear Zone and the Mandel-Ustaoset Line. It is interpreted that these shear zones have had a complex active history from the Gothic orogeny until after formation of the Permian Oslo Graben (e.g. Starmer, 1990; Padget, 1990; Starmer, 1991). Movements along the zones presently expose different levels of crust.

The Kristiansand-Bang Shear Zone is made up of several faults and shear zones. Along the western boundary of the Kongsberg sector it is known as the Friction Breccia which in the northern half follows two mylonite zones: the Saggrenda-Pretfoss and the Pretfoss-Sokna mylonite zones (Starmer, 1985). The Friction breccia is a brittle feature developed post 0.95 Ga, initially under greenschist metamorphic facies during regional uplift following the Sveconorwegian orogeny.

Supracrustal blocks make up about 12% of the exposed bedrock in southern Norway. These crustal blocks, usually less than 10 by 20 km, are surrounded by granitic gneisses. A series of synkinematic granites, augengneisses and migmatites that are often called the Telemark granitic gneiss (Touret, 1968; Martins, 1969) intrude the Telemark suite and Konsgberg and Bamble supracrustal rocks. These rocks make up about 30% of the area of southern Norway. Mixed gneisses make up the remaining 50% (Jacobsen and Heier, 1978). The Telemark granitic gneiss rocks were formed during Sveconorwegian metamorphism between 1.2 and 1.1 Ga. The source rocks were separated from the mantle at about 1.6 Ga (Jacobsen and Heier, 1978).

The Kongsberg and Bamble sectors have a common metamorphic and magmatic history (e.g. Starmer, 1985b; Brickwood and Craig, 1987; Oftedahl, 1980; Starmer, 1991). This was first observed by J. Bugge (1943). It is interpreted that the Bamble and Kongsberg sectors now separated by the Permian aged Oslo graben were once continuous. Presently the structural fabric of the Bamble sector trends to the northeast while the Kongsberg sector

fabric has a northerly trend. This change in fabric is known as the "Bamble-Kongsberg Bend" (Starmer, 1985b; Starmer, 1991). The bend was initiated during initial deformation of the belts and was enhanced during successive mylonitization events along the margins of the Kongsberg-Bamble sector (Starmer, 1985b).

2.3. The Kongsberg sector

The first Norwegian geological establishment was the School for Mining Engineers which opened at the Kongsberg Silver Mines in 1757. The Skuterud mines began producing Co and As around this time also. The Norwegian Geological Survey began in 1858 and produced maps at 1:400.000 and then at 1:100.000 scale. The Kongsberg sector was mapped by A. Bugge (1918), since then it has enjoyed a moderate amount of attention, with recent mapping and studies by Jacobsen and Heier (1978), Starmer (1985), Brickwood and Craig (1987). The Modum complex of the Kongsberg sector has been mapped in detail by Jøsang (1966) and Munz, associated with others (Munz, 1990; Munz and Morvik, 1991; Munz et al., 1994; Munz, et al., 1995).

The Kongsberg sector is overlain in the southeast by Cambro-Ordovician sedimentary rocks of the Oslo region. Along the western margin a 'friction breccia' marks the faulted contact with the Telemark Basement gneiss complex (TBGC). To the north it passes into the TBGC at about the Ådal Granite. The Kongsberg sector is approximately 90 km in length with a NNE trend and with a nearly continuous width of about 30 km.

There is a strong north-south fabric to the rocks of the Kongsberg sector and the dips are in general quite steep to the east, in contrast to the more shallow easterly dips of the Telemark sector (Starmer, 1985b). Initiated in the Gothian orogeny, and extending through the Sveconorwegian orogeny, multiple phases of ductile deformation have affected the sector parallel the metamorphic fabric. Four major and two minor episodes of ductile shearing have

been identified in a zone of protomylonite to ultramylonite along the interface with the Telemark sector (Starmer 1985b). During deformation there was east-west shortening and thrusting of the Kongsberg sector over the TBGC (Starmer, 1985a).

2.3.1. The Modum complex

The north-south elongate Modum complex is about 10 km wide in the centre and about 30 km long. The Modum complex is centrally located in the Kongsberg sector. The western boundary of the Modum complex is fault bounded by the Kröderen-Hokksund fault, a late brittle fault that follows a mylonite zone along it's southern portion (Jøsang, 1966; Starmer, 1980). The eastern margin is defined lithologically.

The bulk of the Kongsberg sector is composed of gneissic and migmatitic rocks with minor metagabbro and related amphibolites. The Modum complex, however, contains significant supracrustal rocks. Quartzites are most common, covering about 30% of the exposed area. Exposed over a somewhat lesser area are muscovite ± sillimanite schists and gneisses. Modum metagabbros and amphibolites constitute about 30% of the exposed area. Various rocks with a strong hydrothermal character and pegmatites make up a significant exposed area, and are derived from the above lithologies. Post-kinematic granites are a minor constituent.

The oldest rocks in the complex are quartzites and other metasedimentary rocks deposited prior to the mid-Gothian intrusive activity of 1.6 Ga, but are younger than 1.7 Ga (Jacobsen and Heier, 1978; Veraschure, 1985). Within south Norway there is no known basement or any rocks that predate 1.7 Ga (Falkum, 1985; Veraschure, 1985). The metasedimentary rocks are lithologically similar to the northeast portion of the Bamble sector (Bugge, 1918; Jøsang, 1966; Starmer, 1981). Two depositional settings proposed describing the origin of the quartzites, plus the more extensive pelitic and gneissic rocks are: (1) The

sediments may be deposited on continental crust and derived from a crustal source to the northwest that is relatively stable and extended under the Kongsberg sector. The latter is indicated by subsequent tectonic activity, with Bamble and Kongsberg sectors thrusting over the Telemark sector (Veraschure, 1985; Starmer, 1990). (2) An oceanic basement for the supracrustal rocks has been proposed by Smalley and Field (1985).

The abundance of coronitic mafic intrusions is one of the noted similarities between the Kongsberg and the Bamble sectors. Within southern Scandinavia, especially in the Bamble sector, the term "hyperite" refers to these intrusions. The intrusions are dominantly olivine metagabbros but range from ultramafic to gabbro and norite (e.g. Brickwood and Craig, 1987; Munz and Morvik, 1991). A coronitic texture is a typical feature of these rocks. Coronas form between olivine and plagioclase surrounding olivine there are rings of: orthopyroxene, clinopyroxene, symplectic amphibole and spinel, and sometimes garnet. Pyroxenes may also be rimmed by amphibole.

The Modum gabbros were emplaced at the beginning of the Sveconorwegian event, a 1.224±0.015 Ga Sm-Nd isochron was obtained from igneous phases (Munz and Morvik, 1991). This is in agreement with a Rb-Sr whole rock date of 1.20±0.05 Ga based on 4 samples from the Western Kongsberg sector. Formation of coronas and recrystallization of clinopyroxene in the Modum metagabbros is calculated to occur at a temperature of 600-800° C and a pressure of 7-10 kbar (Munz and Morvik, 1991). The gabbroic intrusions are pervasively amphibolitized with rare cores of metagabbro. Spatially significant alteration products include scapolitization and albitization, both overlapping with each other. Much of the albitized rock indicates greenschist metamorphic conditions. Munz et al. (1995) calculated conditions for some albitite veins to be 250-300°C and ca. 1-2 kbar.

The supracrustal rocks in the Modum complex were initially metamorphosed at upper amphibolite grade during the Gothian orogeny of 1.7 to 1.55 Ga. Within the Modum complex

and to the east the upper amphibolite grade mineral assemblages are preserved. To the west, however, gneisses preserve granulite metamorphic grade from the Gothian orogeny (Starmer, 1985a). During the Sveconorwegian orogeny the Modum complex reached upper amphibolite metamorphic grade. Munz and Morvik (1991) show that this metamorphism occurred on the retrograde path at about 600°C and at a steady or increasing pressure of 8 to 10 kbars.

Some authors have interpreted only greenschist grade reworking during the Sveconorwegian orogeny in southern Norway (e.g. Field et al., 1985; Brickwood and Craig, 1987). The bulk of recent work supports an amphibolite to granulite grade reworking of the Bamble (e.g. Kullerud and Dahlgren, 1990; Nijland and Senior, 1991; de Haas et al., 1992a; Starmer, 1991). In the Kongsberg sector there is evidence for upper amphibolite to greenschist grade metamorphism during this event (Munz, 1990; Munz and Morvik, 1991; Starmer, 1991).

CHAPTER 3. DESCRIPTION OF ROCK UNITS AND MINERALOGY

3.1. Rock Units

3.1.1. Supracrustal rocks

Metasedimentary rocks in the Modum complex originated as clastic sedimentary rocks, quartzo-feldspathic rocks are dominant. Supracrustal rocks make up about 60% of the exposed rocks in the Modum complex. The metasedimentary rocks are the oldest in the complex, deposited from ~1.7 Ga to ~1.6 Ga as shelf sediments (Starmer, 1985a; Veraschure, 1985) or are as old as 1.9 to 1.7 Ga based on depleted mantle Nd model ages (Andersen and Munz, 1995). Quartz-rich sediments appear to be deposited during marine transgression onto older continental crust. These were overlain by deeper water, more aluminous sediments, the protolith for the para-gneissic and pelitic rocks (Starmer, 1985a).

The metasedimentary rocks were initially deformed during the Gothian (Kongsbergian) orogenic period (~1.7-1.5 Ma), when north-south folding developed as a result of east-west compression. In this period the general north-south trend of the Modum complex was generated. Some structures of this age are preserved or enhanced during the Sveconorwegian orogenic event (~1.2- ~0.9 Ga). The Modum complex is the core of an antiformal structure, exposing quartzites and sillimanite-bearing rocks not observed elsewhere in the Kongsberg sector. It is flanked by structurally overlying, mineralogically-variable (hornblende-plagioclase-biotite-quartz) gneisses in synformal structures. The abundance of quartz-rich metasedimentary rocks in the Modum complex is distinctive when compared to other rocks of the Kongsberg sector and is similar to the Bamble sector; this is the main defining character of the Modum complex (Starmer, 1981).

While the metasedimentary rocks are the oldest rocks, those sampled for this study were chemically affected by fluids after emplacement of the gabbros at 1.224 Ga (Munz and

TABLE 3.1. SUMMARY OF THE UNITS DISCUSSED WITHIN THE STUDY AREA

AGE	ROCK UNIT / EVENT	REFERENCES[1]
post-deformational	Emplacement of calcite units and veins.	Munz et al., 1994.
may be younger than calcite post-deformational	Granites and associated pegmatites.	
1.080 ± 0.003 Ga, some post deformational	Albitization	Munz et al., 1994
1.131 ± 0.03 Ga	Mineralization of fahlbands, introduction of lead into metasedimentary rocks	Anderson and Munz, 1995; This study; Gammon, 1966
	Amphibolite facies retrograde metamorphism leading to: amphibolitization, scapolitization	Munz and Morvik, 1991; This study
1.224 ± 0.015 Ga	Intrusion of gabbros	Dating: Jacobsen and Heir, 1978; Munz and Morvik, 1991
	Granulite to amphibolite facies metamorphism and deformation	
1900-1700†or 1700 - 1550 Ma	Deposition of sedimentary rocks	Age of sediment deposition: †Andersen and Munz, 1995; Starmer, 1985a; Verschure, 1985

[1]Descriptions of all units and relative dating of units other than fahlbands and Co-As mineralization has been discussed by A. Bugge, (1917); J. Bugge, (1943); Jøsang, (1966); Starmer, (1985a).

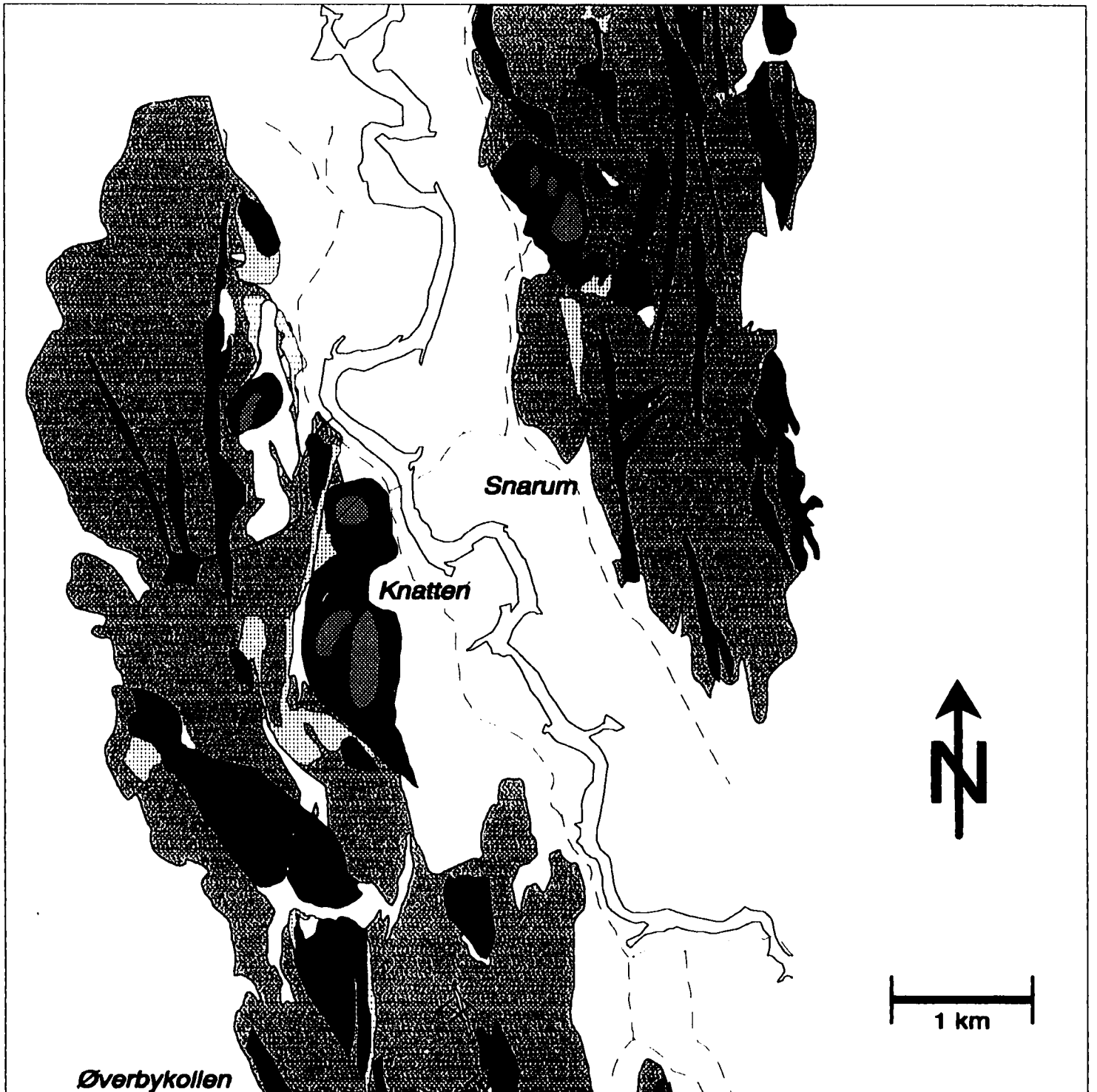
Snarum
Knatten
N
1 km
Øverbykollen

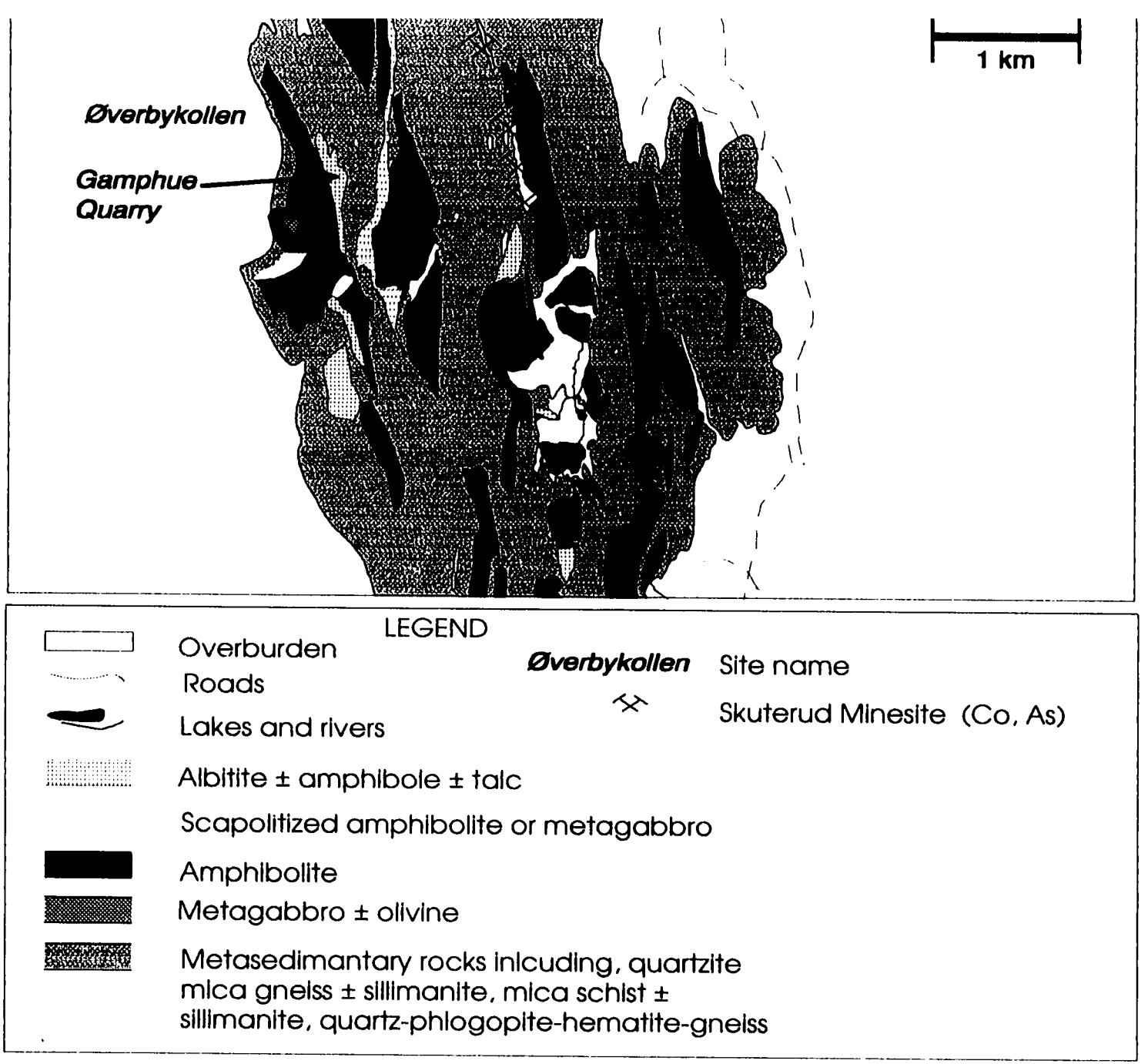

Figure 3.1 Geology of the central portion of the Modum Complex modified after Jøsang (1966)

Morvik, 1991). Evidence for this is local albitization of the metasedimentary rocks (e.g. PWN 058), retrograde muscovite and chlorite growth, and Co-Cu-As-U mineralization (Skuterud ore) (van Autenboer, 1957; Gammon, 1966; Andersen and Munz, 1995; this study). Whole-rock Pb isotope composition date an event of U enrichment at 1.131± 0.03 Ga (Andersen and Munz, 1995), possibly the age of Skuterud ore mineralization. The alteration is variable and complex, leading to some uncertainty about the age of some minerals. The metasedimentary rocks that appear least altered will be described first.

In the geological map (Figure 3.1) rocks of sedimentary origin are indicated to make up approximately 70% of the total outcrop area. The metasedimentary rocks have been subdivided into several units in the map of Jøsang (1966), including the following major units with approximate percentage of the total outcrop area: quartzites (20%), quartz-phlogopite-hematite schist (10%), sillimanite gneiss (10%), and mica schist with local sillimanite (30%). As mapping of the supracrustal rocks was not an objective of this study the reader should consult Jøsang (1966) or Bugge (1943) for more descriptive detail.

Quartzites (>95% quartz) contain minor minerals that include muscovite, biotite, and feldspars. Quartzites grade into gneissic rocks that are dominated by quartz and plagioclase, with muscovite, rutile, feldspar, sillimanite, ± biotite, ± graphite, ± tourmaline, ± titanite (Plates 3.9a and 3.9b). Many of the rocks referred to as mica schists and sillimanite-mica schists by Jøsang (1966) have a significant quartz content. The quartz-phlogopite-hematite schists occur in the western and south western regions, associated with significant albite-rich rocks.

Foliation is typically defined by elongated quartz or gneissic layering. Muscovite and biotite crystals are often not well aligned, muscovite occurs as a replacement of sillimanite. Muscovite, and some biotite grew during retrograde deformation, after the main ductile deformation period (e.g. Plate 3.9a). Some minor thin sulphide-bearing biotite-amphibole schists were observed near the Skuterud mine, generally close to the amphibolite units (i.e. PWN 018, 019 and 096). The occurrence of these schists marginally to the amphibolite, and

the amphibole content has lead to the interpretation that they are derived from the gabbro (Bugge, 1943).

Sillimanite occurs in some of the para-gneissic rocks, often as unoriented fibrolite, in ovoid irregular lenses, that are in the range of 1 cm long, surrounded by quartz and partially or completely replaced by muscovite (as in PWN 012, Plate 3.9a). In other studies the sillimanite nodules have been observed replaced by microcline (Bugge, 1943). Fibrolite is locally observed growing on a biotite substrate, indicating that in this sample the sillimanite post-dates biotite (sample PWN 025). Sillimanite and muscovite may occur in foliated nodules but the muscovite grains are generally unfoliated. Sillimanite is produced at temperatures close to 700°C by the reaction of quartz and muscovite to form sillimanite and K-feldspar (e.g. Ohmoto and Rye, 1972):

$$SiO_2 + H_2KAl_3Si_3O_{12} = Al_2SiO_5 + KAlSi_3O_8 + H_2O \qquad \text{(eq.1)}$$

The observed replacement of sillimanite by muscovite is thus a retrograde reaction. Peak metamorphism has been interpreted to be during the early part of the Kongsbergian orogeny (~1.550-1.525 Ga) (Starmer, 1985).

The oxides in the metasedimentary rocks collected in this study may all date from a period of retrogression that followed the emplacement of the gabbros. Most of the samples were collected close to the Skuterud mine or contain evidence of albitization. Oxides are very sensitive to changes in oxygen fugacity (fO_2) and requilibrate much faster than silicates (e.g. Frost, 1991a). Most of the metasedimentary rocks only contain rutile. The graphite-bearing samples PWN 007, 25, and 73.1 contain ilmenite, as does the gneiss PWN 80.1. The chalcopyrite-rich quartz-muscovite schist PWN 005 contains hematite, some of the strongly albitized metasedimentary rocks also contain hematite (samples PWN 54 and 55). The relationship of the oxide mineralogy and the fO_2 of the rock is discussed in Chapter 5.2.

3.1.2. Fahlbands

In Norway the term "fahlband" has been used to describe elongate zones of low-grade disseminated iron sulphide mineralization in generally gneissic rocks. The term was first used at the Kongsberg silver mines during the 17th century. This important European mining centre, that operated through the 17th, 18th and 19th centuries, is located about 20 km south of the Skuterud mine, in the Kongsberg sector but not within the Modum complex. It was the location of the Kongsberg School of Mines, which likely contributed to the popularization of the use of the term through Europe (Gammon, 1966). The term fahlbands became popular for describing a range of occurrences of disseminated sulphides, more recently the term has fallen into disuse (Gammon, 1966). Currently it is only used when referring to some localities where the term has historically been applied, and in reviews of original literature.

In the Modum complex, and to the south in the Kongsberg district, fahlbands occur within rocks of sedimentary origin. While they parallel the north-south strike of the region, they are not confined to specific units. The fahlbands can have a strike length of over 11 km and a width of up to 200 m. Disseminated iron sulphides occur in foliated, lensoid concentrations of up to 8% sulphides that are in the order of 2 m in length or less (Gammon, 1966). Sulphides occur as individual grains or as aggregates aligned parallel to the foliation. In the Kongsberg fahlbands, pyrite is ubiquitous with lesser chalcopyrite and local pyrrhotite. In the southern portion of the fahlbands in the Modum complex, pyrrhotite is the major sulphide and pyrite is rare or absent. In the north, pyrite is dominant with pyrrhotite being less common (Gammon, 1966). In the Kongsberg district the fahlbands occur in biotite schist, biotite-garnet-schist, chlorite-schist, chlorite-garnet schist, quartz-feldspar-biotite-gneiss, feldspathic-quartzite and quartzite. The fahlbands of the Modum complex are hosted by metasedimentary rocks possibly dominated by sulphide-biotite-muscovite-dravite-sillimanite-plagioclase-quartz gneiss (±graphite). The presence of graphite (up to 5%) in the fahlbands of the Modum complex is distinct from the Kongsberg district fahlbands

(Gammon, 1966). Graphite is present in some of the pyrite-dominant samples of Skuterud ore with fahlband sulphides.

Silver mineralization of the fahlbands in the Kongsberg district is clearly younger than the fahlbands. At the Kongsberg silver deposits, silver is found only at enriched levels where late calcite veins intersect the fahlbands (Neumann, 1944; Gammon, 1966). The calcite and associated quartz veins have been associated through field relations (Neumann, 1944; Gammon, 1966) and isotopically (Moorbarth and Vokes, 1963) with Permian rocks of the Oslo region. The veins contain mainly sphalerite, native silver, chalcopyrite, galena, argentite, and cobalt and nickel arsenides (Gammon, 1966).

At the Skuterud mine Co-As-Cu mineralization is not specifically restricted to fahlbands, but also occurs in younger rocks including amphibolite (PWN 018 and 071) and possibly veins of albite as described below in the mineralization section.

3.1.3. Metagabbroic rocks

From this study samples PWN 050, 051, 053 and 0120 are considered metagabbros. Samples PWN 050, PWN 051 and PWN 053 were collected about 3 km south of Øverbykollen. Sample PWN 120 was collected in the Knatten area, near the bridge crossing the Snarum River.

Metagabbros are defined here as mafic rocks that contain igneous minerals and habits of igneous minerals preserved by uralitic hornblende. Uralitic hornblende was formed by a sub-solidus replacement of olivine and pyroxene (Munz and Morvik, 1991) (Plate 3.4a). The term uralite or uralitic amphibole is used here to refer to an aggregate of pale green, weakly pleochroic amphiboles averaging 0.1 mm across. Metagabbros collected for this study are more altered than some metagabbros observed by some previous workers. Notes from Munz and Morvik (1991) on less altered metagabbros are included (Section 3.2.1). The uralitic habit of the amphiboles is not preserved in the amphibolites. Cumulate igneous plagioclase laths are preserved in the metagabbros and some amphibolites. The gabbros are olivine and

plagioclase cumulates with clinopyroxene and orthopyroxene as the main intercumulate minerals (Munz and Morvik, 1991).

The metagabbro samples from this study contain about 50% plagioclase laths that are 1 mm or finer (Plate 3.4a). Scapolite occurs at the expense of plagioclase in samples PWN 051 and 053 and completely replaces plagioclase in sample PWN 067. About 40% of the metagabbroic samples are composed of secondary hornblende, that is mainly uralitic, but also fine to medium grained. Orthopyroxene, and to a lesser extent clinopyroxene and olivine occur as fine corroded grains surrounded by hornblende. Other minerals observed in the some of the samples are: biotite, garnet, pyrite, pyrrhotite, chalcopyrite, ilmenite, rutile, hematite and gedrite.

3.1.4. Amphibolites

Amphibolites are metamorphic alteration products of the gabbros and are the dominant mafic rock in the Modum complex. The amphibolites represent a recrystallization of the uralitic amphiboles to coarser more stable habits and complete disappearance of pyroxenes. Some smaller units of amphibolites may be derived from older mafic volcanic rocks and related rock types, the presence of which is alluded to in some literature (Starmer, 1985a). Sampling concentrated on larger bodies many of which had either been previously mapped as amphibolites and/or those that contained proto-amphibolites. The transition from metagabbro was not well established during this study. The presence of relict plagioclase laths in protoamphibolites comparable to plagioclase laths in the metagabbro is the main evidence found in this study. At Knatten amphibolite samples PWN 118, 119, and 122 were collected from the same body and within 300 m of the metagabbro sample PWN 120. This study relies mainly on the work of many other studies in this complex (e.g. Jøsang, 1966, Munz and Morvik, 1991) that have determined through more careful mapping and petrographic studies that the amphibolite is derived from the metagabbro.

On the basis of mineral habit, and microstructure amphibolites can be subdivided into proto-amphibolites, amphibolites, gneissic amphibolites, and Na-enriched amphibolites which also has distinct lithogeochemical character. For geochemical interpretations two groups are considered, the Na-enriched or albitized amphibolites and amphibolites (excluding the albitized amphibolites). The proto-amphibolite contains some plagioclase that preserve an igneous lath shaped habit (Plate 3.4b). Munz and Morvik (1991) also observe that plagioclase retains an igneous character in more rocks than pyroxenes or olivine. Some plagioclase grains in the proto-amphibolites and all those in the other amphibolites are finer-grained than the igneous laths, occurring as relatively equant anhedral grains. The equigranular amphibolites contain fine mosaics of equant hornblende and plagioclase, on a hand sample-scale foliation may not be evident. The gneissic samples do not typically have consistent mineral orientations but a mineralogical banding may be developed to a moderate extent. Compared with the metagabbroic rocks there is a general increase in the amount of sulphides, and the habit of the oxides change; this is described more under the mineral headings.

3.1.5. Metasomatic units

There is a range of rock types related to metasomatism that occur in the Modum complex, including scapolitized rocks, orthoamphibole-cordierite schists, albitization along veins and pervasively in rocks, calcite and magnesite veins and deposits, and Co-As mineralization. To a lesser extent even the amphibolites are metasomatic products, as there are significant chemical differences between these and the parent gabbroic rocks. High temperature processes that follow include scapolitization that affect hornblende-bearing rocks including metagabbros and thus would have formed above 500°C since the amphibole is a hornblende. The calcite veins that occur at the low temperature range, they may occur at temperatures below 250°C (Munz et al., 1995). A U-Pb date of 1.080 ± 0.003 Ga is determined for titanite in an albitite dyke (Munz et al., 1994). The post-gabbroic metasomatism began after intrusion of the gabbro at 1.224 ± 0.015 Ga (Munz and Morvik,

1991) A Pb whole-rock age of 1.131±0.030 Ga is found for the metasedimentary rocks, likely reflecting enrichment of U during alteration (Andersen and Munz, 1995); this seems also to be a date of fluid alteration.

Scapolitization primarily affects mafic rocks that contain plagioclase. The larger areas of scapolization are marked on the geology map (Figure 3.1), however, there appears to be a significant number of smaller areas that are not marked. The 15 thin sections that contain scapolite are metagabbros, amphibolites and amphibolites with Na-enrichment. Some of the scapolite-bearing rocks contain hematite as distinct grains or as exsolution from ilmenite (e.g. PWN 054, 057, and 067). Sulphides are not present in all of the scapolite-bearing samples. In the Bamble sector local, scapolite metasomatism of late mafic intrusions ("hyperites") is also observed (e.g. Frodesen, 1968; Elliot, 1973).

Throughout the Modum complex there are discrete and/or diffuse areas of Na-metasomatism, most commonly characterized by plagioclase altering to albite, and albite replacing other minerals in areas of intense metasomatism. Albitites have been noted to locally occur near the margins all of the amphibolite bodies (Munz and Morvik, 1991); this is not immediately obvious in the field and during field work albitites were a somewhat of a challenge to find. Albitization is younger than the age of intrusion of the gabbros (1224±15 Ma, Munz and Morvik, 1991) and has been dated using U-Pb isotopes in titanite as 1080±3 Ma (Munz et al., 1994). Albitite is a rock type that is composed chiefly of albite. The definition of Tomkeieff (1983) indicates that 95% of the rock contains albite, during this study modal concentrations of more than about 80% albite were not observed.

Sample PWN 064 is an example of a metasediment that is albitized (Na_2O = 4.4%). The sample contains about 15% sillimanite but no K-feldspar. Sillimanite and K-feldspar would occur together without element mobility as they are the product of the prograde reaction of quartz and muscovite (equation 1, Section 3.1.1). K-feldspar present at peak metamorphic conditions may have subsequently been replaced by albite. The lack of K in the

sample (K_2O<0.05%) may have prevented retrograde muscovite from replacing the sillimanite.

Some albitite occurs in discrete veins: this may be formed through an addition of material (e.g. sample PWN 016, Plate 3.2a; Plate 3.2b). Albitites considered in this study are products of metasomatism, some albitites were also observed where there was an addition of massive albite, often coarse grained. Replacement is indicated by the local presence of chessboard twinning of albite (Section 3.2.5), by a mineral assemblage similar to the less altered proximal rocks, or by diffuse margins of the albitized area. Where it intensely affects mafic rocks (e.g. PWN 052, 113) it tends to be accompanied by tremolite-actinolite and less commonly talc. Some amphibolites have elevated Na concentration and contain hornblende (e.g. PWN 065, 068, 069, 099). A few of the mafic samples that are moderately albitized contain quartz, suggesting that in some instances silicification accompanies albitization.

In the Na-enriched rocks albite is normally accompanied by minor rutile and titanite. Besides rutile, hematite is the most abundant oxide, present in about half of the samples. Magnetite is only observed in PWN 065 a partially albitized amphibolite, the magnetite is not in equilibrium with the hematite, ilmenite and rutile is surrounded and separated from magnetite by a rim of titanite. Sulphides are uncommon in albitites and when present are only pyrite.

Metasomatism by fluids with a high fugacity of CO_2 occurs to a significant extent in at least three areas within the study area. The Gamphue quarry located at Øverbykollen extends over an area of about 50 m by 50 m, in which coarse calcite constitutes 90% of the rock (Plate 3.3a). Locally within the massive calcite, brecciated fragments of metasomatized remnants of the mafic country rock occur (Plate 3.3b). These are dominated by hematite flakes with pyrite cubes, albite, talc, tremolite and muscovite (samples PWN 028-037). A smaller area of massive calcite and magnesite is observed at Embretfoss (south of what is included in the geological map, Figure 3.1), in this locality there is no prominent clasts or veins enriched in hematite. Small calcite veins are observed infrequently throughout the

study area. The veins may occur as thin subparallel discontinuous veins of less than 1 mm, probably late features along jointing planes. These veins do not visibly affect the wall rock. Several abandoned quarries exist in the Modum complex that contain magnesite and serpentine. One near Embretfoss that is connected to an area of massive calcite, from which calcite or magnesite was extracted. The other, several kilometres south of the Skuterud mine site, is about 15 m across and fairly equant. It is in country rock of amphibolites and contains serpentine, magnesite and magnetite in varying amounts (no hematite or sulphides) (sample PWN 087). The rock is not foliated but slickensides indicating brittle shearing.

The carbonate rock occurrences are formed from fluids with high partial pressures of CO_2. At Øverbykollen the presence of hematite and pyrite indicates that the metasomatic fluid was less than about 500°C and had an fO_2 greater than the HM buffer (Figure 5.1). The presence of magnetite in the rocks from the magnesite quarry (PWN 087) and Embretfoss (PWN 026) places the fluid related to these rocks at a lower fO_2 than the calcite rocks at Øverbykollen. Magnesite was not observed beyond these two quarries. The Øverbykollen calcite quarry and other calcite veins postdate the albitization of the rocks based on cross cutting relationships. The magnesite post-dates the amphibolite based on field relations, but its age relative to albitization and the calcite is not known.

3.1.6. Granites and pegmatites

Post-tectonic granites (sample PWN 048) occur as a minor unit in the Modum complex, as do associated pegmatites. The pegmatites may contain quartz, amphiboles, microcline, micas, albite. There may be multiple generations, but in general the unfoliated granites and pegmatites are a late event, no relationships were observed to compare these with carbonate rocks. Due to the late nature of the granite few samples were taken and only one thin-section made. No interpretations are made from the granite.

3.1.7. Mineralization at the Skuterud mine

In the Modum complex three fahlband zones occur, the Main fahlband, the East fahlband and a few rusty breccia zones further east. The Main fahlband is about 10 km long in a north-south direction and a maximum width of about 150 m. At the Skuterud mine the main fahlband is roughly coincident with disseminated Co-As ore, there is also enrichments of Cu, Au, Ni and U. (Table 4.2).

The Skuterud mine began operations in 1776 and continued until 1898. The mine was briefly reopened during the Second World War by the occupying German forces (J.B. Gammon, personal communication, 1996). Cobalt grades of the crude ore were 0.08 to 0.1% and 0.15% Cu. This was hand sorted to obtain a concentrate of 3% cobalt (Bugge, 1978). Cobalt, Cu and As were extracted at a nearby mill, with the Co being refined to cobalt oxide for cobalt blue pigment. The mineralization at the Skuterud mine is restricted to about 700 m along strike and less than 200 m in width. The mine workings consist of 6 pits up to 100 m long by 20 m wide and 25 m deep; in addition there are two levels of underground workings that extend to a depth of 125 m. At present there appears to be very little exposed rock with significant mineralization; extraction of mineralized rocks during mining was thorough. Ore grades were not very high, some samples collected for this study may be of ore grade (Table 4.2).

Both academic-and economic-oriented work has been carried out on the Skuterud property since the closure of the workings. A study was published a s result of a brief reopening during World War II (Rosenqvist, 1949). A Ph.D. thesis on the Skuterud deposit was carried out by J.B. Gammon, two papers were produced as a result of the research (Gammon, 1966; Gammon, 1967). A systematic rock chip sample survey with analyses for Co, Cu, and Mo was carried out for Falconbridge Nikkelwerk A/S throughout the mine workings (Hygen, 1971). The analysis of Mo was included, based on data indicating some Mo enrichment (Brown, 1952) that proved to be incorrect. About 500 samples were assayed, of this approximately 30% contained concentration of less than detection limits for Co

(0.005%) and Cu (0.01%). Only 21 samples returned assays higher than 0.25% Cu equivalent. The highest concentrations were 0.67% Cu, 0.008% Co; and another at 0.16% Cu and 0.95% Co. Almost all of the Mo concentrations were less than the detection limit of 0.001% and the highest was 0.003%. The samples represented chips collected over a 2 m length. The mineralized samples from this study are comparable with typical ore samples based on lithology (Gammon, 1966) and ore grades (Hygen, 1971) (Table 4.2).

A radiometric study in the area of the Skuterud mine and along the fahlbands found significant U anomalies within the pits of the Skuterud mine. Moderate enrichment of U in the mineralized samples is observed in this study (Table 4.2). The U is mainly hosted in uraninite, and some in monzanite (van Autenboer, 1957): monzanite was observed and probed during this study.

The mineralization occurs along the contact of a large amphibolite body and mixed metasedimentary rocks containing pyritic fahlbands. Most mineralization occurs along the fahlbands in the quartz-rich metasedimentary rocks. To a limited extent mineralization is found in amphibolites such as samples PWN 018 and 071, a feature also observed by Gammon (1966). One heterogeneous vein with areas of albite and chlorite contains high levels of ore mineralization in the chlorititic area (sample PWN 016) (Plate 3.2a). As indicated in Table 4.2 there is a range of rock-types that are mineralized, beyond those associated with the fahlbands. Quartz-plagioclase-dravite-phlogopite-sulphide-schist (±graphite) (Bugge, 1943; Gammon, 1966) was probably the most extensive rock type hosting Co-As-Cu mineralization. Albitization clearly occurs in spatial association with pervasive albitization at the most northern pit (about 500 m north of the main Skuterud mine) (samples PWN 068 to 073).

Embretfoss is the only location where a marginal enrichment in Co was observed beyond the Skuterud mine. It is located about 10 km south of the Skuterud mine, in an area of amphibolites, mixed gneissic rocks and is the location of a magnesite quarry. Gammon

(1966) reported only trace concentrations of Cu and no Co enrichment in the Modum complex fahlbands beyond the Skuterud mine.

The large amphibolite unit bounding the Skuterud workings to the east is foliated, the metasedimentary rocks appear to be more intensely deformed. Small-scale, tight folds observed in the metasedimentary rocks are not observed in the amphibolites. While the mineral foliation appears stronger in the metasedimentary rocks it is not possible to say that they are more deformed during the Sveconorwegian Orogeny. The metasedimentary rocks have been significantly deformed prior to the emplacement of the gabbros at about 1.5 Ga (Bugge, 1943; Jøsang, 1966; and Starmer 1985a). At the Skuterud mine foliations are consistently north-south with a near vertical dip, which is typical of the Modum complex. The pits of the Skuterud mine expose N-S near-vertical brittle shearing. The pit walls are grooved and some large scale stepping of the rock suggests late dextral movement (Plate 3.1b). Possibly related to the lensoid occurrence of sulphide concentrations observed in fahlbands (Gammon, 1966), rock exposed on the wall of the mine pits separates into prolate lenses with the long direction being horizontal (Plate 3.1b). The fluids responsible for this mineralization were focused along this anastomosing shear zone.As indicated in Table 3.3. Skuterud ore mineralization occurs as sulphides and skutterudite. Cobalt and As sulphides are

TABLE 3.3. SULPHIDES AND ARSENIDES FOUND IN SAMPLES FROM THE SKUTERUD MINE.

Mineral Name	Formula	From literature	Observed, this study
Skutterudite	(Co, Ni)As_{2-3}	yes	
Cobaltite	(Co, Fe)AsS	yes	yes
Pyrite	FeS_2	yes	yes
Arsenopyrite	FeAsS	yes	
Chalcopyrite	$CuFeS_2$	yes	yes
Hexagonal? Pyrrhotite	~Fe_9S_{10}		yes
Monoclinic Pyrrhotite	~Fe_7S_8		?
Siegenite	$(Co, Ni)_3S_4$		yes

in general fine grained, irregular and ragged in habit. Microprobe results indicate that much of the mineralization occurs in pyrite and pyrrhotite. Pyrite and chalcopyrite are the only sulphides observed in concentrations greater than one percent. Most sulphides are disseminated within the metasediments. Some veins dominated by albite occur but are minor, discrete, and not clearly related to mineralization. At the most northern pit that occurs about 500 m north of the main Skuterud mine there is a spatial association between albitization and mineralization. The pit occurs at the contact of amphibolite and quartz-tourmaline-muscovite gneiss with local graphite, as is generally typical. In the amphibolite beyond 125 m across strike from the pit there is some veining of albitite (sample PWN 068). Closer to the pit, Na-alteration is more diffuse and pervasive. In the field the metasedimentary rock did not appear to be strongly albitized but the sample from the immediate hanging wall (sample PWN 073.1) is strongly albitized, graphitic and moderately enriched in As, Cu and Au. Sample PWN 071 from this area is an example of mineralized albitized mafic rock (Table 4.2). Reflected light characteristics in air for the observed Co-As-bearing sulphides are almost indistinct from those of pyrite and pyrrhotite. Most of the sulphides other than pyrite, pyrrhotite and chalcopyrite were identified based on microprobe analysis. Microprobe results also indicate that pyrite in the mineralized sections can contain minor Co (2.22 and 2.97 weight percent) or trace Ni (0.65 weight percent). Pyrite with similar impurities is often anisotropic or may have a more creamy hue.

Sulphides appear to be in equilibrium with each other. The occurrence of sulphides related to the fahlbands were not distinguished from sulphides related to Skuterud mineralization. It is likely that substantial recrystallization of fahlband-aged pyrite occurred during the mineralization of the Skuterud ore. Sulphides in mineralized samples appear to post date silicates and graphite (Plate 3.9b).

3.2. Mineralogy of non-opaque minerals

The non-opaque minerals are each described separately, generally in an order that is grouped in assemblages from oldest to youngest, and therefor they are generally grouped by rock type in the following descriptions. Sulphides and oxides are not described by mineral type but by rock type due the nature of chemical equilibrium that dominates this Fe-Ti-S-O system. Notes on minerals from the metagabbros examined by Munz and Morvik (1991) (Section 3.2.1) are kept separate as this section is composed of direct quotes and paraphrases of other's work.

3.2.1. Notes on igneous minerals, from Munz and Morvik (1991)

Munz and Morvik (1991) described metagabbros from the Modum complex that have mineral assemblages and microstructures that are less altered by sub-solidous recrystallization and metamorphism than those collected for this study. The following section is largely quoted directly from Munz and Morvik (1991, pages 101-102).

The primary igneous assemblage consists of olivine, plagioclase, clinopyroxene, and with or without orthopyroxene, ilmenite, titanite, biotite and apatite. The metagabbros are coarse-grained and all have a subophitic texture with olivine and plagioclase as the major cumulus phases and clinopyroxene and ilmenite as the major intercumulus phases. Even the least altered igneous assemblage displays corona texture.

Olivine

One of the cumulate phases, olivine is observed as euhedral grains. Surrounding the euhedral igneous olivine grains are multiple discontinuous to continuous corona that may completely replace olivine. Phases occurring as corona in successive surrounding rings moving outward from olivine are orthopyroxene, ±clinopyroxene, amphibole with titanite, ±garnet at the contact with plagioclase. The presence of coronas in the six mafic bodies (one without olivine in the cores) indicates the ubiquitous presence of igneous olivine.

Plagioclase

Plagioclase occurs as laths that are typically clouded or zoned. Plagioclase has the highest preservation potential during alteration.

Pyroxenes

Clinopyroxene fills most of the intersticies in optical continuity enclosing both plagioclase and olivine grains. Ilmenite occurs as very fine needles within grains and occasionally as coarser exsolution. Alteration of clinopyroxenes may lead to replacement by secondary pyroxene and or amphibole. Initially there is a loss of colour in the pyroxene. More altered samples contain a mosaic of fine clinopyroxene ±orthopyroxene sometimes completely filling interstices.

Orthopyroxene occurs as an intercumulus mineral in some of the bodies in observed concentrations of 5 modal % or less. Unlike clinopyroxene the grains are not in optical continuity. Alteration is observed as a rim of secondary clinopyroxene and amphibole.

The chemistry of pyroxenes of igneous origin and those related to alteration processes is shown to be distinct for orthopyroxenes. Orthopyroxenes of metamorphic "coronitic" origin have a lower Ca content and a higher Fe content. Clinopyroxenes contain a range of Ca contents from igneous through metamorphic grains.

Ilmenite

In addition to occurring as exsolution within clinopyroxene ilmenite is observed as interstitial grains in all samples. The interstitial grains are commonly rimmed by coronas of amphibole or amphibole with garnet.

Spinel

Spinel has been observed as an intergrowth with ilmenite in two samples.

Biotite

Biotite may be a late igneous phase occurring in some samples up to 2-3 modal %.

Apatite

Apatite makes up less than 1 modal % as rounded 0.1 to 0.3 mm grains.

Alteration Products

Scapolite is described in veins usually less than 1 mm wide but up to 5 mm wide (with amphibole). Scapolite also occurs in one sample beyond a corona of orthopyroxene and amphibole with spinel.

3.2.2. Pyroxene

Orthopyroxene is observed in concentrations of <10% in the metagabbros. All grains are corroded, occurring as groups of relic islands derived from the same crystal and rarely as single subhedral grains. With the exception of PWN 067 and PWN 118B, the grains are surrounded by uralitic hornblende (Plate 3.4a). The orthopyroxene grains are up to 1 mm in size surrounded by an aggregate of uralitic hornblende at least 2 mm in diameter. Typically two or more grains occur together, and intergrowths are frequent.

The other microstructure observed for pyroxene is poikiolitic and fairly ragged anhedral grains, present in samples PWN 118B and 067. The corroded grains are up to 2 mm across. These grains have well defined inclusions of hornblende. Hornblende in these samples is not uralitic and do not surround these grains. PWN 067 also contains very strongly corroded and poorly defined grains of orthopyroxene engulfed in single hornblende grains that are medium grained. The two microstructures of orthopyroxene may result from each replacing different minerals, leading to different growth histories.

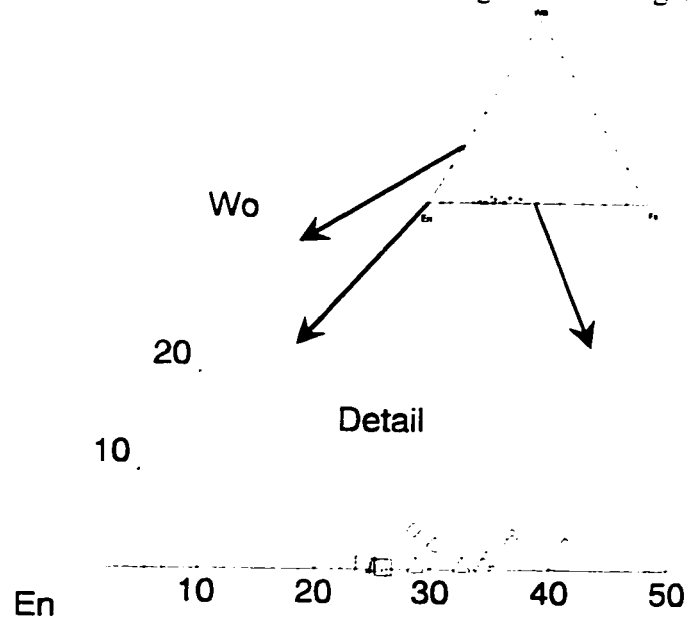

Figure 3.2. Wo-Fs-En diagram for probed orthopyroxenes from this study (open) and from Munz and Morvik (1991) (shaded). The diamond shapes represent grains interpreted to be igneous, the triangles are from coronas, open squares are from PWN 050, and the circle is from PWN 067. The samples from this study are similar to orthopyroxene from coronas though they do not share the same habits.

Clinopyroxene is a dominant primary cumulate mineral, but it was not positively identified within the samples used in this study. Optically it appeared that clinopyroxene occurs as a lesser intergrowth or cryptocrystalline exsolution with some of the orthopyroxene in sample PWN 051. No evidence for any was found during microprobe studies of other pyroxenes.

Microprobe analyses for samples PWN 053 and PWN 067 are presented in Appendix 2 using a Wo-En-Fs ternary graph. The orthopyroxenes are in the enstatite to hypersthene compositional fields, most being bronzite. The habit of orthopyroxene observed in this study is different than coronitic pyroxene that occurs as a rim around a core of olivine. Chemically, however, the orthopyroxenes from this study are similar to the orthopryoxenes interpreted by Munz and Morvik (1991) to be formed during corona growth: they contain less Ca and Fe than the igneous orthopyroxenes (Figure 3.2). The increase in the Mg content of the secondary orthopyroxene makes Fe available to the system. It is consumed by another ferromagnesian mineral (hornblende), by an oxide as Fe^{2+} or Fe^{3+} or to form an iron sulphide.

3.2.3. Olivine

Olivine is only observed in PWN 50, occurring as moderately corroded subhedral grains within uralitic hornblende. Orthopyroxene (secondary) occurs adjacent to one grain, but there was not a coronitic relationship of orthopyroxene rimming olivine as observed by Munz and Morvik (1991).

3.2.4. Garnet

Garnet is a minor constituent in metagabbroic samples PWN 50 and PWN 120, and amphibolite PWN 119. In the metagabbros, garnet is not surrounded by hornblende, it occurs as medium-grained irregular subhedral grains. Amphibolite bodies typically do not host garnet; those that do typically contain concentrations of 5 to 10% coarse subhedral equant garnets. Microprobe chemistry is not available for any garnets from this study, though some

analyses are available in Munz and Morvik (1991). There is no clear microstructural differences except that the garnets of the amphibolites may be larger (up to 3 cm across) and possibly closer to euhedral in habit. The presence of garnets in metagabbros and amphibolites weakly correlates with samples that contain higher MnO concentrations.

3.2.5. Plagioclase

Igneous plagioclase occurs as generally medium-grained cumulate laths, that are partially preserved in the metagabbros and protoamphibolites. Samples from Knatten (sample PWN 118B and PWN 120) contain some zoned plagioclase with anorthositic cores and intermediate rims. The plagioclase may show very slight turbid alteration as in PWN 120. The turbid texture is due to porosity created during the alteration of plagioclase to finer, more equant plagioclase. Two microprobe analyses in metagabbros found plagioclase compositions of An_{59} and An_{62}.

The habit of the plagioclase in the amphibolites is equant, fine-grained, and generally is not foliated. No microprobe results for plagioclase were collected from amphibolites. Using the Michel-Levy microscope method to identify plagioclase composition through extinction angles of polysynthetic albite twins, no difference in composition was observed between plagioclase of metagabbros and amphibolites. Moderately Na-enriched amphibolites contain plagioclase that is more albitic but in general is of the same habit of plagioclase occurring in other amphibolites.

Strongly albitized rocks contain albite that is variable but generally fine-grained occurring in an interlocking habit (Plate 3.5a). The composition of plagioclase in PWN 52 appears somewhat variable based on probe results, but it is dominantly albite (An_{0-5}) (Appendix 2) and microscopic estimates using the Michael-Levy method. "Chessboard twinning" is observed in some of the strongly albitized rocks, a feature also observed by Munz et al. (1994) (Plate 3.5a). The texture of chessboard twinning has been attributed to formation of albite through replacement (Smith, 1974). It is morphologically characterized by

dense arrays of narrow discontinuous albite lamellae. The twin boundaries are usually stepped or lenticular with abrupt terminations (Barth, 1969). It is confined to albite that is close to pure end-member. Chessboard twinning has a low level of stability and tends to recrystallize during annealing processes (Barth, 1969), supporting the interpretation that albitization occurred late in the metamorphic history.

3.2.6. Scapolite

Scapolite is the sole mineral directly associated with the process of scapolitization (described in section 3.1.5). Scapolite is a secondary alteration mineral occurring in 2 of 4 metagabbro samples, 9 of 28 amphibolite samples, 4 of 7 Na-enriched amphibolite samples, 1(?) of the metasedimentary rocks and none of the strongly albitized rocks. In scapolitized protoamphibolite PWN 067, fine-grained scapolite completely replaces plagioclase. Other samples in which scapolite has replaced all, or almost all of the plagioclase are: 092, 105, and 057, other samples appear to contain some plagioclase. In most samples scapolite is medium-grained and anhedral. Scapolite is locally observed to occur as a replacement along grain boundaries. Scapolite does not generally directly replace plagioclase, but do occur at the expense of plagioclase. Microprobe analyses of scapolite from metagabbro PWN 051, and amphibolites PWN 067 and 057 give similar results (Appendix 2). The analyzed scapolites are very rich in Cl (3.07 wt. % on average) with minor SO_2 (0.33 wt. % on average), with little CO_2 and undetectable levels of OH and F. The scapolite is moderately towards the Na end member, the variety is on average Me_{35} (chloride dipyre) (Appendix 2). The most Cl-rich scapolites reported occur in the Bamble sector, containing up to 3.91 wt. % Cl, from the apatite deposits at Ødegården (Lieftink et al., 1993). Frodesen (1973) reports that the completely scapolitized rocks (ødegårdites) of the Hiåsen gabbro (Bamble sector) contain scapolites that are of Me_{35} (chloride dipyre).

3.2.7. Biotite

Biotite is a common accessory mineral, occurring in all rock types. Biotite is observed in two of the metagabbros. In PWN051, PWN053 and PWN090 it contains needles of rutile that are oriented within the 001 plane at 60° to each other. Biotite has been observed in an albitized amphibolite to be intergrown with lamellae of hematite (sample PWN 054). Biotite from a hematite-bearing albitized amphibolite (PWN 057, Appendix 2) has a Fe/(Fe+Mg) composition of 0.3, this composition and the association with hematite is compatible with oxidation at or above the hematite-magnetite buffer (Wones and Eugster, 1965; Speer, 1984). A biotite from a scapolitized protoamphibolite (PWN 067) is measured to have an exceptionally high level of chlorine at 0.97 wt.% (Appendix 2) (Munoz, 1984); the grain was intergrown with amphibole and it is possible that there is contamination from amphibole. The albitized amphibolite (PWN 057) contains moderately high Cl concentrations at 0.25 and 0.28 wt.%; while a mineralized sample (PWN 009) from lower metamorphic grade does not contain measurable Cl. Biotite is usually not foliated with the any gneissic foliation defined by hornblende and plagioclase.

3.2.8. Amphiboles

Hornblende occurs in the metagabbros and in the amphibolites and gneisses related to the alteration and metamorphism of the gabbro. The Na-enriched amphibolites often contain hornblende, though some contain actinolite-tremolite. The strongly albitized rocks contain tremolite-actinolite, tremolitic hornblende was observed once through microprobe analyses. Orthoamphiboles are observed in one of the metagabbros as a trace phase and a major phase of the orthoamphibole-cordierite rock that occurs locally in the Modum complex (Munz, 1990).

Amphiboles with a uralitic habit occur as a secondary mineral rimming and replacing mafic minerals in the metagabbros; in which they make up about 60% of the rock. Uralite is a typical replacement product of augite, in metagabbro samples it is observed replacing

pyroxene and olivine. In the coronitic gabbro it is expected to occur as the outer rim in a symplectic intergrowth with spinel, however, spinel is not observed in rocks of this study. Chemically, samples of uralites are found to be tschermakitic, pargasitic, and magnesio-hastingsitic by microprobe analysis (Appendix 2). The pargasitic amphiboles and the magnesio-hastingsite have by definition slightly more total Ca, Na, K than the tschermakitic amphiboles. The uralitic amphiboles have high contents of Cl, the highest of the measured amphiboles.

In metagabbros from this study uralite appears to be a product of orthopyroxene, clinopyroxene and plagioclase. The equations roughly balance when 1 plagioclase, 2 orthopyroxene and 1 clinopyroxene is consumed and Na and H are added to produce 1 Ca

TABLE 3.4. RELEVANT NAMES AND FORMULAS OF AMPHIBOLES FROM HAWTHORNE (1983)

End Member	Formula
	Calcic Amphiboles
Tremolite - Ferro-actinolite	$Ca_2Mg_5Si_8O_{22}(OH)_2$ - $Ca_2Fe^{2}_5Si_8O_{22}(OH)_2$
Pargasite	$NaCa_2Mg_4AlSi_6Al_2O_{22}(OH)_2$
Ferro-pargasite	$NaCa_2Fe^{2}_4AlSi_6Al_2O_{22}(OH)_2$
Hastingsite	$NaCa_2Fe^{2}_4Fe^{3}Si_6Al_2O_{22}(OH)_2$
Magnesio-hastingsite	$NaCa_2Mg_4Fe^{3}Si_6Al_2O_{22}(OH)_2$
Alumino-tschermakite	$Ca_2Mg_3Al_2Si_6Al_2O_{22}(OH)_2$
Ferro-alumino-tschermakite	$Ca_2Fe^{2}_3Al_2Si_6Al_2O_{22}(OH)_2$
Ferri-tschermakite	$Ca_2Mg_3Fe^{3}_2Al_2Si_6Al_2O_{22}(OH)_2$
Ferri-ferro-tschermakite	$Ca_2Fe^{2}_3Fe^{3}_2Si_6Al_2O_{22}(OH)_2$
Alumino-ferro-hornblende	$Ca_2Fe^{2}_4AlSi_7AlO_{22}(OH)_2$
	Orthorhombic Amphiboles
Magnesio-gedrite	$Mg_5Al_2Si_6Al_2O_{22}(OH)_2$
Ferro-gedrite	$Fe^{2}_5Al_2Si_6Al_2O_{22}(OH)_2$
Sodium-gedrite	$Na(Mg,Fe^{2})_6AlSi_6Al_2O_{22}(OH)_2$

amphibole. If clinopyroxene is consumed then Na must be derived externally. Since the gabbros did contain clinopyroxene, it appears that Na was from an external source; rigorous calculations are not possible with the present data and the samples.

Amphibolites do not contain uralitic amphiboles, but are fine-to medium-grained anhedral to subhedral hornblendes. Specifically, microprobe results indicate compositions of tschermakitic and hastingsitic amphiboles. Tschermakitic amphiboles are known to occur in rocks of high metamorphic grade. They are common in eclogites replacing omphacite as an early retrograde product.

The orthorhombic amphibole gedrite was observed and analyzed in metagabbro PWN051. This metamorphic amphibole is a trace phase occurring as well-formed, fine grains. The orthoamphibole-cordierite rocks of the Modum complex contain gedrites that also fall in the gedrite to sodium gedrite field (Munz, 1990).

From metagabbro to amphibolite there is a decrease in Al and an increase in Ti in the amphiboles (Appendix 2). This is also observed in the whole-rock data (Chapter 4). The changes in the Ti and Al content of the hornblendes during amphibolization may be in response to the enrichment in Ti in the rock. Metamorphic conditions during crystallization may also play a role. The relationship of Ti and Al in hornblende has been related to pressure for granodiorites with a specific assemblage and has been used as a geobarometer (e.g. Hammarstrom and Zen, 1986; Hollister et al., 1987).

Hornblende and what appears to be actinolite-tremolite occurs in Na-enriched amphibolites. Amphiboles in two probed samples PWN 057 and 071 are found to be magnesio-hastingsite (Appendix 2). Sample PWN 071 with Skuterud ore mineralization also contains about 10% epidote. Some examples of measured amphibole compositions and optical observations indicate that many Na-enriched amphibolites contain some hornblende, evidence for albitization during amphibolite facies metamorphism. The amphiboles often do not have as dark a colour as hornblendes from the amphibolites. The habit also is in general

irregular. In this general group of rocks actinolite has been identified in some samples. These samples contain somewhat less Cl.

The amphibole-bearing, strongly albitized rocks contain amphiboles from the actinolite-tremolite solid solution series. The amphiboles are more irregular in habit as is the albite of these rocks (Plate 3.4b). The difference between the amphiboles measured in sample PWN 052 and in the metagabbros is increased Cr and Mg, and less Na and K in the albitized sample. Consistent with the biotites in the greenschist-grade mineralized rocks these amphiboles contain very little Cl.

The ubiquitous presence of hornblende in the amphibolites is a strong indication that the alteration of the metagabbro occurred at amphibolite-grade conditions. Albitized rocks with amphiboles may contain either tremolite-actinolite or hornblende. Strongly albitized samples such as PWN 052 and PWN 113 contain actinolite or tremolite that is indicative of greenschist-grade metamorphism. The moderately albitized amphibolite gneiss with Skuterud mineralization contains hornblende and epidote suggesting that it is transitional between greenschist and amphibolite-grade metamorphic conditions: or the epidote and the hornblende are not in equilibrium with each other suggesting dis-equilibrium.

3.2.9. Potassium feldspar

This mineral is conspicuous more in its absence than in its presence. To identify K-feldspar, all of the polished thin sections were stained following the cobaltinitrite-aramath method. As expected most of the mafic rocks do not contain K-feldspar. Some of the metasediment samples from near Butjern Lake, and a sample of a late granite contain K-feldspar. As described in 3.1.5, K-feldspar may be replaced during albitization

3.2.10. Titanite

Titanite is an accessory mineral that is observed to occur in some of the samples that contain rutile. Usually it is subordinate in concentration to rutile. It may rim rutile or composite grains of rutile, hematite and ilmenite as in PWN 067. Titanite is especially

common in the Na-metasomatized rocks (samples PWN 052, 055, 65). The role of titanite in the oxide system and its role in controlling oxygen fugacity is not known.

3.2.11. Spinel

Spinel is not observed in the thin sections. It is expected to occur in a symplectic relationship with coronitic amphibole in metagabbroic rocks. Possibly the alteration of the metagabbros is too far advanced, and this phase has become unstable.

3.2.12. Apatite

Apatite occurs in all rock types; it is the main or the only phosphorous-bearing mineral in the samples. It is typically fine-grained and equant. Normative values of apatite in the rocks have been calculated by the CIPW method: mafic rocks contain 0.15 - 0.5 % apatite; rocks with over 30% normative albite contain 0.07 - 1.52% apatite; and metasedimentary rocks contain as much as 1.66% apatite (PWN 025). The chlorite-albite vein (sample PWN 016) contains the most apatite (4.26%).

Limited microprobe analyses were carried out for apatite in this study. Appendix 2 contains 4 quantitative analyses of apatite, also several qualitative analyses were carried out, though not reported beyond this summary. Some of the apatites are found to contain moderate concentrations of Cl (up to 1.04 wt. %), these are less than the most Cl-rich apatites from the Bamble sector that range from 5.3 to 6.73 wt. % Cl (Nijland et al., 1993; and Lieftink et al., 1995), these samples include the highest concentrations of Cl reported for apatite. Fluorine was not detected in any of the apatite grains analyzed in this study. Minor Sr and SiO_2 were measured in two samples, both from PWN 009, a mineralized metasediment.

Cl-free apatite from PWN 090 has a distinct character; it is nearly opaque with a dusty appearance and the grains are about 1 mm in size. The appearance and chemistry of these apatite grains is similar to hydroxylapatite from apatite-phlogopite veins in the ancient Ødegården mines in the Bamble sector (Lieftink et al., 1994). It has been interpreted that

these hydroxylapatites form as a replacement of the Cl-bearing apatites (mentioned above). The loss of Cl is accompanied by losses in REE, Fe, Na (Lieftink et al., 1994).

3.3. Mineralogy of opaque minerals

3.3.1. Rutile

Rutile is found in most of the metagabbros as a high temperature deuteric oxidation product of ilmenite. In amphibolites it is only observed in some of the Na-enriched samples (PWN 038, 066, and 069). In the strongly albitized samples, rutile along with hematite is the dominant oxide. The metasedimentary rocks also commonly contain rutile as the sole oxide, usually of a ragged character that is not likely detrital in origin, or if so, has re-crystallized.

3.3.2. Graphite

Graphite occurs in 4 thin sections. The samples are moderately aluminous to aluminous metasedimentary rocks (samples PWN 007, 025, 072.1 and 073.1). The graphitic samples are collected from the immediate area within and around the mine workings. Minor amounts of graphite are characteristic of the metasedimentary rocks hosting the fahlbands of the Modum complex (Gammon, 1966). Stable isotope evidence (see Geochemistry chapter) suggests that the graphite is of organic origin. The graphite is deformed, and has recrystallized under metamorphic conditions as indicated by its coarse size. The graphite is moderately foliated but flakes are generally bent out of the foliation plane, affected by neighboring minerals and unknown factors. Most of the graphite-bearing samples are variably enriched in pyrite, with the exception of PWN 73.1 a sample located within 3 m of the most northern pit. The pyrite crystallization appears to postdate graphite (Plate 3.9b).

3.3.3. Oxides

Observed minerals that directly relate to oxygen fugacity during formation of the rocks are: graphite, pyrrhotite, pyrite, magnetite, ilmenite, rutile, hematite and scapolite. In this section the minerals magnetite, ilmenite, rutile and hematite are discussed together as

they have a strong interdependency. The oxygen fugacity of the fluids is addressed in Chapter 5.

Metagabbroic rocks contain trace amounts of ilmenite that has exsolved rutile, and in one sample also hematite. Samples PWN 050 and 051 contain rutile with a graphic looking texture replacing ilmenite (Plate 3.8b). PWN 053 contains ilmenite (analysis 5311IL, 8% hematite) that has been partially replaced by a mottled to graphic appearing assemblage of rutile (analysis 53124, 97% TiO_2) and hematite (analysis 53123, with 6.4% TiO_2) (Plate 3.7b). The assemblage of ilmenite, rutile and hematite is stable below about 600°C (Figure 5.2) and the presence of hematite represents an oxygen fugacity higher than ilmenite alone or ilmenite and rutile. The observed textures and phase compositions are indicative of high temperature deuteric oxidation of discrete ilmenite grains as described by Haggerty (1991). Exsolution of rutile is a slightly less advanced stage of oxidation than exsolution of rutile and hematite according to Haggerty (1991). The oxygen fugacity of these rocks and the fluids affecting them is discussed in Section 5.2. The presence of a high temperature fluid is also required for the formation coronitic microstructures.

There is a higher abundance of ilmenite in the amphibolites than in the metagabbros and they do not preserve similar relations with rutile; possible exceptions are PWN 073.2, 062. Rutile generally occurs as distinct grains. The increase in ilmenite is reflected in the whole-rock analyses by an increase in TiO_2 content; see mass balance calculations: Section 4.3. Recystallization of the ilmenite during amphibolization did not appear to preserve habits observed in the metagabbroic rocks.

Ilmenite occurs in a range of habits but always anhedral and usually irregular fine to medium grains. In many of the samples thin parallel lamellae of hematite have exsolved from ilmenite (Plate 3.8a). In a lesser number of samples thicker exsolution of magnetite occurs as well. The amount of hematite exsolution in ilmenite ranges from trace amounts to 10 or 20%. At least one Na-enriched amphibolite (PWN 065, Plate 3.8b) contains about 45% hematite lamellae in ilmenite.

Albitites and Na-enriched samples tend to contain hematite rather than other iron oxides. Hematite and ilmenite is observed in some samples (e.g. PWN 065 (Plate 3.8b) and 099). Many albitized samples contain no oxides (e.g. PWN 111). Other samples contain rutile ± titanite that tends to rim rutile. PWN 110 contains 2% rutile and is located close to PWN 111 with no oxides.

Hematite may occur as flakes without exsolution of other oxides or in grains as an exsolution product with ilmenite. The moderately Na-enriched samples more commonly display exsolution with ilmenite. Sample PWN 065 contains about 2% composite grains of ilmenite and hematite, with hematite making up about 45% of the grains (Plate 3.8b). The oxide grains in PWN 065 are irregular in habit, similar to the habit of ilmenite grains in oxides. Strongly albitized samples (albitites) contain hematite that may have a flake-like habit (e.g. PWN 052) and may be interstitial to some silicates; sample PWN 057 contains hematite that is interstitial to hornblende but not interstitial to albite. The grains with exsolution of ilmenite and hematite appear to represent oxidation of preexisting ilmenite dominant grains, while the hematite flakes appear to be new mineral growths contemporaneous with albitization.

Along the western margin of the Modum complex hematite-bearing units are particularly common (Figure 3.1) (Jøsang, 1966). These units include the clearly metasomatic albitized rocks and the calcite dominated rocks at the Gamphue quarry, but also a unit labeled quartz-phlogopite-hematite schist. It is expected that the hematite in this unit is secondary as observed metasedimentary rocks are more reduced, some containing graphite. Microprobe analyses of hematite from altered metasedimentary rocks near Øverbykollen could discriminate the source, low Ti content of hematite is typical of sedimentary hematite. The presence of abundant hematite-bearing metasomatic rocks in the area suggests that the metasedimentary rocks in the area have been affected.

The calcite-dominated metasomatic rocks at the Gamphue quarry contain hematite and pyrite in equilibrium. Calcite- and magnesite-rich rocks at Embretfoss contain magnetite

and ilmenite. Beyond the oxides there is a different character to the metasomatism at the two locales. The one thin section from the magnesite and calcite quarry at Embretfoss is not strongly altered by greenschist facies processes as indicated by the presence of hornblende (PWN 026). At the Gamphue quarry country rock is strongly altered, including albitized (Plate 3.3b).

Magnetite is observed in some mafic rocks, a late granite (sample PWN 048) and a serpentine-magnesite rock (sample PWN 87). Rarely, amphibolite samples that contain ilmenite with hematite exsolution also contain thicker exsolution bands of magnetite or proximal separate grains. One of the more advanced metagabbros (sample PWN 118.2) contains this texture as well. Magnetite mainly occurs intergrown with pyrite. The intergrowth is interpreted as being related to either of two processes, oxidation of pyrrhotite to pyrite and magnetite, or oxidation of pyrite liberating sulphur into a fluid. The alteration of pyrrhotite to pyrite plus magnetite is observed in gabbros of the Bamble sector (Cameron et al., 1993) where pyrrhotite is partially replaced by a loose aggregate of pyrite cubes with interstitial magnetite. Pyrite and magnetite occur together in a similar habit in a few amphibolites and protoamphibolites in this study (Plate 3.6b). Pyrite also appears to be partially replaced by magnetite in other samples (Plate 3.6a).

3.3.4. Sulphides in the unmineralized samples

Pyrite is ubiquitous in the mafic rocks and metasedimentary rocks of the study area, but the most strongly albitized rocks rarely contain any sulphides. In metagabbroic rocks, sulphides are observed in concentrations of << 1%, while in amphibolites it tends to occur in amounts of <1%. In both rock types pyrite is fine grained, though it is somewhat coarser and more irregular shape in the amphibolites.

Pyrrhotite is observed in trace amounts in metagabbros PWN 050, 120 and possibly in 118.2. Pyrrhotite in these samples is extremely fine and scarce, Plate 3.5b contains typical pyrrhotite that is at the lower limit of optical resolution. In sample PWN 050 trace amounts

of pyrrhotite occur as part of a composite with pyrite and chalcopyrite (Plate 3.5b) and on one occasion with magnetite in composite grains. Above 742 °C pyrrhotite but not pyrite is stable (Barton, 1969; Barton and Skinner, 1979), rocks that crystallized at high temperatures are expected to contain pyrrhotite. Recrystallization at lower temperatures would tend to produce pyrite, as expected for the relatively oxidized fluids observed in this system.

The Fe-Ni sulphide from PWN 042.2 is from an unusual 2 mm wide vein of plagioclase where Py and Po appear to coexist. One 100 μm grain of pyrite contained minor blebs of Ni-bearing Fe sulphide (pentlandite?) as indicated by microprobe. The occurrence is not typical of pentlandite that most commonly occurs as flames in pyrrhotite; the mineral is not clearly pentlandite.

Many amphibolite samples that contain magnetite, have pyrite intergrown with some of the magnetite grains (as in Plate 3.6a, 3.6b, 3.8a). Pyrite that is associated with magnetite sometimes has a microstructure similar to pyrite and magnetite replacing pyrrhotite (Cameron et al, 1993) (Plate 3.6b).

Photographic Plates

Plate 3.1a. (facing page, top)

A view looking north from near the south end of the Skuterud mine workings. The building is a replica of an original mine building, part of a plan to use the sight as an open air museum. Hidden pits, elongate in the direction of the photograph, occur to the left of the building; they are the main workings of the mine. Two levels of underground workings also exist. Waste rock piles are the main visible feature.

Plate 3.1b. (facing page, bottom)

A view into a central pit at the Skuterud mine. Note the distinct horizontal grooving exposed in the vertical foliation plane. The shear zone has been affected by brittle dextral (?) strike slip shearing. The asymmetry in step direction in the grooved fault surface suggests the dextral sense. The fault planes have an anastomosing nature resulting in relatively coherent elongate lenses separated by more schistose zones. A truncated portion of a lense is exposed to the north (right) of the 3 m high mine portal.

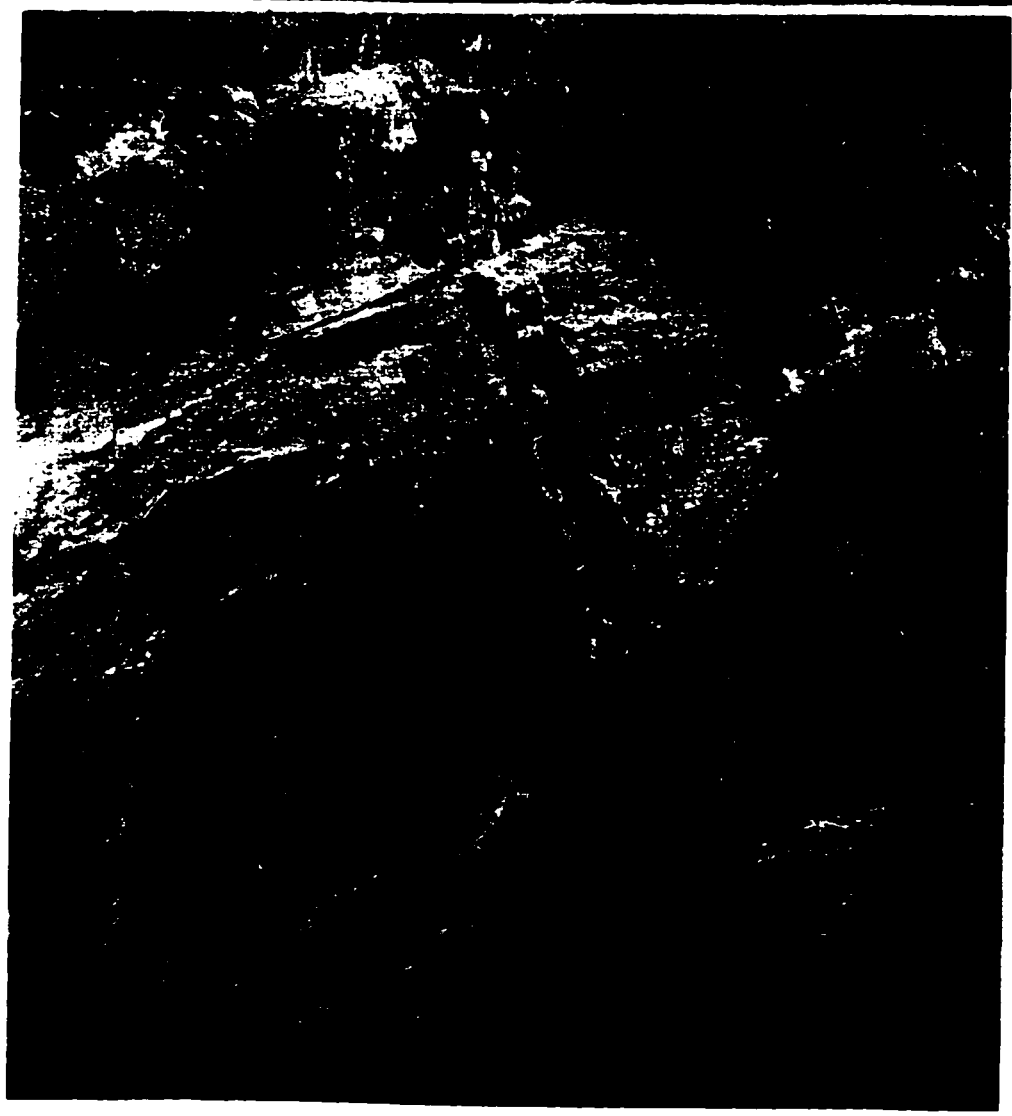

Plate 3.2a. (facing page, top)

Vein of albite with local concentrations chlorite, pyrite and magnetite (sample PWN 016) from about 1 km south of the Skuterud mine. There is moderate Cu and As concentrations in the sample, though albite-rich rocks are normally not observed to be mineralized. 10 cm knife for scale.

Plate 3.2b. (facing page, bottom)

This albite vein from Skuterud mine workings contains unfoliated albite and crosscuts the fabric of the micaceous shear zone that makes up the wall rock. The photograph is from near sample PWN 019, red knife is 10 cm long.

Plate 3.3a. (facing page, top)

Gamphue calcite quarry at Øverbykollen. Mixed angular blocks of mainly altered mafic rock in a massive very coarse calcite matrix. Some calcite crystals are 2 m across. There is significant Na-alteration in the general surrounding area.

Plate 3.3b. (facing page, bottom)

Gamphue calcite quarry at Øverbykollen. Metasomatized older mafic block with albite-rich rim in a calcite matrix. Metasomatized fragments are often dominated by hematite with clots of pyrite

PHOTOMICROGRAPHS

Plate 3.4a. (facing page, top)

Metagabbro with igneous laths of intermediate plagioclase (Pl), uralitic hornblende (Hbl) replacing orthopyroxene grains (Opx). minor scapolite (Scp) occurs replacing plagioclase. (sample PWN 050, field of view 3.38 mm, crossed polars).

Plate 3.4b. (facing page, bottom)

This Na-rich protoamphibolite with relic turbid igneous laths of plagioclase (Pl-1) that are characteristic of the rocks termed protoamphibolites in this study. There is significant recrystallized plagioclase, which in this sample is albitic (Pl-2). The hornblende is characteristic of the more equigranular amphibolites (sample PWN 099, field of view 3.38 mm).

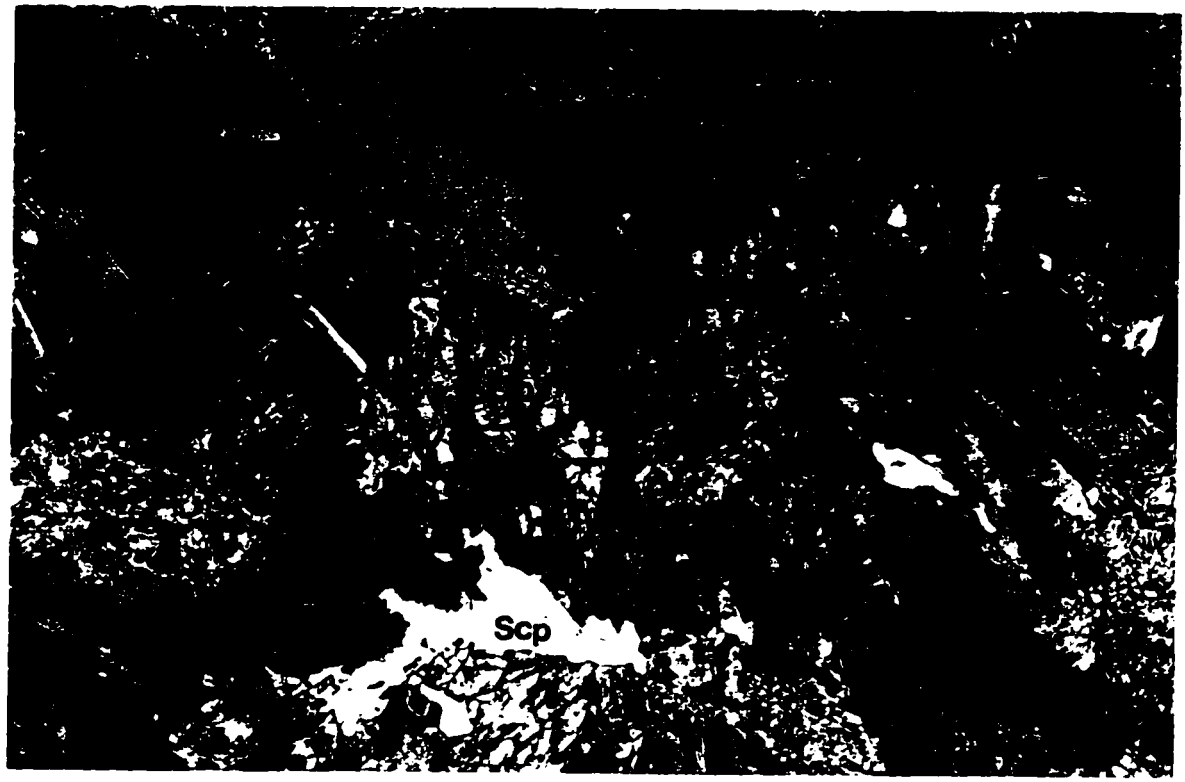
Scp


I-1

Plate 3.5a. (facing page, top)

Strongly albitized metagabbro containing mainly albite and minor tremolite-actinolite. Well formed "chessboard" twinning of the albite is common, this is a type of twinning that associated with pure albite formed via replacement of other minerals: especially K-feldspar: some examples are marked (cb). unfoliated actinolite (Cam) occurs in his rock that occurs within hornblende-bearing metagabbros: probe results indicate the presence of actinolite and a tremolitic hornblende (sample PWN 052, field of view = 3.38, crossed polars).

Plate 3.5b. (facing page, bottom)

Metagabbro: a composite grain of pyrite (Py) with lesser pyrrhotite (Po) and chalcopyrite (Ccp). The instability of pyrite above about 741°C indicates that pyrite cannot be igneous, pyrrhotite and chalcopyrite may be igneous. (sample PWN 50, field of view = 0.019 mm, reflected light).

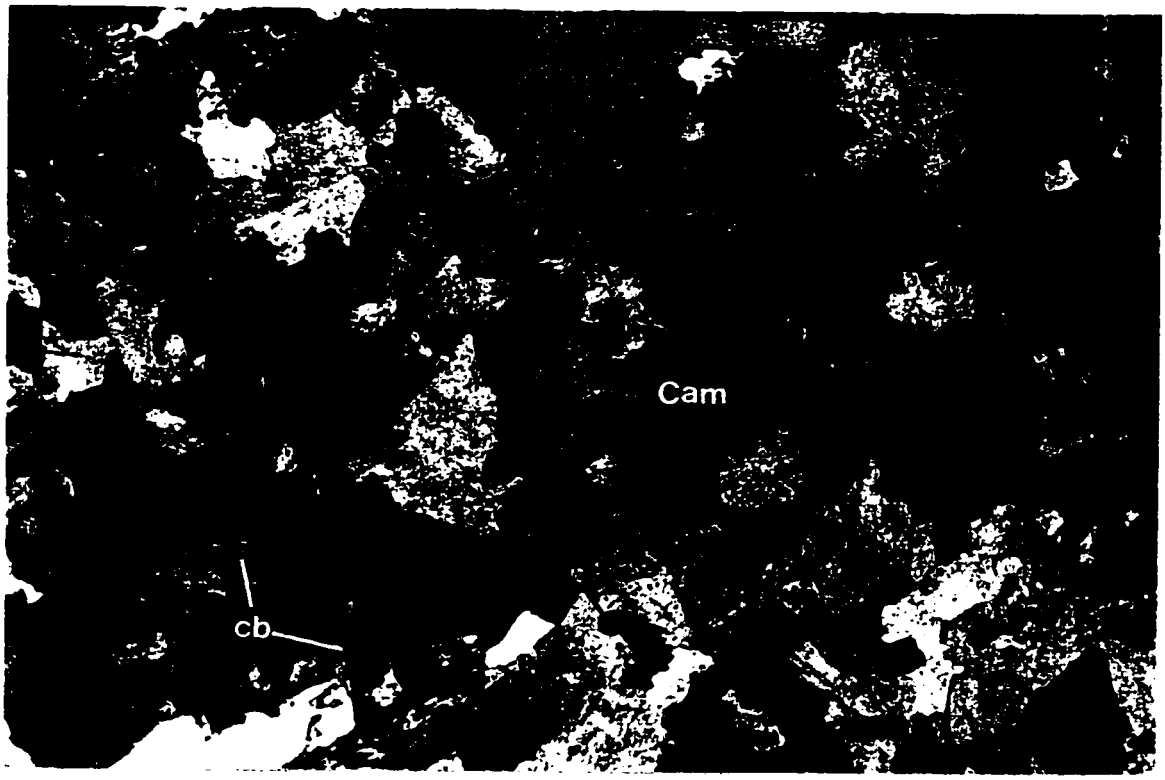
Cam
cb


Po
Py
Ccp

Plate 3.6a. (facing page, top)

Equigranular amphibolite with a pyrite (Py) grain that is partially replaced by magnetite (Mag). Slight low-temperature oxidation of the pyrite occurs on the margin between the pyrite and the magnetite. Magnetite and pyrite often occur together in the amphibolites in this example the magnetite appears to have formed after the pyrite during metamorphic oxidation (sample PWN 061, field of view = 0.55 mm, reflected light).

Plate 3.6b. (facing page, bottom)

A protoamphibolite displaying pyrite (Py) and magnetite (Mag), the microstructure of pyrite occurring in an aggregate of cubes with lesser magnetite is a habit typically observed when pyrrhotite is oxidized to pyrite and magnetite (Cameron et al., 1993) (sample PWN 118.1, field of view = 0.48 mm, reflected light).

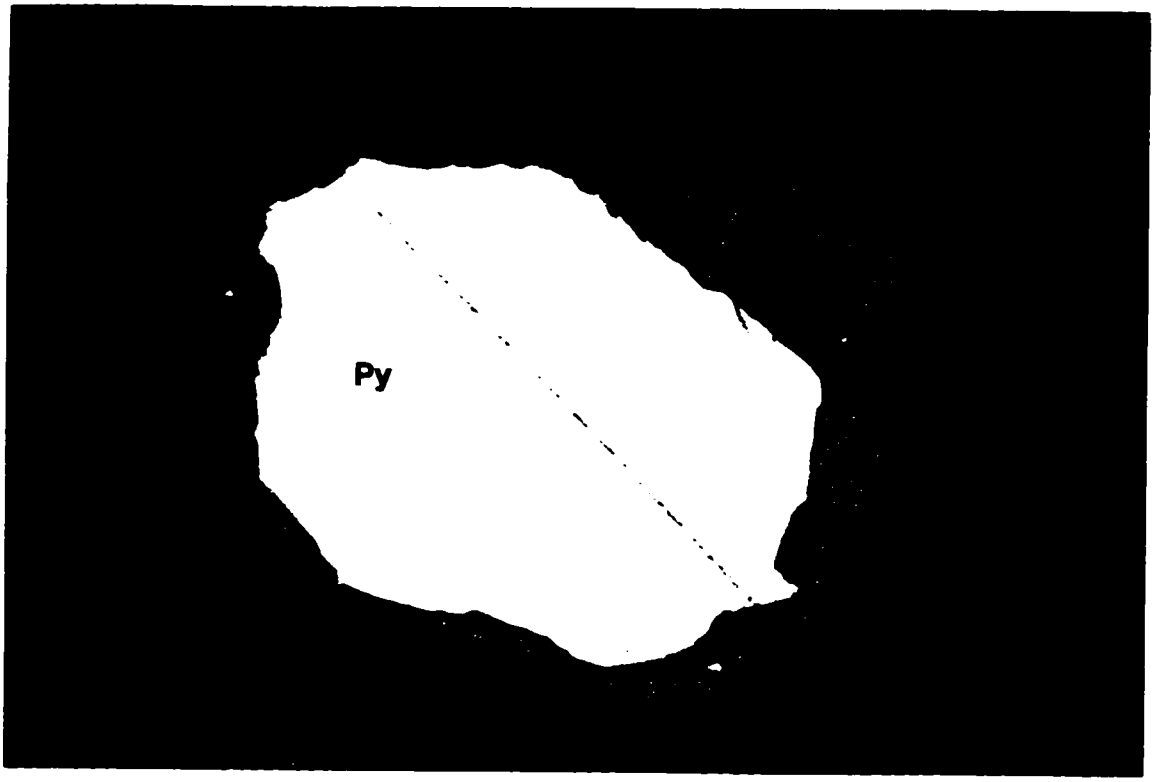
Py

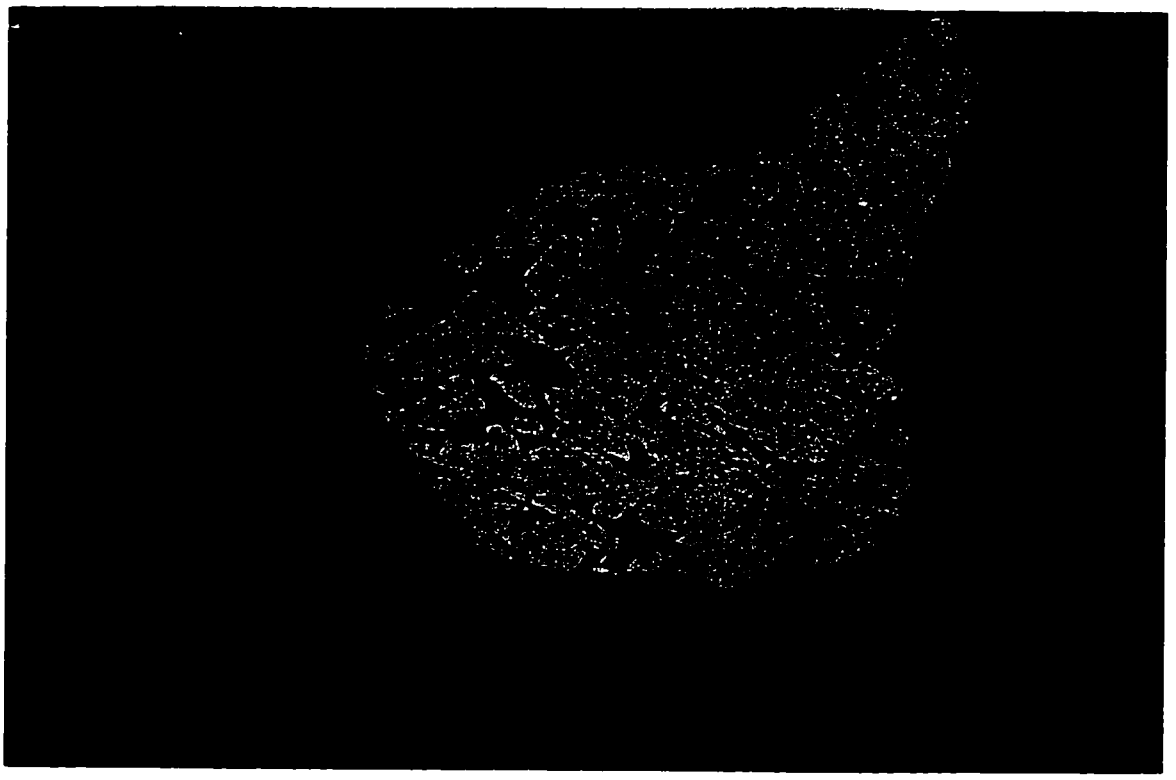

Plate 3.7a. (facing page, top)

Microphotograph of metagabbro containing trace ilmenite (Ilm) containing lesser rutile (Rt). Rutile appears to be due to high temperature deuteric oxidation of ilmenite (sample PWN 50.1, field of view = 0.96 mm, reflected light).

Plate 3.7b. (facing page, bottom)

A backscatter SEM image of a metagabbro containing an ilmenite grain (mid-grey) partially replaced by a mottled to graphic appearing texture of rutile (mid-dark grey) that is surrounded by hematite (light grey).The proportions of each phase in the composite grain that is photographed are calculated to be 33.7% rutile, 32.6% ilmenite, and 33.7% hematite. Raster analysis of a digital image of the mottled portion of this grain was used for the calculation. The grain is bounded to the left by a large area of silicate (dark grey). This metagabbro contains an advanced stage of high temperature oxidation (sample PWN 053)..

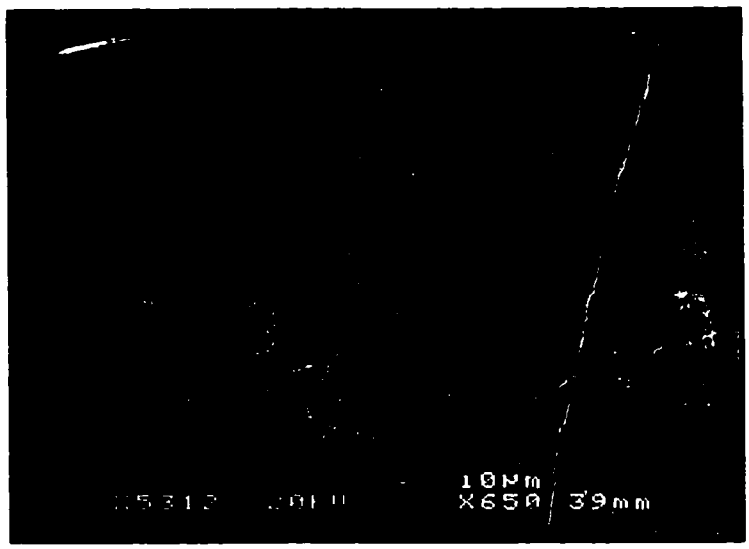
10Nm
X650 39mm

Plate 3.8a. (facing page, top)

Protoamphibolite containing Ilmenite (Ilm) with thin exsolution lamellae of hematite (Hem), and more irregular exsolution of magnetite (Mag).The darker lenses have been found to be titanite (Ttn). Pyrite (Py) and chalcopyrite (Ccp) occur marginally. (sample PWN118.1, field of view = 0.96 mm, reflected light).

Plate 3.8b. (facing page, bottom)

Na-enriched amphibolite: Hematite (Hem) exsolution as the dominant phase in a grain of ilmenite (Ilm) The amount of hematite varies but point counting indicates an average of 45% of the ilmenite. Some grains contain areas of rutile as well, this was not factored into the point count but makes up about 20% of the composite grains. All of the composite grains are rimmed by titanite (Ttn). A single discrete ragged magnetite grain occurs it is not rimmed by titanite The oxidation appears to be related to Na-enrichment observed in the sample. (sample PWN 065, field of view = 0.48, reflected light).

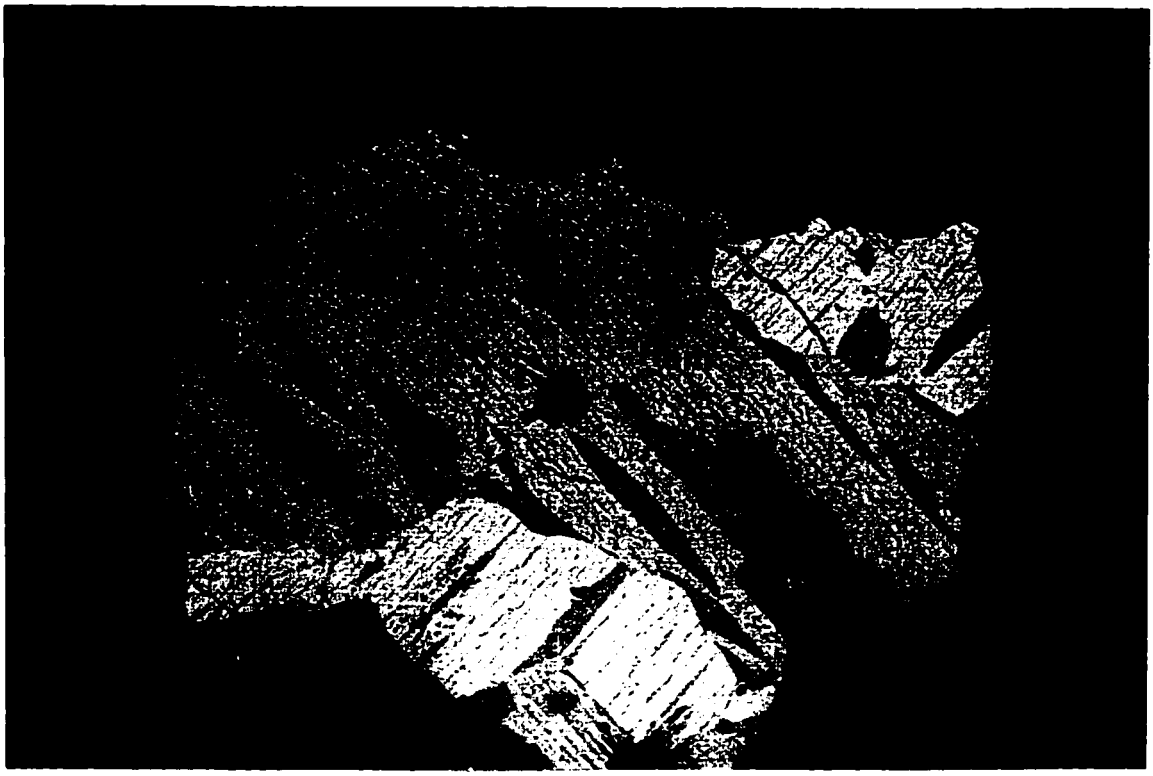

Plate 3.9a. (facing page, top)

Mineralized metasediment from the Skuterud mine, the low relief colourless mineral is quartz (Qtz) occurring as irregular equant grains about 0.2 mm across. The knot of muscovite (Ms) appears to be a replacement of a sillimanite knot. The muscovite composition included in the microprobe results is an analysis of a similar knot in this section. Other minerals include rutile (Rt), tourmaline (Tur), unfoliated biotite (Bt); the sample is dominated by quartz and feldspar (sample PWN 012, field of view = 0.95 mm, uncrossed polars).

Plate 3.9b. (facing page, bottom)

Mineralized metasediment with pyrite (Py) possibly bearing some Co and Ni, and graphite (Gr). The size of the graphite indicates that it has recrystallized metamorphically. While the graphite is generally oriented along a foliation plane most flakes are bent. Pyrite growth appears to be postdate graphite, based on mineral relationships throughout the section (sample PWN 025, field of view = 0.49 mm, reflected light).


Bt
5


Py

3.4. Summary

This chapter in a broad way describes the petrology of samples of the main rock types under investigation which include the metagabbro and rocks derived from it. Some of the observations will be used in discussions within Chapter 5. Some of the important points from Chapter 3 are as follows.

(1a) The gabbros are altered to coronitic gabbros with hornblende that contains significant Cl; some metagabbros contain scapolite. (1b) The ilmenite of the metagabbros is oxidized during the formation of the metagabbro. (1c) The sulphides are mainly pyrite (secondary) but there is local pyrrhotite (primary?).

(2a) The amphibolites contain hornblende (amphibolite-grade): this hornblende also contains significant Cl. (2b) The oxides are dominated by ilmenite with some hematite and rutile: there are more oxides than in the metagabbros. (2c) Pyrite is the dominant sulphide: it is often associated with magnetite: there are generally more sulphides in the amphibolites than in the metagabbro.

(3a) Many of the moderately albitized amphibolites preserve hornblende (amphibolite-grade). Strongly albitized mafic rocks contain tremolite-actinolite ± epidote (upper greenschist facies): Cl contents are moderate in the volatile hosting minerals. (3b) The albitized rocks generally contain rutile, and may contain hematite and titanite. (3c) Sulphides are not common in the albitized rocks, pyrite occurs rarely.

(4a) The calcite-rich metasomatic rocks locally contain metasomatized country-rock fragments with significant Na-enrichment. (4b) Hematite and pyrite occur together, in veins and in the fragments.

CHAPTER 4. GEOCHEMISTRY

This chapter is based on whole rock data listed in Appendix 3. The rock types considered in this chapter are metagabbro, amphibolite, albitite and Skuterud ore type. This chapter has the following main objectives.

1. The metagabbro samples are described to better understand the tectonic environment where these mafic rocks were generated and emplaced.
2. The amphibolites are compared to the metagabbro samples to understand the chemical changes related to amphibolitization.
3. The characteristics Skuterud-ore-bearing rocks are described.
4. The character of strongly albitized samples is examined and in general compared to the amphibolite and metagabbro source rocks.
5. The concentration of gold in the rocks is examined, mobility of gold in the rocks is discussed here and in Chapter 5.

X-Y scatter diagrams and rare earth element plots are presented here to graphically describe the dataset. Observations from the scatter diagrams are related to mineralogical and petrolocical observations. Some discrimination diagrams are used to describe the gabbro and the tectonic environment of emplacement is predicted. To compare the amphibolites to the metagabbro samples a graphical variant (Grant, 1986) of the mass balance method of Gresens (1968) is used. Some stable isotope data are presented for graphite in the metasediments, and pyrite and calcite in the calcite dominated metasomatic rocks.

Samples listed in Table 4.1 have been determined to be metagabbro , amphibolites or albitized mafic rocks on petrological and mineralocgical grounds as described in Chapter 3 (and summarized below). The samples considered to be mineralized are classified as such based on elevated Co and Cu concentration. The four metagabbro samples (Table 4.1) all contain igneous laths of plagioclase, recrystallized plagioclase, relict (secondary)

Table 4.1. Representative samples (used for geochemistry): locations and mineral assemblages; see also Appendix 1

Sample	Rock type	Sample location	Py	Ccp	Po	Ilm	Mag	Hem	Rt	Ttn	Cal	Cam	Pl	Qtz	Bt	Kfs	Ms	Sil	Scp	Other minerals
	METAGABBRO SAMPLES																			
PWN 50	metagabbro	South of Overbykollen-from behind houses in Bingås area	y	n	y	y	y		y	n	n	Hbl	y	n	n	n	n	n	n	Opx, Ol?
PWN 51	scapolized-metagabbro	South of Overbykollen-from behind houses in Bingås area	y	y	n	y	n	n	y	y	n	Hbl	y	n	y	n	y	n	y	Opx
PWN 53	metagabbro	Block, from behind houses in Bingås area	y	n	n	y	n	y	y	n	n	Hbl	y	n	y	n	n	n	y	Opx
PWN 120	metagabbro	Road cut at Knatten, about 200 m south of the Snarum bridge	y	y	y	y	n	n	n	n	y	Hbl	y	n	n	n	n	n	n	Grt, Srp, tr Ep
	AMPHIBOLITE SAMPLES																			
PWN 2	Hbl-Bt gneissic amphibolite	Amphibolite unit 100m east of Mellemgrube (at Skuterud)	y	y	n	y	n	n	n	n	n	Hbl	y	n	y	n	n	n	y	
PWN 17	gneissic amphibolite	East of Butjern lake, this sample from amphibolite bluff	y	n	y	y	n	y	n	n	n	Hbl	y	n	y	n	n	n	?	tr Srp, Ep?
PWN 42 1	proto-amphibolite	Overbykollen road,nw from 041-beyond the intersection	y	y	y	y	n	n	n	n	n	Hbl	y	n	n	n	n	n	n	
PWN 42 2	proto-amphibolite	Overbykollen roadnw from 041-beyond the intersection	y	y	y	y	n	n	n	n	n	Hbl	y	n	n	n	n	n	n	
PWN 42 3	proto-amphibolite	Overbykollen road, nw from 041-beyond the intersection	y	n	n	y	n	y	n	n	n	Hbl	y	n	y	n	y	n	n	
PWN 61	equigranular amphibolite	310m on traverse east from Butjern lake	y	y	n	y	y	n	y	n	n	Hbl	y	n	y	n	n	n	n	
PWN 67	scapolitized proto-amphibolite	410m on traverse east from Butjern lake	y	n	n	y	y	y	n	n	n	Hbl	n	n	y	n	n	n	y	
PWN 80 2	proto-amphibolite	From a traverse SW of Søndregrube		n	n	y	n	n	n	n	n	Hbl	y	n	y	n	n	n	n	Ap
PWN 90	equigranular amphibolite	Magnesite quarry, on o/c SE and above quarry	n	n	n	y	n	n	n	n	n	Hbl	y	n	y	n	n	n	n	Ap
PWN 102 1	equigranular amphibolite	On hill NW of Søndregrube(Skuterud)	y	n	n	y	n	y	y	n	n	Hbl	y	n	y	?	n	n	?	
PWN 118 2	proto-amphibolite	At Knatten, from slope near bridge	y	y	y	y	?	y	n	n	n	Hbl	y	n	n	n	n	n	n	Opx?
PWN 119	gneissic amphibolite	At Knatten 100m south of bridge,	y	y	n	y	n	n	n	n	n	Hbl	y	n	n	n	n	n	n	Grt
PWN 121	gneissic amphibolite	About 400 m south of 120 on road	y	n	n	y	n	n	n	n	n	Hbl	y	y	y	n	n	n	n	Ap
PWN 122	gneissic amphibolite	Knatten bridge										Hbl								
	ALBITIZED MAFIC SAMPLES																			
PWN 40	Act-Ab gneiss	Overbykollen on road, 30m nw of 039	n	n	n	n	n	y	n	n	n	Act	y	n	n	n	n	n	n	
PWN 47	albitite	Overbykollen road sw of quarry	y	n	n	n	n	n	y	n	n	Tr	y	y	n	?	n	n	n	Ap, Tc
PWN 52	Act-albitite	South of Overbykollen-from behind houses in Bingås	n	n	n	y	n	y	y	y	n	Act	y	n	n	n	n	n	?	
PWN 65	Na-enriched-proto-amphibolite	410m on traverse east from Butjern lake	n	n	n	y	y	y	y	y	n	Act	y	n	n	?	n	n	y	
PWN 66	Na-enriched-proto-amphibolite	410m on traverse east from Butjern lake	n	n	n	n	?	y	y	y	y	Tr	y	y	y	n	n	n	n	Chl
PWN 69	Na-enriched amphibolite	Around separate Skuterud pit (to the north), 30m west of 068	n	n	n	n	n	y	y	y	n	Hbl	y	n	n	n	n	n	y	
PWN 73 1	Ab-Chl-Rt-Gr-Bt-Ms-Tur schist	Around separate Skuterud pit (to the north), west side of pit	y	y	n	n	n	n	y	y	y	n	y	y	y	n	y	n	n	Tur, Chl, Gr
PWN 110	albitite	On dirt road, 100m south of magnesite quarry road	n	n	n	n	n	n	y	y	n	Act	y	n	y	n	n	n	n	
PWN 111	albitite	About 50 m nnw of Overbykollen quarry	n	n	n	n	n	n	n	y	y	Act	y	y	n	n	n	n	n	Zm?, Chl
PWN 113	albitite	About 50 m nnw of Overbykollen quarry, 200m se of PWN 111	y	n	n	n	y	n	y	n	y	Act	y	n	n	n	n	n	n	Chl
	MINERALIZED SAMPLES																			
PWN 5	Qtz-Ms-sulphide schist	100 m east of the north end of Mellemgrube, Skuterud	y	y	y	n	n	y	n	n	n	n	n	y	n	y	y	n	n	Chl
PWN 7	Qtz-Bt-Ms-Gr-Rt schist	100 m northeast of the north end of Mellemgrube, Skuterud	y	y	y	n	n	n	n	n	n	n	y	y	y	y	y	n	n	Gr
PWN 9	Ab-Bt-Ms-Chl schist	Near north end of an open pit at the south end of Skuterud	y	y	n	n	n	n	y	n	n	n	y	y	y	y	y	n	n	Ap,xenotime,Mnz,Chl
PWN 10	Qtz-Ms-Sil quartzite	Along northwest margin of the Søndregrube pit, Skuterud	y	y	n	y	n	n	n	n	n	n	y	y	n	y	y	y	n	Col, skutterudite, Chl
PWN 12	Ms-Sil-Tur-Bt gneiss	Along northeast margin of the Søndregrube pit, Skuterud	y	y	n	n	n	n	y	y	n	n	n	y	y	n	y	y	n	Tur, Chl
PWN 14	Qtz-Bt-Ms schist	East side of middle pit, Skuterud	y	y										y	y		y	?		
PWN 15	Bt-Ms quartzite	NE side of central pit, Skuterud	y	n	n	n	n	n	n	n	n	n	n	y	y	y	y	n	n	Chl
PWN 25	Bt-Tur-Sil-Py-Gr schist	Forhngenes stoll, Skuterud	y	y	y	y	n	n	n	n	n	n	n	y	y	n	n	y	n	Tur, Chl
PWN 71	Act-Ab-Qtz-Ep-Py gneiss	Around separate pit (to the north), waste rock pile, Skuterud	y	y	n	n	n	n	n	n	n	Hbl	y	y	n	y	n	n	n	Co-rich Py, Ep

Notes on some locations Bingås is is about 1 km south of Overbykollen (the metagabbro body is marked on Figure 3.1). The Magnesite quarry referred to is located just to the south of the map and about half way across the mapped body

orthopyroxene, uralitic amphibole, minor ilmenite, rutile, and trace pyrite. Some of the metagabbro samples contain garnet, scapolite; minor amounts of relict clinopyroxene, relict olivine, biotite; and trace amounts of gedrite, pyrrhotite, magnetite and hematite. The presence of uralitic amphibole and relict pyroxene and olivine are the characteristic features of this rock type that were used to distinguish this group.

The gabbroic intrusions, of which metagabbro may be preserved in the core, were extensively amphibolitized. The assemblage observed in the amphibolites consists of the major minerals hornblende, plagioclase, and in a few samples, scapolite and the minor minerals pyrite, ilmenite and apatite. In some samples minor or trace garnet, biotite, rutile, and hematite are observed. Plagioclase may occur as relict igneous laths or finer recrystallized equant grains. The hornblende is fine to medium grained but not uralitic. None of the samples considered amphibolites have significant Skuterud ore mineralization or distinct albitization.

Samples with select metals above background levels are included in Table 4.2. Of these samples only samples from the pits or the vicinity of the Skuterud mine are classified as "mineralized" rocks and also termed "Skuterud ore" (Table 4.1). The typical host rock for mineralization is muscovite-sillimanite-tourmaline-biotite ± quartzite and rarely amphibolite (PWN 071); this mineralogy is also observed by other workers (e.g. Gammon, 1966). The samples all come from within 10 m of the pits of the Skuterud mine including the extreme northern Skuterud pit. There is a spatial relationship between the Fe-sulphide-bearing fahlbands and Skuterud ore mineralization (e.g. Gammon, 1966). In the continuation of the fahlbands north and south from the mine Co mineralization has not been observed (Gammon, 1966; Hygen, 1971). Most samples in this study with Skuterud ore mineralization are contained within fahlband zones. Unmineralized metasediments with or without fahlbands were not well sampled during this study.

As can be seen in Table 4.2, some of the moderately mineralized samples have not been included in the group of Skuterud ore samples. Some amphibolites enriched in Cu have not been included, the lack of As or Co enrichment suggests that this is related to a separate process. Sample PWN 016.1 is a very heterogeneous sample that is not typical of the mineralization and the geochemistry for the sample may include unrepresentative wall rock material. PWN 073.1 is an albitized mineralized metasedimentary sample, it has arbitrarily been included with the albitized samples though it could be in the mineralized group.

The samples of albitized rock are characterized by a metasomatic enrichment in albite. Albite-rich rocks (albitites) from the area have previously been found to contain 5-7% Na_2O (Munz et al., 1994), in this study concentrations of up to 9% Na_2O are observed: pure albite contains about 11.4 wt.% Na_2O. The concentration of 5% Na_2O is an arbitrary lower limit defined for albitized rocks. With the exception of PWN 073.1 (5.99% Na_2O) (a metasediment), albitized mafic rocks contain amphiboles. The presence of mafic rocks bordering the albitized rock is also evidence supporting a mafic source.

The scatter plots include a number of unclassified samples, that are outside the above classification. The unclassified samples include unmineralized or weakly mineralized metasedimentary rocks, serpentinites, carbonate-altered samples, cordierite-orthoamphibole schists, weakly albitized rocks, and micaceous zones derived mainly from the mafic intrusive rocks.

4.1. Geochemical results, (X-Y) plots of all samples

Harker variation diagrams of igneous rocks typically have SiO_2 or MgO for the X-axis plotted against other elements (e.g. Cox et al., 1979), this is to describe changes associated with magmatic evolution. This study, however, investigates metamorphic and metasomatic changes in rocks. The aim was to find an element for the X-axis that separates the important rock types. Na_2O was chosen because each rock type plots in a distinct range of Na_2O concentration, and Na_2O is key in the albitization process.

The igneous chemical character of the gabbro is interpreted to be preserved in the metagabbro in which the igneous olivine, clinopyroxene and orthopyroxene are mainly replaced by uralitic amphibole. The uralitic amphiboles preserve concentrations that are similar to the igneous mafic minerals; for example high Ni and MgO contents (Appendix 2) that are reflective of concentrations in olivine. The concentrations of MgO and Ni are higher and FeO is lower in the uralitic amphibole compared with the amphibole of the amphibolite:

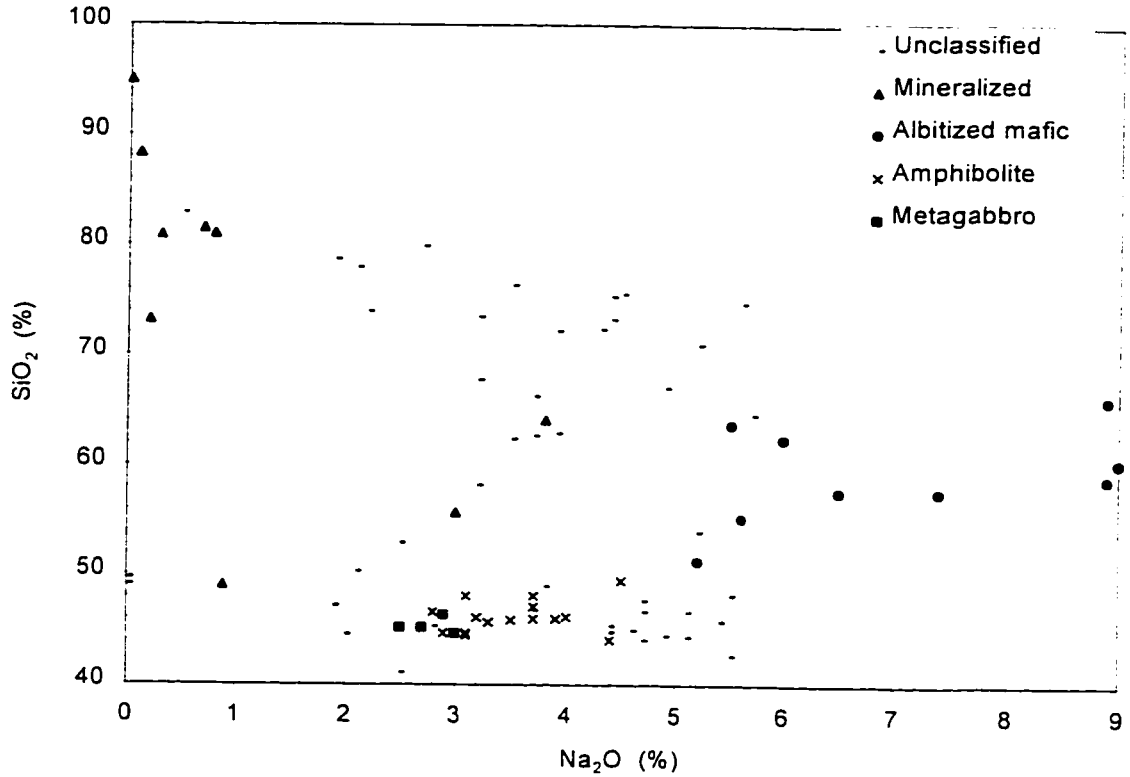

Figure 4.1. Plot of SiO_2 vs. Na_2O for all samples. SiO_2 concentrations are highest for the low Na_2O mineralized metasediments, though these show considerable variation related to different quartz contents. There is considerable range in SiO_2 at most Na_2O concentrations. The general decrease in maximum Na_2O with increasing SiO_2 is at least partially related to dilution by SiO_2. The albitized rocks approach SiO_2 concentrations of pure albite (68% SiO_2) with lesser concentrations of SiO_2. An increase in SiO_2 accompanies the increase in Na_2O with albitization of the mafic rocks. There is no change in SiO_2 with amphibolitization, an increase would be expected if the amphibolites represented more fractionated igneous rocks.

this mirrors changes in whole rock composition.

4.1.1. Sodium

Na_2O is used for the X-axis of the plot (Figures 4.1 - 4.8, 4.10 - 4.12 and 4.15). Most of the mineralized samples have Na_2O concentrations of less than 1%. The exceptions to this are samples PWN 007 (3.0% Na_2O), an albitized (?) micaceous schist that is visually estimated to contain about 30% strongly altered plagioclase, and PWN 071 (3.8% Na_2O) that is estimated to contain about 70% actinolite and 30% albite. Few unmineralized, unaltered

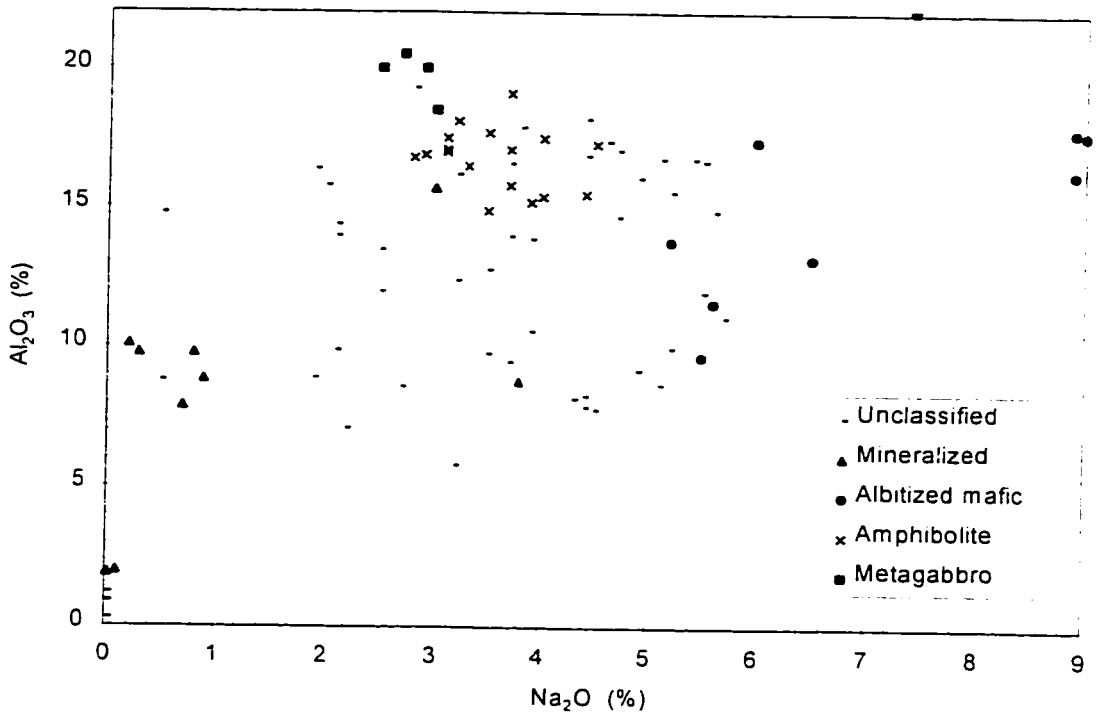

Figure 4.2. Plot of Al_2O_3 vs. Na_2O for all samples. There is a clear decrease in the average Al_2O_3 concentration from the metagabbro samples to the amphibolites. Lower Al concentrations are measured in the hornblendes of the amphibolites than in uralitic hornblendes of the metagabbro samples. Most mineralized rocks have low Al_2O_3, they are quartzites and have low abundance of Al-bearing minerals. The albitized samples contain a variable amount of Al_2O_3, but the concentration approaches that of pure albite (19.5% Al_2O_3 at 11.3% Na_2O).

metasediments were collected, metasediments (?) PWN 060 and PWN 098 contain 1.9 and 2.2% Na_2O respectively. Without metasediments that are clearly unaffected by the Skuterud mineralizing event it is not possible to describe chemical changes related to mineralization. The unclassified samples with low SiO_2 and Na_2O are serpentine and magnesite-rich samples (PWN 087.1, 087.2 and 087.3). PWN 073.1 is the metasediment with the highest concentration of Na_2O at 5.99 %, the other albitized rocks appear to have a mafic protolith

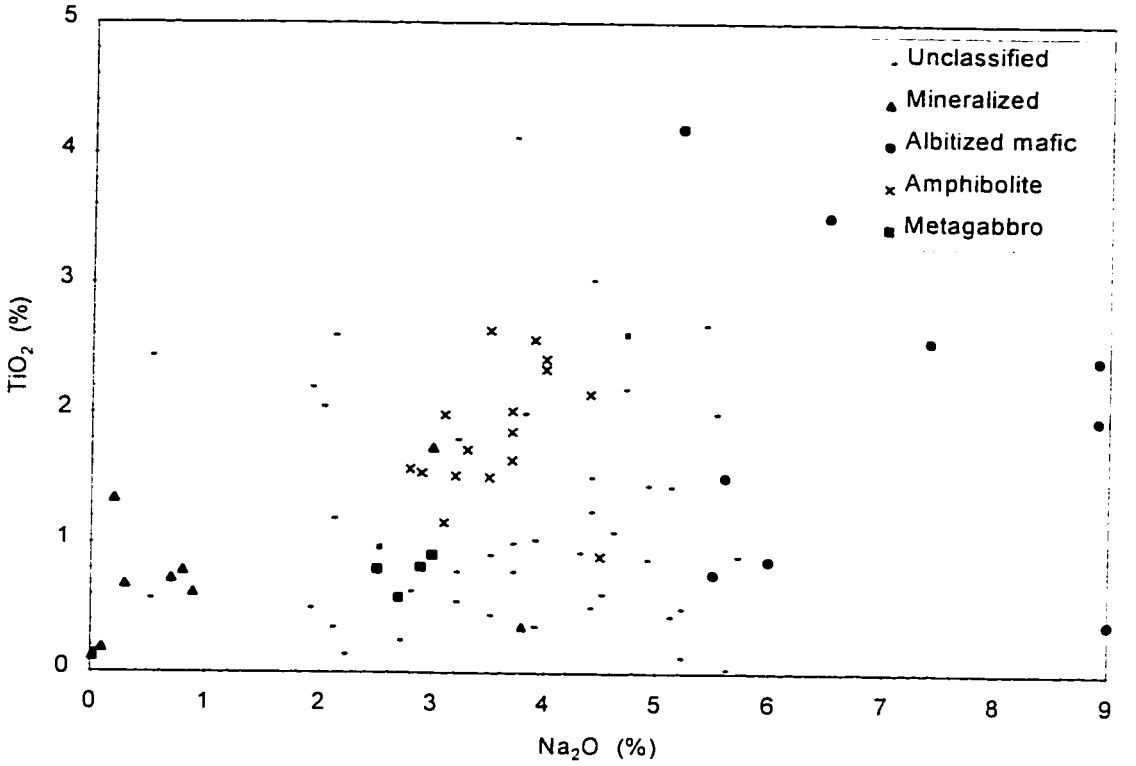

Figure 4.3. Plot of TiO_2 vs. Na_2O for all samples. TiO_2 concentration increases strongly from the metagabbro to the amphibolite. There is a large range in concentrations of TiO_2 the amphibolites and especially in the albitized rocks. The concentration of TiO_2 is low in the mineralized samples. In the mineralized and the albitized samples Ti occurs mainly in rutile. In the metagabbroic rocks and the amphibolites Ti occurs mainly in hornblende, ilmenite and rutile. The Ti contents of hornblendes in the amphiboles is higher than the metagabbro samples. The variation in Ti content in different rocks is largely observed as variations in oxide content.

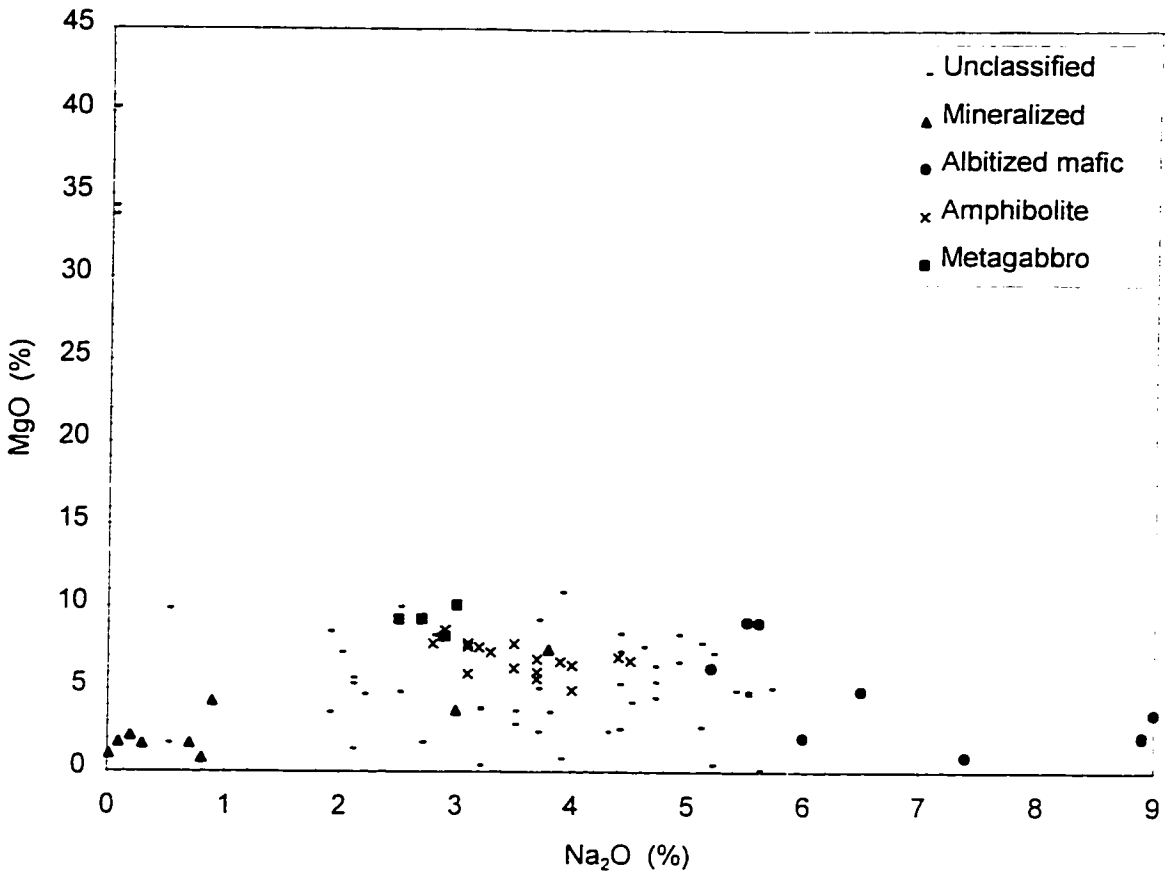

Figure 4.4. Plot of MgO vs. Na_2O for all samples. The concentration of MgO is, as expected, very high in the magnesite-serpentinite samples (unclassified, $Na_2O < 0.1\%$). The MgO concentration of the metagabbro samples show little variation, with an average of 9.2% MgO. The range in MgO from hyperites from the Bamble sector is large (3 - 25%) (de Haas, 1992). The MgO concentration is also lower for a metagabbro from the Øverbykollen (6.63 %) area as reported by Munz et al. (1994). These rocks are olivine cumulates and thus MgO is affected by fractionation of olivine. The concentration is lower in the amphibolites and the variability is only slightly higher than the metagabbro samples. The lower concentration of MgO and Ni in the amphibolites may relate to fractionation of these minerals into olivine or mobility during metamorphism; this will be discussed later. The albitized samples have a large range with concentrations similar to the samples with lower Na_2O contents. Samples with the highest Na_2O contents have marginally lower concentrations of MgO; due to dilution effects with increasing albite concentration. The sensitivity of MgO to early fractionation of olivine or orthopyroxene likely contribute to the variability of this element in the metagabbro samples of this period.

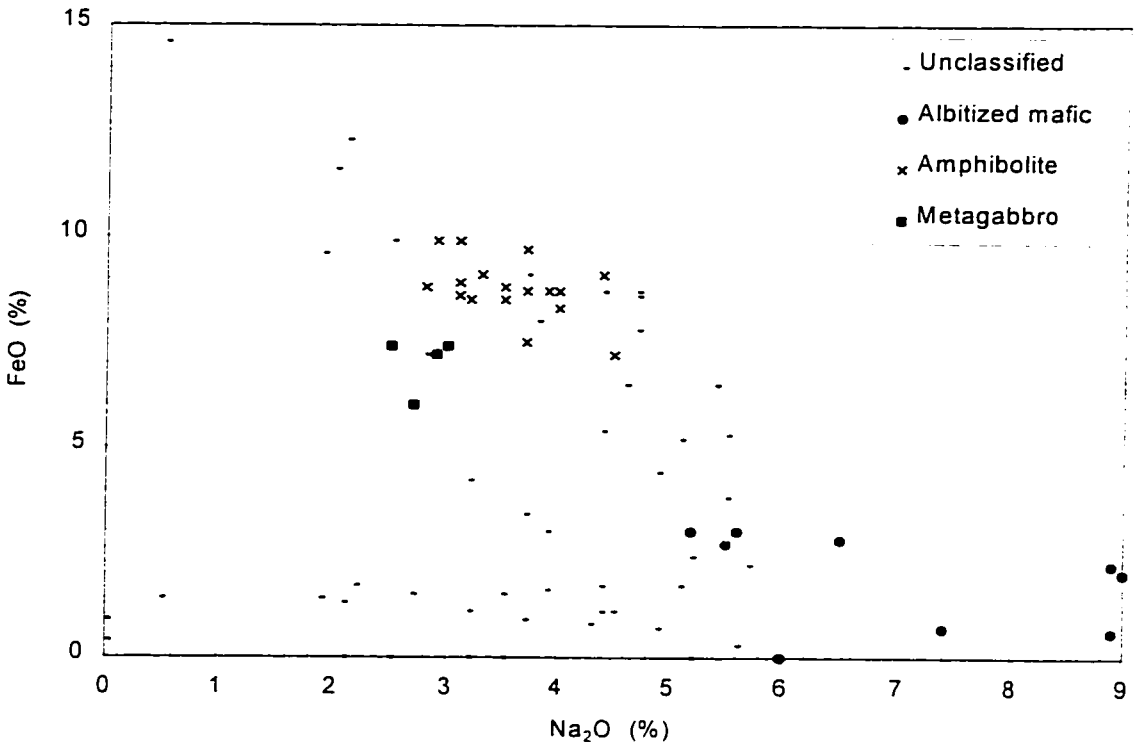
15
10
5
0
FeO (%)
0
1
2
3
4
5
6
7
8
9
Na2O (%)
Unclassified
Albitized mafic
Amphibolite
Metagabbro

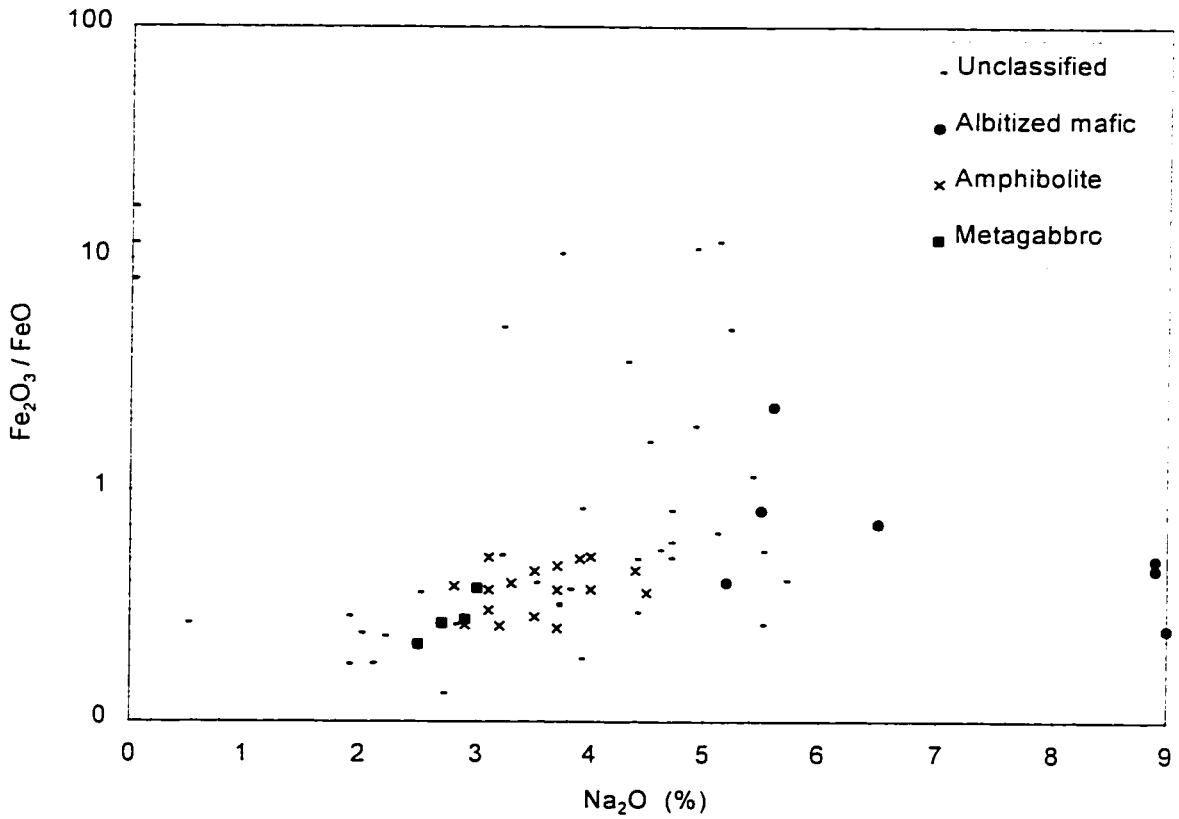
100
10
1
0
Fe2O3 / FeO
0
1
2
3
4
5
6
7
8
9
Na2O (%)
Unclassified
Albitized mafic
Amphibolite
Metagabbro

Figure 4.5 a, b (previous page). Plot of Fe vs. Na_2O for all samples. The Fe content was analyzed for both valences and reported as FeO and Fe_2O_3. Fe analysis of sulphide-rich samples was inaccurate and is not reported; accuracy is adversely affected by the Fe in sulphides. Most of the Fe in silicate minerals occurs as FeO. Fe_2O_3 occurs in oxides and silicates. There is an increase in concentration of Fe_2O_3 from metagabbro to amphibolite, this is also observed to a lesser extent for FeO. Metagabbro samples and the amphibolites show a limited range in Fe contents. The albitized rocks contain significantly less FeO than the mafic rocks. The amphiboles (actinolite-tremolite) of the albitites has a higher ratio of MgO/FeO (Appendix 2), this is also evident in the whole rock data. There is no trend of varying FeO within the group of albitites. The ratio of Fe_2O_3 / FeO indicates oxides are more common in the amphibolites than the metagabbro samples. The albitites show a large variation in this ratio. Hematite is observed in some of the albitized rocks, low concentrations of FeO in the albitized rocks make this ratio sensitive to small variations in the iron oxide content.

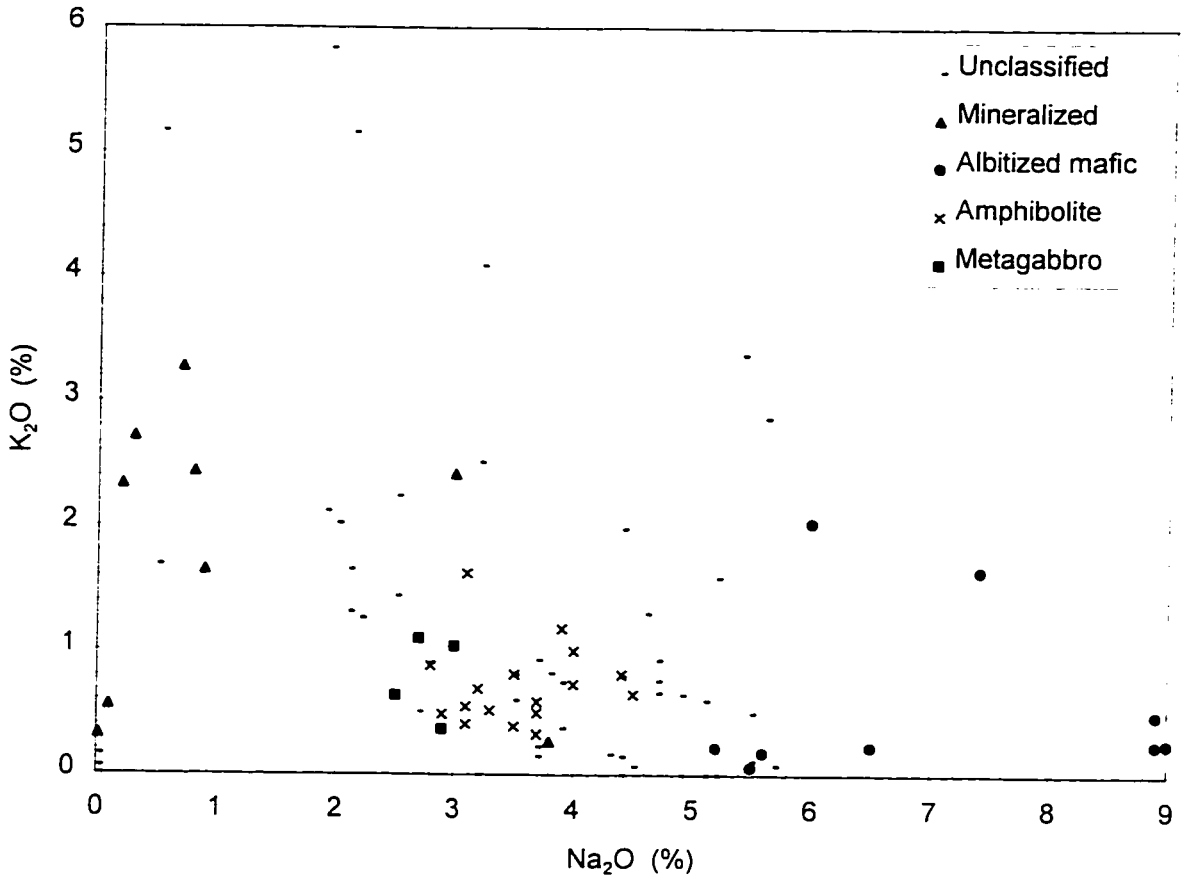

Figure 4.6. Plot of K_2O vs. Na_2O for all samples. There appears to be a general inversely proportional relationship between K_2O and Na_2O for all samples: related to the different mineralogical associations. The mineralized samples have a moderate variability in K_2O concentration and in general they are not as K_2O-rich as some other low Na_2O samples. This is expressed in low concentrations of K-feldspar and micas in the mineralized samples. Most of the albitized samples have low concentrations of K_2O. K_2O-bearing minerals such as biotite and K-feldspar are not preserved in albitized samples. Rb and Ba vary in a manner very similar to K_2O, for this reason only K_2O is plotted

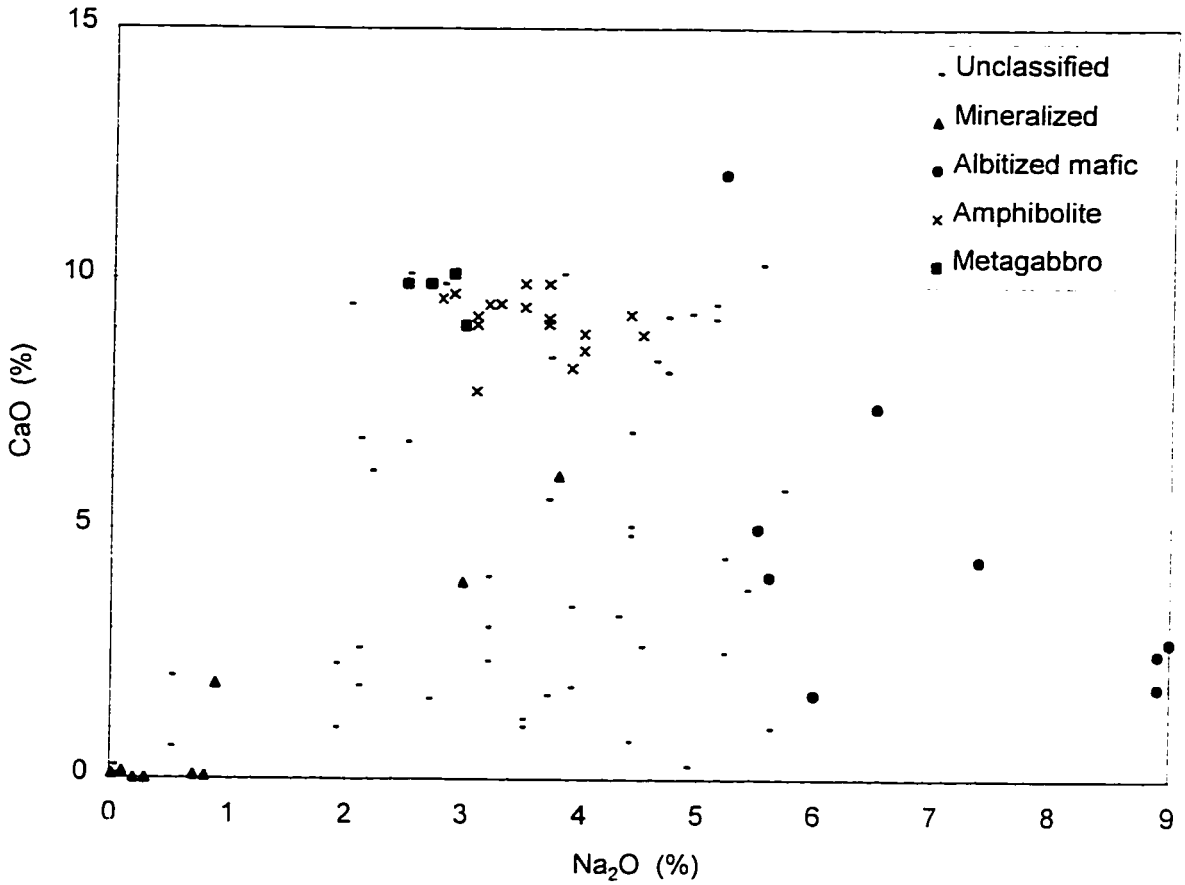

Figure 4.7. Plot of CaO vs. Na_2O for all samples. Similar concentrations of CaO are observed in metagabbro samples and amphibolites, with amphibolites slightly depleted. CaO in amphiboles appears similar for both rock types, the concentration in plagioclase of the amphibolites may be slightly less but this is not well documented (Appendix 2). Some of the samples rich in CaO contain calcite (e.g. PWN 028, 15.3% CaO). Albitized sample PWN 069 contains about 3% titanite and about 50% hornblende that contributes to a high concentration of CaO (12.10%). The concentration of CaO in the albitized rocks is lower at high Na_2O values, plagioclase from these rocks is almost pure albite (Appendix 2). There is good correlation between CaO and Sr, as Sr substitutes for Ca in minerals such as plagioclase.

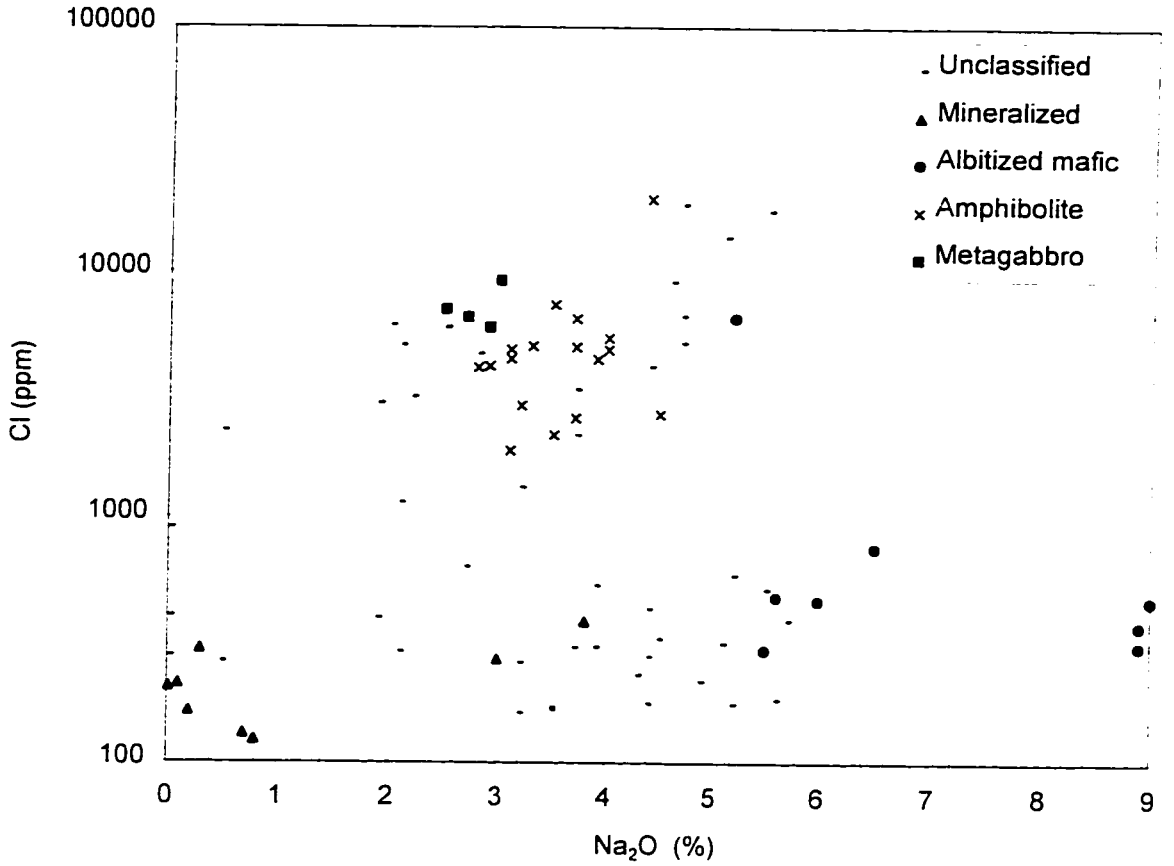

Figure 4.8. Plot of Cl vs. Na_2O for all samples. The metagabbro samples, amphibolites and mafic rocks of the unclassified group contain very high concentrations of Cl, from 1000 ppm to over 2%. Some of the most Cl-enriched samples have elevated concentrations of Na. The mineralized samples, including the mafic sample (PWN 071), contain values of Cl that are less than 1000 ppm, as do the albitized samples. The metagabbro samples contain significant uralitic hornblende with high concentrations of Cl in these rock types. Scapolite-bearing mafic rocks tend to have high Cl contents (e.g. PWN 067). The values recorded in the mafic rocks are well above typical concentrations of Cl in mafic rocks including other amphibolites from southern Norway. In amphibolitized hyperites from the Bamble sector, Cl is measured in concentrations of up to 3100 ppm and at an average of 1500 ppm, the gabbros average 300 ppm (Field and Elliott, 1974). A similar study of the 1500 Ma Värmland Hyperite suite reports average Cl concentrations of 169 ppm and 827 ppm for gabbros and amphibolites respectively.

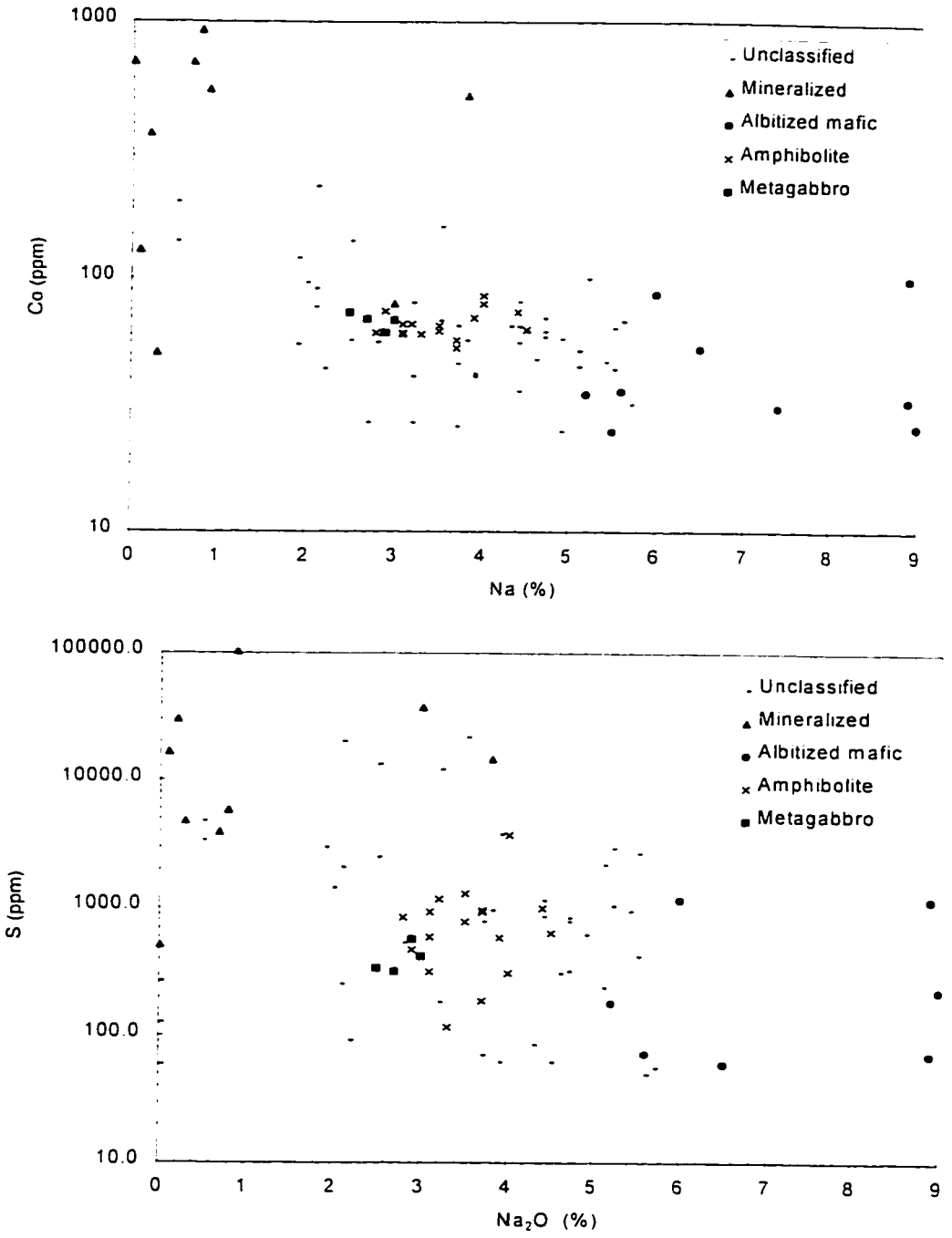

Figure 4.9 a. b. Plot of Co. S vs. Na_2O for all samples: see section 4.1.2 for description.

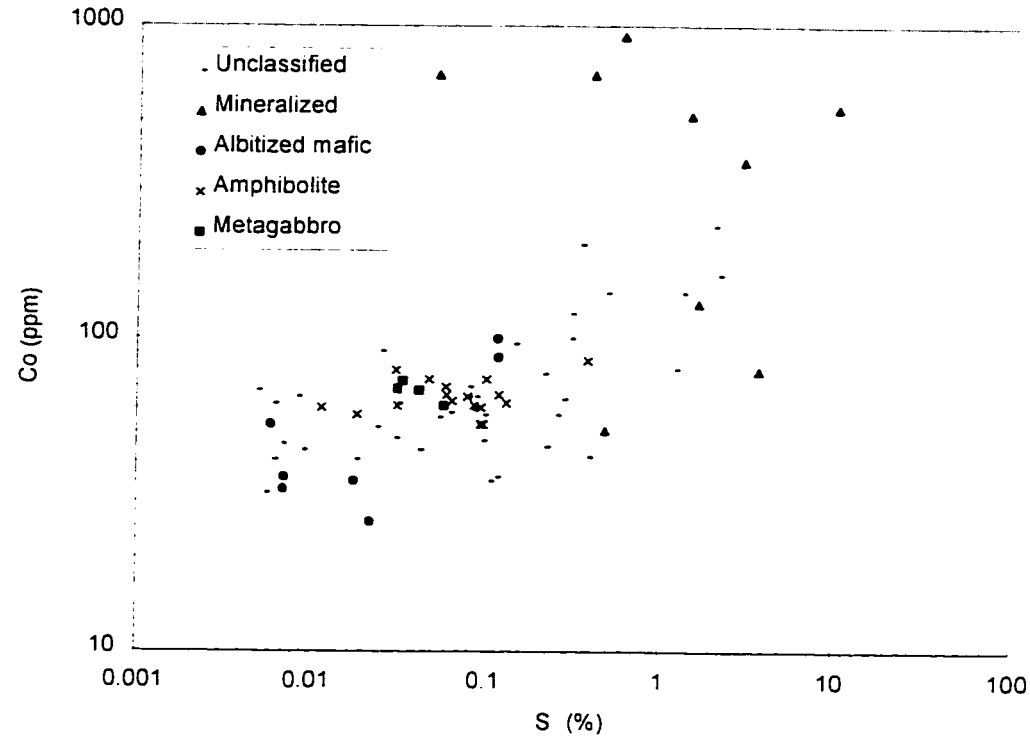

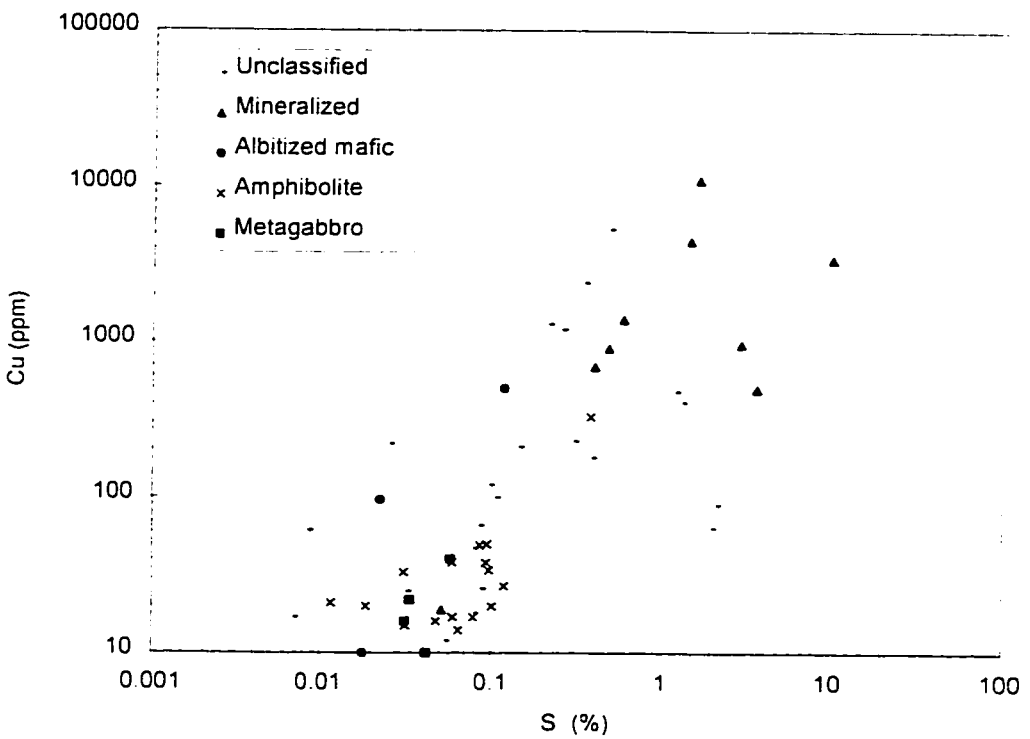

Figure 4.10 a, b. Plot of Cu, Co vs. S for all samples: see section 4.1.2 for description.

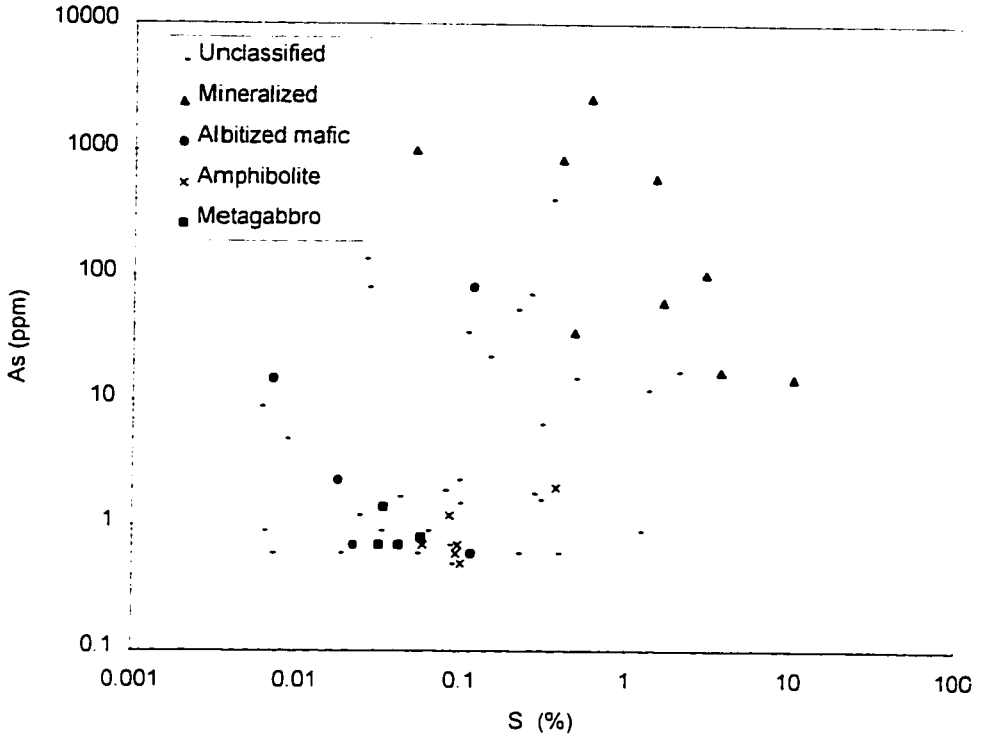

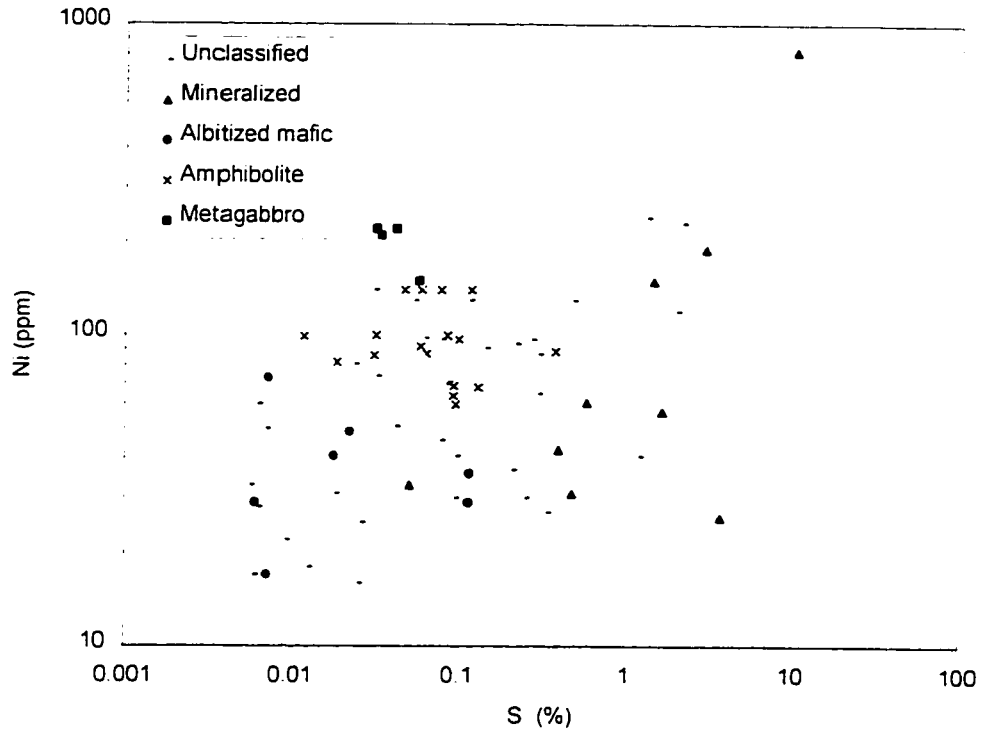

Figure 4.11 a. b. Plot of As. Ni vs. S for all samples: see section 4.1.2 for description.

based on the presence of actinolite and the field relationships, i.e. being in an area of mafic rocks. The intermediate range of Na_2O includes the metagabbroic rocks, amphibolites and most of the unclassified rocks. The unclassified rocks are altered amphibolites, gneisses, pegmatites, granitoids; many have uncertain alteration. The amphibolites have concentrations of Na_2O that are in general higher than those of the metagabbro samples.

4.1.2. Ore Metals (Cobalt, Arsenic, Copper, Nickel)

The Skuterud ore (mineralized samples) contain variably elevated concentrations of As, Co, Cu, S and slightly elevated Ni (Figures 4.13 and 4.14). During mining Co and As were extracted form the ore. The concentrations of Ni in the metagabbro samples are clearly higher than in the amphibolites. This is not observed for As, Cu or Co; and is due to the loss of olivine in which significant Ni occurs. Concentrations of Cu, Co, and Ni in the metagabbro are examined in Chapter 5 with respect to the possibility that an immiscible sulphide liquid was removed from the gabbro magma. Albitized samples have variably low S, Co, Ni, Cu, and As; this reflects low concentrations of sulphides in the albitized samples.

Enrichment of As correlates poorly with the S content in the Skuterud ore samples. A variable enrichment of As is observed for the mineralized samples. Notably, PWN 015 has a high As (1000 ppm) and Co (700 ppm) content (Table 4.2), while the S content is low (513 ppm). This relationship suggests the presence of an arsenide such as (Co, Ni)As_{2-3}. (skutterudite) This and two other similar samples indicate the mineralization is not always accompanied by Fe-sulphide. Moderate As enrichment is observed in a few of the albitized samples. The amount of pyrite present in fahlbands may also be significant in the amount of S relative to ore metal that is present.

4.1.3. Sulphur

There is enrichment of S in the pyrite of the fahlbands, and some samples with high concentrations of scapolite contain moderate enrichments of S. Most of the Skuterud ore

TABLE 4.2 SAMPLES CONTAINING "SKUTERUD ORE" TYPE ELEMENT ENRICHMENTS†.

Sample (PWN)	Rock type	Co (ppm)	Cu (ppm)	As (ppm)	Ni (ppm)	Au (ppb)	S (%)	U (ppm)
2	Hbl-Bt gneissic amphibolite	85	330	2	85	<2	0.37	0.8
3	Pl-Bt vein	42	180	0.6	5	<2	0.38	6
4	Pl-Kfs-Qtz-Bt vein	80	480	0.9	44	3	1.22	3.2
5*	Qtz-Ms-sulphide schist	130	11000	61.6	24	18	1.67	21.4
7*	Qtz-Ms-Bt-Gr schist	79	500	17	33	5	3.73	3.4
9*	Ab Qtz-Bt-Ms-Chl schist	930	1400	2600	47	42	0.58	6.4
10*	Ms-Sil quartzite	700	690	845	45	11	0.39	4
12*	Ms-Sil-Tur-Bt quartzite	370	970	103	180	8	3.01	5.6
14*	schist	51	910	35	41	2	0.48	5.1
15*	Bt-Ms quartzite	700	19	1000	41	<4	0.05	1.9
16.1	Mag-Py-Chl-Oam-Tlc? vein	230	64	17	110	11	2.03	1.1
18	Ccp-Bt-Cam amphibolite	140	5300	15	120	1100	0.48	1.3
19	Bt-Hbl-Qtz-Czo-Chl gneiss	120	230	6.4	79	<2	0.30	1.6
20.2	amphibolite, at albite vein	57	1200	70.1	5	25	0.25	1.2
21	amphibolite	77	1300	53.2	30	60	0.33	2.6
22	Ms-Tur-Sil quartzite	200	2400	404	20	29	0.34	3.5
23	amphibolite	96	210	22	75	<2	1.34	1.2
24	Ms-Tur-Bt schist	91	220	135	16	7	0.03	23.5
25*	Bt-Tur-Sil-Gr gneiss	550	3400	15	860	8	10.3	7.5
25.1	Bt-Tur-Sil-Gr gneiss	1600					7.27	
26	Mgs?-Cal-Hbl amphibolite	140	410	12	280	7	1.34	0.7
26.1	Mgs?-Cal-Hbl amphibolite	290					1.5	
37	Cal-Hem-Py-Ab-Tc vein	100	5	1.6	53	<2	0.30	<0.2
41	Tur-Ab-Hbl gneiss	57	120	1.5	39	<2	0.10	0.6
71*	Py-Qtz-Ep-Ab-Act gneiss	520	4500	600	130	56	1.5	2.9
73.1	Gr-Ms-Tur-Bt-Ab-Qtz schist	87	500	81.1	18	30	0.12	3.1
87.1	Mgs-Serpentinite	8	5	80.5	13	<2	0.03	0.4

* samples used as representative mineralized rocks for geochemical interpretations.

†Prerequisites Co>100 ppm, Cu>100 ppm, As>50 ppm or U>2 ppm.

The following samples are not from the Skuterud mine:

PWN 016 (1 km south of the mine), 026, 037, 041, and 087.1.

occur within fahlbands. Sulphur concentrations of the mineralized samples are mainly with pyrite related to the fahlbands, lesser amounts of S is associated with mineralized sulphides. The albitized samples contain less than 1000 ppm S, within the range of the other

unmineralized samples. There is a larger variance of S concentration in the amphibolites than the metagabbro samples. During metamorphism S is typically mobile, and appears to be during amphibolitization.

4.1.4. Gold concentrations in the rocks

The investigation of Au mobility during alteration of the gabbroic rocks is a major goal of this project. The INAA method that is used for most of the Au analyses has a minimum detection limit of 2 ppb. With the exception of the samples listed in Table 4.2 and some of the samples listed in Table 4.3, all samples are measured to contain less than the 2 ppb detection limit for Au. To describe concentrations below this detection limit the metagabbro samples, some amphibolites and albitized rocks were analyzed by XRAL Laboratories using a specialized preparation method and graphite furnace atomic absorption spectrometer (GFAAS) method that reports concentrations of Au to 0.1 ppb; the method is described in Appendix 3. The GFAAS Au results did not produce clear results (Table 4.3). It can be observed that there is significant differences between the repeat analyses for each sample (e.g. PWN 120 and 102.1) and between the blind duplicates (PWN 119 and 122). This may be due to heterogeneous Au concentrations in the sample powder, or poor analysis precision.

It is considered in the following calculations that the concentration of 8 ppb in amphibolite PWN 102.1 is an erroneous result; it may alternatively indicate that the heterogeneity of Au distribution requires more analyses for a more complete description of distribution. The average gold concentrations of Au in the GFAAS analyzed metagabbro samples and amphibolites (Table 4.3) are 0.84 and 0.41 ppb respectively. The statistical two-tailed t-test indicates that the averages are not significantly different at the 95% confidence level. The average of all GFAAS analyses is 0.58 ppb, the median is 0.4 ppb; the average 4.1 ppb Au based on 196 samples, with the lowest concentration observed concentration

TABLE 4.3 CONCENTRATION OF AU FOR SAMPLES ANALYZED BY INAA AND GFAAS EXCLUDING SAMPLES IN TABLE 4.2 AND SAMPLES REPORTED AS <2 PPB.

Sample		Rock type	Au concentration (ppb)			
			INAA	GFAAS-1	GFAAS-2	GFAAS-3
PWN	50	metagabbro	<2		0.2	
PWN	51	metagabbro	<2	0.3	1.8	
PWN	53	metagabbro	<2	0.5	0.8	
PWN	120	metagabbro	<2	0.7	2.0	0.4
PWN	20.1	amphibolite	4			
PWN	42.1	amphibolite	<2		0.2	
PWN	65	amphibolite	<2		0.4	
PWN	68	amphibolite	2			
PWN	100	amphibolite	<2		0.3	
PWN	102.1	amphibolite	<2	0.8	8.0	0.6
PWN	113	amphibolite	<2		0.4	
PWN	118.2	amphibolite	<2		0.4	
PWN	119	amphibolite	<2		0.2	
PWN	119(d)	amphibolite	<2		0.1	
PWN	121	amphibolite	<2		0.1	
PWN	122	amphibolite	<2		0.2	
PWN	122(d)	amphibolite	<2	1.9	1.2	
PWN	14	pegmatite	2			
PWN	28	Cal albitite	<2	0.5	0.6	
PWN	32	coarse Cal vein	3			
PWN	38	Act-Pl gneiss	<2		0.3	
PWN	52	Act albitite	<2		0.3	
PWN	87.2	Mgs-Srp rock	2			
PWN	88	Qtz-diorite	2			
PWN	98	albitite	<2	0.8	0.4	
PWN	99	Ab amphibolite	<2		0.4	

(d) = blind duplicate

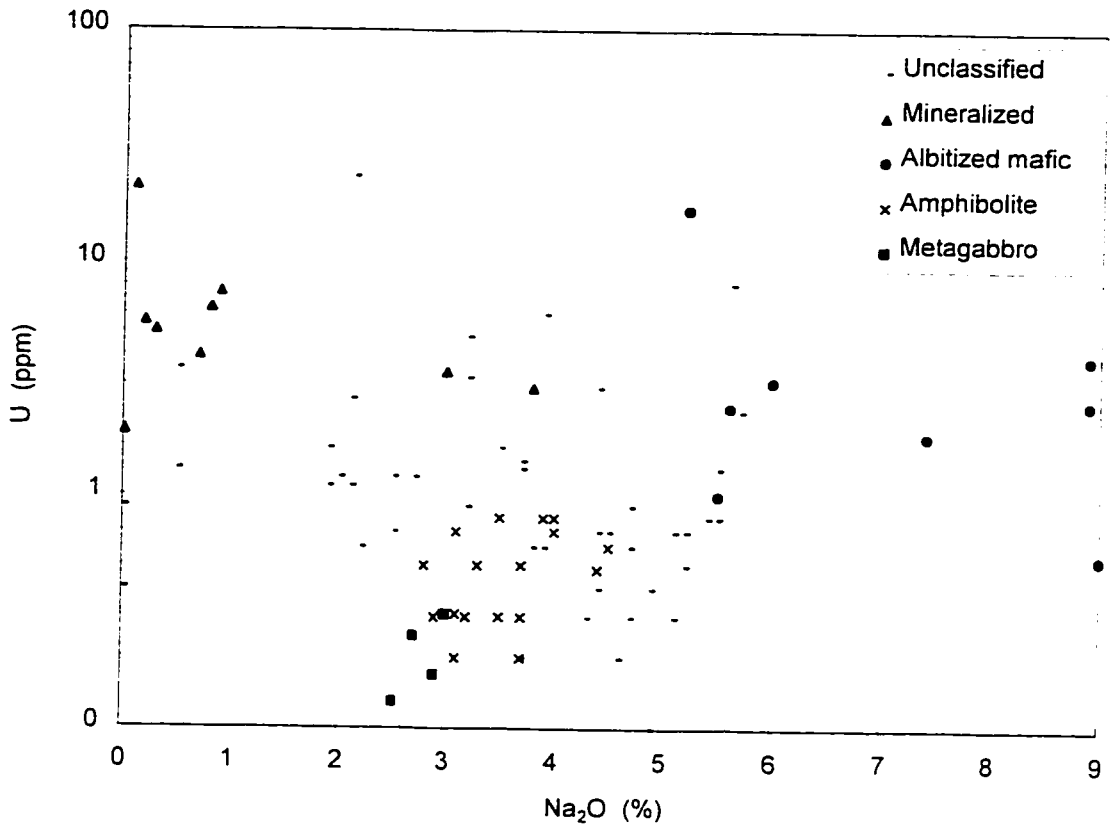

Figure 4.12. Plot of U vs. Na_2O for all samples .Some amphibolites contain higher concentrations of U relative to the metagabbro samples. The average concentration of U in the metagabbro samples is in the range of the average composition for basalts (0.75 ppm) (average of Turekian and Wedepohl, (1961) and Vinogradov (1962)). The albitites have concentrations of U that are in the similar or higher than those observed in granites (3 ppm) (Turekian and Wedepohl, 1961). An average concentration of U for sandstones is 0.45 ppm (Turekian and Wedepohl, 1961), in the mineralized samples of this study the average is close to 8 ppm. The highest concentration of U is observed in a sample of quartz-rich metasediment (unclassified) just at the contact with an amphibolite (PWN 024, Figure 4.13). The sample is mainly composed of the muscovite-tourmaline-sillimanite quartzite with lesser inclusions of metagabbro derived biotite schist, which is similar to sample PWN 018.

plus 2 standard deviations would be 1.62 ppb. The average including PWN 102.1 for amphibolites is 0.99 ppb and for all samples the average increases to 0.93 ppb.

Average values for the concentration of Au in gabbroic rocks have been estimated by various workers. Korobenikov (1986) measures Au concentrations that are on average

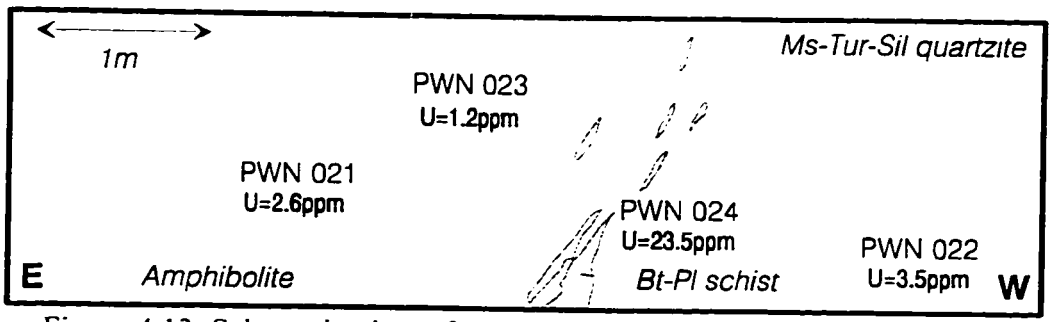

Figure 4.13. Schematic view of rock face in Forhaabningenes Stoll (southern adit of the central Mellemgrube pit). Skuterud mine with sample locations circled. The samples include PWN 024 which contains the highest concentrations of U found during the study, though it does contains only moderate enrichment in ore sulphides. Sample PWN 25 (U = 7.5 ppm) was collected from a 7m wide discrete zone of sulphide concentration 25 m to the west. The biotite-plagioclase schist (e.g. PWN 018) is interpreted to be an altered and sheared product of the amphibolite, a similar interpretation has been made in the past (Bugge, 1943).

3.1 ppb, based on 793 samples of intrusive gabbros, gabbro-diabases and gabbro-diorite of all ages. A study of Proterozoic greenschist-grade metagabbro samples found an average of being 2.3 ppb Au (Korobenikov, 1991). Boyle and Jonasson (1984) report an average composition of 4.1 ppb Au for mafic igneous rocks. The concentrations of Au observed in the mafic rocks of this study is well below the typical values observed in gabbroic rocks.

4.1.5. Association of Uranium and Skuterud Mineralization

Concentrations of U have been observed with Skuterud ore during a radiometric survey of the Modum area (van Autenboer, 1957). Quantitative radiometric analyses by van Autenboer (1957) reported concentrations of as much as 0.31% U (Forhaabningenes Stoll: southern open pit). A decrease in radioactivity with depth correlates with a decrease in Co mineralization with depth (Rosenqvist, 1949). The radioactive minerals are mainly uraninite in cubic crystals with some monazite (van Autenboer, 1957). Elevated concentrations are observed in and near Skuterud ore (Figure 4.12, 4.13).

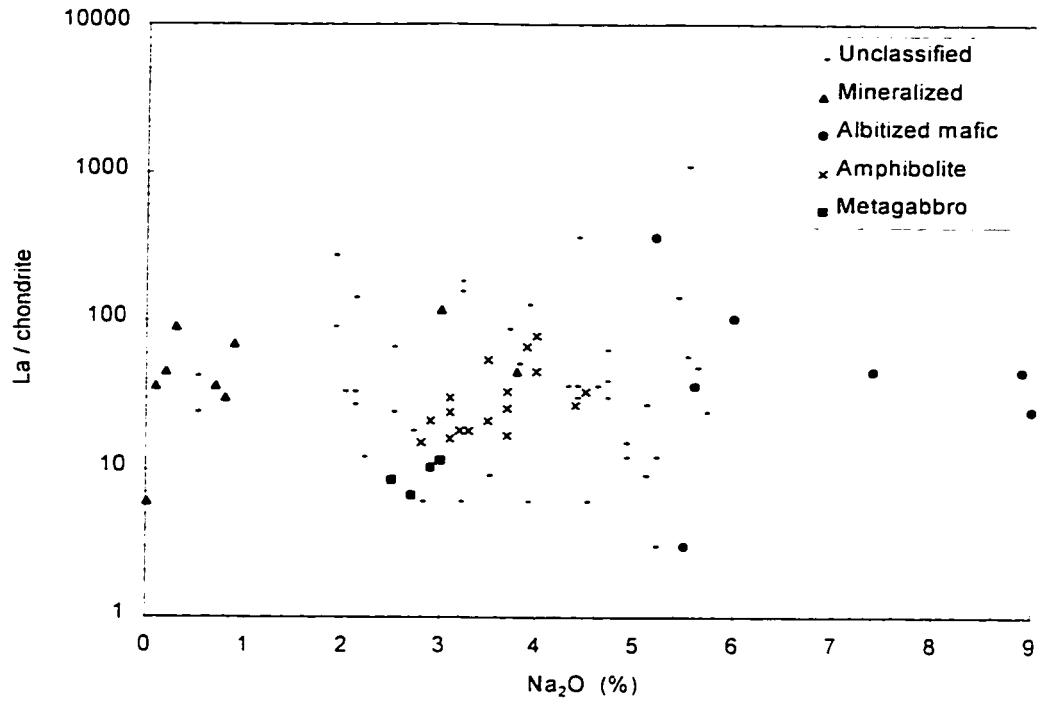

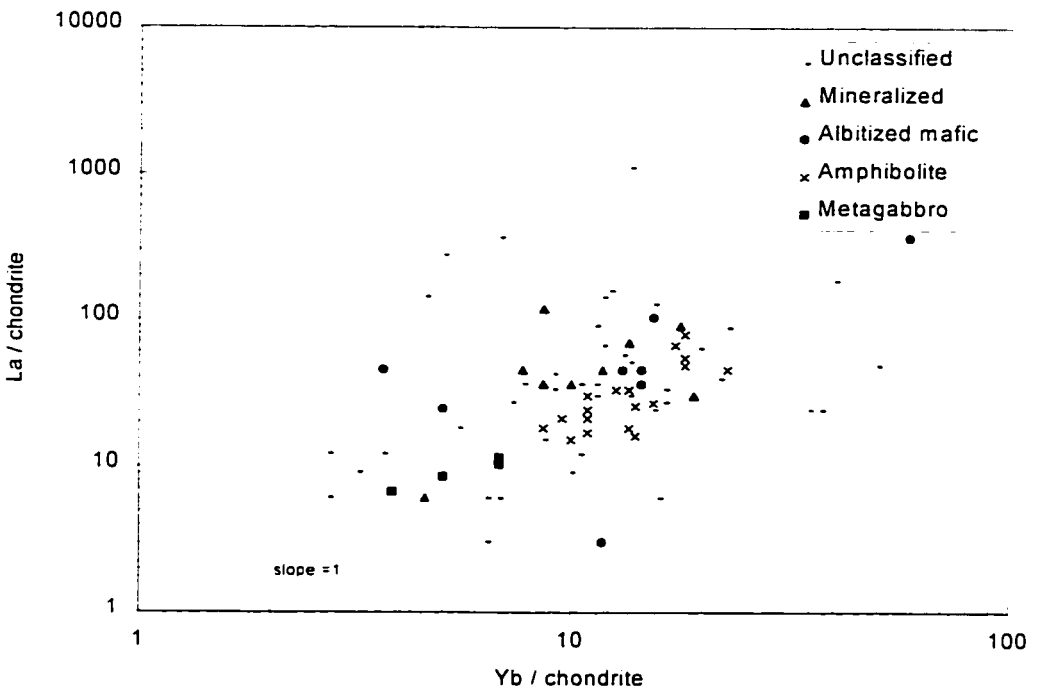

Figure 4.16 a, b. Plot of La vs. Na_2O and La vs. Yb for all samples normalized to chondrite (Sun, 1980). See section 4.1.6 for details.

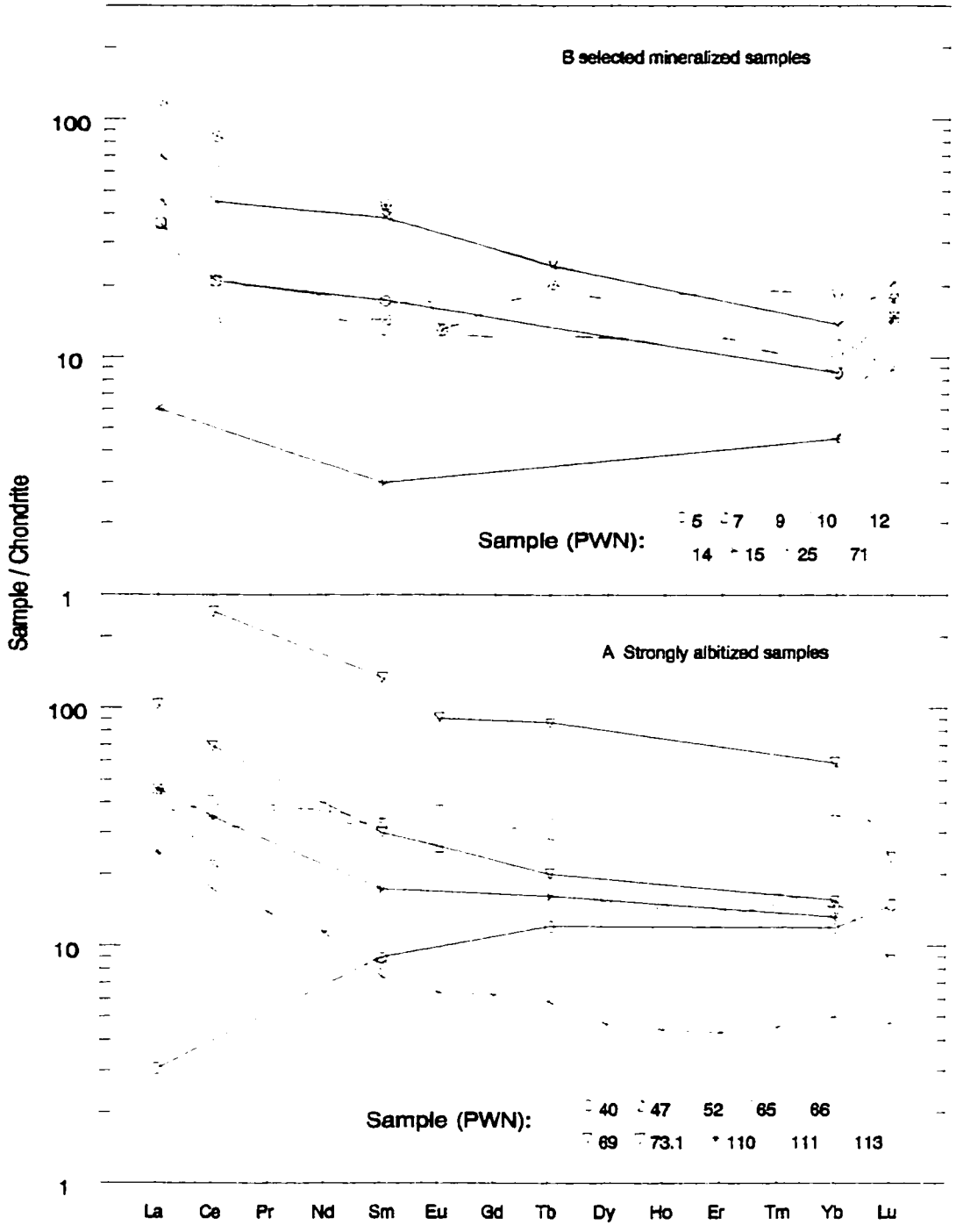

Figure 4.15. Rare earth element plots for mineralized samples and strongly albitized samples, normalized to chondrite (Sun, 1980). Data is from whole rock geochemistry (Appendix 3) including both INAA and ICP-MS methods. Results for elements that are below the detection limit of the technique are not plotted.

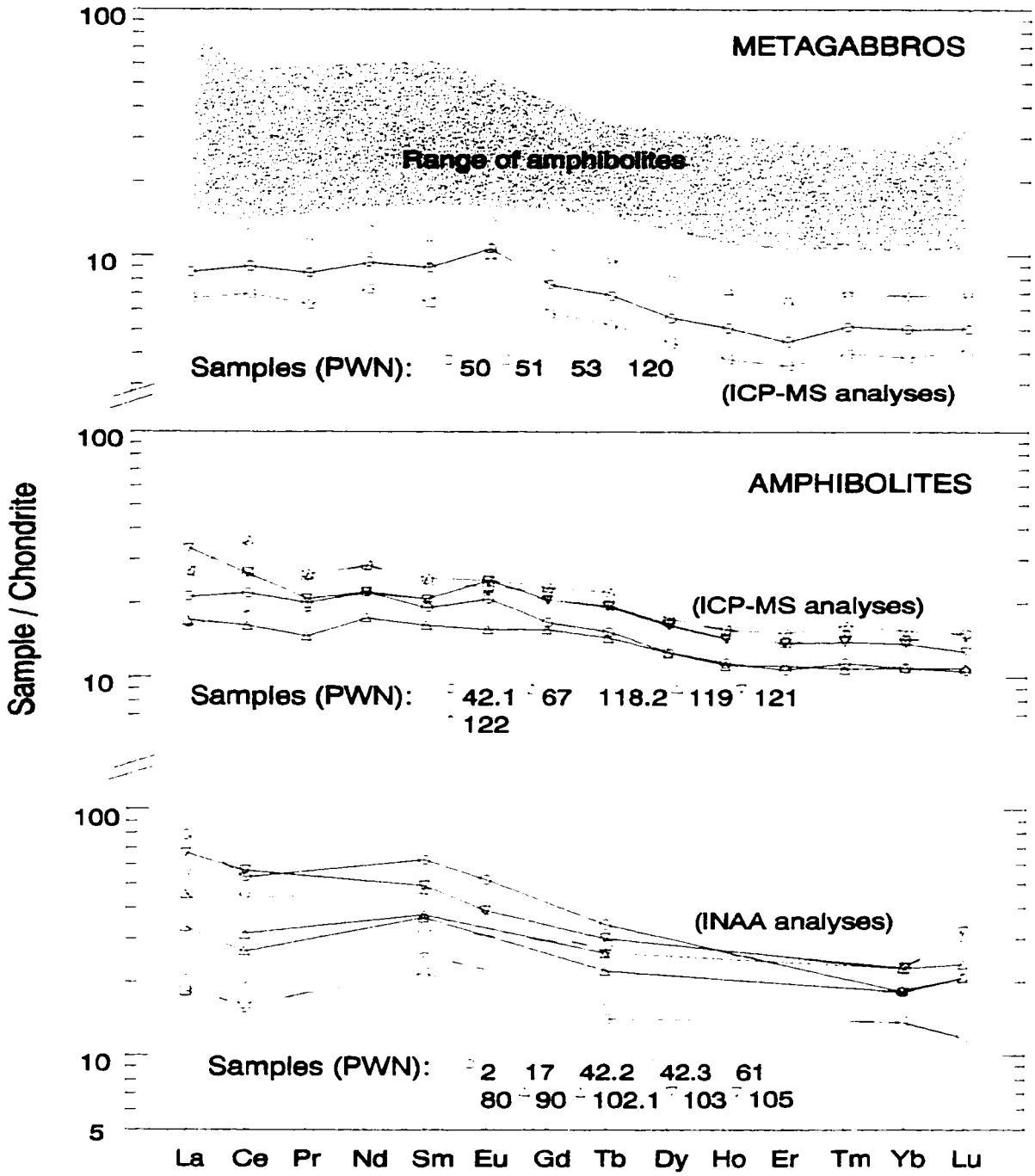

Figure 4.16. Rare earth element plots for metagabbro and amphibolite samples, normalized to chondrite (Sun, 1980). Data is from whole rock geochemistry (Appendix 3) including both INAA and ICP-MS methods. The INAA analyses of amphibolite samples give poor resolution for some elements (e.g. many samples have the same Eu value and Lu at higher concentrations than Yb). Overall the slope and position of the trends is comparable to the ICP-MS results. The shaded area in the metagabbro plot reflects the ranges of amphibolite values.

4.1.6. Rare earth elements

Rare earth element (REE) trends of samples, in general show a larger enrichment of light rare earth elements (LREE) relative to chondrite than the enrichment of heavy rare earth elements (HREE) relative to chondrite (Figure 4.14b La vs. Yb, the negative slope of Figure 4.16). There is a range of LREE enrichments from less than 3 to just over 1000 times chondrite. The samples analyzed by ICP-MS methods returned values for more of the REE elements, with lower detection limits, and more consistent trends than the INAA analyses. The ICP-MS is considered to be more accurate and more precise (Figures 4.15 and 4.16). The INAA data contains Eu results that are limited to 1 ppm increments of resolution, and samples are often below the detection limit of 1 ppm.

The REE plot of the mineralized samples (Figure 4.15) are LREE-enriched, there is a spread from about 2 to 108 times chondrite. The samples form a scattered LREE group, plus PWN 015 with lower LREE concentrations. PWN 015, a chlorite - muscovite quartzite, is the most quartz-rich sample. Quartz tends to contain very low abundance of REE and quartz-rich rocks may be enriched in (HREE) (McLennan, 1989). The sample most enriched in HREE, PWN 009, contains the HREE-enriched minerals xenotime and monazite, see Appendix 2 for probe results. For most samples Eu concentration levels are below the detection limit of 1 ppm. A negative Eu anomaly is indicated for samples PWN 007, 014 and 025; it cannot be judged for the samples with lower REE concentrations. The REE plot of the mineralized samples is similar to REE plots of typical terrigenous clastic sedimentary rocks (e.g. Turekian and Wedepohl., 1961; McLennan, 1989) including the negative Eu anomaly.

The REE trends of the metagabbro samples are slightly LREE-enriched with slight positive Eu anomalies (Figure 4.16). The trends of metagabbroic samples from a metagabbro south of Øverbykollen (PWN 50, 51, 53) and one near Knatten (PWN 120) are all similar. The positive Eu anomaly is due to divalent Eu being enriched in the cumulate plagioclase. The slight LREE-enriched trend is similar to the LREE-enriched Vestre Dale and Flosta gabbros of the Bamble sector (de Haas et al., 1993), though they have smaller Eu anomalies

than the samples from this study. The concentrations of REE in the metagabbro, and the shape of the trends including the positive Eu anomaly is very similar to two hyperites from Valberg at Kragerø and Barmen at Risør (Smalley and Field, 1991).

Three reasons suggest that the metagabbro samples from this study preserve primary REE values. (1) The general similarity with all other reported REE trends from similar rocks of the Bamble sector and strong similarity with some of them. (2) The similarity of all four samples to each other. (3) The REE trends are similar in slope and level of enrichment to tholeiitic island-arc volcanic rocks (Wilson, 1989).

The chondrite-normalized REE concentrations of the amphibolites are nearly flat to slightly more LREE-enriched than the metagabbro samples. Significantly, the amphibolites have a distinctly higher overall concentration and greater spread in values. The amphibolites have a higher REE concentration than the metagabbro samples by a factor of 1.3 to 2.5 times (Table 4.4). The REE trends of most amphibolite samples do not have distinct positive Eu anomalies, most are close to flat. Two samples have negative LREE slopes (PWN 080 and

The strongly albitized samples display a large variation in REE concentrations and trends. All samples but the HREE-enriched PWN 040 and 060, are LREE-enriched. The LREE enrichment in albitized rocks is variable but is on average larger than that of the amphibolites (Figure 4.14b). The overall concentration of the REE is in a overlapping, slightly higher range than the amphibolites (Figure 4.14). The Eu anomalies are generally very minor to flat, indicating that Eu was behaving as Eu^{3+}; the valence associated with more oxidizing conditions (e.g. Weaver and Tarney, 1980). Sample PWN 073.1 has a minor negative Eu anomaly, a characteristic observed in the other metasedimentary rocks. It is not clear that the high REE values of PWN 073.1 are related to albitization since this sample is relatively aluminous; clay-rich sedimentary rocks are associated with higher REE concentrations (McLennan, 1989).

4.2. Geochemical and petrogenetic classification of the gabbros

The purpose of this section is to describe the geochemistry of the gabbroic rocks using major and minor element concentrations in the metagabbro samples. The petrogenesis of the metagabbroic rocks is described using elements that appear to be immobile during alteration. The high level of mobility that appears to be associated with alteration of the gabbro to amphibolite cannot be assumed to be excluded from involvement in modification of the gabbros to form metagabbro. The metagabbro samples may be compositionally intermediate between the gabbro and the amphibolite.

The uralitic amphiboles in the metagabbroic samples are evidence for alteration, and some chemical mobility has been shown to be related to amphibolization in many examples. Fractional crystallization and metamorphism affects the concentration of the major elements and may affect compatible trace elements. Fractional crystallization is important in plutonic rocks especially those with cumulate minerals such as these metagabbro samples. Incompatible trace elements have ions with radii that are dissimilar to major elements (Zr, Y, Nb, Hf, Ta, Th and REE), are not strongly affected by fractional crystallization, and are generally considered immobile during alteration (Cann, 1970; Nicholls and Islam, 1977). These trace elements have been used extensively as petrogenetic indicators for volcanic rocks (e.g. Wilson, 1989).

The four metagabbro samples that are used are: PWN 050, PWN 051, PWN 053 and PWN 120. The metagabbro samples all preserve some orthopyroxene (probably not igneous), plagioclase laths and contain uralitic hornblende that rims and replaces orthopyroxene, clinopyroxene and olivine. Metagabbro samples PWN 051 and PWN 053 contain some scapolite; these samples cannot be shown to have a significantly different geochemistry than those without scapolite.

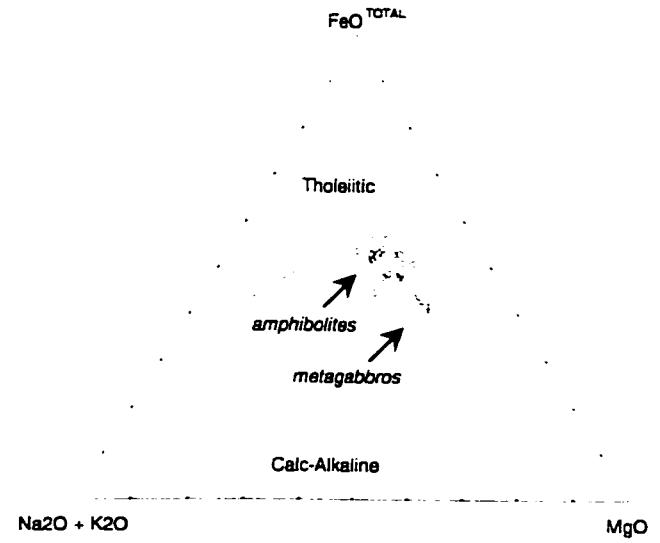

Figure 4.17. Ternary diagram based on major elements to discriminate calc-alkaline and tholeiitic basalts (Irvine and Baragar, 1971). Both the metagabbro samples and the amphibolites plot as transitional between tholeiitic and calc-alkaline basalts. This plot suggests that the amphibolites are derived from a more evolved igneous source, though differentiation has not been described for these intrusions. Coherent major element mobility is indicated for the amphibolites that do not plot with the less altered metagabbro samples.

4.2.1. Classification by major element geochemistry

Based on major element data, the metagabbro samples are transitional between calc-alkaline and tholeiitic basalts (Figure 4.17). Trace element data can be used to discriminate calc-alkaline and tholeiitic basalts. Discrimination methods based on trace elements with low mobility generally indicate a tholeiitic composition. In these discrimination methods, the amphibolites often plot over a larger range suggesting mobility during metamorphism (as discussed below). Major element geochemistry is reported for one metagabbro from the Øverbykollen area by Munz et al., (1994). Unlike the metagabbro samples in this study orthopyroxene occurs in a corona as amphibole does. The MgO content of this sample is lower (6.63%) than concentrations observed for metagabbro samples collected for this study. This low concentration of MgO places this sample in the field occupied by amphibolites in Figure 4.17.

4.2.2. Classification of the metagabbro based on trace elements

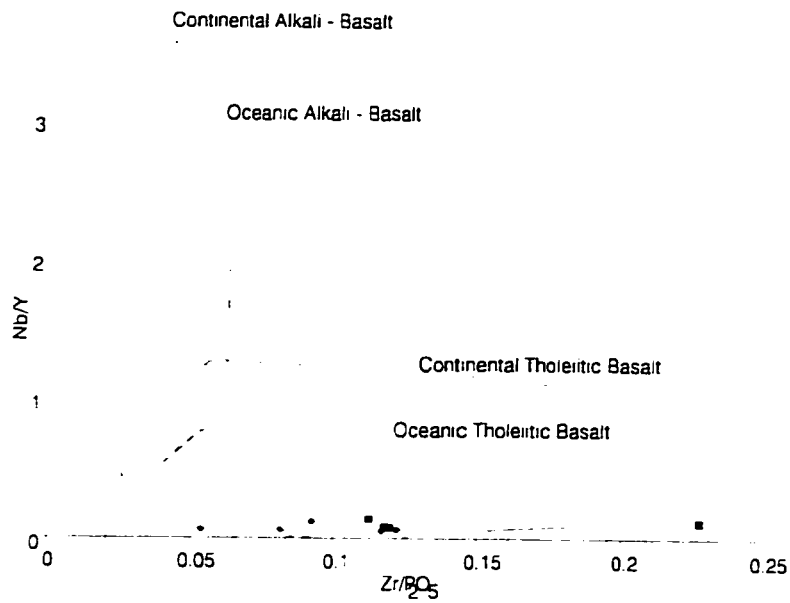

Figure 4.18. The Nb/Y vs. $Zr/(P_2O_5 * 10\ 000)$ diagram to distinguish alkali and tholeiitic basalts based on trace elements (Floyd and Winchester, 1975). The square symbols represent metagabbro samples and the diamond shapes are amphibolites from this study.

Floyd and Winchester (1975) discriminate volcanic rocks based on Y/Nb vs. Zr/P_2O_5, the metagabbro samples from this study also plot well within the tholeiite field (Figure 4.18). The REE trends of the metagabbro samples are nearly flat and have enrichments less than 100 times chondrite. The REE profiles of the metagabbro samples are not as LREE-enriched as expected for calc-alkaline rocks (Figure 4.16). The modified spiderdiagram (Figure 4.19) most similar to a tholeiitic trend. The metagabbro samples appear from the above evidence to be transitional to tholeiitic.

Metagabbro samples of the Modum complex are indicated by Sm-Nd isotopes to have been derived from a depleted mantle source (Munz et al., 1994) (Table 4.7); which are similar to the hyperites of the Bamble sector (Dahlgren et al., 1993).

4.2.3. Tectonic discrimination of emplacement setting

The modified spiderdiagram of Pearce (1983) (Figure 4.19) is useful to interpret the tectonic setting of the Modum gabbros. The plot contains elements that are in general increasingly incompatible from left to right. For normalization a Phanerozoic MORB composition is used, this diagram and normalization values have elsewhere been used to interpret Late Precambrian rocks (Smith and Holm, 1990; Field and Smalley, 1990). The shape of the spiderdiagram (Figure 4.19) is similar to basalts from active destructive margins (Pearce, 1983), where the magma is derived from a subducting oceanic slab. Alkali elements (Sr - Ba) are strongly enriched in the metagabbro relative to MORB as these elements preferentially enter the melt from the subducted slab. High Ba and Rb concentrations have been interpreted to be derived from oceanic sediments (Hole et al., 1984). The more incompatible elements (Nb - Yb) are generally less than MORB concentrations, with a near horizontal trend and a hump about Zr and Hf. A horizontal line drawn at the level of the lowest immobile elements (Nb, Yb) represents the theoretical composition of the magma without input from the subducting slab. Displacement of this line from the MORB concentrations (1.0) is a reflection of varying degrees of partial melting and crystal fractionation (Wilson, 1989). Crustal contamination also enriches the rock with alkali elements and to a lesser extent the more incompatible elements are also enriched. Field evidence indicates that the gabbros emplaced in a gneissic crustal sequence but there appears to be minimal crustal contamination, based on the values of many of the incompatible elements below MORB concentrations and the near horizontal trend of the incompatible elements (Pearce, 1983; Wilson, 1989). The lack of strong positive Ce, P and Sm peaks is similar to a tholeiitic trend. The concentration peak in the metagabbro samples for Zr and the trough for Nb are typical of tholeiites (Winchester and Floyd, 1975).

The profile of Figure 4.19 is very similar to hyperites from the Bamble sector (Smalley and Field, 1991), they have an enrichment of almost 10 times MORB for Sr to Ba, a trough at Ta and Ce to Yb being close to MORB values. The hyperites of the Bamble sector

are also interpreted to be formed from a subducting slab (Field and Smalley, 1991; Atkins and Brewer, 1990).

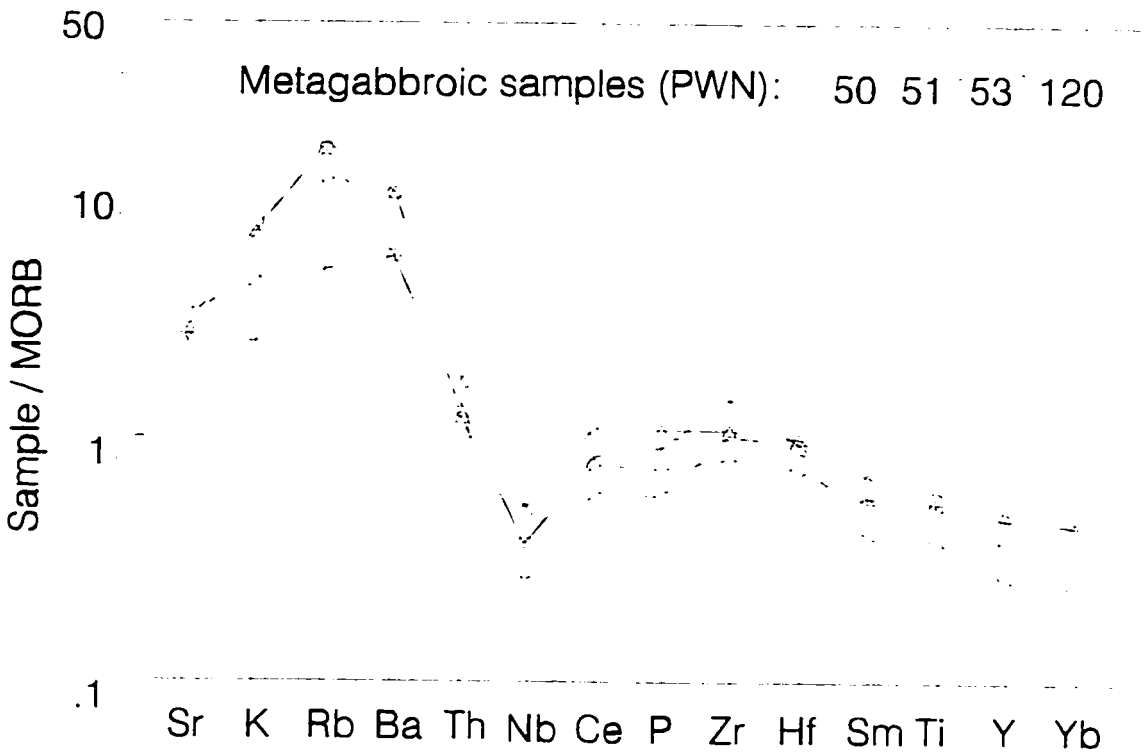

Figure 4.19. MORB normalized modified spiderdiagram with the elements in the order of Pearce (1983). The shape is characteristic of a tholeiitic magma formed at a compressive margin with little crustal contamination; see text for details.

Similar enrichments of Ta and Nb are expected during igneous processes, typically, in a collisional setting these elements plot together as a trough. ICP-MS analyses produced Ta concentrations three to six times MORB values, significantly higher than Nb. INAA results for Ta indicate that all metagabbro samples are less than the 0.5 ppm detection limit, while the ICP-MS results average 0.73 ppm. Ta concentration is interpreted to be inaccurate, possibly enriched during crushing in the W-carbide ring mill used for powdering of the sample.

4.3. Comparison of metagabbro and amphibolite geochemistry

In the Bamble sector metamorphism of the gabbro to amphibolite has been found to be non-isochemical (Frodesen, 1968; Frodesen, 1973; Elliot, 1973; Field and Elliott, 1974; Cameron, 1989b; Smalley and Field, 1991; Cameron et al., 1993). The chemistry of the transition has not been described in much detail for the Kongsberg rocks. The gains and losses between the rock types is quantitatively described here using the "isocon" method of Grant (1986), a graphical solution to the mass balancing equation of Gresens (1967).

Field relations suggest that the amphibolites are derived from the gabbros via hydrous metamorphic alteration (Bugge, 1943; Jøsang, 1966; Munz and Morvik, 1991; Chapter 3 this study). Comparison of the geochemistry between these two rock types is useful to describe chemical mobility and the character of the altering fluid. For this comparison of metagabbro samples and amphibolites only samples collected during field work for this study were used. In this study each rock type is grouped and the averages compared for the mass balance calculations. Metagabbroic rocks were not paired with spatially associated amphibolites, due to the rarity of metagabbroic rocks and that the metagabbroic samples did not all have amphibolites that were proximally associated.

Differences between the gabbros and the amphibolites are made in X-Y scatter diagrams 4.1-4.12, 4.13-4.14 and in the normalized REE plot 4.16. Another qualitative graphical comparison is made in Figure 4.20 that compares elements that generally increase in incompatibility from left through Lu, with some transition metals, S, and Cl at the far right. The compatible elements K to Ba (mainly alkali elements) (Figure 4.20) show no clear difference or are at lower concentrations in the amphibolite samples. The relatively incompatible elements Th to Lu are concentrated 2 to 3 times higher in the amphibolites than in the metagabbro samples. Many of these elements have ions that have charges of +3 or greater (as described elsewhere). The metals Sc to Cr display various changes, and have different affiliations. V and Sc behaves somewhat similar to Ti and shows an enrichment in

the amphibolites (mainly occurring in oxides). Ni is depleted, probably due to the disappearance of olivine as discussed above.

Considering trace element concentration changes during a slight magmatic differentiation process in a hyperite of the Bamble sector, Frodesen (1973) observed a marginal increase in V and Cr in later differentiates, attributed to late crystallization of magnetite. Like the later differentiates Ti is at higher concentrations in the amphibolites of this study, but there is not a significant change in Cr (Table 4.4). Frodesen (1973) did not observe significant changes in the other 15 trace elements. It is concluded that magmatic differentiation was not a significant process in distinctly characterizing these rocks.

With the exception of Na, Fe^{2+}, V, Ga, and F, all of the elements that are in higher concentrations (beyond one standard deviation) in the amphibolite form trivalent or more positive ions. These include the trivalent ions Ti, Fe^{3+}, P, Sc, Y, V, Ga, and REE; the tetravalent ions Ti, V, Hf, Th, and U; the pentavalent ions P and V; and the hexavalent ion U. V and Ga more commonly as more positive ions and U is the most mobile as a hexavalent ion.

Some elemental variations can be accounted for by inversely proportional relations. To an extent the lower concentration of Al corresponds with and higher cocentration of Ti and Fe^{3+}, this can be observed in the amphiboles where Ti and Fe^{3+} are more abundant in the hornblende of the amphibolite than in the uralitic amphiboles; they both occupy the Al site. This change is possibly driven by pressure changes, as in calc-alkaline plutons in which the Al content of hornblende decreases with increasing temperature (e.g. Hammarstrom and Zen, 1986). The increase in Na and decrease in Ca may be related to compositional changes in plagioclase, i.e. the plagioclase becoming more albitic; microprobe results from this study did not establish a change in chemistry.

Sulphides and oxides are highly mobile in hydrothermal settings and an enrichment of both is observed in the amphibolites. This enrichment is supported by the measured variable increases in S, Cu, Ti, V, Fe^{3+} and Cr. Some of these minerals especially Ti and Fe^{3+} occur

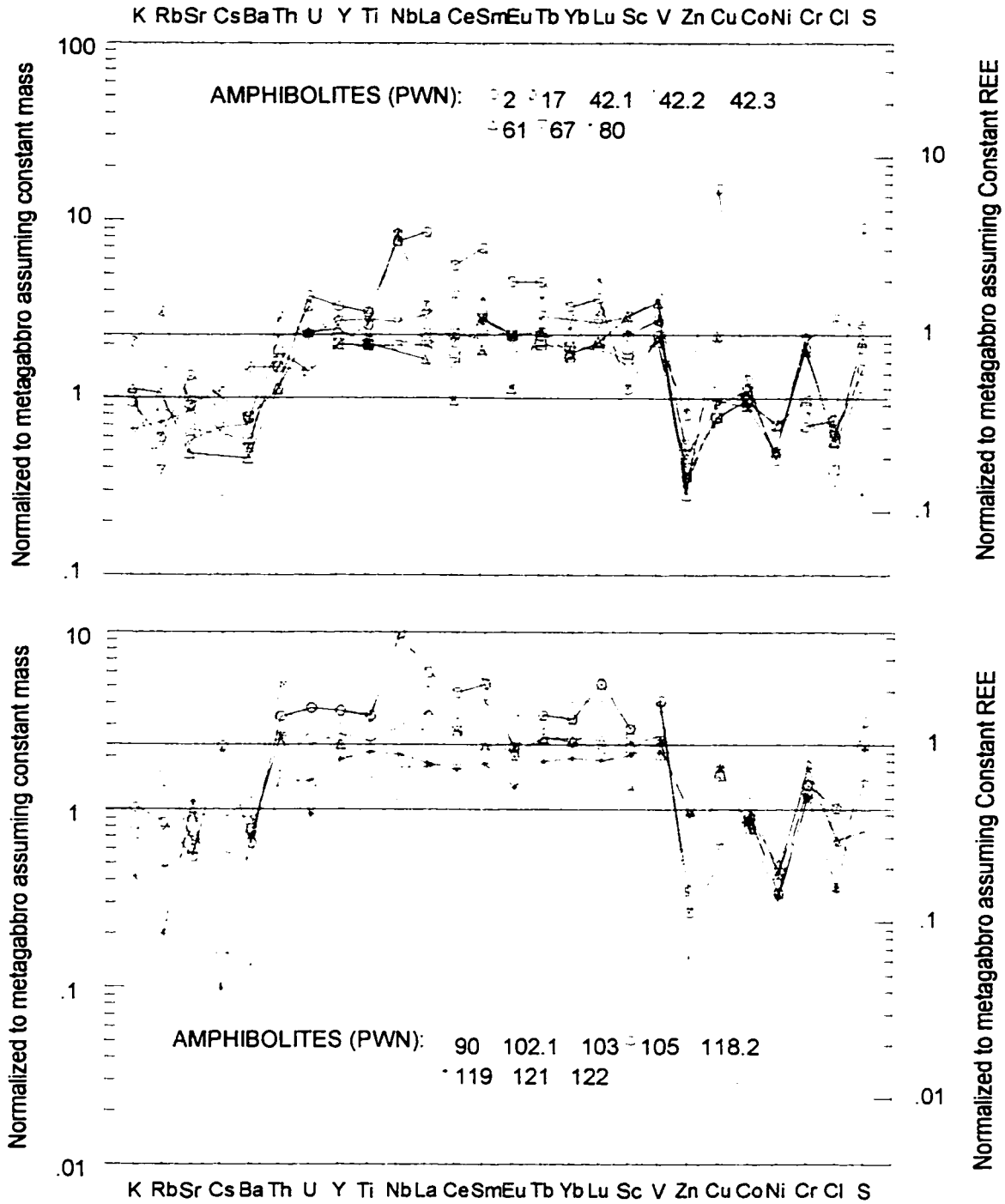

Figure 4.20. Concentrations of trace elements and K in amphibolites normalized to the average of the metagabbro samples assuming constant mass (left scale, lower horizontal line) and assumming constant REE (right scale, upper horizontal line); two graphs are used due to the number of samples. Some samples are analyzed by the more sensitive and complete ICP-MS method, this replaces the INAA results for these elements. See text for description of data.

in silicates as well as oxides, some S occurs in scapolite in both metagabbroic rocks and amphibolites. The amphibolites are enriched in U, but this is the only element of those associated with Skuterud ore that is enriched in either rock-type.

Significantly lower concentrations of Cl are described in amphibolites of the Bamble sector (Figure 4.8), though Cl was at higher concentrations in the corresponding amphibolites. In some locales of the Bamble sector very high concentrations of Cl are observed in minerals including apatite (Lieftink et al., 1994) and scapolite (Lieftink et al., 1993). Similar to these rocks, the amphibolitized hyperites of the Bamble sector have an increased Fe^3/Fe^2 level, indicating a probable increase in oxygen fugacity. REE elements are interpreted to be immobile in the similar studies from the Bamble sector (Table 4.4, de Haas, 1992a). A high fluid to rock ratio in Modum complex is supported by the extensive nature of the formation of amphibolites and the extent of element mobility.

4.3.1. Method used for mass balance calculations

The isocon (line of equal mass) is calculated from the following formula which is derived from the formula of Gresens (1967) by replacing volume and density with mass (Grant, 1986).

$$\Delta M_i=[(M^A/M^O)C_i^A - C_i^O]M^O$$

where:

O = Superscript for original sample

A = Superscript for altered sample

i = Subscript for component

M = Mass of Sample

C = Concentration

ΔM_i = Gain or loss of mass component i relative to the reference mass

A graph of C^A vs. C^O for all components will allow a straight line to be plotted from the origin through those elements which show similar changes in concentration. The slope of the line will produce a constant for the equation

$$C_i^A = (M^O / M^A) C_i^O$$

where the constant (M^O / M^A) is the dilution or concentration factor that can be applied to all components.

4.3.2. Mass balance results

To calculate the gains and losses of elements during alteration of the gabbro to the amphibolites, the metagabbro samples were averaged and used as the starting composition (gabbro). The graphical results are presented in Figures 4.22 a and b (major and trace element plots respectively). Table 4.4 also contains the mass balance data and results. This table indicates which changes are significant and compares them with the results from studies in the Bamble sector. The difference is considered "significant" and identified with bold lettering when the higher average minus one standard deviation is greater than the average of the smaller one plus one standard deviation. The isocons constant mass and constant REE are used in Table 4.4as factors for the concentration change column. Some elements have a large variation of concentration within a rock type (Figure 4.20), for these elements the accuracy of the average is poor; examples of these elements are Cu, S, Rb, Cl, and Br.

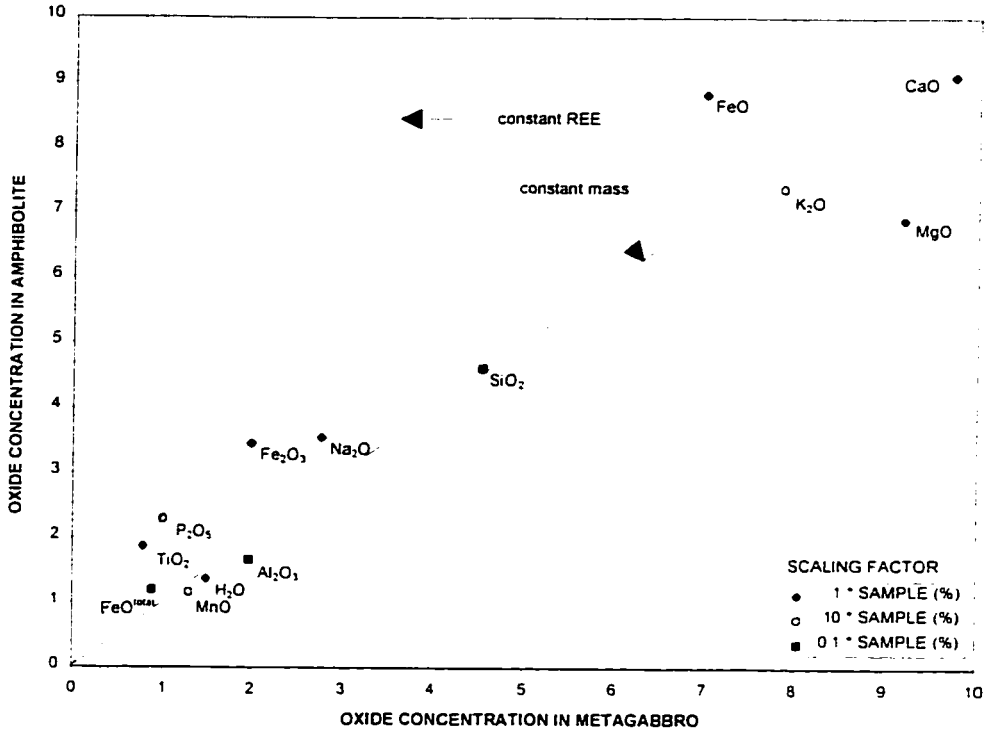

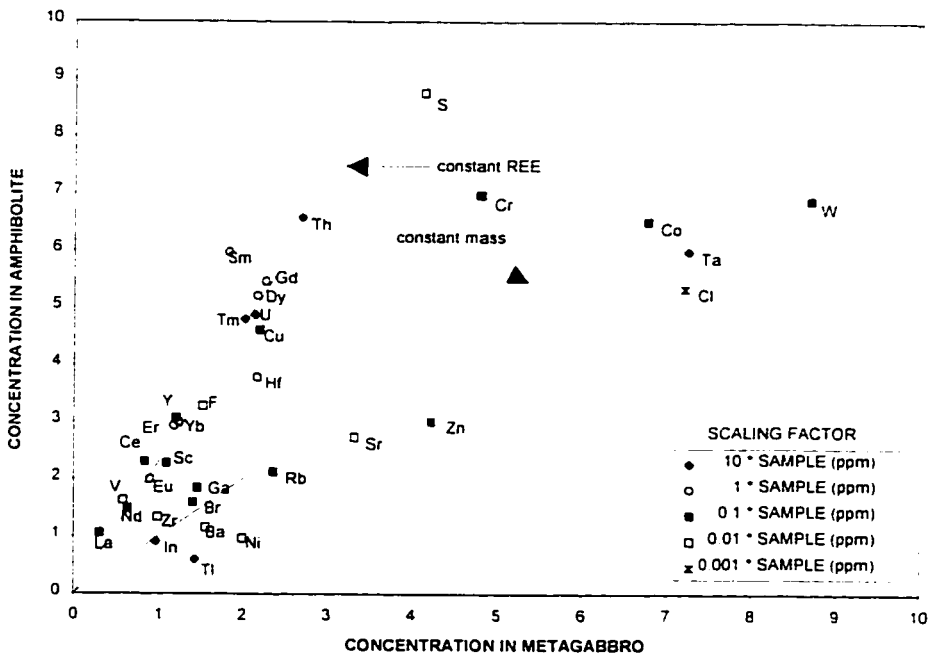

Figure 4.21 a, b. Isocon diagrams comparing the average concentration of elements and oxides in the metagabbro samples and the amphibolite samples. The averages are multiplied by the scaling factors shown to fit in the range of 1 to 10. See text for details.

Table 4.4. Geochemical changes during amphibolitization in this and other studies from southwest Scandinavia

ELEMENT / OXIDE	KONGSBERG SECTOR (This study)								BAMBLE SECTOR							SWEDEN
	METAGABBRO			AMPHIBOLITE			Percent Increase		Locatio	Hiåsen		Valberg, Laget + Barmen			Tvedestran	Varmland
									Ref	1,2	1 2	3	4	5	6	7
	Av	Std Dev	No of Samples	Av	Std Dev	No of Samples	Assuming No Mass Change	Assuming Contstant REE	Process	Scapolitize	Amphibolitization					
									No of Sample	?	35	16 pairs			2 pairs	39
Major Oxides (weight %)																
SiO2	45 38	0 72	4	46 1	1 4	17	0 02	-0 55		-	x	-?				x
TiO2	0 78	0 14	4	1 9	0 5	17	**1.40**	0 06		x	x	x				x
Al2O3	19 75	0 87	4	16 6	1 0	17	**-0.16**	-0 63				x?				x
Fe2O3	2 00	0 57	4	3 5	0 7	17	**0.73**	-0 24				+				+
FeO	7 00	0 67	4	8 8	0 7	17	**0.26**	-0 44		-	x	-				+
FeO total	8 80		4	11 9		17	**0.37**	-0 40				x				+
MnO	0 13	0 03	4	0 1	0 0	17	-0 11	-0 61		-	-	x				+
MgO	9 20	0 76	4	6 9	0 9	17	**-0.25**	-0 67		+		x				x
CaO	9 74	0 46	4	9 1	0 6	17	-0 06	-0 59				-				-
Na2O	2 78	0 22	4	3 5	0 5	17	**0.28**	-0 44		+		x				+
K2O	0 79	0 35	4	0 7	0 3	17	-0 06	-0 59				+			x	+
P2O5	0 10	0 03	4	0 2	0 1	17	1 29	0 01				+			x	x
H2O	1 50	0 37	4	1 4	0 5	17	-0 09	-0 60				+				+
Transition Metals (ppm)																
Cr	48	11	4	69 9	22.4	17	0 46	-0 36		x	x				x?	
Ni	200	34	4	97 2	27 4	17	**-0.51**	-0 79					x		x	x?
Co	68	5	4	65 2	8 8	17	-0 04	-0 58		x	x		-?		x	
Sc	11	2	4	22 8	6 2	17	**1.10**	-0 08							x	
V	58	13	4	162 9	40 7	17	**1.80**	0 23		x	x		+			
Cu	22	13	4	46 2	76 6	17	1 10	-0 08		x	x				-	x?
Pb	2		4	~1		6										
Zn	42	14	4	30 1	27 1	17	-0 29	-0 69		x	x		-		-?	+
Granitiod (ppm)																
In	0 10	0 02	4	0 1	0 04	6	-0 05	-0 58								
W	87 0	9 6	4	68 9	27 6	17	-0 21	-0 65								
Mo	0 3	0 1	4	<1		17										
Miscellaneous (ppm)																
S	412 8	116 1	4	876 3	841 7	17	1 12	-0 06					-?		-	-
Sb	0 17	0 06	4	<0 1		17									-	
Low field strength (ppm)																
Rb	23 7	10 1	4	21 3	16 5	17	-0 10	-0 60		x	+		+		-	+
Cs	0 92	0 33	4	<0 5		6										
Ba	155	52	4	116 0	40 3	17	-0 25	-0 67		-	x		±		x	x?
Sr	333	42	4	273 5	77 1	17	-0 18	-0 64		-	x		±		x	x
Tl	0 14	0 04	4	0 1	0 0	6	**-0.58**	-0 81								
Ga	14 5	0 6	4	18 5	1 8	6	**0.28**	-0 44		-	x					
High field strength (ppm)																
Ta	0 73	0 22	4	0 60	0 14	17	-0 17	-0 64						x		
Nb	1 32	0 37	4	<10	0 00	17				x	x					
Hf	2 18	0 26	4	3 79	1 28	17	**0.74**	-0 23						x		
Zr	99 00	23 18	4	133 47	50 24	17	0 35	-0 41		x	x		-?			x
Y	11 98	3 20	4	30 71	6 62	17	**1.56**	0 13		x	x					x
Th	0 27	0 05	4	0 66	0 35	17	1 44	0 07						x		+
U	0 22	0 08	4	0 49	0 21	17	1 27	0 00								
Rare Earth Elements (ppm)																
La	3 05	0 70	4	10 61	6 17	17	**2.48**	0 53		x	x			+?	x	
Ce	8 33	2 07	4	23 12	11 76	17	**1.78**	0 22		x	x			x	x	
Pr	1 16	0 28	4	2 70	0 54	6	**1.34**	0 03								
Nd	6 33	1 54	4	14 83	2 71	6	**1.35**	0 03						x		
Sm	1 83	0 41	4	5 98	2 63	17	**2.27**	0 44						x	x	
Eu	0 90	0 15	4	2 01	0 66	17	**1.24**	-0 01						x	x	
Gd	2 28	0 56	4	5 47	0 84	6	**1.40**	0 06						x		
Tb	0 38	0 10	4	1 06	0 29	17	**1.77**	0 22						x	x	
Dy	2 18	0 59	4	5 22	0 72	6	**1.40**	0 06								
Ho	0 44	0 12	4	1 06	0 15	6	**1.42**	0 06								
Er	1 18	0 33	4	2 93	0 39	6	**1.50**	0 10								
Tm	0 20	0 05	4	0 48	0 07	6	**1.37**	0 04						x		
Yb	1 24	0 32	4	3 00	0 83	17	**1.43**	0 07						x	x	
Lu	0 20	0 05	4	0 60	0 23	17	**2.06**	0 35						x	x	
Halogens (ppm)																
F	152	35	4	328	137	17	**1.17**	-0 05								
Cl	7210	1400	4	5340	4200	17	-0 26	-0 67		+			+			+
Br	14 0	6 2	4	16 0	29 9	17	0 14	-0 50								
Be	<0 5		4	0 95	0 38	17										

* changes larger than 1 standard deviations are in bold

KEY				
	+	increase	x	unchanged
	-	decrease	±	variable
	?	uncertain		results unlike this study

REFERENCES

1 Frodesen (1968), 2 Frodesen (1973), 3 Elliot (197 5 Smalley and Field (1991), 6 Cameron et al (1993)
4 Field and Elliott (1974), 6 Zeck and Willadsen, 1990

Elements occuring along an "isocon" (trend line) can be interpreted to have behaved in a similar manner chemically. The typical cause for multiple elements to occur along one line is that they were immobile. Samples that plot above the "constant mass" isocon occur in higher concentrations in the amphibolites than in the metagabbro samples, and visa versa for those below the isocon. An isocon is drawn through the REE ("constant REE"), but there are no other groups of elements that warrant an isocon. Both isocons are used as normalizing factors in Figure 4.20.

The "constant REE" isocon is placed along a concentration of trace elements and major elements (TiO_2 and P_2O_5). The group is dominated by elements with valences of +3 or more, the exceptions are Cu, S, and F which all are values with high standard deviations. The only trivalent element significantly away from this isocon is Al. Notably, no elements concentrated at over 3% in the rock follow this isocon. Assuming constant mass, the "constant REE" trend represents elements increased by a consistent factor of 1.3 times from metagabbro samples to amphibolite. If the "constant REE" isocon represents immobile elements then there would have been loss in mass by a factor of about 0.55 (55%) from the metagabbro to the amphibolite samples. The "constant REE" isocon may not represent immobile elements, but elements that are geochemically coupled and increased together. No field or petrographic evidence was found to indicate a large loss in mass (volume) associated with the amphibolites, such as migmatization, or mylonite fabric. Few similar geochemical changes from metagabbro to amphibolite are observed in studies of the Bamble sector and the Värmland hyperite suite, as indicated by Table 4.4. These other studies have assumed constant mass, or in one case a $2 \pm 0.5\%$ increase in rock volume during the partial formation of amphibolites for the 1500 Ma gabbros of the Värmland hyperite suite (Zeck and Willadsen, 1990). If "constant REE" is assumed for this study then the findings of constant REE, Sc, Y, and Ti in other studies is coincedent with this study, but depletions of many of the other elements is not observed in the other studies.

4.3.3. Geochemical differences related to hydrothermal processes

The favoured mechanism of alteration from metagabbro to amphibolite is one dominated by hydrothermal fluid interaction. This general interpretation is the accepted interpretation made by workers for the Modum complex (e.g. Bugge, 1943; Jøsang, 1966; Munz and Morvik, 1991) and alteration of the hyperites of the Bamble sector (e.g. Frodesen, 1968; Elliot, 1973; Brickwood and Craig, 1987; Smalley and Field, 1991). Indicators of this process are as follows: the presence of hydrothermal alteration products in the area such as albitites; and hydrous minerals such as amphiboles and scapolite replacing anhydrous pyroxene, olivine and plagioclase. Two possible scenarios are considered: (1) The constant REE isocon represents immobile elements and thus there was a large loss (55%) of mass; (2) Elements following the constant REE isocon were enriched and there was a lesser but unknown change in mass of the samples.

Reduction in mass may acompany shearing. Along the Fries ductile deformation zone, southern Appalacians (United States) enrichments of Ti, Zr, P, Y, V and some LREE have been attributed immobility of these elements during large volume losses (60% at Hot Springs window) (O'Hara and Blackburn, 1987; O'Hara, 1988; O'Hara and Blackburn, 1989). The rocks from that deformation zone are granitic to granodioritic gneisses deformed to mylonites. In the mylonites there is a decrease in grain size, an overall increase in phyllosilicates, quartz grains may be annealed, plagioclase is often kinked and feldspars display brittle deformation during breakdown. The rocks of the Modum complex do not show similar mylonitic textures, foliation is low to moderate in the amphibolites and metagabbro samples. The Kongsberg sector including the Modum complex has undergone repeated ductile deformation (e.g. Starmer, 1980; Starmer, 1985b). The amphibolite samples do not exhibit mylonitic microstructure, this may be due to post-deformation recrystalization of the amphibolites. The metasediments and especially the fahlbands appear to have accepted more of the strain during Sveconorwegian deformation (Jacobsen and Heir, 1978) phyllosilicates and quartz in these rocks do not appear highly strained, or as is the case with the micas, they

have recrystallized post-deformationally with no typical mylonitic textures present (this study). The REE plots of the metagabbros and the amphibolites do have a similar slope and shape, with the exception of the lack of an Eu anomally in the amphibolites. The lack of a positive Eu anomaly in the amphibolite samples may be interpreted to be related to the loss of plagioclase, and therefore the Eu^{2+} sites. The relatively oxidizing conditions (Chapter 5) indicates that Eu would have more affinity for the trivalent state in the amphibolite samples. Titanium lies along the constant REE trend, modelling indicates that this element is expected to be immobile for fluid / rock ratios as high as 10^4 (Weaver and Tarney, 1981; O'Hara and Blackburn, 1989). With the exception of F, S and Cu the elements along the constant REE trend are typically comparatively insoluble in the aqueous fluids and siliceous melts which are considered to be derived from the subducting slab (e.g. Tatsumi, 1989; Pearce and Norry, 1979; Tatsumi et al., 1986; Defant and Drummond, 1990). It is consistantly the more soluable elements (Rb, Sr, Si, K, Na) that are at lower and more variable concentrations (i.e. not following a single isocon) and would represent depleated elements

Migmatization or some other partial melting processes can be considered as a possible cause of volume reduction. Some large-ion lithophile elements (LIL), also known as hygromagmatophile elements, are depleted as a group (K, Rb, Sr, Ba, Zr) if the "constant REE" isocon is assumed to represent immobile elements, but not Th and LREE which would be expected to be depleted with the others (Figure 4.21, Table 4.4). LIL elements as well as SiO_2 and Na_2O tend to be removed in the melt phase (leucosome) during migmatization. Evidence to indicate migmitization was not observed during this or in the literature. At about 700°C a mafic rock may begin partial melting (Best, 1982), making this process a possible factor though it is not clearly supported by the geochemical evidence.

The high Cl content of rocks in this study indicates a halogenated fluid; in such a fluid REE have higher mobilities (Taylor et al., 1981; Haas et al., 1995). The interpretation of mobile REE has been made for albitites of the Modum complex, but the trace element character of the amphibolite formatation process does not appear to have been studied (Munz and Morvik, 1991; Munz et al., 1994).

4.3.4. Geochemical differences related to igneous processes

The differences between the metagabbro and amphibolite samples may be assigned to igneous or metamorphic / hydrothermal processes. In some respects the amphibolites have characteristics of more fractionated gabbros than the metagabbro samples. As the intrusions have a cumulate component (plagioclase and olivine) one possibility to consider is that fractionation of the intrusion has lead to the differences in chemisry between metababbro and amphibolite samples. Variable concentrations of the cumulus minerals will affect the geochemistry of the rock. To preserve the equal SiO_2 contents of the amphibolite and the metagabbro samples olivine (36% SiO_2) and plagioclase (50% SiO_2) would need to be removed from the melt at a ratio of 10 parts plagioclase to 1 part olivine. To attribute geochemical differences between the metagabbro samples and amphibolites only to igneous differences the above fractionation should be used. Two trends support the involvement of

removal of plagioclase and olivine in the geochemical characterization of the amphibolites. (1) Some elements, incompatible with plagioclase or olivine, are more enriched in the amphibolites, including: Th, U, Hf and Ta (Figure 4.21). (2) Nickel is compatible in olivine and is relatively depleted in the amphibolites. However, these trends are also explained by metamorphic processes elsewhere through mobility in a oxidized fluid with high Cl activity and reduced compatibility in the secondary mineral assemblage.

Five points argue against igneous processes being the dominant processes in the characterization of the amphibolites. (1) Significant removal of plagioclase with positive peaks of Eu should lead to negative Eu anomalies in the normalized REE trends of the residual magma; generally flat trends are observed (Figure 4.16). (2) Chromium, while variably compatible in olivine, has higher concentrations in the amphibolites than in the metagabbro samples. (3) Barium and Sr are variably compatible with plagioclase, but are not clearly depleted in the amphibolites. (4) Potasium is compatible in neither olivine or plagioclase, but no enrichment in the amphibolites is observed. (5) The study lacks samples that plot intermediate between the metagabbro samples and the amphibolites. For many elements separate clusters are observed without intermediate points for amphibolites and metagabbro samples. Of the samples from this study, there are no amphibolites that plot with the metagabbro samples; including samples PWN 118 to 122 which are all collected from within about 300 m radius.

Fractional crystallization may play a lesser role in accounting for the differences between the metagabbro samples and the amphibolites but does not provide a complete model. The coronitic alteration is an indication of the presence of fluid during subsolidous reactions. The elements enriched in the amphibolites, which includes many trivalent ions, are interpreted to be derived from the metamorphic fluid. On formation of the coronitic gabbros the fluid responsible certainly introduced and removed some matter. H_2O and the halogens Cl and Br are concentrated in the metagabbro samples in concentrations well above what is expected in gabbros (e.g. Turekian and Wedepohl, 1961). These elements, at least H_2O, are

required for formation of amphiboles and thus are probably the most reactive elements in the fluid. Other elements, such as REE and Ni, preserve values that are as expected for gabbroic rocks, and are interpreted to be igneous concentrations.

4.4. Geochemical changes related to albitization

As illustrated in Figures 4.1-4.12 and 4.14-4.15 relative to the metagabbro and amphibolite protoliths the albitized rocks contain higher concentrations of Na_2O, Si_2O and U; and contain higher concentrations of MgO, FeO, CaO and Cl. A plot of trace elements in albitized samples normalized to the average of the metagabbro samples (Figure 4.22) produces enrichments and depletions similar to those observed in the amphibolites (Figure 4.20). Most albitites are replacements of amphibolites, the trace element geochemical changes for these occurrences are smaller than indicated in Figure 4.22. Sample PWN052 is an albitite that is hosted by metagabbro (PWN 050, 051), and displays a trace element pattern typical of the albitized rocks hosted by amphibolites. Compatible elements K-Ba are generally slightly depleted in the albitite. Incompatible elements Th-Sc are at higher concentrations in most samples. The metals are generally lower as sulphides are scarce or absent in albitized samples (Chapter 3). There is variable gains and losses of Cr; in one of the enriched samples (PWN 052) Cr is measurable in the amphiboles (Appendix 3). The depletion of Sr, can be related to lower compatibility in albite than in more calcic plagioclase. The heterogeneous nature of albitite geochemistry is illustrated by the range of REE values (Figure 4.15) and the scatter in Figure 4.22. The range of REE values includes the range of values measured in the amphibolites and has a similar average slope (Figure 4.16). Mobility of Nd and Sm has also been observed by Munz et al. (1994). Contributing to the large range in geochemistry of the albitized samples are variations in the intensity of albitization, varying metamorphic conditions during albitization, geochemistry of the protolith and the locally variable nature of alteration. A larger dataset of albitized samples would help to make more quantitative interpretations.

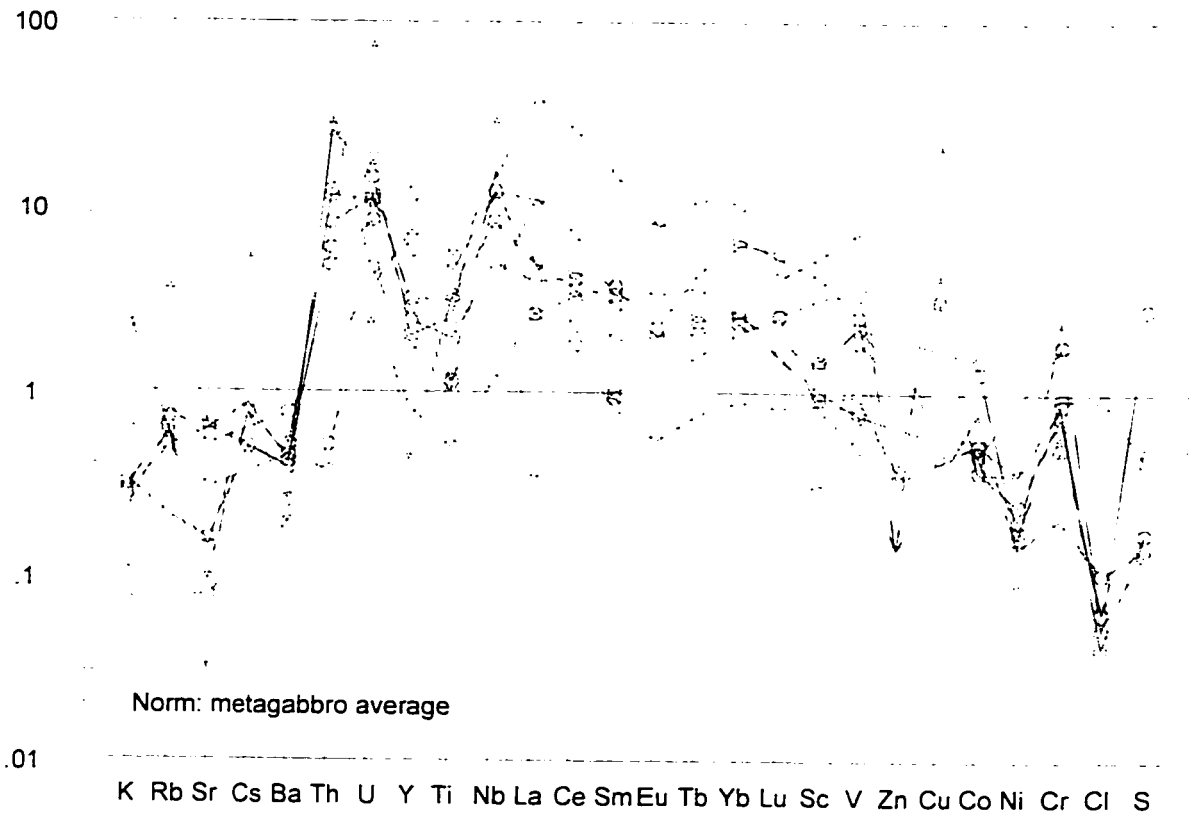

Figure 4.22. Extended element comparison of the albitized mafic samples: normalized to the average of the four metagabbro samples. Cu is below the detection limit for 5 samples.

4.5. Stable isotopes

Stable isotope analyses have been carried out on some of the mineralized metasediments of the Skuterud Mine (Table 4.5). Stable isotope analyses were carried out for two rock types: graphite and pyrite from the Co-As-Cu mineralized fahlband-bearing quartzite, and calcite and pyrite from the massive calcite of the Gamphue quarry at Øverbykollen. The pyrite analyzed for this study contain 2 to 10% S, mainly as pyrite, the analyzed sulphide may contain minor to trace amounts of other sulphides including cobaltite and arsenopyrite.

The graphite is medium grained, foliated and bent, this habit indicating that it has been recrystallized and deformed during metamorphism and deformation. The strongly depleted $\delta^{13}C$ values observed in the graphite (Table 4.5) are indicative of an organic source for the graphite (e.g. Faure, 1986). A hydrothermal fluid originating from a high-temperature

source at -5 ‰ $\delta^{13}C_{PDB}$ (i.e. magmatic source (Ohmoto, 1972)) would be expected to produce graphite with a $\delta^{13}C$ value of greater than -15 ‰ $\delta^{13}C_{PDB}$ (Bottinga, 1969). Silicic metasedimentary rocks from the Arendal area in the Bamble sector contain graphite with an average $\delta^{13}C$ value of -20.2‰, interpreted to be of an organic source (Andreae, 1974).

TABLE 4.5. STABLE ISOTOPE RESULTS IN FAHLBANDS AT THE SKUTERUD MINE, AND IN PYRITE FROM MASSIVE CALCITE FROM THE GAMPHUE QUARRY (PWN 033).

$\delta^{13}C$ in graphite		$\delta^{34}S$ in pyrite	
Sample Number	$\delta^{13}C_{PDB}$ (‰)	Sample Number	$\delta^{34}S_{CDT}$ (‰)
PWN 007B	-23.44	PWN 025	20.1
PWN 025	-20.62	PWN 071	20.7
PWN 072A	-24.68	PWN 033*	-4.3

Pyrite from the mineralized fahlbands contains an approximate value of $\delta^{34}S_{CDT}$ of 20‰ (Table 4.5). The only likely source for the S is seawater. Sulphur from igneous rocks of mantle derivation is expected to be 0±10‰ (Faure, 1986). A pyrite-bearing metagabbro (PWN 050) and an amphibolite (PWN 043.1) have $\delta^{34}S$ values of 7.1 and 5.4‰ respectively; analyzed using the Kiba method. Metamorphosed mafic intrusions from the Bamble sector have been found to have $\delta^{34}S$ values ranging from 0 to 4‰ (Andreae, 1974). The $\delta^{34}S$ of the fahlbands is distinctly more enriched than would be expected for an igneous source. Sulphur associated with the mantle, and some lode Au deposits are not as $\delta^{34}S$ enriched as pyrite from the fahlbands (Figure 4.23). These examples show that the pyrite of the fahlbands contains S that is unlike igneous and hydrothermal material that is interpreted to have a mantle or lower crust source.

The metasedimentary rocks that host the fahlbands were deposited as early as 1.9 Ga (Andersen and Munz, 1995) or after 1.7 Ga (Veraschure, !985), sulphide in metasedimentary rocks within this age range can be found with $\delta^{34}S$ values similar to the pyrite from the fahlbands. Andreae (1974) observed a range of $\delta^{34}S$ values from -3 to +18‰ for

metasediments from the Arendal area of the Bamble sector. Carbonates of the Aphebian Lower Albanel Formation, Québec contain $\delta^{34}S$ values that average 24‰ (range = -3 to +54‰), the heavy values are interpreted to be due to formation through sulphate reduction in a restricted basin (Mirota and Veizer, 1994). Sulphides of the Mid-Proterozoic Newland Formation, Belt Supergroup, Montana (ca. 1.3 Ga) range from -14 to +18‰ (Strauss and Schieber, 1990). Australian Mid-Proterozoic sediments, the McArthur Group (1.6 Ga) and the Mount Isa Group (1.65 Ga) have $\delta^{34}S$ values that range from -8 to +30‰ (Strauss and Schieber, 1990). In the ~1.9 Ga Rove Formation near Thunder Bay, Ontario, early diagenetic pyrite is found to have $\delta^{34}S$ values ranging from +13 to +21‰, the relatively heavy values are interpreted to be due to formation in a partly closed basin (Carrigan, 1990). Mid Proterozoic seawater had a $\delta^{34}S$ value in the range of +15 to +20‰ (Mirota and Veizer, 1994). Values of $\delta^{34}S$ similar to seawater can be interpreted to have formed in a restricted basin where there is a limited source of sulphur. The fahlbands of the Modum complex are compatible with formation through sulphate reduction in a sedimentary setting, possibly a restricted basin. Percolation of seawater/brines into fault systems during a late phase of the Sveconorwegian is not supported for the origin of the fahlbands, as suggested for some quartz veins in the Modum complex (Munz et al., 1995). Graphite in the fahlbands has been metamorphosed and deformed, beyond what would be expected for lower greenschist facies. Cobaltite crystallization postdates graphite (Chapter 3) and has an ordered structure indicating that it has been metamorphosed (Gammon, 1967).

Pyrite from sample PWN 033 (Gamphue quarry) coexists with calcite and hematite and appears to be emplaced under greenschist facies conditions. The pyrite grain has a more negative $\delta^{34}S$ value than sulphides of mantle derivation, or from the selected lode Au deposits(Figure 4.23), but is within the range of igneous rocks (Faure, 1986). In the fluid, SO_4^- and H_2S would have similar activities (Figure 5.1), this oxidized composition can lead to more negative $\delta^{34}S$ values (Ohmoto, 1972).

TABLE 4.6. STABLE ISOTOPE DATA OF CALCITE FROM ØVERBYKOLLEN.

Sample Number	$\delta^{18}O_{SMOW}$ (‰)	$\delta^{18}O_{PDB}$ (‰)	$\delta^{13}C_{PDB}$ (‰)
PWN 26	7.66	-22.56	-7.88
PWN 27	6.36	-23.82	-4.05
PWN 28	4.76	-25.37	-3.86
PWN 29	4.42	-25.70	-3.92
PWN 31	5.41	-24.74	-4.99
PWN 33	4.81	-25.32	-4.77
PWN 35	5.92	-24.24	-4.88

The calcite is from two locations, sample PWN 026 is collected from Embretfoss and the rest are from the Gamphue calcite quarry. Sample PWN 026 from Embretfoss has slightly more negative $\delta^{13}C$ values. The area at Embretfoss is not well understood and will not be examined in detail.

Calcite from the Gamphue quarry and the quarry at Embretfoss (PWN 026) (Table 4.6) does not appear to be of a sedimentary origin. Calcite occurs as massive unfoliated, generally coarse to pegmatitic grains. Locally it is the matrix for brecciated, metasomatized amphibolite and other rocks; no field or microscopic observations indicate a sedimentary origin. Åtangen metasedimentary calcite-marble from the Bamble sector has a $\delta^{13}C_{PDB}$ and $\delta^{18}O_{SMOW}$ content with -3 to 0‰ and 14 to 16‰ respectively (Dahlgren et al., 1993). The range of marine limestone is -3 to 4‰ $\delta^{13}C$ (Ohmoto and Rye, 1979). The measured calcite from the Gamphue quarry has lighter values than these sedimentary carbonates (Figure 4.24b).

A carbonatite origin for the calcite-rich areas in the Modum complex and the Kragerø dolomites is not favored. Trace elements show some distinctions from carbonatites: The Fen carbonatite contains 3980 ppm Sr, 310 ppm Ba and 2 ppm Sc (Dahlgren et al., 1993); in contrast the most calcite-rich sample (PWN 28) contains 50 ppm Sr, and 40 ppm Ba and 20 ppm Sc. Silicate contamination may account for high Sc concentrations but not low Sr or Ba

concentrations. The $\delta^{18}O$ values in calcite from the Gamphue quarry has a lower range than known carbonatites (Figure 4.24a). The calcite rocks from the Gamphue quarry have negative ε_{Nd} strongly positive ε_{Sr} values (Table 4.7). the Fen carbonatites in contrast have negative ε_{Nd} and positive ε_{Sr} values (Andersen, 1987). The whole rock chemistry, including isotopic values, is distinctly unlike the Fen carbonatite.

Dolomite marbles emplaced in the Kragerø area of the Bamble sector are in many ways similar to the calcite rocks of the Gamphue quarry and may have a genetic link. Sm-Nd isotope data indicates an age of 1175±37 Ma (Dahlgren et al., 1993); the calcite rocks of the Gamphue quarry are also interpreted to be Sveconorwegian in age (e.g. Jøsang, 1966; Munz et al., 1994; this study). Some trace elements of both areas are similar, specifically both have low concentrations of Ba and Sr and high levels of Sc. The $\delta^{18}O$ values of the Gamphue rocks are slightly lighter than those of the Kragerø dolomite (Figure 4.24b). The $\delta^{13}C$ values have a large overlap (Figure 4.24b). Similar to calcite rocks from the Gamphue quarry, Kragerø dolomites have negative ε_{Nd} strongly positive ε_{Sr} values (Table 4.7).

A hydrothermal origin for calcite at the Gamphue quarry has been interpreted in the past (e.g. Jøsang, 1966; Munz and Morvik, 1991; Munz et al., 1994) a hydrothermal origin is also interpreted for the Kragerø dolomites (Dahlgren et al., 1993). There are different interpretations in the two areas for the source of the hydrothermal fluids.

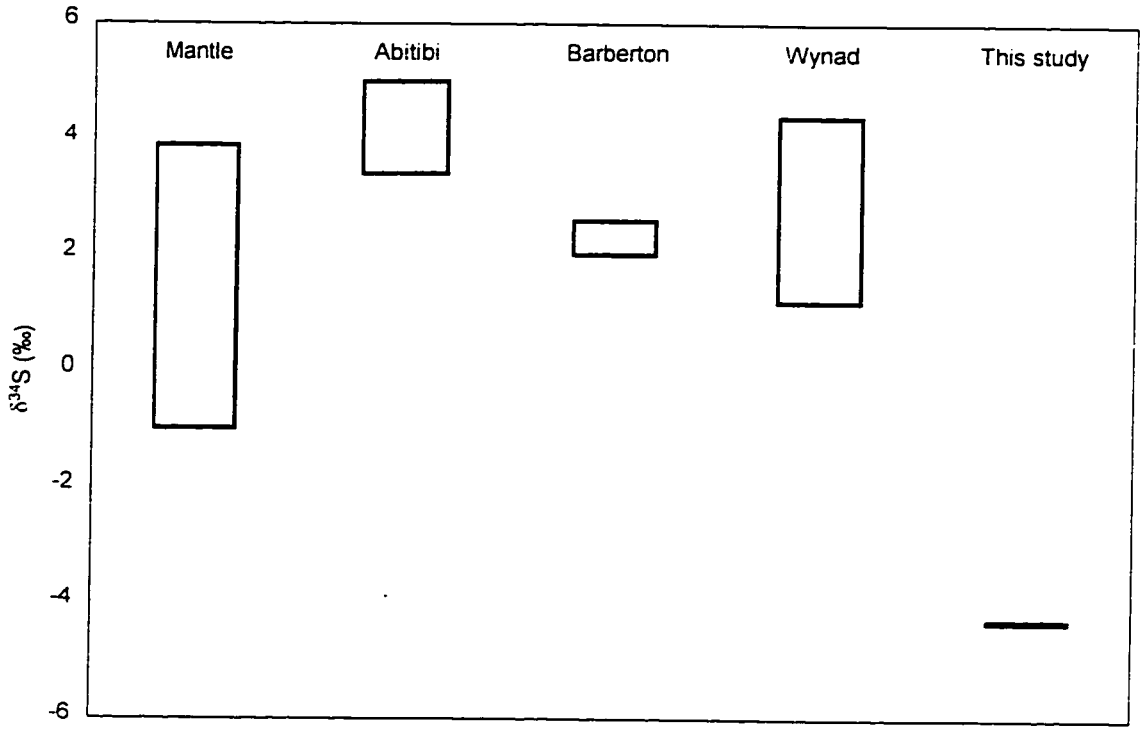

Figure 4.23. Sulphur isotope data for sample PWN 033 from the Gamphue calcite compared with carbonates from the mantle (Chaussidon, 1989); three Archean gold mines/regions the Abitibi (Canada), Barberton (South Africa), and Wynad (India) (Ronde et al., 1992; Santosh et al., 1995).

TABLE 4.7. SUMMARY OF RELEVANT PUBLISHED Sm AND Nd ISOTOPE STUDIES

	No. of Samples	ε_{Nd}	ε_{Sr}	Model Age
Modum complex (Munz et al., 1994)				
Metagabbro	1	5.3	-12.3	1224 Ma
Albitized mafic rocks	2	-0.9 to -0.3	5.6 to 160	1080 Ma
Gamphue calcite rocks	3	-1.6 to -0.9	120 to 125	1080 Ma
Bamble sector (Dahlgren et al., 1993)				
Hyperites	5	3 to 6	-10 to -5	1150 Ma
Kragerø Dolomites	8	-2 to 1	40 to 80	1150 Ma

A mantle or lower crustal source for the dolomites of the Kragerø area has been interpreted based on low Sr and Ba and high Sc, Cr and Ni concentrations as well as Sr-Nd isotope data (Dahlgren et al., 1993). The formational fluids may have escaped during late crystallization of the charnockite-mangerite intrusions (Dahlgren et al., 1993). Concentrations

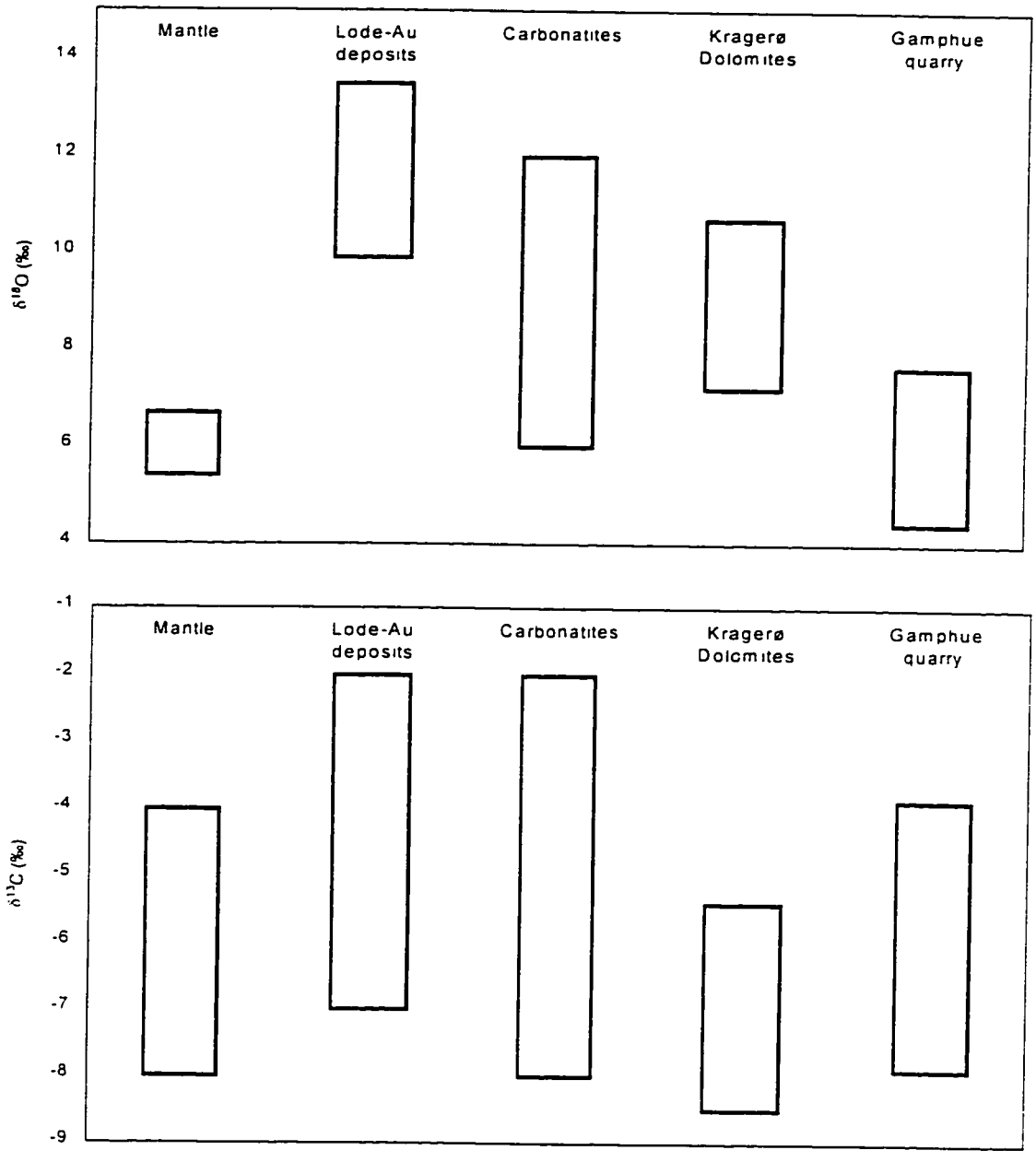

Figure 4.24 a, b. Oxygen and carbon isotope data for calcite samples from the Gamphue calcite quarry at Øverbykollen compared to 4 other carbonate types and mantle values. Archean Au deposits include Yilgarn Block (in Western Australia), Abitibi (in Canada) and Barberton (in South Africa) (Ronde et al., 1992). Mantle O values reflect average composition (Taylor, 1980) and slightly more enriched values observed in Hawaiian tholeiites (Kyser et al., 1982). Mantle C isotopes include the range for MORB values (Hoefs, 1987). Carbonatite values represent 91% and 75% of known compositions for C and O isotopes respectively (Deines, 1991). Kragerø dolomite isotope values from Dahlgren et al. (1993).

of Sc between 30 and 150 ppm found in carbonate minerals of the Tarr albitite complex, southeast Sinai have been used to suggest a mantle/ophiolite affinity (Bogoch et al., 1984). The Gjeving charnockites have ε_{Sr} ranging from 15 to 55 and ε_{Nd} from 3 to -4 and the Arendal granulites have average ε_{Nd} of -1 and ε_{Sr} of 450 (Dahlgren et al., 1993), derivation from these or similar lower crustal rocks could lead to the observed values. An alternate interpretation is that fluid was derived from a hypothetical devolatilizing carbonated upper mantle (Dahlgren et al., 1993). For the rock of the Gamphue quarry Munz et al. (1994) advocate a crustal source and disturbance of the Sm-Nd system through REE mobility.

4.6. Summary

Pyrite in the fahlbands has $\delta^{34}S$ values indicating formation during sedimentation, through reduction of sulphate, possibly in a restricted basin. The four metagabbro samples, from 2 locales display internally consistent geochemical character. The magma is derived from the partial melting of a subducted oceanic plate, with little crustal contamination. The amphibolites have more internal variation than the metagabbro samples but display many consistent chemical variations from the metagabbro samples. *A mass change during alteration of the metagabbro to amphibolite of less than 20% is interpreted in this study, based on similar major element geochemistry and petrography. The significant changes in major element concentration are higher concentrations of* Na_2O, TiO_2, P_2O_5 *and decreased* Al_2O_3. There is a general increase in the trace element content. The trace element content is higher in the amphibolites, many elements exhibit strong increases in concentration. Elements that tend to exist as ions with a +3 or higher valency (REE, U, Y, Ti, and P) are enriched in the amphibolites. There is little consistency between geochemical changes related to amphibolitization of gabbros of this study and amphibolitization of hyperites in the Bamble sector. The very high Cl content of the metagabbro samples and amphibolites suggests a strongly halogenated fluid, high fluid to rock ratios are also suggested for the amphibolitization process.

The albitization process appears to mainly affects the metagabbro samples and amphibolites. There is a continuity of concentrations of Na_2O between the amphibolites and the metagabbro samples and similar trace element trends. The interpretation that the albitites formed via hydrothermal replacement of existing rock is supported (e.g. Jøsang, 1966; Munz et al., 1994).

Skuterud ore has been documented to contain patchy, disseminated, sub-economic enrichments of Co, As, Cu, U and Ni (Gammon, 1966; Hygen, 1971; van Autenboer, 1957), this is supported and locally anomalous concentrations of Au are found in this study. As observed before, Skuterud ore is mainly enriched in the fahlbands and locally in marginal rocks: amphibolite, quartzite, and biotite schist derived from the gabbro at the contact with the metasediments.

Calcite rocks of the Gamphue quarry have a stable isotope character similar to hydrothermal dolomites from the Kongsberg sector, and like these rocks may also have a source from the lower crust or mantle.

CHAPTER 5. DISCUSSION

Four important rock types that have resulted from rock-fluid interactions have been described in Chapters 3 and 4: amphibolite, albitite, Skuterud ore, and massive calcite. Considering these rock types, this chapter will focus on: (1) Fluid conditions during the Sveconorwegian polyphase orogenic event that affected the rocks of the Modum Complex after intrusion of the gabbros. (2) Whether there is a genetic relationship between the fluids responsible for the different alterations and metasomatic products. (3) Possibilities for mobility of Au from the gabbro and conditions that lead to the low concentrations of Au in the metagabbros and amphibolites. The observed geochemical changes are summarized in Table 5.1. Semi-quantitative mass-balance calculations are made for the amphibolitization process, others are less well constrained.

TABLE 5.1. CONCENTRATION CHANGES OBSERVED RELATIVE TO METAGABBROIC ROCKS

Alteration Event	Protolith	Geochemical changes
Amphibolitization	metagabbros	-increases in elements with high field strength high ionic strength (Ti, REE, U, Th, Nb), Na, P and Fe -decreased Al, Mg, Ca variable S, Cu, Cl, and compatible elements (K, Rb, Sr, Cs, Ba)
Albitization	mainly metagabbros and amphibolites	-increased Na, Si, U, Nb, LREE, HREE? -variable Ti, -decreased Mg, Fe, Ca, Cl, Ni, S, Sr
Skuterud ore	mainly graphitic-pyritic quartzite	-increased Co, Cu, As, Au, and U -locally increased Ni
Gamphue Calcite rocks	addition of material, metasomatism of albitized and amphibolite rock	-increased Ca, CO_2, Sr, -decreased Rb, -variable REE

5.1. Nature of amphibolitization

Trace element patterns indicate that metagabbros in this study preserve largely igneous characters (Chapter 4). Sveconorwegian amphibolitization of gabbros in southwest Scandinavia has been consistently found to be nonisochemical (Table 4.4). Geochemical changes from metagabbro to amphibolite are observed to be inconsistent when the studies from southwest Scandinavia are compared (Table 4.4). Some gabbros from other studies may have been emplaced earlier than the Modum gabbros; igneous ages for these older intrusives ranges between *ca.* 1200 and 1500 Ma (de Haas et al., 1992b, Zeck and Willadsen, 1990). Amphibolitization is interpreted to be Sveconorwegian in all instances.

It was suggested by Zeck and Willadsen (1990) that it is possible to define typical geochemical changes during amphibolitization of the gabbros. Geochemical comparison of rocks from this study and others (Table 4.4) indicates significant geochemical differences between study areas. The most consistent geochemical change observed in this study, is higher concentrtions of P and the high-field strength elements including Ti, Th, U, Nb, Y and the REE elements in the amphibolites (Figure 4.20). These elements are normally relatively immobile (e.g. Weaver and Tarney, 1981), and are commonly used as petrogenetic indicators (e.g. Pearce, 1983). Possible mobility of these elements provides an example of an occasion where the altered rock does not necessarily preserve the petrogenetic character of the igneous precursor, in contrast with some rocks from the Bamble Sector (Field and Smalley, 1991). Major element changes consistent between this and other studies are increases in Fe_2O_3 and unchange SiO_2. The low-field strength elements all have large variations, increases in Rb and K observed in other studies are not observed here. The Cl content of the metagabbros and amphibolites in this study is higher by an order of magnitude than found in other studies, suggesting that the Cl activity of the altering fluid was higher than in the other areas. Cl will complex with many elements at temperatures above 350°C, it is an important transport agent in this aqueous fluid (e.g. Brehler and Fuge, 1973; Crerar and Barnes, 1976; Cathles, 1986; Haas et al., 1995). Chlorine is interpreted to have been added during subsolidous

recrystallization. Chlorine is not compatible with the igneous assemblage plagioclase, olivine and pyroxene. Differences in geochemistry due to alteration between the igneous gabbro the initial rock used for comparison (metagabbro) affect results. The metagabbros for this study contain secondary Cl, H_2O, and those with scapolite have secondary SO_2. Other studies may incorporate more or less altered rocks. A high water-rock ratio is suggested for the study area based on the large change in REE elements and the pervasive nature of amphibolitization. The altering fluid affecting the metagabbros in this study area was relatively oxidizing. Other gabbros (hyperites) in southwest Scandinavia are amphibolitized by a relatively oxidizing fluid (Table 4.4).

A large variability of S concentrations is observed by all studies and in both the metagabbros (gabbros) and amphibolites. Field and Elliott (1974) report 500 ppm and 1300 ppm S in the hyperite and amphibolite respectively. Zeck and Willadsen (1990) report 1346 ppm in the hyperite depleted to 466 ppm S in the amphibolite. In this study, and possibly that of Zeck and Willadsen (1990), scapolite occurs locally, containing SO_2. Scapolite-bearing rocks were excluded from the study of Field and Elliott (1974). The presence of secondary scapolite confirms that H_2S and SO_2 were both mobile. H_2S has a solubility similar to HCl and slightly less then H_2O in aqueous fluids in the appropriate temperatures

5.2. Nature of albitization

Albitization occurs locally at the margins of all major gabbroic intrusions in narrow veins to diffuse zones tens of metres wide (e.g. Munz and Morvik, 1991, Jøsang, 1966). Albitized rocks may contain actinolite (e.g. PWN 052 and 065) or less commonly hornblende (e.g. PWN 057 and 069); indicating that the albitization occurred at amphibolite facies, but primarily at greenschist metamorphic facies. A date for some fine-grained albitized rocks has been interpreted at 1080±3 Ma (a concordant U-Pb date for sphene) (Munz et al., 1994). General changes interpreted for the albitized samples are indicated by scatter-plots (Figures 4.1 to 4.14) and a plot of trace elements normalized to the metagabbro average (Figure 4.22).

A continuum of Na_2O concentrations is observed from the metagabbros up to the strongly albitized samples. Albitites have a pattern of trace element variations (Figure 4.22) similar to those of amphibolites (Figure 4.20). In contrast with the amphibolites, high values of Cl were not recorded in the amphiboles or other hydrous minerals of the albitized rocks (Appendix 2). Strontium is depleted in the albitite while it is variable in the amphibolites. The major element changes listed in Table 5.1 are relative to the amphibolites and the metagabbroic rocks.

There are some differences between the albitites and amphibolites in terms of chemistry, mineralogy and occurrence: but also many similarities as described above. It is possible that there is a genetic connection between the fluid responsible for the respective alterations, this is considered in Section 5.10. Amphibolites have virtually completely replaced the metagabbro, but amphibolite grade hydration and alteration is not observed to effect the metasediments. Albitization is observed in metagabbros, amphibolites, and also affects some metasedimentary rocks. Intense albitization tends to occur in veins and local zones of up to about 100 m long but does not pervasively affect units as amphibolitization does. The lower metamorphic grade of the albitites as well as field relations indicate that the albitites post-date the amphibolites. Within the group of samples considered there is a variation in some trace elements that makes characterization of albitization complex. Without a larger database of albitized samples it is not possible to accurately describe the character of these rocks.

Albitites are also observed in the Bamble Sector and are especially frequent in the Kragerø area (Green, 1956). These albitites have been interpreted to be of metasomatic origin (Green, 1956). They have the following characteristics that are similar to the albitites of the Modum Complex (from Green, 1956): (1) They occur within amphibolites and have gradation contacts with them. (2) The amphiboles are more magnesian than in the amphibolites. (3) There is local concentrations of rutile, locally as a major component

(Kragerøites), evidence of high TiO_2 concentration. (4) local actinolite and chlorite indicate greenschist facies metamorphic conditions.

5.3. Nature of Skuterud mineralization

The Skuterud mineralization is marginal to one of the major gabbroic intrusions, and is generally coincident with pyrite-bearing fahlbands. Due to a lack of unaltered samples, these rocks were not compared to other metasedimentary rocks from this area. Beyond enrichment of the elements Co, Cu, As, Ni, Au and U no definite variations from the chemistry of typical metasedimentary rocks was observed. The mineralized samples are typically siliceous metasedimentary rocks with concentrations of Na_2O, CaO, Al_2O_3, TiO_2 and REE that is similar to of rocks of sedimentary origin (Turekian and Wedepohl, 1961; Vinodgradov, 1962; McLennan, 1989). The presence of local mineralization in the amphibolite indicates that mobility of ore elements post-dates intrusion of the gabbros. Metasedimentary rocks with Skuterud ore mineralization tend to contain chlorite and retrograde muscovite, but a mineralized amphibolite (PWN 071) contains hornblende (Appendix 3). The presence of arsenopyrite in the Modum deposit (Gammon, 1967) restricts the mineralized assemblage to below 491°C (Clark, 1960). The presence of chlorite indicates a temperature below about 550°C (assuming a pressure of 4 to 8 kbar). The ordering of the cobaltite structure (Gammon, 1967) indicates ore deposition during or prior to metamorphism. The disseminated mineralization style and lack of brittle deformation related to mineralization indicates that metamorphic conditions were in the upper greenschist range or higher. Enrichment of U in the metasedimentary rocks has been dated at 1181 Ma (with a high level of uncertainty) by U-Pb whole rock methods (Andersen and Munz, 1995). There is a moderate spatial relationship between albitization and mineralization but the age relationship is unclear.

5.4. Nature of local calcite metasomatism

Two areas of massive calcite were sampled: the Gamphue quarry at Øverbykollen and a magnesite/calcite quarry at Embretfoss (south of the area covered by the geological map). Occurrences of minor, discrete calcite veining were observed rarely elsewhere throughout the study area. The calcite at the Gamphue quarry is associated with albitization and is bordered by an amphibolite unit. The changes interpreted for the calcite rocks from the Gamphue quarry (Table 5.1) are based on limited trace element data for samples PWN 028 and 031 in Appendix 3 and three samples from Munz et al. (1994). No isotopic date is available for this unit. Field relations indicate that it postdates or is synchronous with albitization. Associated muscovite and chlorite indicate greenschist grade metamorphic conditions. The interpreted Sveconorwegian age is supported (Munz et al., 1994). The trace element and stable isotope character is similar to hydrothermal dolomite from the Kragerø area of the Bamble Sector. A hydrothermal origin is indicated for the calcite rocks of this area.

5.5. Oxygen fugacity of fluids affecting the rocks

5.5.1. approach used to calculate fO_2

The oxygen fugacity (fO_2) of altered rocks describes the oxygen activity in the magma or altering fluid. The fO_2 of hydrothermal fluids plays an important role in defining the solubility of speciation of S in the fluid and the solubility of Au. At temperatures above about 350°C Cl^- complexes become more significant in the solubility of Au (Cathles, 1986; Seward, 1984; Zotov et al., 1989). The solubility of Au as $AuCl_2^-$ increases with fO_2; making an oxidized high temperature fluid suitable to mobilize appreciable Au (Seward, 1984). An oxidized magmatic system may favour the partitioning of Au into magmatic aqueous fluids (Cameron and Hattori, 1987). A high fO_2 fluid will oxidize pyrrhotite to pyrite and magnetite, this can mobilize Au contained within pyrrhotite (Cameron et al., 1993). Evidence of ore-fluids with high fO_2 are observed at Hemlo, McIntyre-Hollinger, Macassa, Lake Shore, and Ross all in Ontario, and Kalgoorlie in Australia.

The fO_2 at which the rock mineral assemblage equilibriated is described by the mineral assemblage and mineral composition, mainly Fe oxides, including hematite, magnetite and ilmenite. In the Fe oxides the Fe^{2+} / Fe^{3+} composition may adjust along solid solution ranges, or recrystallization to different oxides can accommodate the change in fO_2 (e.g. Frost, 1991a). Some silicates, including amphibole, biotite and chlorite, can accommodate a limited amount of Fe^{3+}. In silicates, Fe^{3+} substitutes primarily for Al. Fe^{3+} in silicates is not used as an indicator of oxidation state in this study, partially due to inaccurate stoichiometric distinction of Fe^{2+} to Fe^{3+} concentrations based on microprobe results (P. Jones, personal communication, 1993). The oxide assemblage is interpreted to have approached equilibrium with the fluids that have passed through the rock.

Commonly acting as buffers to the fO_2 of the fluids affecting rocks of this study are redox reactions of sulphide-sulphate and graphite-CO_2 in some metasedimentary rocks. Oxidation-reduction reactions are typically insensitive to pressure; fugacities of equilibria are often plotted on fO_2 or ΔfO_2 vs. temperature plots that include experimentally calculated buffers. The ΔfO_2 format used here is fO_2 normalized to the fO_2 of the fayalite-magnetite-quartz buffer (FMQ). The oxygen buffers used in Figure 5.1 are from equilibrium calculations by Frost (1991a), they are calculated at 2 kbar, though they are relatively insensitive to pressure.

The sulphide-sulphate fence is the locus of points where the fugacities of SO_2 and H_2S are equal. SO_2 is the dominant species above the fence and H_2S dominates at fO_2 below the fence (Frost, 1991c); related to the following equilibrium:

$$2H_2S + 3O_2 = 2H_2O + 2\ SO_2$$

The presence of sulphate-bearing scapolite is presumed to reflect oxygen fugacities near or above this fence, literature calculating the fO_2 stability range of SO_2-bearing scapolite was not uncovered. The sulphate-sulphide fence in Figure 5.1 is from Whitney (1988), it is calculated for 1 kbar and is close to isobaric.

The graphite-CO_2 fence represents the upper stability limit of graphite in fO_2 -T space. The curve used in Figure 5.1 is from Ohmoto and Kerrich (1977), it is calculated for 4 kbar; with increasing pressure, the curve occurs at slightly higher fO_2 values.

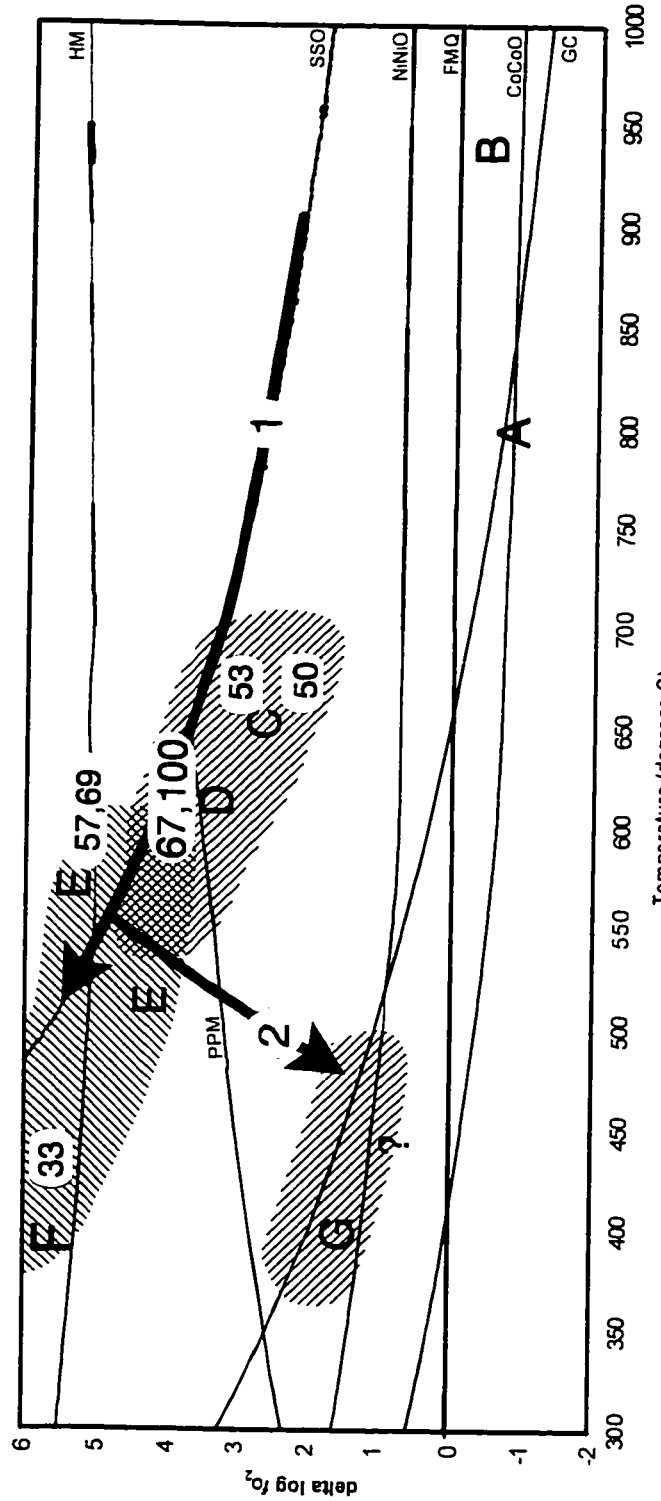

Figure 5.1. Diagram of $\Delta \log f_{O_2}$ vs. temperature with common oxygen fugacity buffers and significant stability fences normalized to the FMQ buffer, see Table 5.2 for abbreviations. The interpreted oxidation conditions are graphitic supracrustals (peak metamorphic assemblage), **A**; gabbros, **B**; metagabbros, **C**; amphibolites, **D**; albitized rocks, **E**; calcite rocks, **F**; and Skuterud ore, **G**. The hatched areas represent the ranges for the enclosed fields. Numbers identify approximately located samples e.g. 33 represents PWN 033. Two interpretive fluid evolution trends are marked. Trend ① describes the fO_2-T evolution of a fluid along the SSO fence. The character of this fluid matches that of the fluid responsible for the metagabbros, amphibolites, albitites and calcite rocks. Trend ② represents reduction of fluid ① by graphitic metasedimentary rocks, inducing Skuterud ore to precipitate from the fluid.

TABLE 5.2. ABBREVIATIONS USED IN FIGURE 5.1.

Buffer/Fence abbreviations	Buffer reactions/ Fence
CoCoO	cobalt to cobalt oxide
FMQ	fayalite to magnetite-quartz
PPM	pyrrhotite to pyrite-magnetite
MNO	manganosite to hausmannite
MH	magnetite to hematite
CC	copper to cuprite
GC	graphite-carbon dioxide
SSO	sulphide-sulphate, ($fH_2S = fSO_2$)

5.5.2. fO_2 of gabbros

The positive Eu anomaly in the metagabbros is not observed in the amphibolites (Figure 4.16), indicating that Eu occurred as a 2+ ion in the gabbroic magma and as a 3+ ion in the hydrothermal fluid responsible for amphibolitization. The valency of Eu indicates that the gabbroic magma was less oxidized than the amphibolites and Field **B** (Figure 5.1) is placed at a lower fO_2; there are no other factors used to constrain the fO_2.The temperature for area B is placed at near 1000°C. Munz and Morvik (1991) predict 1000-1100°C.

5.5.3. fO_2 of metagabbros

The mineral assemblages of the metagabbros indicate metamorphism at amphibolite facies conditions; pressure is estimated at about 5-8 kbar (Munz and Morvik, 1991). At these pressures hornblende is stable between 500 to 700°C. Rutile and hematite locally partially replaces ilmenite as high temperature oxidation products (Haggerty, 1991). The occurrence of rutile and $ilmenite_{ss}$ (Plate 3.7a) indicates an fO_2 between NiNiO and HM (Lindsley, 1991). The assemblage of rutile + $ilmenite_{ss}$ + $hematite_{ss}$ observed in sample PWN 053 (Plate 3.7b), associated with a slightly higher fO_2 , also below HM, is present in the assemblages at 600 through 400°C (Lindsley, 1991).

Trace pyrite ± pyrrhotite is observed in all metagabbros and SO_2-bearing scapolite is present in contact with pyrite in two of the metagabbros (PWN 053 and PWN 051). Samples

with scapolite and a sulphide are placed on the SSO buffer. Pyrite and magnetite is observed replacing pyrrhotite in samples PWN 118.2 and 50, putting these at temperatures below about 630°C and above the PPM buffer. The temperature- fO_2 range for oxides of the metagabbros is interpreted to be the hatched area C of Figure 5.1.

5.5.4. fO_2 of amphibolites

The amphibolites are not distinguished from metagabbros in fO_2-temperature space: they share the same hatched field in Figure 5.1 (Field **D**). The temperature range, like the metagabbros, is delimited by the presence of hornblende. The amphibolites typically contain ilmenite with minor exsolution of hematite in thin lenses. Assemblages where hematite and ilmenite are both present can be placed between the NiNiO and HM buffers (Lindsley, 1991). Trace magnetite occurs in some amphibolites, always in equilibrium with pyrite (Plate 3.6b) including samples PWN 061, 067, 068, 100, 103, 114, 118.1 and 118.2. The presence of magnetite and pyrite places these samples above the PPM buffer, placing an upper temperature limit on these rocks. The upper limit of fO_2 is described as being close to the SSO fence by the presence of pyrite with all 13 occurrences of scapolite, and below the HM buffer by the absence of hematite without ilmenite.

5.5.5. fO_2 of albitized rocks

Mafic rocks that have been partially or intensely albitized contain significant hematite. Some of the Na-enriched mafic rocks such as PWN 054, 065, 096 and 099 contain composite grains where lenses of hematite constitute more than 10% of the host ilmenite grain. In PWN 065 exsolution of hematite accounts for about 45% of the grain area. Two Na-enriched amphibolites samples contain isolated grains of hematite and some hornblende (PWN 057, 069, Figure 5.1). Intensely albitized rocks contain only hematite, if they contain an Fe oxide e.g. PWN 40, 52 and 56; these have stabilized above or near the HM buffer. Most of the albitized samples contain actinolite or tremolite and no hornblende, this indicates

that metasomatism occurred below 500°C. The albitized rocks tend to fall in Field **E** of Figure 5.1.

5.5.6. fO_2 of graphitic fahlbands and Skuterud mineralization

Field **A** (Figure 5.1) represents the general area at which sillimanite and graphite-bearing fahlbands would have equilibriated during peak conditions of Svecofennian metamorphism. Chlorite and muscovite growth during Sveconorwegian metamorphism indicates retrograde greenschist metamorphism. Hatched Field **G** (Figure 5.1) represents a rough fO_2 range for these retrograded metasedimentary rocks (including fahlbands) that contain local graphite and includes the Skuterud ore. Fluid trend **2** (Figure 5.1) represents the reduction of a relatively oxidized fluid due to intersecting the reduced graphitic rocks.

5.5.7. fO_2 of Calcite rocks at Øverbykollen

Calcite-rich samples from the Øverbykollen contain hematite and pyrite in equilibrium. This assemblage places the rocks near or above the magnetite-hematite buffer and below the sulphide-sulphate fence (area **F**, Figure 5.1). The presence of local chlorite in breccia fragments is congruent with the rock forming at lower temperatures.

5.6. pH of fluid as indicated by mineralogy

Figure 5.3 illustrates conditions that may be broadly similar to fluids considered in this study, limitations on the understanding of the fluid and conditions prevent modeling for this fluid. Figure 5.3 can be used to estimate the relative pH range based on the stable and replaced mineral assemblage. For fixed levels of a_K and a_{Na} increasing a_{H^+} (pH) will form a positive slope intersecting various stability fields. A fluid with a pH close to neutral may precipitate muscovite (or biotite) while a more alkaline fluid would precipitate albite or K-feldspar depending on the activities of K and Na. The stability fields are also affected by factors such as temperature, pressure and rock chemistry; a fluid with fixed activities (i.e.

fixed location on Figure 5.3) may cause different alteration depending on these conditions (Böhlke, 1989).

Most amphibolites do not contain biotite (which would roughly occupy the muscovite field), they may have a more alkaline pH. The dominance of albitite and normal lack of muscovite in albitized samples is consistent with an alkaline fluid. The fluid associated with the calcite rocks of the Gamphue quarry has a lower limit on pH marked by the stability of calcite; in metasomatized rock fragments within the calcite both albite and muscovite occur. The presence of muscovite and lack of K-feldspar in some metasediments appears to be an indication of acidic conditions.

5.7. Skuterud mineralization model

The pyritic-graphitic fahlbands host most of the Skuterud ore. As stated in Chapter 2 fahlbands refer to the N-S bands of disseminated pyrite ranging throughout the Kongsberg Sector and/or pyrrhotite with local areas that are also graphitic. As indicated in Chapter 4, the pyrite and graphite of the fahlbands have S and O stable isotope characters indicating that they have originated from a sedimentary source. The pyrite appears to be formed through reduction of seawater sulphate. Local remobilization of the fahlband pyrite during metamorphism is possible.

Skuterud ore (enriched in Co, As, Cu, U, Au, Ni) is interpreted here to postdate the fahlband formation for five main reasons. Sulphides locally rim graphite and muscovite, indicating late mobility of sulphides (Plate 3.9b). Some mineralization occurs in amphibolites (PWN 025 and 071). Cobalt mineralization only occurs marginal to the amphibolitized gabbroic intrusion and not beyond (Gammon, 1966). The mineral association is atypical of known sedimentary deposits (e.g. Guilbert and Park, 1986). An uncertain date for U enrichment is 1181 Ma (U-Pb whole rock) (Andersen and Munz, 1995) indicating a Sveconorwegian origin for U. Mineralization is interpreted not to post-date Sveconorwegian

metamorphism based on the sulphide association with chlorite and the ordered structure of cobaltite suggested to be a metamorphic affect (Gammon, 1967).

The presence of muscovite as the dominant retrograde mineral in metasedimentary rocks indicates a neutral to acidic pH (Figure 5.3, 5.4), stability of graphite indicates reduced conditions (Ohmoto, 1972). Premineralization the fahlbands had a reduced and acidic nature; under different fluid conditions than illustrated in Figure 5.4 graphite and pyrite may be stable together (e.g. Leitch et al., 1991).

The mineralizing fluid may initially be near the hematite-pyrite fence and within the albite stability field; evidence for fluids with lower fO_2 levels has not been observed. At the extreme northern pit of the Skuterud mine, hematite-bearing albitized rock occurs marginal to the ore (e.g. PWN 070). This fluid was reduced (and probably acidified) upon reaction with graphite in the fahlbands, forming CO_2 (Trend 2, Figure 5.1). Reduction and acidification(?) of the fluid lead to metal precipitation (Section 5.8). Sulphur contained in the ore minerals such as Co-bearing pyrite, cobaltite, arsenopyrite and chalcopyrite may either be from the hydrothermal fluid or remobilized from fahlband pyrite.

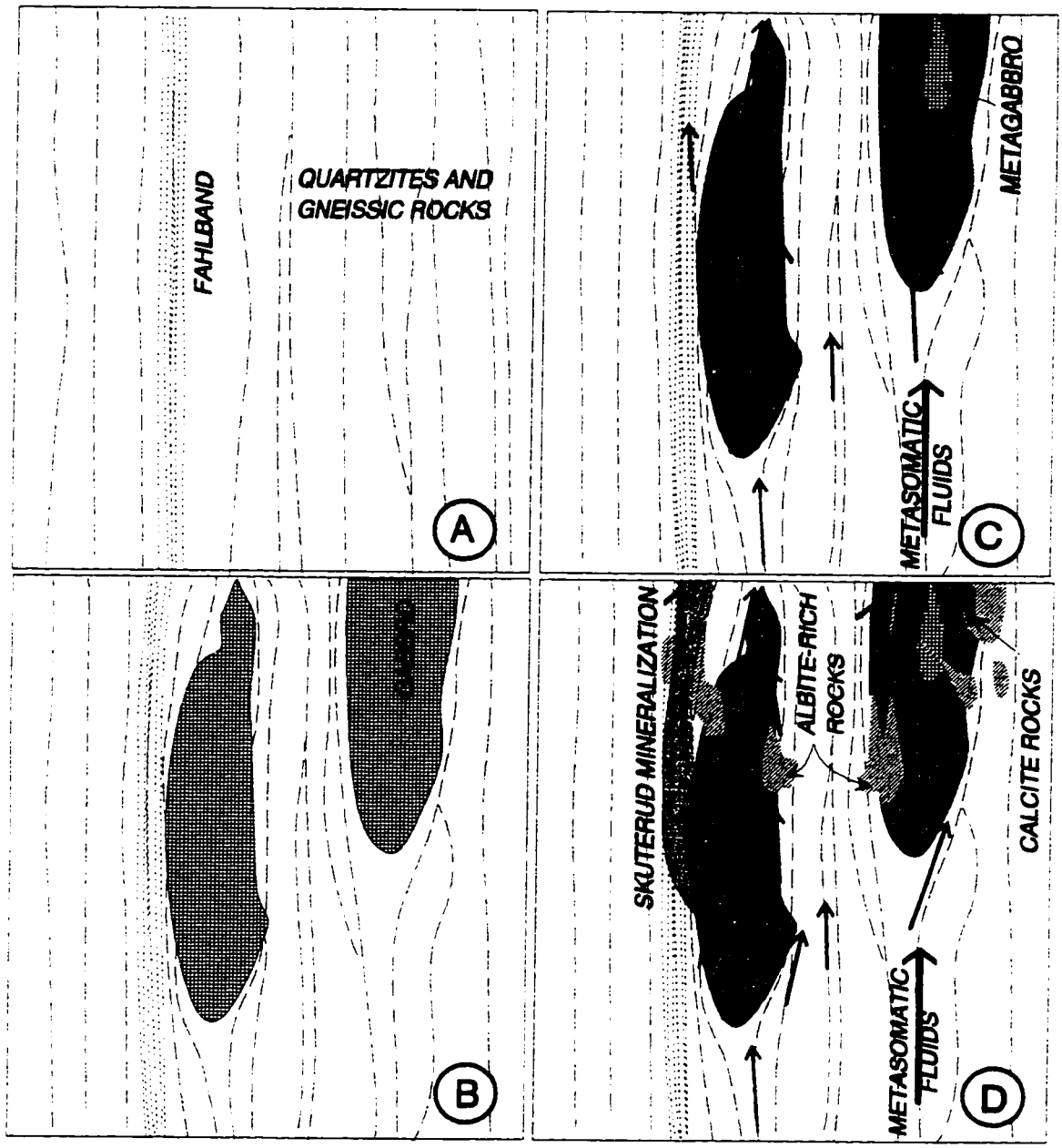

Figure 5.2. Sequential idealized cross-sections for intrusion of gabbros and hydrothermal alteration in the Modum Complex. A strike width of about 500 m is represented. In frame **A** metasedimentary rocks including pyrite-graphite-bearing fahlbands affected by ductile deformation and sillimanite grade metamorphism in a mainly transpressive tectonic environment are represented. Frame **B** shows intrusion gabbros during a transtensional tectonic setting. Frame **C** represents isobaric cooling of the area with metasomatic high fO_2 fluids altering the gabbro to amphibolite, metagabbro is preserved in some cores. In frame **D** high fO_2 fluids produces albite-rich rocks, Skuterud mineralization and calcite rocks mainly at greenschist grade metamorphic conditions.

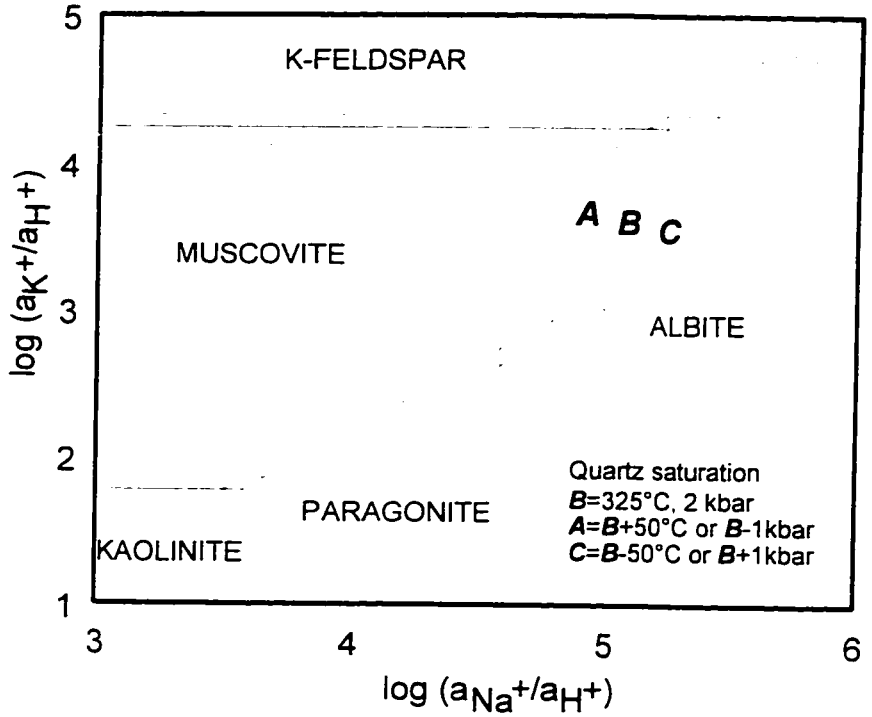

Figure 5.3. Activity diagram showing the relative stability fields of Al-bearing phases in amphibolite. Activities are based on activities of analyzed phases from amphibolites in Alleghany, California. The considered physical conditions are indicated by the fields A, B and C. The stability field of muscovite expands with decreasing Al/(Cr+Mg+Fe), the muscovite field is larger for ultramafic rocks and smaller for granites. Albite can precipitate when conditions move fluid within the albite field, this same fluid may not precipitate albite for a different set of conditions or in a different host rock (After Böhlke, 1989).

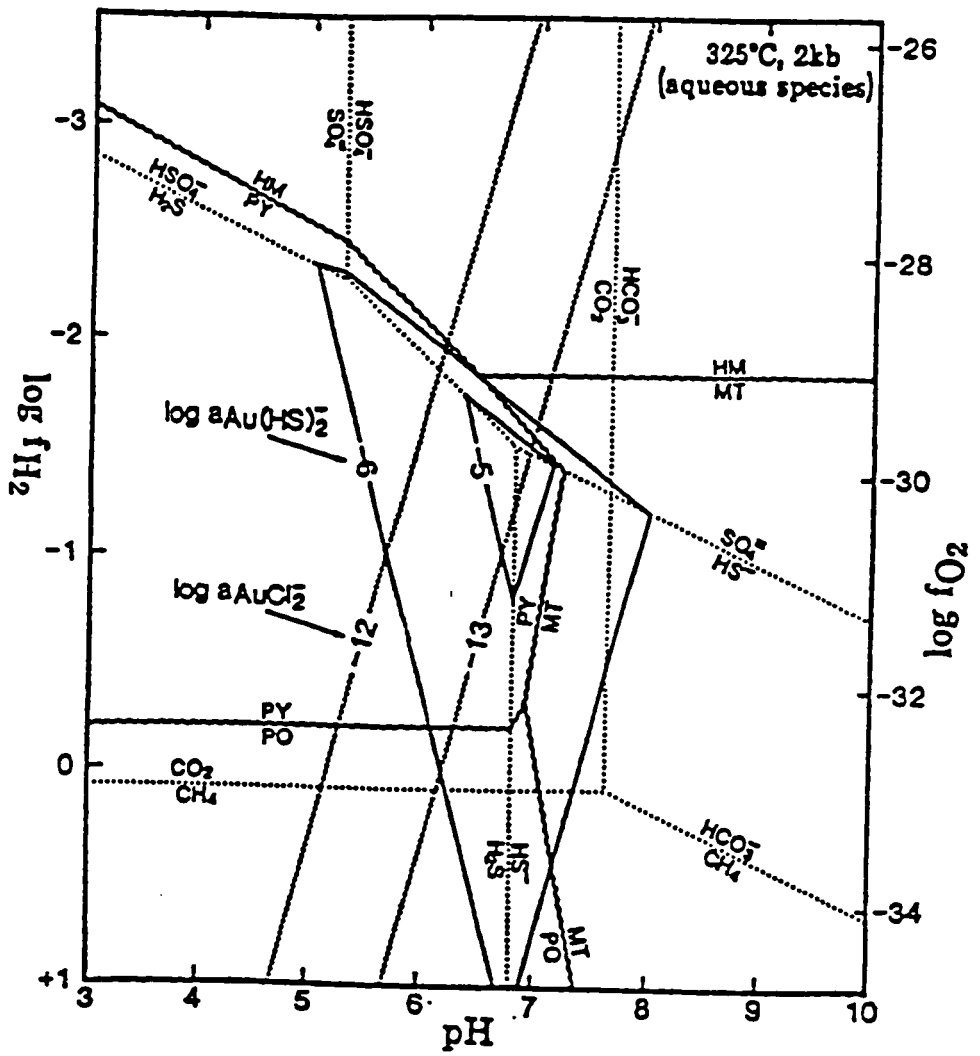

Figure 5.4. Simplified log fO_2 vs. pH diagram with activities contours of $AuCl_2^-$ and $Au(HS)_2^-$. Fluid parameters are those used by Böhlke (1989). The gold is at saturation, log $aAu(H)2^-$ = -6.0 is approximately equal to 0.5 ppm. Fence lines for equal activities of carbon and sulphur are shown for reference. Symbols are as follows PO = pyrrhotite, PY = pyrite, MT = magnetite and HM = hematite. For a typical amphibolite albite is stable above a pH of about 5.8, and muscovite is stable at lower pH levels (After Böhlke, 1989).

The mineralizing fluid, if related to albitization, would have a pH that is likely alkaline (Figure 5.3, albite stable), be close to the sulphate - sulphide fence and within the pyrite stability field (Figure 5.4). The presence of hematite in albitized rocks proximal to mineralization indicates an fO_2 that is close to or above the magnetite buffer. On Figure 5.4 the mineralizing fluid would plot close to the region of maximum Au solubility. Intersection with the fahlbands converts graphite to CO_2; consuming O_2 in the fluid and acidifying the fluid by addition of CO_2 (Leitch et al., 1991). Either or both of these changes will lead to reduced solubility of Au and precipitation. These changes are indicated by the low Na_2O content of the mineralized samples, the typical presence of muscovite, and the presence of ilmenite (PWN 010, 025) or no oxides. The fluid chemistry and physical conditions for the Skuterud mineralization may be somewhat different than Figure 5.4, but this is conceptually representative. Other representations of Au solubility in fO_2-pH space are similar (Seward, 1984; Hayashi and Ohmoto, 1991): most gold in the modeled temperature range (up to 350°C) is complexed as $Au(HS)_2^-$ and $HAu(HS_2)$ with lesser $AuCl_2$.

The precipitation of some of the other metals is also explained by the above model. Uranium is mobilized as a +6 ion. Reduction of U^{6+} causes precipitation, in this case forming uraninite. Modeled at 250° and 350°C and, it is interpreted that CuCl will be the predominate Cu complex in typical mineralizing solutions; which are more saline than typical Au mineralizing fluids. Solubility of Cu and other metals complexed with Cl decreases with increased activity of H_2S, increased pH, decreased Cl^- concentration (e.g. dilution) decreased temperature, or fO_2 is decreased (Crerar and Barnes, 1976; Barnes, 1979). Arsenic commonly occurs with Au in lode gold deposits, chemical behavior similar to Au is expected.

Gammon (1966) notes that Co mineralization only occurs proximal to the amphibolite unit, suggesting that the Co originates from the mafic unit. Co falls within a narrow concentration range for both metagabbros and amphibolites (Figure 4.22), suggesting that it is not mobile. S and Cu, in contrast, appear to be very mobile. Ni is depleted during

amphibolitization, though there is only a minor enrichment of Ni in the Skuterud ore. Levels of As generally below detection limit in the metagabbros and amphibolites restrict interpretations of mobility. The apparent immobility of Co suggests that the mafic rocks were not a source for Co, but the mobile character of S and Cu make interpretation tenuous. Comparing metals in the amphibolite unit adjacent to the mineralization to the other intrusions in the study area may indicate that this body is depleted; an interpretation of this sort is not possible with the samples for this study. Three U-bearing deposit types have some similarities with the Skuterud mineralization: arsenide vein silver, uranium deposits (e.g. Cobalt, Ontario silver mines); unconformity-associated uranium deposits (e.g. Athabasca type deposits such as Rabbit Lake); and uranium deposits in the Lagoa Real region of Brazil. The unconformity-associated U deposits contains U ore and byproducts Co, As, Se, Ag and Mo. The mineralization may be from circulation of oxidized groundwater? or diagenetic? waters (Tremblay and Ruzicka, 1984). Arsenide veins may contain ores of Ag, U and byproducts of As, Co, Ni, Cu, and Bi; a generalized genetic model is one fluids circulating, possibly initiated by mafic sills that may be the source of the metals. In the Lagoa Real district associated with the U is V, Pb and Sr; Sr isotopes indicate that the fluid is not locally derived (Lobato and Fyfe, 1990).

There is not a definitive alteration assemblage associated with Skuterud ore. Most ore occurs in fahlbands, but it is also found in amphibolites and albitized rocks. As considered further below, a single fluid may be responsible for the higher temperature amphibolitization and the subsequent lower temperature albitization. Reduction of this fluid during the different alteration processes can explain the different alteration associated with the mineralization.

In Figure 5.2 the fluid is shown to come from below. Munz et al. (1995) interpret methane and other hydrocarbons in fluid inclusions within quartz veins to have an organic source. The quartz veins are interpreted to have formed at 1-2 kbar and 250-300°C based on fluid inclusions. While quartz veins are not observed to be related to mineralization a surface derived fluid could be used to interpret an Athabasca unconformity type U mineralization

event. The disseminated mineralization does not appear to be related to brittle deformation and it is difficult to produce deep conditions where $P_{fluid} > P_{lithostatic}$ by a descent model: especially in plastic rocks (Lobato and Fyfe, 1990). The lack of chlorite in the amphibolites suggests that the Skuterud ore formed at lower temperatures, there is however, an overlap in the stability range of hornblende and chlorite between about 450 and 550 °C.

Alteration or albitization is commonly observed with Au mineralization. Examples of albitization include Alleghany, California (Böhlke, 1989); Bardoc-Kalgoolie area, Western Australia (Witt, 1991); and McIntyre-Hollinger, Timmins (Spooner et al., 1985; Wood et al., 1986). It is indicated above that a fluid that precipitates albite (Figures 5.3, 5.4) may be in the pH range where Au is most soluble. This may be also true for potassic alteration. Böhlke (1989) illustrates that for different wall rock assemblages or for similar fluids under different temperature and pressure conditions different alteration assemblages may stabilize. Gold is at a low concentrations in the mafic rocks prior to albitization, and albitized rocks also have less than 2 ppb Au.

Fluid inclusion studies of hydrothermal rocks in Modum Complex generally indicate high salinities which is not expected for fluids related to lode Au deposits. Orthoamphibole-cordierite rocks and white-schists that record Sveconorwegian isobaric cooling in the range of 800-600°C and 6-8 kbar (Munz, 1990) contain fluid inclusions of brines, secondary trails of CO_2 or CH_4 also occur (I. A. Munz unpublished data, see Munz et al., 1995). Quartz veins interpreted by Munz et al., (1995) to be related to albitization contain fluid inclusions with salinities that range from 0 to 23% or with hydrocarbons that are interpreted to have a biogenetic source. During field work by this author, the minor local quartz veins appeared to have a less than clear association with albitization, though quartz veins were not investigated intensely.

The metal assemblage of the Skuterud ore is not typical of lode Au mineralization, the ratio Au to base metals is normally higher than observed here; As and to a lesser extent Cu may be enriched (E.g. Guilbert and Park, 1985). The fluids that lead to the Skuterud

mineralization were probably more saline than typical fluids related to lode Au processes (Chapter 1) based on the base metal content, some saline inclusions and Cl-rich assemblages. It may be possible that phase separation of the fluid could produce a brine and a Au-bearing CO_2-rich, low salinity fluid, but this is speculative and no evidence for such a process is interpreted.

5.8. Au depletion in metagabbros and amphibolites

There are low concentrations of Au observed in the metagabbros and amphibolites (0.58 ppb) relative to the average concentrations observed for similar rocks types by others (e.g. 4.1 ppb (Boyle and Jonasson, 1984)); as described in Section 4.5. Possible causes for the low Au values are described in the following three sections. The Au either was not present in the gabbroic magmas, the Au was removed from the magma or the Au was removed from the rock during initial alteration of the gabbro to metagabbro.

5.8.1. Magmatic immiscibility of a sulphide phase

This section considers the possibility that Au was removed from the gabbro prior to emplacement. Magmatic sulphide deposits including the Merensky Reef of the Bushveld, Noril'sk, Kambalda, and some of the mines in the Sudbury Complex form a generalized deposit type occurring in utramafic to mafic igneous rocks. They are characterized by rocks enriched in Ni, Cu, PGE, and Au. Within southern Norway there is an abundance of small deposits hosted by mafic to ultramafic intrusions. In the event that a sulphide phase separated from the gabbroic magmas of the Modum Complex some Au would have been removed from the silicate melt to the sulphide phase. This would account for the low Au concentrations measured in the metagabbros. The most significant contributing factors to formation of an immiscible sulphide liquid phase in the silicate melt is higher concentrations of S and ferrous Fe, and increases in oxygen fugacity of the silicate melt.

Distribution coefficients between silicate and sulphide phases for platinum group elements and Au is not well constrained; estimates range from 100 to 100,000 (Barnes et al.,

1987; Boyd et al., 1988). Naldrett et al. (1979) assume values of 1500 for Pd and 1000 for Pt based on unpublished data from others. The relative concentrations of PGE and Au is generally maintained within an order of magnitude between the mantle concentrations and those observed in magmatic sulphide deposits (Barnes et al., 1988).

Norway has historically been a major producer of nickel, supplying half of the worlds nickel during the period from 1843 to 1880 when there were up to 40 mines operating in southern Norway. The deposits occur within norites, with most of them along the coast in the Bamble Sector and to a lesser extent in the Kongsberg Sector. Mineralization typically occurs near the basal portion of the intrusions and is generally thought to have formed through liquid immiscibility in sulphide-silicate melts; these interpretations were introduced in the region by Vogt (1893). The host rocks are thought to be of a similar age as the Modum Gabbros (Boyd et al., 1987). The Ringerike area in the northern part of the Kongsberg Sector contains small deposits in a north-south zone 2 km by 25 km long. The Ertelien deposit is the largest of these, having produced 1500 tonnes of nickel and half this tonnage of copper (Bugge, 1978). The deposit can be separated into two zones, a central zone of Ni>Cu and a peripheral area of veins where Ni>>Cu, with Au concentrations that average 111 and 1434 ppb respectively (Boyd et al., 1988). The deposit is associated with a small noritic plug that is 600 by 450 m in area at surface.

The metagabbros used in this study all contain trace amounts of fine pyrite, one sample contains slight trace amounts of pyrrhotite (PWN 050). As discussed in Chapter 4 the pyrite in these samples is likely a replacement of igneous pyrrhotite. The presence of igneous sulphides indicates that at some point the S concentration in the silicate liquid exceeded the level for saturation forming a sulphide phase, typical of gabbros. The observed concentrations of sulphides in the metagabbros and protoamphibolites are low (<<1%). Exsolution of a sulphide phase may have occurred earlier in the igneous process, however, no sulphide clots were observed in the amphibolites or metagabbros in the area, this phase, if it exists, has separated from the gabbro.

A hypothetical sulphide phase would have needed to have been removed from the Modum gabbros and possibly concentrated in unobserved massive lenses. No sulphide clots were observed during field work for this study, nor are they described by previous mappers (Jøsang, 1966; Munz and Morvik, 1991).

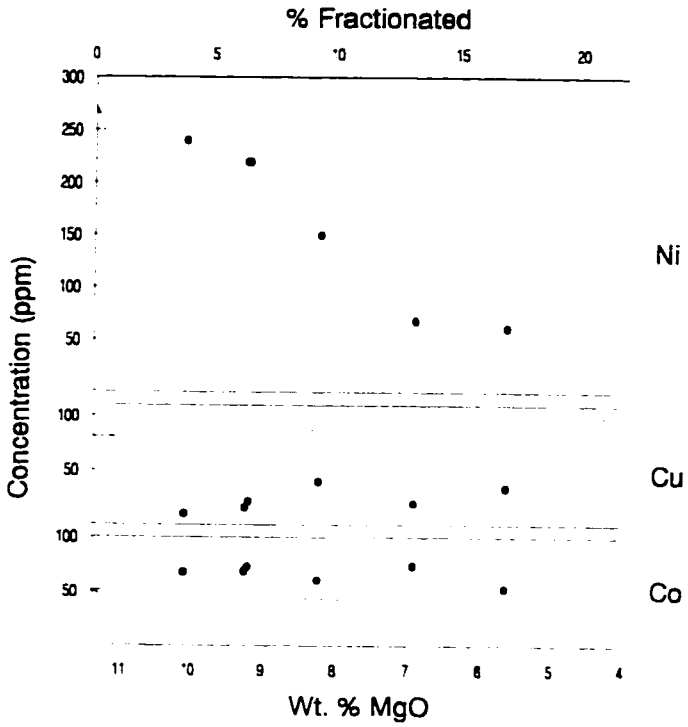

Figure 5.5. A computer simulation of the fractionation of chalcophile elements versus MgO using initial compositions corresponding to the most magnesium-rich MORB from FAMOUS area of the Mid-Atlantic ridge (Duke, 1979). The fractionation trends are a result of removal of only olivine for a sulphide under-saturated magma (solid lines), and removal of olivine and a sulphide phase for the trends where sulphide saturation is reached in the magma (dashed lines). Short dashed lines represent a silicate / sulphide phase concentration ratio of 100 and long dashed lines represent a ratio of 10. Sample points are for metagabbros from this study and two proto amphibolites (lower MgO concentrations). Ni follows the trend of a magma that does not have an extracted sulphide phase. Co and Cu do not appear to be affected by fractionation or indicate extraction of a sulphide phase.

Through field observations or geochemical interpretations there is no evidence for extraction of a sulphide phase from the silicate phase of the gabbroic melt. As stated before

no magmatic concentrations of sulphides have been observed in the study area. Compared to MORB from the Mid-Atlantic ridge (Duke, 1979), the metagabbros have a high concentration of Co and a low concentration of Cu. Ni concentrations are comparable. The decrease in Ni with MgO is compatible with fractionation of olivine from the melt, also indicated by the cumulate habit of olivine in the metagabbros (e.g. Munz and Morvik, 1991).

5.8.2. Partitioning of Au into an aqueous magmatic phase

Magmas derived from a subducting oceanic plate will be hydrated due to partial melting of altered oceanic rock. The ubiquitous subsolidous recrystallization (coronitic texture) is evidence for an aqueous phase affecting the rocks during crystallization. A basaltic magma at 8 kbar may contain up to 12 wt. % H_2O and moderately less HCl and H_2S (Burnham, 1979). An aqueous phase will separate from the magma before or during crystallization and will affect the process of crystallization (Burnham, 1979). Chalcophile elements are strongly partitioned into the aqueous phase (Holland, 1972).

5.8.3. Extraction of Au by a fluid from the gabbro during formation of the coronas

During subsolidous and any metamorphic alteration that occurred in the metagabbro Au may have been transported from the rock. Most Au present in the magmatic phase of the gabbroic intrusions would precipitate within pyrrhotite grains; pyrite is not stable above 742° C (Barton, 1969; Barton and Skinner, 1979). In the metagabbros trace pyrite is observed in all samples and trace pyrrhotite in two samples (PWN 050 and 120). The pyrite is a secondary mineral indicating recrystallization of the sulphides in the metagabbro. Pyrrhotite may be oxidized to form pyrite and magnetite according to the following reaction which occurs along the PPM buffer (Figure 5.1):

$$6FeS + 2O_2 = 3FeS_2 + Fe_3O_4$$

Magnetite is observed with pyrite and pyrrhotite in PWN 050 and with pyrite in several amphibolites. Recrystallization of pyrrhotite formed at high temperatures to pyrite has been observed to cause a net loss of Au in the sulphide (Cameron et al., 1993). Several pyrite

grains from the samples PWN118.1 and PWN 067 contain pyrite grains with associated magnetite mantling the grain and as inclusions with some 90 degree angles (Plate 3.6b); this texture is the same as observed in sulphides from the Bamble Sector that have recrystallized from pyrrhotite (Cameron et al., 1993). Especially in the amphibolites, where variable S contents suggest mobility, it is unlikely that all pyrite associated with magnetite is a recrystallization of pyrrhotite. Magnetite can also be formed according to the reaction:

$$3FeS_2 + 6H_2O = 6H_2S + O_2 + Fe_3O_4$$

5.9. Model of fluids and synopsis

A possibility introduced in the Skuterud ore mineralization discussion, is that the fluid responsible for albitization is the same as the fluid responsible for amphibolitization at higher temperatures. One apparent major difference between the amphibolites and the albitites is the pervasive nature of amphibolitization and the local nature of albitization. During amphibolitization the metagabbroic rocks may have had a higher permeability, possibly due to a minor volume loss. The greenschist facies conditions of albitization should be more brittle than during amphibolitization, and the mafic bodies may have been hotter than the surrounding rock during amphibolitization. Oliver et al. (1990) experimentally found that during deformation of a rigid body with in a weaker matrix, low pressure zones will occur marginal to the rigid body (i.e. amphibolite); these zones become favorable pathways for fluid flow (e.g. albitizing fluid). Plastic deformation of the mafic bodies would not produce these high permeability strain zones (amphibolitization)

The hypothesis of genetically linked fluids responsible for amphibolitization and albitization is supported by the observed similarities in trace elements (Figures 4.20 and 4.22), the increased Na_2O in amphibolites and the spatial association with gabbroic intrusions. As illustrated in the scatter-plots of Chapter 4 there is a continuum of Na_2O concentrations from the amphibolite to the samples considered albitized. Similar ε_{Nd} and ε_{Sr}

values for amphibolites and albitites have been measured (Munz et al., 1994; as reported in Chapter 4).

An apparent difference in fluid composition arises when the lower Cl content of amphiboles and micas in the albitized samples (Appendix 3) are compared to the Cl-rich amphiboles of the amphibolites. However at temperatures below 350°C Cl is effectively totally ionized in a hydrothermal solution (Barnes, 1979) and should be less reactive with wall rocks. In muscovite and chlorite of the metasedimentary rocks Cl concentrations are below the detection limit (Appendix 2). Apatite in PWN 009 (mineralized amphibolite) is observed to contain some Cl (0.21 and 0.48%), the age of this apatite is unknown and it may predate mineralization. The whole-rock results indicate that the metasedimentary rocks are not enriched in Cl, neither is the mineralized amphibolite (PWN 071).

Some indicated characteristics of a fluid that may be responsible for amphibolitization, albitization, Skuterud ore mineralization, and possibly related to the calcite rocks at the Gamphue quarry are: high fO_2; an alkaline pH; high concentrations of Cl, probably associated with Na; the ability to transport high field strength elements; high ε_{Sr} and low ε_{Nd}.

In addition to all hydrothermal rocks in this study area being enriched in U, granite on the north margin of the Kongsberg Sector (the Flå granite) and several others throughout southwest Scandinavia are enriched in U during Sveconorwegian metamorphism (Killeen and Heir, 1974; Killeen and Heier, 1975). The U content of other rocks from the Bamble Sector is not known. An enrichment in U is possible though, as associations between albitites and U-mineralization is common in Russia, Ukraine and elsewhere (Lobato and Fyfe, 1990). In Brazil at Lagoa Real, U mineralization with albitization occurs in response to reduction of the hydrothermal fluid.

In the Modum Complex, a crustal or surface brine source for hydrothermal fluids has been interpreted (Munz et al., 1994; Munz et al., 1995). It is thought by this author that a fluid source from the lower crust or upper mantle was dominant during all but possibly the

latest hydrothermal activity (which is not documented in this study). A late involvement of surface brines is compatible with a heat anomaly produced by the U enrichment similar to the Athabasca-type deposits. U mineralization may have driven a convection cell drawing down surface fluids via a fault-valve type model (Oliver et al., 1990). Another possible source for a late surface type fluid is if thrusting over the Telemark Sector (to the west) (Starmer, 1993) caused dewatering in Telemark sediments; similar to the interpretation for U mineralization in Lagoa Real in Brazil (Lobato and Fyfe, 1991).

The similarities between hydrothermal events the Bamble sector and the Kongsberg Sector suggest that a large scale process affected these rocks. A lower crustal (derived for underplating magmas) or mantle source (devolatilizing of a hypothetical carbonated upper mantle) for the Kragerø dolomites has been interpreted (Dahlgren et al., 1993; Cameron, 1993). Similar processes can explain the hydrothermal activity in the Modum complex, the chemical differences of the amphibolites suggest some differences in the fluid chemistry or amount of fluid passing through the rocks. A different orientation of structural fabric in the Kongsberg Sector compared to the Bamble Sector may have influenced the relative amount of extension during Sveconorwegian deformation. Gold was mobilized by Skuterud ore-bearing fluids at greenschist facies, but this fluid appears to post-date the generation of low Au values in the metagabbros and amphibolites. Extraction of Au from mafic rocks in the Modum Complex is not interpreted to be related later hydrothermal processes that may have occurred during isothermal uplift . This interpretation has been made for areas of the Bamble Sector that attained Granulite facies during Sveconorwegian metamorphism (Cameron, 1993).

5.9. Conclusions

1. The stable isotope values of $\delta^{13}C$ in graphite and the $\delta^{34}S$ in pyrite in the fahlbands is indicative of a sedimentary origin.

2. Geochemical evidence from the metagabbros indicates a tholeiitic composition, that is derived from a subducting oceanic slab, little crustal contamination is indicated.

3. The metamorphism of metagabbro to amphibolite is not isochemical. The amphibolites have much higher concentrations of Fe_2O_3, TiO_2, P_2O_5, REE, Y, Sc, and V. There are moderately higher concentrations of Na_2O and FeO. There is a probable higher concentrations of Cr, U and Th. The amphibolites are relatively depleted in MgO, Al_2O_3 and Tl. The geochemical changes observed during amphibolitization are in detail unlike other studies of Sveconorwegian amphibolitization from southwest Scandinavia. There may have been mobility and enrichment of typically immobile trace elements or a significant loss of volume with the elements that occur at higher concentrations representing immobile elements

4. The metagabbros and amphibolites have below normal concentrations of Au. It is not clear whether the Au was depleted by an metamorphic/subsolidous process prior to amphibolitization or if the low concentration is a primary igneous feature.

5. The hydrothermal fluids responsible for amphibolitization, albitization, Skuterud ore mineralization, and massive calcite at the Gamphue quarry (at Øverbykollen), have an fO_2 that is high relative to that of the protolith (gabbro).

Field relations indicate that Co-Cu-As-U-Au mineralization at the Skuterud mine post-dates gabbroic intrusion; the greenschist mineralization assemblage indicates that it also post-dates

amphibolitization. Mineralization of Skuterud ore is interpreted to result from reduction of an oxidized hydrothermal fluid in graphitic fahlbands.

LIST OF REFERENCES

Andersen, T. (1987): Mantle and crustal components in a carbonatite complex, and the evolution of carbonatite magma: REE and isotopic evidence from the Fen complex, southeast Norway. *Chem. Geol.* **65**, 147-166.

Andersen, T. and Munz, I.A. (1995): Radiogenic whole-rock lead in Precambrian metasedimentary gneiss from south Norway: evidence of Sveconorwegian LILE mobility. *Norsk Geol. Tidssk.* **75**, 156-168.

Andreae, M.O. (1974): Chemical and stable isotope composition of the high grade metamorphic rocks from the Arendal area, southern Norway. *Contrib. Mineral. Petrol.* **47**, 299-316.

van Autenboer (1957): The radiometric survey of the Modum Area. Report for the Geological Survey of Norway, 28 pp.

Barnes, S.J. (1988): The effects of partial melting, crystal fractionation and sulphide segregation on Ni/Pd, Cu/Rh and Cu/Pt ratios; with examples from Norway and Quebec. *Goldschmidt conference.* **28**.

Barnes, S.J., Boyd, R., Korneliussen,A., Nilsson, L.P., Often, M., Pedersen, R.B. and Robins, B. (1988): The use of mantle normalization and metal ratios in discriminating between the effects of partial melting, crystal fractionation and sulfide segregation on platinum-group elements, gold, nickel, and copper: Examples from Norway. *In* Geo-Platinum 87 (H.M. Prichard, P.J. Potts, J.F.W. Boyles, and S.J. Cribb, eds.). Elsevier Applied Science Publishers, London, 113-143.

Barovich, K.M., Patchett, P.J., Peterman, Z.E. and Sims, P.K. (1989): Nd isotopes and the origin of 1.9-1.7 Ga Penokean continental crust of the Lake Superior region. *Geol. Soc.*

of Am. Bull. **101**, 333-338.

Barth, T.F.W. (1969): Granulite facies rocks of the Precambrian of south Norway, particularly around Arendal. *Sci. Terre* **14**, 361-369.

Barton, P.B. Jr (1969): Thermochemial study of the system Fe-As-S. *Geochim Cosmochim. Acta* **33**, 841-857.

Barton, P.B. Jr and Skinner, B.J. (1979): Sulphide mineral stabilities. *In* Geochemistry of Hydrothermal Ore Deposits, 2nd ed. (H.L. Barnes, ed.). John Wiley and Sons Inc., 404-460.

Best, M.G. (1982): Igneous and metamorphic petrology. W. H. Freeman and Company, NewYork, 630 pp.

Bogoch, R., Eldad, H. and Nathan, Y. (1984): Scandium-bearing carbonatites of the Tarr complex, southeast Sinai. *Geochim. Cosmochim. Acta* **48**, 885-887.

Böhlke, J.K. (1989): Comparison of metasomatic reactions between a common CO2-rich vein fluid and diverse wall rocks: intensive variables, mass transfers, and Au mineralization at Alleghany, California. *Econ. Geol.* **84**, 291-327.

Bottinga, Y. (1969): Calculation of fractionation factors for carbon and oxygen isotopic exchange in the system calcite-carbon dioxide-water. *Jour. Phys. Chem.* **72**, 800-808.

Boyd, R., Barnes, S.J. and Gonlie, A. (1988): Noble metal geochemistry of some Ni-Cu deposits in the Sveconorwegian and Caledonian orogens in Norway. *In* Geo-Platinum 87 (H.M. Prichard, P.J. Potts, J.F.W. Boyles and S.J. Cribb, eds.). Elsevier Applied Science Publishers, 113-143.

Boyle, R.W. (1979): The geochemistry of gold and its deposits. *Geological Survey of Canada*

Bulletin **280**, 584 pp.

Boyle, R.W. and Jonasson, I.R. (1984): The geochemistry of antimony and its use as an indicator element in geochemical prospecting. *J. Geochem. Explor.* **20**, 223-302.

van Breemen, O., Halliday, A.N., Johnson, M.R.W. and Bowes, D.R. (1978): Crustal additions in late Precambrian times. *In* Crustal evolution in northwestern Britain and adjacent regions (D.R. Bowes and B.E. Leake eds.) *Geol. J.* **10**, 81-106.

Brehler, B. and Fuge, R. (1974): Chlorine. *In* Handbook of Geochemistry (K.H. Wedepohl, ed.). Springer-Verlag, Berlin 17-A-1 to 17.

Brickwood, J.D. and Craig, J.W. (1987): Primary and re-equilibrated mineral assemblages from the Sveconorwegian mafic intrusions of the Kongsberg and Bamble areas, Norway. *Norges Geol. Unders. Bull.* **410**, 1-23.

Bridgewater, D. and Windley, B.F. (1973): Anorthosites, post-orogenic granites, acid volcanic rocks and crustal development in the Atlantic shield during the mid-Proterozoic. *In* Symposium on granite, gneisses and related rock, (L.A. Lister, ed.). *Geol. Soc. S. Africa Spec. Pub.* **3**, 307-317.

Brown, I.C. (1952): A nomenclature of igneous rocks. *Can. Min. Metall. Bull.* **477**, 54-57.

Bugge, C. (1918): Kongsbergfeltests geologi. *Nor. Geol. Unders.* **82**, 272pp.

Bugge, J.A.W. (1943): Geological and petrological investigations in the Kongsberg-Bamble formation. *Nor. Geol. Unders.* **160**, 150pp.

Bugge, J.A.W. (1978): Norway. *In* Mineral deposits of Europe (S.H.U. Bowie, A. Kvalheim and H.W. Haslam, eds.). **1**, 199-249.

Burnham, C.W. (1979): Magmas and hydrothermal fluids. *In* Geochemistry of Hydrothermal

Ore Deposits. 2nd ed. (H.L. Barnes. ed.). John Wiley and Sons. Inc. 71-136.

Cameron. E.M. (1988): Archean gold: relation to granulite formation and redox zoning in the crust. *Geol.* **16**. 109-112.

Cameron. E.M. (1989): Derivation of gold by oxidative metamorphism of a deep ductile shear zone: Part 1. Conceptual model. *J.Geoch. Expl.* **31**. 135-147.

Cameron. E.M. (1989): Derivation of gold by oxidative metamorphism of a deep ductile shear zone; Part 2. Evidence from the Bamble belt. south Norway. *J. of Geoch. Expl.* **31**. 149-169.

Cameron. E.M. (1989): Scouring of gold from the lower crust. *Geol.* 17. 26-29.

Cameron. E.M. (1993): Depletion of gold and LILE in the lower crust:comparison of Scourian complex. Scotland. and Bamble shear belt. Norway. Manuscript.

Cameron. E.M. and Hattori. K. (1987): Archean gold mineralization and oxidized hydrothermal fluids. *Econ. Geol.* **82**. 1177-1191..

Cameron. E.M.. Cogulo. E.H. and Stirling. J. (1993): Mobilization of gold in the deep crust: evidence from mafic intrusions in the Bamble belt. Norway. *Lithos* **30**. 151-166.

Cann. J.R. (1970): Rb. Sr. Y. Zr and Nb in some ocean-floor basaltic rocks. *Earth Planet. Sci. Lett.* **10**. 1-10.

Carrigan. W.J. (1990): Stable isotope ratios of cabonate and sulphide minerals from the gunflint formation: evidence for the origin of iron-formations. unpublished PhD. Thesis. University of Ottawa. 199 pp.

Cathles. L.M. (1986): The geologic solubility of gold from 200-350°C. and its implications for gold-base metal ratios in vein and stratiform deposits. *Can. Bull. Min. Metall.* **38**.

187-210.

Chaussidon, M., Albarede, F. and Sheppard, S.M.F. (1989): Sulphur isotope variations in the mantle from ion microprobe analyses of micro-sulphide inclusions. *Earth Planet.Sci. Lett.* **92**, 144-156.

Clark, L.A. (1960): The Fe-As-S system: phase relations and applications. *Econ. Geol.* **55**, 1345-1381.

Corfu, F., Krogh, T.E., Kwok, Y.Y. and Jenson, L.S. (1989): U-Pb geochronology on the southwestern Abitibi greenstone belt, Superior province. *Can. J. Earth Sci.* **26**, 1747-1763.

Corfu, F. and Andrews, A.J. (1987): Geochronological constraints on the timing of magmatism, deformation, and gold mineralization in the Red Lake greenstone belt, northwestern Ontario. *Can. J. Earth Sci.* **24**, 1302-1320.

Crerar, D.A. and Barnes, H.L. (1976): Ore solution chemistry V. solubilities of chalcopyrite and chalcocite assemblages in hydrothermal solutions at 200 ° to 350 ° celcius. *Econ. Geol.* **71**, 772-794.

Cox, K.G., Bell, J.D. and Pankhurst, R.J. (1979) The interpretation of igneous rocks.Unwin Hyman, London, 450 pp.

Curti, E. (1987): Lead and oxygen isotope evidence for the origin of the Monte Rosa gold lode deposits (Western Alps, Italy): a comparison with Archean lode deposits. *Econ.Geol.* **82**, 2115-2140.

Dahlgren, S., Bogoch, R., Magaritz, M. and Michard, A. (1993): Hydrothermal dolomite marbles associated with charnockitic magmatism in the Proterozoic Bamble shear belt, south Norway. *Contrib. Min. Petrol.* **113**, 394-409.

Defant, M.J. and Drummond, M.S. (1990): Derivation of some modern arc magmas by melting of young subducted lithosphere. *Nature* **347**, 662-665.

Dons, J.A. (1972): The Telemark area, a brief presentation. in Recherche cooperative sur Programme (R.C.P.) 193, Scandinavie, Socle-Caledonides: Premiere partie; Le socle precambrien de la Norvege meriodionale. *Sci. Terre* **17**, 25-29.

Duke, J.M. (1979): Computer simulation of the fractionation of olivine and sulfide from mafic and ultramafic magmas. *Can. Mineral.* **17**, 507-514.

Elliot, R.B. (1973): The chemistry of gabbro/amphibolite transitions in south Norway. *Contrib. Mineral.Petrol.* **38**, 71-79.

Emslie, R.F. and Hunt, P.A. (1990): Ages and petrographic significance of igneous-charnockite suites associated with massif anorthosites, Grenville Province. *J. Geol.* **98**, 213-232.

Ernst, R.E., Bell, K., Ranalli, R. and Halls, H.C. (1987): Mafic dyke swarms: a collection of papers based on the proceedings of an international conference. *In* Mafic dyke swarms (H.C. Halls and W. F. Fahrig eds.).*Geol. Assoc. Can. Spec. Pap.* 123-135.

Falcum, T. (1985): Geotectonic evolution of southern Scandinavia in light of a late-Proterozoic plate-collision. *In* The deep Proterozoic crust in the north Atlantic provinces. .(A. C. Tobi and J. L. R. Touret eds.) NATO Adv. Study Inst., Ser.C **158**, 309-322.

Faure, G. (1986): Principles of Isotope Geology, 2nd ed. Wiley, New York, 589pp.

Ferguson, S.A., Buffam, B.S.W., Carter, O.F., Griffis, A.T., Holmes, T.C., Hurst, M.E., Jones, W.A., Lane, H.C. and Langley, C.S. (1968): Geology and ore deposits of Tisdale Township, District of Cochrane. *Ont. Dep. Mines Geol. Rep.* **58**, 1-177.

Field, D. and Elliott, R.B. (1974): The Chemistry of Gabbro/Amphibolite transitions in south Norway II trace tlements. *Contrib. Mineral. Petrol.* **47**, 63-74.

Field, D., Smalley, P.C., Lamb, R.C. and Raheim, A. (1985): Geochemical evolution of the 1.6-1.5 Ga-old amphibolite-granulite facies terrain, Bamble sector, Norway: dispelling the myth of Grenvillian high-grade reworking. *In* The deep Proterozoic crust in the north Atlantic provinces. .(A. C. Tobi and J. L. R. Touret eds.) NATO Adv. Study Inst., Ser.**C** **158**, 567-578.

Floyd, P.A., Winchester, J.A. (1975): Magma type and tectonic setting discrimination using immobile elements *Earth Planet. Sci. Lett.* **27**, 211-218.

Frarey, M.J. and Krogh, T.E. (1986): U-Pb zircon ages of late internal plutons of the Abitibi and eastern Wawa subprovinces, Ontario and Quebec. **86-1A**, 43-48.

Fripp, R.E.P. (1976): Stratabound gold deposits in Archean banded iron-formation, Rhodesia. *In Current Research, Part A, Geological Survey of Canada Econ. Geol* **71**, 58-75.

Frodesen, S. (1968): Petrographical and chemical investigations of a Precambrian gabbro intrusion, Hiasen, Bamble area, south Norway. *Norsk Geol. Tidsskr.* **48**, 281-306.

Frodesen, S. (1973): Trace elements in a Precambrian gabbro intrusion, Hiasen, Bamble area, South Norway. *Norsk Geol. Tidsskr.* **53**, 1-10.

Frost, B.R. (1991a): Introduction to oxygen fugacity and its petrologic importance. *In* Oxide Minerals: Petrologic and Magnetic Significance (D.H. Lindsley, ed.). *Rev. Mineral.* **25**, 1-9.

Frost, B.R. (1991b): Stability of oxide minerals in metamorphic rocks. *In* Oxide Minerals: Petrologic and Magnetic Significance (D.H. Lindsley, ed.). *Rev. Mineral.* **25**, 469-487.

Fyfe, W.S. (1973): The generation of batholiths. *Tectonophysics* **17**, 273-283.

Fyfe, W.S. and Henley, R.W. (1973): Some thoughts on chemical transport processes, with particular reference to gold. *Minerals Sci. Eng.* **5**, 295-303.

Gallagher, David. (1940): Albite and gold. *Econ. Geol.* **35**, 698-736.

Gammon, J.B. (1966): Fahlbands in the Precambrian of southern Norway. *Econ.Geol.* **61**, 174-188.

Gammon, J.B. (1967): Some observations on minerals in the system CoAsSFeAsS. *Norsk Geol. Tidsskr.* 405-431.

Gee, D.G. and Sturt, B.A. (1985): The Caledonide orogen - Scandinavia and related areas, I-II. Wiley & Sons, 1266.

Goldfarb, R., Leach, D.L., Miller, M.L. and Pickthorn, W.J., (1986): Geology, metamorphic setting and genetic constraints of epigenetic lode-gold mineralization within the Cretaceous Valdez Group, south-central Alaska. *In* Turbidite-hosted gold deposits (Keppie, J.D., Boyle, R. W., and Haynes, S.J., eds.). *Geological Association of Canada Special Paper* **327**, 87-105.

Goldfarb, R.J., Leach, D.L., Pickthorn, W.J. and Paterson, C.J. (1988): Origin of lode-gold deposits of the Juneau Gold Belt, southeastern Alaska. *Geol.* **16**, 440-443.

Goldfarb, R.J., Snee, L.W., Miller, L.D. and Newberry, R.J. (1991): Rapid dewatering of the crust deduced from ages of mesothermal gold deposits. *Nature* **354**, 296-298.

Goldschmidt, V.M. (___): Die kontactmetamorphose im kristianiagbeit. Kristiana Vidensk. Skr., 1, Math.-Naturv. Kl.11,.

Gorbatschev, R., Solyom, Z. and Johansson, I. (1979): The Central Dolerite group in

Jaamtland, Central Sweden. *Geologiska Fooreningens i Stockholm Foorhandlinger* **101**, 177-190.

Gorbatschev, R., Lindh, A., Solyom, Z., Laitakari, I., Aro, K., Markov, M.S., Ivliev, A.I. and Bryhni, I. (1987): Mafic dyke swarms of the Baltic Shield. *In* Mafic Dyke Swarms (H.C. Halls and W.F. Fahrig eds.). *Geol. Assoc. Can. Spec. Pap.* **34**, 362-372.

Gower, C.F. and Owen, V. (1984): Pre-Grenvillian and Grenvillian lithotectonic regions in Eastern Labrador-correlations with the Sveconorwegian Orogenic belt in Sweden. *Can. J. Earth Sci.* **21**, 678-693.

Gower, C.F., Ryan, A.B. and Rivers, T. (1990): Mid-Proterozoic Laurentia-Baltica: an overview of its geological evolution and a summary of the contributions made by this volume. *In* Mid-Proterozoic Laurentia-Baltica (C.F. Gower, T. Rivers and B. Ryan eds.).*Geol. Assoc. Can., Spec. Pap.* **38**, 1-20.

Grant, J. (1986): The isocon diagram-a simple solution to Gresens' equation for metasomatic alteration. *Econ. Geol.* **81**, 176-182.

Green, J.C. (1956): Geology of the Storkollen-Blankenberg area, Krageroe, Norway. *Norsk Geol. Tidssk.* **36**, 89-140.

Gresens, R.L. (1967): Composition - volume relationships of metasomatism. *Chem. Geol.* **2**, 47-65.

Griffis, A.T. (1968): McIntyre Porcupine Mines, Limited *In* Geology and ore deposits of Tisdale township. *Ontario Dept. Mines Geol. Rept.* **58**, 122-130.

Groves, D.I., Phillips, G.N., Ho, S.E., Houstoun, S.M. and Standing, C.A. (1987): Craton-scale distribution of Archean greenstone gold deposits; predictive capacity of the metamorphic model. *Econ. Geol.* **82**, 2045-2058.

Guilbert, J.M. and Park, C.F. Jr. (1986): The geology of ore deposits. W. H. Freeman and Company, New York 965 pp.

de Haas, G.J.L.M., Nijland, T.G., Huijsmans, J.P.P., Maijer, C. and Dam, B.P. (in press?): The magmatic history of a gabbroic intrusion in the Bamble sector, Vestre Dale, Norway. Neues Jahrbuch für Mineralogie/Abhandlungen,.

de Haas, G.J.L.M. de, Verschure, R.H. and Maijer, C. (in press?): Isotopic constraints on the timing of crustal accretion of the Bamble sector, Norway, as evidenced by coronitic gabbros. *Precamb Res.*

Haas, J.R., Shock, E.L. and Sassani, D.C. (1995): Rare earth elements in hydrothermal systems: Estimates of standard partial molal thermodynamic properties of aqueous complexes. *Geochim. Cosmochim.* **59**, 4329-4350.

Haggerty, S.E. (1991): Oxide textures-a mini-atlas. *In* Oxide Minerals: Petrologic and Magnetic Significance (D.H. Lindsley, ed.). *Rev. Mineral.* **25**, 129-219.

Hammarstrom, J.M. and Zen, E. (1986): Aluminum in hornblende: An empirical igneous geobarometer. *Amer. Mineral.* **71**, 1297-1313.

Hayashi, K. and Ohmoto, H. (1991): Solubility of gold in NaCl- and H_2S-bearing aqueous solutions at 250 to 350°C. *Geochim. Cosmochim. Acta* **55**, 2111-2126.

Henley, R.W., Norris, R.J. and Paterson, C.J. (1976): Multistage ore genesis in the New Zealand geosyncline; a history of post-metamorphic lode emplacement *Mineral. Deposita* **11**, 180-196.

Hodgson, C.J. (1982): Gold deposits of the Abitibi belt, Ontario. *In* Ontario Geological Survey Miscellaneous Paper **106**, 192-197.

Hoefs, J., (1987): Stable Isotope Geochemistry. 3rd edition, Springer-Verlag, Berlin.241 pp.

Hole, M.J., Saunders, A.D., Marriner, G.F. and Tarney, J. (1984): Subduction of pelagic sediments: implications for the origin of Ce-anomalous basalts from the Mariana Islands. *J. Geol. Soc. Lon.* **141**, 453-472.

Holland, H.H. (1972): Granites, solutions, and base metal deposits. *Econ. Geol.* **67**, 281-301.

Hollister, L.S., Grissom G.C., Peters, E.K., Stowall, H.H. and Sisson, V.B. (1987): Confirmation of the empirical correlation of Al in hornblende with pressure of solidification of calc-alkaline plutons. *Amer. Mineral.* **72**, 231-239.

Hygen, G.K. (1971): Report on underground sampling programme at the Sutterud Mines' Modum, Norway. Report for Falconbridge Nikkelverk A/S, Project 905-14, 22 pp., 8 maps.

Irvine, T.N. and Baragar, W.R.A. (1971): A guide to the chemical classification of the common volcanic rocks. *Can. J. Earth Sci* **8**, 523-548.

Jacobsen, S.B. and Heier, K.S. (1978): Rb-Sr isotope systematics in metamorphic rocks, Kongsberg sector, south Norway. *Lithos* **11**, 257-276.

Johnson, M. C. and Rutherford, M.J. (1989): Experimental calibration of the aluminum-in-hornblende geobarometer with application to Long Valley Caldera (California) volcanic rocks. *Geol.* **17**, 837-841.

Kerrich, R. and Fryer, B.J. (1979): Archaean precious-metal hydrothermal systems, Dome Mine, Abitibi Grennstone Belt. II. REE and oxygen isotope relations. *Can. J. Earth Sci.* **16**, 440-458.

Kerrich, R. and Fyfe, W.S. (1981): The gold-carbonate association: source of CO_2, and CO_2

fixation reactions in Archaean lode deposits. *Chem. Geol.* **33**, 265-294.

Kerrich, R. and Wyman, D. (1990): Geodynamic setting of mesothermal gold deposits: An association with accretionary tectonic regimes. *Geol.* 18, 882-885.

Killeen, P.G. and Heier, K.S. (1975): A uranium and thorium enriched province of the Fennoscandian shield in southern Norway. *Geochim. Chosmochim. Acta* **39**, 1515-1524.

Kontak, D.J., Smith, P.K., Chaterjee, A.K., Giles, P.S. and Reynold, P.H. (1989): (40)Ar-(39)Ar geochonological studies in the Beaver Dam-Liscomb area, southern Nova Scotia: Recognition of a major 370 Ma magmatic-metallogenic event. *Geol. Assoc. Can. Prog. with Abs.* **14**, A11.

Korobeynikov, A.F. (1986): The gold distribution in differention products of basic and acid magmas of various ages. *Geochemistry International* **23**, no.7, 101-110.

Kretz, R. (1983): Symbols for rock-forming minerals. *Amer. Mineral.* **68**, 277-299.

Kullerud, L. and Dahlgren, S.H. (): Sm-Nd geochronology of Sveconorwegian granulite facies mineral assemblages in the Bamble Shear Belt, South Norway. Unpublished for Precambrian Research Spec. vol.

Kyser, T.K., O'Neil, J.R. and Carmichael, I.S.E. (1982): Genetic relations among basic lavas and ultramafic nodules; evidence from oxygen isotope compositions. *Contrib. Mineral.and Petrol.* 81, 88-102.

Landefeld, L.A. (1988): The Geology of the Mother Lode Gold Belt, Sierra Nevada Foothills Metamorphic Belt, California. *In* Bicentennial Gold, Gold 88. *Geol. Soc. Australia Abs.* **22**, 167-172.

Layer, P.W., McMaster, N.D. and York, D. (1987): The dating of Ontario's gold deposits.

Ontario Geol. Surv. Miscellaneous Pap. **136**, 27-34.

Leake, B.E. (1978): Nomenclature of amphiboles. *Amer. Mineral.* **63,** 1023-1053.

Leitch, C.H.B. (1990): Geology, wall rock alteration and characteristics of the ore fluids at the Bralorne Mesothermal gold vein deposit, Southwestern British Colombia. *In* Greenstone gold and crustal evolution; NUNA conference volume (F. Robert, P.A. Sheahan and S.B. Green) Geol. Assoc. Canada, 183-184.

Leitch, C.H.B., Godwin, C.I., Brown, T.H. and Taylor, B.E. (1991): Geochemistry of mineralizing fluids in the Bralorne-Pioneer mesothermal gold vein deposit, British Columbia. *Econ.Geol.* **86**, 318-353.

Lieftink, D.J., Nijland, T.G. and Maijer, C. (1993): Cl-rich scapolite from Ødegårdens verk, Bamble, Norway. *Nor. Geol. Tidsskr.* **73**, 55-57.

Lieftink, D.J., Nijland, T.G. and Maijer, C. (1994): The behavior of rare-earth elements in high-temperature Cl-bearing aqueous fluids: results from the Ødegårdens verk natural labratory. *Can. Mineral.* **32**, 149-158.

Lindsley, D.H. (1991): Experimental studies of oxide minerals. *In* Oxide Minerals: Petrologic and Magnetic Significance (D.H. Lindsley, ed.). *Rev. Mineral.* **25**, 69-106.

Lobato, L.M. and Fyfe, W.S. (1990): Metamorphism, metasomatism, and mineralization at the Lagoa Real, Bahia, Brazil. *Econ. Geol.* **85**, 968-989.

Lumbers, S.B., Heaman, L.M., Vertolli, V.M. and Wu, T.W. (1990): Nature and timing of middle Proterozoic magmatism in the Central Metasedimentary belt, Grenville province, Ontario *In* Mid-Proterozoic Laurentia-Baltica (C.F. Gower, T. Rivers and B. Ryan eds.).*Geol. Assoc. Can., Spec. Pap.* **38**, 243-276.

Martins, J.A. (1969): The Precambrian rocks of the Telemark area in the south central Norway: no. VII, The Vraadal area. *Norg. Geol. Unders.* **258**, 267-301.

Mason, R. and Melnik, N. (1986): The anatomy of an Archean gold system - the McIntyre-Hollinger complex at Timmins, Ontario, Canada. *In* Gold '86 (A.J. Macdonald, ed.)., 40-55.

McLelland, J.M. and Chiarenzelli, J.R. (1990): Isotopic constraints on the emplacement of anorthositic rocks of the Marcy Massif, Adirondack Mountains, New York. *J. of Geol.* **98**, 19-41.

McLennan, S.M. (1989): Rare earth elements in sedimentary rocks: influence on provenance and sedimentary processes. *In* Geochemistry and mineralogy of rare earth elements (B.R. Lipin and G.A. McKay, eds.). *Rev. Mineral.* **21**, 169-200.

McNaughton, N.J. and Dahl, N. (1987): A geochronological framework for gold mineralization in the Yilgarn block, Western Australia. Recent advances in understanding Precambrian gold deposits University of Western Australia, Geology Department and University Extension Publication 11, 29-49.

Mirota, M.D. and Veizer, J. (1994): Geochemistry of Precambrian carbonates: VI, Aphebian Albanel Formations, Quebec, Canada. *Geochim. Cosmochim.* **58,** 1735-1745.

Mitchell, R.H. (1967): The Precambrian rocks of the Telemark area in south central Norway: V, The Nissedal supracrustal series. *Nor. Geol. Tidsskr.* **47**, 295-332.

Moorbarth, S. And Vokes, F.M. (1963): Lead isotope abundance studies on galena occurances in Norway. *Norsk Geol. Tidsskr.* **43**, 283-343.

Munoz, J.L. (1984): F-OH exchange in micas with applications to hydrothermal ore deposits. In Mica (S.W. Bailey, ed.).*Rev. Mineral.* **13**, 469-493.

Munz, I.A. (1990): Whiteschists and orthoamphibole-cordierite rocks and the P-T-t path of the Modum complex, south Norway. *Lithos* **24**, 181-200.

Munz, I.A. and Morvik, R. (1991): Metagabbros in the Modum complex, southern Norway; an important heat source for Sveconorwegian metamorphism. *Precam. Res.* **52**, 97-113.

Munz, I.A., Wayne, D. and Austrheim, H. (1994): Retrograde fluid infiltration in the high-grade Modum complex, south Norway: evidence for age, source and REE mobility. *Contrib. Mineral. Petrol.* **116**, 32-46.

Munz, I.A., Yardley, B.W.D. Banks, D. and Wayne,D. (1995): Deep penetration of sedimentary fluids in basement rocks from southern Norway: evidence from hydrocarbon and brine inclusions in quartz veins. *Geochim. Cosmochim.* **59**, 239-254.

Neumann, H. (1944): Silver deposits at Kongsberg. *Norsk. Geol. Unders.* **162**.

Nijland, T.G. and Senior, A. (1991): Sveconorwegian granulite facies metamorphism of polyphase migmatites and basic dikes, South Norway. *J. of Geol.* **99**, 515-525.

Nijland, T.G., Jansen, B.H., Maijer, C. (1993): Halogen geochemistry of fluid during amphibolite-granulite metamorphism as indicated by apatite and hydrous silicates in basic rocks from the Bamble sector, South Norway. *Lithos*, **27** 167-189.

Nunes, P.D. and Pyke, D.R. (1980): Geochronology of the Abitibi metavolcanic belt, Timmins-Matachewan area-Progress report. *In* Summary of geochonological studies 1977-1979 (E.G. Pye ed.). *Ontario Geol. Surv. Miscellaneous Pap.* **92**, 34-39.

Oftedahl, C. (1980): The geology of Norway. *Nor. Geol. Unders.* **319**, 3-114.

O'Hara, K. and Blackburn, W.H. (1989): Volume-loss model for trace-element enrichments in mylonites. *Geol.* **17**, 524-527.

O'Hara, K (1988): Fluid flow and volume loss during mylonitixation-An origin for phyllonite in an overthrust setting, North Carolina, U.S.A.. *Tectonophys.* **156**, 21-36.

O'Hara, K. and Blackburn, W.H. (1987): Fluid fow and volume loss during mylonitization: Evidence from the western Blue Ridge, North Carolina. *Geol. Soc. Amer. Abs. with Prog.* **19**, 792.

Ohmoto, H. (1972): Systematics of sulfur and carbon isotopes in hydrothermal ore deposits. *Econ. Geol.* **67**, 551-578.

Ohmoto, H. and Rye, R.O. (1979): Isotopes of sulfur and carbon. *In* Geochemistry of hydrothermal ore deposits (H.L. Barnes, ed.). John Wiley & Sons, New York, NY, 509-567.

Oliver, N.H., Valenta, R.K. and Wall, V.J. (1990): The effect of heterogeneous stress and strain on metamorphic fluid flow, Mary Kathleen, Autralia, and a model for large-scale fluid circulation. *J. Metamorphic Geol.* **8**, 311-331.

Padget, P. (1990): Tectonic and lithostratigraphic relationships in the Bamble sector, south Norway: an Intrerpretive view. *In* Mid-Proterozoic Laurentia-Baltica (C.F. Gower, T. Rivers and B. Ryan eds.).*Geol. Assoc. Can., Spec. Pap.* **38**, 307-316.

Patchett, J., Bylund, G. and Upton, B.G.J. (1978): Palaeomagnetism and the Grenville Orogeny: New Rb-Sr Ages from the Dolerites in Canada and Greenland. *Earth Planet. Sci. Lett.* **40**, 349-364.

Pearce, J.A. (1983): Role of the sub-continental lithosphere in magma genesis at active continental margins. *In* Continental basalts and mantle xenoliths (C. J.Hawkesworth and M. J. Norry eds.) papers prepared for a UK Volcanic Studies Group meeting at the University of Leicester.230-249.

Pearce, J.A. and Norry, M.J. (1979): Petrogenetic implications of Ti, Zr, Y, and Nb variations in volcanic rocks. *Contrib. Mineral. Petrol.* **69**, 33-47.

Ramsay, J.G. and Huber, M.I. (1987): The techniques of modern structural geology, volume 2: fold and fractures. Academic Press Limited, London 700 pp.

Ridler, R.H. (1976): Regional metallogeny and volcanic stratigraphy of the Superior Province. Can., Geol. Surv., Pap (**76-1A**). *Report of activities. Part A.*, 399-405.

Robert, F. (1989): Internal structure of the Cadillac tectonic zone southeast of Val d'Or, Abitibi greenstone belt, Quebec. *Can. J. Earth Sci.* **26**, 2661-2675.

de Ronde, C.E.J., Spooner, E.T.C., de Wit, M.J. and Bray, C.J. (1992): Shear zone-related Au quartz vein deposits in the Barberton greenstone belt, South Africa: field and petrographic characteristics, fluid properties, and light stable isotope geochemistry. *Econ. Geol.* **87**, 366-402.

Rosenqvist, I.T. (1949): Noen observasjoner og refleksjoner omkring Modum koboltgruver (Nedl.): I, Fahlbandene. *Norsk. Geol. Tidssk.* **27**, 187-216 (Norwegian, Engl. summ.).

Sandiford, M. and Keays, R.R. (1986) Structural and tectonic constraints on the origin of gold deposits in the Ballarat Slate Belt, Victoria. *In* Turbidite hosted gold deposits (J.D. Keppie; R.W. Boyle and S.J. Haynes eds.). *Geol. Assoc. Can. Spec. Pap.* **32**, 15-26.

Santosh, M., Nadeau, S. and Javoy, M. (1995): Stable isotopic evidence for the involvement of mantle-derived fluids in Wynad gold mineralization, South India. *J. Geol.* **103**, 718-728.

Seward, T.M. (1984): The transport and deposition of gold in hydrothermal systems. *In* Gold '82: The geology, geochemistry and genesis of gold deposits (R.P. Foster, ed.). A.A. Balkema, Rotterdam 165-181.

Sims, P.K., Schulz, K.J. and Kisvarsanyi, E.B. (1989): Proterozoic anorogenic granite-rhyolite terranes in the Midcontinental United States; possible hosts for Cu-, Au-, U-, and REE-bearing iron-oxide deposits similar to the Olympic Dam orebody. *In* U.S. Geological Survey-Missouri Geological Survey symposium; mineral-resource potential of the Midcontinent; program and abstracts.(W. P. Pratt and M. B. Goldhaber eds.). U. S. Geol. Surv., Open-File-Report 40.

Smalley, P.C. and Field, D. (1985): Geochemical constraints on the Evolution of the Proterozoic Continental Crust in Southern Norway (Telemark sector). *In* The deep Proterozoic crust in the north Atlantic provinces. .(A. C. Tobi and J. L. R. Touret eds.). *NATO Adv. Study Inst., Ser.***C 158**, 551-566.

Smalley, P.C. and Field, D. (1991): REE, Th, Hf, Ta in Bamble gabbros (southern Norway) and their amphibolitized equivalents: implications for gabbro tectonic setting. *Precamb. Res.* **53**, 233-242.

Smith, J.P., Spooner, E.T.C., Broughton, D.W. and Ploeger, F.R. (1990): Grant 364 The Kerr Addison-Chesterville Archean Gold-Quartz Vein System, Virginiatown: Time Sequence and Associated Mafic "Albitite" Dike Swarm. Ontario Geoscience Research Grant Program, Summary of Research 1989-1990, *Ontario Geol. Surv., Miscellaneous Pap.* **150**, 175-199.

Smith, J.V. (1974): Feldspar Minerals, volumes 1 and 2.

Smith, P.M. and Davis, D.W. (1989): Gold mineralization, a byproduct of Late-Arhean accretion: Evidence from precise U-Pb geochronology, Lake of the Woods area, Superior Province, Canada. *Geol. Assoc. Can. Prog. with Abs.* **14**, A119.

Smith, T.E. and Holm, P.E. (1990): The petrogenesis of mafic minor intrusions of the Central Metasedimentary Belt, Grenville Province, Canada: MORB and OIB sources. *Precamb.*

Res **48**, 361-373.

Speer, J.A. (1984): Micas in igneous rocks. *In* Micas (S.W. Bailey, ed.).*Rev. Mineral.* **13**, 299-356.

Starmer, I.C. (1980): A Proterozoic mylonite zone in the Kongsberg series north of Hokksund, south central Norway. *Norsk. geol. Tidsskr* **60**, 189-193.

Starmer, I.C. (1981): The northern Kongsberg series and its western margin. *Norges geol. Unders.* **370**, 25-44.

Starmer, I.C. (1985a): The evolution of the south Norwegian Proterozoic as revealed by the major and mega-tectonics of the Kongsberg and Bamble sectors *In* The deep Proterozoic crust in the north Atlantic provinces. .(A. C. Tobi and J. L. R. Touret eds.) NATO Adv. Study Inst.. Ser.**C 158**, 259-290 .

Starmer, I.C. (1985b): The geology of the Kongsberg district and the evolution of the entire Kongsberg sector, south Norway. *Nor. Geol. Unders.* **401**, 35-58.

Starmer, I.C. (1990): Mid-Proterozoic evolution of the Kongsberg - Bamble belt and adjacent areas, southern Norway. *In* Mid-Proterozoic Laurentia-Baltica (C.F. Gower, T. Rivers and B. Ryan eds.).*Geol. Assoc. Can., Spec. Pap.* **38**, 279-305.

Starmer, I.C. (1991): The Proterozoic evolution of the Bamble sector shear belt, southern Norway; correlations across southern Scandinavia and the Grenvillian controversy. *Precamb. Res.* **49**, 107-139.

Stearn, J.E.F. and Piper, J.D.A. (1984): Palaeomagnetism of the Sveconorwegian mobile belt of the Fennoscandian shield. *Precamb. Res* **23**, 201-246.

Stott, G.M., Sanborn-Barrie, M. and Corfu, F. (1987): Major transpression events across

Archean subprovince boundaries in northwestern Ontario. *Geol. Assoc. Can., Yellowknife '87 Prog. Abs.* **16**, (unpaginated).

Strauss, H. and Schieber, J. (1990): A sulfur isotope study of pyrite genesis: The Mid-Proterozoic Newland Formation, Belt Supergroup, Montana. *Geochim. Cosmochim. Acta* **54**, 197-204.

Tatsumi, Y. (1989): Migration of fluid phases and genisis of basalt magmas in subduction zones. *J. Geophys Res.* **94**, 4697-4707.

Tatsumi, Y., Hamilton, D.L. and Nesbitt, R.W. (1986): Chemical characteristics of fluid phase released from a subducted lithosphere and origin of arc magmas: evidence from high-pressure experiments and natural rocks. *J. Volcanol. Geotherm. Res.* **29**, 293-309.

Taylor, H.P. Jr. (1980): The effects of assimilation of country rocks by magmas on $^{18}O/^{16}O$ and $^{87}Sr/^{86}Sr$ systematics in igneous rocks. *Earth Planet. Sci. Lett* **47**, 243-254.

Taylor, R.P., Strong, D.F. and Fryer, B.J. (1981): Volatile control of contrasting trace element distributions in peralkaline granitic and volcanic rocks. *Contrib. Mineral. Petrol.* **72**, 267-271.

Thorpe, R.I. and Franklin, J.M. (1984): Volcanic-associated vein and shear zone gold *In* GSC *Econ.Geol.* report 36, Canadian mineral deposit types: a geological synopsis (O.R. Eckstrand ed.), 38-39.

Tomkeieff, S.I. (1983): Dictionary of Petrology. Chinchester: Wiley 680pp.

Touret, J. (1968): The Precambrian rocks around the Lake Vegar. *Norges Geologiske Undersokelse* **257**, 45 pp.

Touret, J.L.R. (1985): Fluid regime in southern Norway: the record of fluid inclusions. *In*

The deep Proterozoic crust in the north Atlantic provinces. .(A. C. Tobi and J. L. R. Touret eds.) NATO Adv. Study Inst., Ser.**C 158**, 517-549.

Tremblay, L.P. and Ruzicka, V. (1984): 21. Unconformity-associated uranium. *In* GSC Economic Geology report 36. Canadian mineral deposit types: a geological Synopsis (Eckstrand, O.R., ed.). 61.

Turekian, K.K. and Wedepohl, K.H. (1961): Distribution of the elements in some major units of the Earth's crust. Bull. Geol. Soc. Am. **72**, 175-191.

Veraschure, R.H. (1985): Geochronological framework for the late-Proterozoic evolution of the Baltic shield in south Scandinavia. *In* The deep Proterozoic crust in the north Atlantic provinces. .(A. C. Tobi and J. L. R. Touret eds.) NATO Adv. Study Inst., Ser.**C 158**, 381-410.

Vinogradov, A.P., Grinenko, V.A. and Ustinov, V.I. (1962): Isotopic composition of sulfur compounds in the Black Sea. *Geochemistry (USSR)*, no.10, 973-997.

Vogt, J.H.L. (1893): Bildung von Erzlagerstaatten durch differentiationsprocesse in basischen Eruptivmagmata. II. *Z. prakt. Geol.* 125-143.

Weaver, B.L. and Tarney, J. (1981): Chemical changes during dyke metamorphism in high-grade basement terrains. *Nature* **289**, 47-49.

Wilson, M. (1989): Igneous Petrogenesis. Chapman and Hall, 446 pp.

Winchester, J.A. and Floyd, P.A. (1976): Geochemical magma type discrimination: application to altered and metamorphosed basic igneous rocks. *Earth Planet. Sci. Lett.* **28**, 459-469.

Witt, W.K. (1992): Porphyry intrusions and albitites in the Bardoc-Kalgoorlie area, Western

Australia and their role in Archean epigenetic gold mineralization *Can. J. Earth Sci.* **29**, 1609-1622.

Wones, D.R. and Eugster, H.P. (1965): Stability of biotite, experiment, theory, and application. *Am. Mineral.* **50**, 1228-1272.

Wood, P.C., Burrows, D.R., Thomas, A.V. and Spooner, E.T.C. (1986): The Hollinger-McIntyre Au-quartz vein system, Timmins, Ontario, Canada: geological characteristics, fluid properties and light stable isotope geochemistry. *In* Gold '86 (A.J. Macdonald, ed.), 56-80.

Wyman, D. and Kerrich, R. (1988): Alkaline Magmatism, Major Structures, and Gold Deposits: Implications for Greenstone Belt Gold Metallogeny. *Econ.Geol.* 83, 454-461.

Zeck, H.P. and Willadsen, K. (1990): The ca. 1500 Ma Varmland Hyperite Suite, Southwest Sweden - petrography, magma chemistry and metasomatic changes of a series of partly recrystallized gabbroic intrusions. *In* Mid-Proterozoic Laurentia-Baltica (C.F. Gower, T. Rivers and B. Ryan eds.).*Geol. Assoc. Can., Spec. Pap.* **38**, 461-470.

Zotov, A.V., Baranova, N.N., Dar'yina, T.G. and Bannykh, L.N. (1989): Experimental study of complex-formation of gold in the system KCl-HCl-H_2O at 450°C and 500 atm. *Geokhimiya* 541-551.

APPENDIX 1. PETROGRAPHIC DESCRIPTIONS

Mineral symbols used in Appendix 1 and within the text are from Kretz (1983). the following is a summary of used abreviations

Act	actinolite	Ms	muscovite
Ab	albite	Ol	olivine
Ath	anthophillite	Oam	orthoamphibole
Ap	apatite	Pn	pentlandite
Bt	biotite	Pl	plagioclase
Cam	Ca clinoamphibole	Py	pyrite
Cpx	Ca clinopyroxene	Po	pyrrhotite
Cal	calcite	Qtz	quartz
Ccp	chalcopyrite	Rt	rutile
Chl	chlorite	Scp	scapolite
Cld	chloritoid	Srp	serpentine
Crd	cordierite	Siil	sillimanite
Ep	epidote	Spl	spinel
Grt	garnet	Tlc	talc
Gr	graphite	Ttn	titanite
Hbl	hornblende	Ts	tschermaakite
Ilm	ilmenite	Tur	tourmaline
Kfs	K feldspar	Tr	tremolite
Mag	magnetite	Zrn	zircon
Mnz	monzanite	w/	with

Sample: 2 **Rock type :** Hbl-Bt gneissic amphibolite

Field notes: from 5-10cm vein: 60% Hbl, 30%Pl

Sample location: amphibolite unit 100m east of Mellemgrube (at Skuterud)

Strike: 001 **Geochemical analysis:** 100, some wall

Dip: 52 **Microprobe analysis:**

y: tr. v. fine **Po:** 0 **Ccp:** tr. fine

Ilm: tr. med grained, no exsolution **Hem:** 0

Mag: 0 **Gr:** 0

Opaque mineralogy notes: several fine grains of cobaltite in Pl rich area; Ilm is more abundant in the Pl rich area than in the Cam area, though no textural difference is observed

Plagioclase (Pl) ***General:*** 40% med. gr. mosaic

Alteration : yellow Scp? Ep along fractures ***extinction angle:*** 30

Qtz: 0 **Scp:** tr.

Amphiboles: 40%, med. gr. unfoliated Hbl **Cal:**

Bt: <5%, orange, unoriented **Ms:** 0

Kfs: 0 **Sil:** 0 **Tlc:** 0

Others : **Chl:** 0

Notes: vein doesn't seem to be albitite, Po? in Pl area

Sample: 4 **Rock type :** Pl-Kfs-Qtz vein

Field notes: 30cm Pl.-Bt vein, from central zone, dominated by well lineated Bt, sample also contains a rock with contact of marginal zone (this is probably the thin section)

Sample location: amphibolite unit 100m east of Mellemgrube (at Skuterud), 20 m south of PWN002

Strike: 001 **Geochemical analysis:**

Dip: 40 **Microprobe analysis:**

y: fine - tr. porous **Po:** possible **Ccp:** tr.

Ilm: tr. pourous (altered?) fine gr., no ex. **Hem:** 0

Mag: 0 **Gr:** 0

Opaque mineralogy notes: seems that the rock may be affected by weathering, fieldnotes describe the outcrop as rust coloured; Py may be late

Plagioclase (Pl) ***General:*** 60%, fine mosaic, triple junctions moderately well formed

Alteration : light patchy ***extinction angle:*** 20

Qtz: 30% similar habit as Pl. **Scp:** 0

Amphiboles: **Cal:** 0

Bt: <10%, well oriented,locally concentrated **Ms:** 0

Kfs: tr., local with Bt **Sil:** 0 **Tlc:** 0

Others : **Chl:**

Notes:

Sample: 5 **Rock type :** Qtz-Ms-sulphide schist

Field notes: Ms-Qtz schist, weathered, high porosity?

Sample location: 100 m east of the north end of Mellemgrube

Strike: **Geochemical analysis:**

Dip: **Microprobe analysis:**

y: tr. **Po:** tr. **Ccp:** 2%

Ilm: 0 **Hem:** tr.

Mag: 0 **Gr:** 0

Opaque mineralogy notes: minor Po,Py in the Ccp, Po may be in contact with Ilm, Po in contact with Rt, coarse Ms flakes cut into Ccp

Plagioclase (Pl) ***General:*** 0

Alteration : 0 ***extinction angle:*** 0

Qtz: >30%, fine granular and coarse recrystallized **Scp:** 0

Amphiboles: **Cal:** 0

Bt: 0 **Ms:** minor, fine grained

Kfs: tr. **Sil:** 0 **Tlc:** 0

Others : **Chl:** minor, local

Notes: Ms and Chl in area with Py, not foliated

Sample: 7 **Rock type :** Qtz-Bt-Ms-Gr-Rt schist

Field notes: sheared hydrothermal rock, 007b- Po in small piece?-thin section evidence (graphite, rounded grains) suggests a sediment

Sample location: 100 m northeast of the north end of Mellemgrube

Strike: **Geochemical analysis:** 100

Dip: **Microprobe analysis:**

y: minor, probably late **Po:** tr. **Ccp:** tr. with Py

Ilm: 0 **Hem:** 0

Mag: 0 **Gr:** tr.

Opaque mineralogy notes: Py may suround Gr and other minerals, minor Rt some touching Gr; 1 Po grain; Py is coarse but in the matrices so inclusions of all silicates are more abundant than sulphide

Plagioclase (Pl) ***General:*** 30%, fine grained

Alteration : strong ***extinction angle:*** ?

Qtz: >30%, fine grained **Scp:** 0

Amphiboles: **Cal:**

Bt: >10%, coarse-med. grained **Ms:** 10%, med. grained

Kfs: tr. **Sil:** 0 **Tlc:**

Others : **Chl:**

Notes: Gr foliated 0.5 mm logn bent grains

Sample: 9 **Rock type :** albitized Qtz-Bt-Kfs-Ms-Chl s

Field notes: high grade sample of a rock that is strongly albitized and sulphidized along discrete zones parallel foliation

Sample location: near north end of an open pit at the south end of Skuterud

Strike: **Geochemical analysis:** 100

Dip: **Microprobe analysis:** Ap.xenotime.Kf.Mnz.Rt

y: tr.fine grained, with Ccp **Po:** 0 **Ccp:** minor.

Ilm: 0 **Hem:** 0

Mag: 0 **Gr:** 0

Opaque mineralogy notes: Ccp quite porous, mainly in coarser vein with some Bt, disemminated minor Rt

Plagioclase (Pl) ***General:*** 20%,fine grained

Alteration : moderate ***extinction angle:*** ?

Qtz: >30%, fine, granular **Scp:** 0

Amphiboles: **Cal:**

Bt: minor, moderate foliation **Ms:** tr, fine, unfoliated, with Bt

Kfs: 30% in some areas **Sil:** 0 **Tlc:**

Others : minor Rt, Ap (some with chlorine), tr. xenotime, tr. Mnz **Chl:** trace, chlorine free, with Ms

Notes: Chl probably late, no chlorine in the Chl but in the Ap; Ms may be younger than Bt

---

Sample: 10 **Rock type :** Qtz-Ms-Sil quartzite

Field notes: quartzite,5% Ms, fine grained, weakly layered

Sample location: along northwest margin of the Sondregrube pit

Strike: 178 **Geochemical analysis:** 0

Dip: 70 **Microprobe analysis:** cobaltite, Py

y: fine - tr.porous (low temp.) **Po:** 0 **Ccp:** y, tr.

Ilm: 0, minor Rt **Hem:** 0

Mag: 0 **Gr:** 0

Opaque mineralogy notes: disseminated colbaltite, skutterudite?

Plagioclase (Pl) ***General:*** minor fine grained

Alteration : unaltered ***extinction angle:***

Qtz: >30% **Scp:** 0

Amphiboles: **Cal:** 0

Bt: 0 **Ms:** 5% weak foliation

Kfs: 30% **Sil:** tr., clusters of rods **Tlc:** 0

Others : ore sulphides **Chl:** 5%

Notes:

Sample: 12 **Rock type :** Ms-Sil-Tur-Bt gneiss

Field notes: Qtzite with minor Bt/alb, see diagram

Sample location: along northeast margin of the Søndregrube pit (footwall)

Strike: **Geochemical analysis:** au

Dip: **Microprobe analysis:** y

y: tr. fine-med. porous (low temp.) **Po:** 0 **Ccp:** tr.

Ilm: 0 **Hem:** 0

Mag: 0 **Gr:** 0

Opaque mineralogy notes: Rt, possible Ttn; coarse, porous Po?

Plagioclase (Pl) ***General:*** 0

Alteration : 0 ***extinction angle:***

Qtz: >30% **Scp:** 0

Amphiboles: **Cal:** 0

Bt: tr. **Ms:** 10%

Kfs: **Sil:** coarse nodules, mow **Tlc:**

Others : tr. Tur **Chl:** minor

Notes: Ttn may be assoc. with nodules, unoriented late Ms replaces Sil nodules

---

Sample: 13.1 **Rock type :** Oam-Ms-Crd rock

Field notes: rad. clusters of 2cm Oam, no Crd identified, o/c that I.A.Munz pointed out

Sample location:

Strike: **Geochemical analysis:** 100

Dip: **Microprobe analysis:**

y: **Po:** 0 **Ccp:**

Ilm: 0% **Hem:** 5% ilmohematite

Mag: 0 **Gr:** 0

Opaque mineralogy notes: Tr. Rt. with hematite

Plagioclase (Pl) ***General:*** fine grained, unconfirmed albitized

Alteration : light patchy ***extinction angle:*** 5

Qtz: 10% **Scp:** 0

Amphiboles: <20%, anthophillite **Cal:**

Bt: 0 **Ms:** 10%

Kfs: **Sil:** 0 **Tlc:**

Others : minor Crd **Chl:**

Notes: Cam is a lighter than normal colour

Sample: 13.2 **Rock type :** pegmatite

Field notes: x-ray of Pl.

Sample location: 10cm from A

Strike: **Geochemical analysis:**

Dip: **Microprobe analysis:**

y: **Po:** 0 **Ccp:** tr.

Ilm: 0 **Hem:**

Mag: 0 **Gr:**

Opaque mineralogy notes:

Plagioclase (Pl) ***General:***

Alteration : 0 ***extinction angle:***

Qtz: 0 **Scp:** 0

Amphiboles: **Cal:**

Bt: 0 **Ms:** 0

Kfs: **Sil:** 0 **Tlc:** 0

Others : **Chl:**

Notes: no thin section

Sample: 15 **Rock type :** Bt-Ms quartzite

Field notes: Qtzite w/ pathches of Ms

Sample location: NE side of central pit

Strike: **Geochemical analysis:** au

Dip: **Microprobe analysis:**

y: tr.cubic **Po:** 0 **Ccp:**

Ilm: 0 **Hem:**

Mag: 0 **Gr:** 0

Opaque mineralogy notes: Py probably late

Plagioclase (Pl) ***General:*** 0

Alteration : 0 ***extinction angle:*** 0

Qtz: 90% **Scp:** 0

Amphiboles: **Cal:** 0

Bt: tr **Ms:** 5%

Kfs: tr. **Sil:** 0 **Tlc:** 0

Others : 0 **Chl:** tr

Notes:

Sample: 16 **Rock type :** Chl-Py-Oam?-Mag vein

Field notes: abundant coarse Ab and Qtz (pegematitic) w/ lesser Cam in monomineralic aggregates, sample includes chips from Cam and Qtz clot and seen in phot 2-1, note magnetic Ilm

Sample location: Northeast of Butjern lake, normally foliated amphibolite with garnet, this sample from amphibolite bluff, near north end of face

Strike: 50 **Geochemical analysis:** geochem sampl

Dip: 90 **Microprobe analysis:**

y: 20% **Po:** 0 **Ccp:**

Ilm: 0 **Hem:**

Mag: 5% **Gr:** 0

Opaque mineralogy notes: sulphide in area with only orthoamphiboles

Plagioclase (Pl): ***General:*** 0

Alteration : 0 ***extinction angle:***

Qtz: 0 **Scp:** 0

Amphiboles: 20%, orthoamphibole **Cal:** 0

Bt: trace **Ms:** 0

Kfs: **Sil:** 0 **Tlc:**

Others : 20% Oam? **Chl:** 20%, all in foliated area

Notes: the coarse Mag and Py intergrowth seems cogenetic, crosscuts, deflects foliation

---

Sample: 17 **Rock type :** gneissic amphibolite

Field notes: med grained amphibolite, with vein of Ab?

Sample location: East of Butjern lake, normally foliated amphibolite with garnet, this sample from amphibolite bluff, near north end of face

Strike: **Geochemical analysis:** 100

Dip: **Microprobe analysis:**

y: fine - tr. **Po:** possible tr. **Ccp:**

Ilm: tr.with exsolved Hem **Hem:** tr.

Mag: 0 **Gr:** 0

Opaque mineralogy notes: I think that with Py surrrounding Ilm and visa versa Py is not shallow, exsolution of Ccp, po from Py--high temp?

Plagioclase (Pl): ***General:*** fine grained

Alteration : strong, sericitic ***extinction angle:*** ?

Qtz: 0 **Scp:** possible

Amphiboles: >20% **Cal:**

Bt: 1,brown+green **Ms:** 0

Kfs: 0 **Sil:** 0 **Tlc:**

Others : tr. Srp **Chl:** tr.

Notes: Pl alt may be Ep

Sample: 18 **Rock type :** Bt-Hbl-Ccp amphibolite

Field notes: Bt amphibolite vein (about 2m) with 5% foliated parallel to country rock, possibly shear zone.

Sample location: Forhaabningenes stoll, at entrance.

Strike: **Geochemical analysis:**

Dip: **Microprobe analysis:**

y: some as exsolution in Ccp **Po:** 0 **Ccp:** 2%, fine-med

Ilm: tr. **Hem:** 0

Mag: 0 **Gr:**

Opaque mineralogy notes: fine Ilm occurs between Bt grains and one med.grain with exsolution of Ccp

Plagioclase (Pl) ***General:*** 0

Alteration : ***extinction angle:***

Qtz: minor? **Scp:** possible tr.

Amphiboles: 30%, coarse hastingsite **Cal:**

Bt: 50% coarse flakes **Ms:** 0

Kfs: tr. **Sil:** 0 **Tlc:**

Others : **Chl:**

Notes: Pl possibly in small veins and along cleavage- biaxial but not twined

---

Sample: 19 **Rock type :** Bt-Hbl-Qtz-Czo-Chl gneissic

Field notes: shear zone 3m wide, albitite veins crosscut shear zone (see photos)

Sample location: traverse into Forhaabningenes Stol (adit?), see graph paper, 18m in

Strike: 001 **Geochemical analysis:** ?

Dip: 56 **Microprobe analysis:**

y: minor, late? **Po:** tr. in Py **Ccp:** tr

Ilm: tr. **Hem:**

Mag: tr. in a Py grain **Gr:** 0

Opaque mineralogy notes:

Plagioclase (Pl) ***General:*** fine grained, unconfirmed albitized

Alteration : light patchy ***extinction angle:*** 10

Qtz: 10% **Scp:** 0

Amphiboles: 20%, appears to be replaced by Bt. **Cal:** 0

Bt: 40% **Ms:** 0

Kfs: 0 **Sil:** 0 **Tlc:** 0

Others : Czo up to 10% 0.2mm subhedral, zoned, replacing Pl + Bt **Chl:** tr. replaces Bt?

Notes:

Sample: 20.1 **Rock type :** Hbl-Bt-Ab amphibolite

Field notes: albitite, some of the largest pieces have wall rock in them, wall rock is very similar to 21, a refers to geochem sample-mainly Ab some wall rock

Sample location: traverse into Forhaabningenes stol (adit?), see graph paper, 19m in

Strike: 001 **Geochemical analysis:** 20a Ab vein, 2

Dip: 60 **Microprobe analysis:**

y: minor, rimmed by silicate (Qtz?) **Po:** 0 **Ccp:** minor

Ilm: 0 **Hem:**

Mag: 0 **Gr:** 0

Opaque mineralogy notes: no oxides observed

Plagioclase (Pl) ***General:*** minor, coarse grained, unconfirmed albitized

Alteration : strong ***extinction angle:***

Qtz: <5%, fine rim around sulphides **Scp:** 30%, Qtz rim between Sc and Py

Amphiboles: >20% **Cal:**

Bt: 10% **Ms:** 0

Kfs: minor **Sil:** 0 **Tlc:** 0

Others : 0 **Chl:**

Notes: Scp has replaced some Pl, seems to have wall rock not vein

---

Sample: 22 **Rock type :** Ms-Tur-Sil quartzite

Field notes: quartzite

Sample location: traverse into Forhaabningenes stol (adit?), see graph paper, 30m in, see drawing p 41

Strike: **Geochemical analysis:**

Dip: **Microprobe analysis:**

y: tr. corroded grains **Po:** 00 **Ccp:**

Ilm: 0 **Hem:**

Mag: 0 **Gr:** 0

Opaque mineralogy notes: trace Rt.

Plagioclase (Pl) ***General:*** 0

Alteration : unaltered ***extinction angle:*** 0

Qtz: >30%, fine equant grains, with 10mm ribbons **Scp:** 0

Amphiboles: **Cal:**

Bt: 0 **Ms:** Minor

Kfs: tr **Sil:** tr. clots **Tlc:**

Others : 5% Tur **Chl:**

Notes: the lack of oxides explains the Fe3/Fe2 ratio.scapolite after foliaton, minor Tur

Sample: 25 **Rock type :** Pl-Qtz-Bt-Tur-Sil-Py-Gr schis

Field notes: chip sample, in rusted zone

Sample location: Forhnigenes stoll, 70m in

Strike: **Geochemical analysis:** ?

Dip: **Microprobe analysis:** y,should probe sulphides

y: >1% fine porous **Po:** possible tr. **Ccp:** 1%

Ilm: possible **Hem:** 0

Mag: 0 **Gr:** 1%

Opaque mineralogy notes: no ore minerals found by probe, only Py with some ni;

Plagioclase (Pl) ***General:*** 0

Alteration : moderate ***extinction angle:***

Qtz: 30% **Scp:** 0

Amphiboles: **Cal:**

Bt: 10% **Ms:** 0

Kfs: 0 **Sil:** tr. fibrolite on Bt **Tlc:**

Others : Tur **Chl:** tr.

Notes:

Sample: 26 **Rock type :** Hbl-Ep-Mgs amphibolite

Field notes: h.s: med gr. amp. w/ blebs of Qtz rimming magnesite

Sample location: Embretfoss, sample from waste rock pile outside magnesite quarry

Strike: **Geochemical analysis:** au

Dip: **Microprobe analysis:** xray analysis of whole rock powder, major Pl and ort

y: 10%, coarse **Po:** 0 **Ccp:** 2%

Ilm: 0 **Hem:**

Mag: 1%, with and in Py **Gr:**

Opaque mineralogy notes:

Plagioclase (Pl) ***General:*** fine grained, unconfirmed

Alteration : strong ***extinction angle:*** ?

Qtz: 0 **Scp:** 0

Amphiboles: >20%, coarse hornblende **Cal:** <5%

Bt: 0 **Ms:** 0

Kfs: 0 **Sil:** 0 **Tlc:**

Others : minor Ep **Chl:** minor

Notes:

Sample: 28 **Rock type :** Ab-Cal-Act-Chl rock

Field notes: Cal albitite vein with Py, Hem

Sample location: Overbykollen Cal quarry

Strike: **Geochemical analysis:**

Dip: **Microprobe analysis:**

y: tr. equant **Po:** 0 **Ccp:**

Ilm: 0 **Hem:** tr. fine plate habit

Mag: 0 **Gr:**

Opaque mineralogy notes:

Plagioclase (Pl) ***General:*** 10%, chessboard twinning

Alteration : 0. ***extinction angle:*** 30

Qtz: 0 **Scp:** 0

Amphiboles: minor Act **Cal:** >5%

Bt: 0 **Ms:** 0

Kfs: **Sil:** 0 **Tlc:**

Others : **Chl:** 10%

Notes:

Sample: 30 **Rock type :** fine grained albitite

Field notes: fine to med gr with tr Py

Sample location: Overbykollen, on road 100m up from waste rock pile

Strike: **Geochemical analysis:**

Dip: **Microprobe analysis:**

y: 0 **Po:** 0 **Ccp:** 0

Ilm: 0 **Hem:** 1% fine equant to elongate

Mag: 0 **Gr:**

Opaque mineralogy notes:

Plagioclase (Pl) ***General:*** 20%

Alteration : 0 ***extinction angle:*** 30

Qtz: 30% **Scp:** 0

Amphiboles: 10% fine Tr **Cal:** >5%

Bt: 0 **Ms:** probable,fine clots,unfoliated

Kfs: 0 **Sil:** 0 **Tlc:** minor probable

Others : **Chl:**

Notes: Qtz and Cal may be med. grained but most minerals fine grained fairly evenly distributed

Sample: 31 **Rock type :** Cal-Ab rock

Field notes: sample of alb1 with reminant rounded frags. of amph. these are enriched in Hem and Py

Sample location: Overbykollen Cal quarry

Strike: **Geochemical analysis:**

Dip: **Microprobe analysis:** x-ray mineral analysis of rock powder. major Ab; mi

y: coarse **Po:** one coarse grain **Ccp:**

Ilm: 0 **Hem:** local 30% fine plates

Mag: 0 **Gr:**

Opaque mineralogy notes: Hem equant fine plates in area of Cal and Tlc?

Plagioclase (Pl) ***General:*** fine Ab dominant in area of low Hem

Alteration : 0 ***extinction angle:***

Qtz: minor in low Hem area **Scp:** 0

Amphiboles: possible Tr. **Cal:** <5% in section. with

Bt: 0 **Ms:** probable

Kfs: **Sil:** 0 **Tlc:** 20%

Others : **Chl:**

Notes: about 20% of the area is Tlc and/or Ms probably both. Tr?

Sample: 32 **Rock type :** coarse Cal vein

Field notes: Ab. calcite. vein in Amp w/ Pyand Hem

Sample location: Overbykollen Cal quarry

Strike: **Geochemical analysis:**

Dip: **Microprobe analysis:**

y: >5%. coarse occuring in a vein **Po:** 0 **Ccp:** 0

Ilm: tr., weak anisotropy **Hem:** tr

Mag: 0 **Gr:** 0

Opaque mineralogy notes: Ilm and Hem occur together in relict grains with rhomic intergrowths maginal to massive Py

Plagioclase (Pl) ***General:*** possibly .fine grained

Alteration : strongly altered if present ***extinction angle:***

Qtz: 0 **Scp:** 0

Amphiboles: ? **Cal:** 80%

Bt: 0 **Ms:** 0

Kfs: 0 **Sil:** 0 **Tlc:** 10%. fine grained disseminated

Others : **Chl:**

Notes: carbonate vein.

Sample: 35 **Rock type :** Qtz-Ab-Act?-Ms-Cal-Chl brec

Field notes: Ab-rich matrix with rounded frags up to 50cm across of mafic (80%) and metaQtzite(20%). most clasts are 3cm or less. matrix has some amphiboles thoughout. few oxides or suphides

Sample location: Overbykollen. sample from lunch spot

Strike: **Geochemical analysis:**

Dip: **Microprobe analysis:** xray analysis of rock powder. major quartz; minor C

y: 0 **Po:** 0 **Ccp:** 0

Ilm: 0 **Hem:** 1% dissem. fine gr

Mag: 0 **Gr:** 0

Opaque mineralogy notes: a coarse grey low reflectant grain w/ red internal reflections not identified

Plagioclase (Pl) ***General:*** 30% med grained equant-irregular

Alteration : light patchy ***extinction angle:*** 20

Qtz: 60% med grained irregular **Scp:** 0

Amphiboles: 10% Act **Cal:** <5%

Bt: 0 **Ms:** 5%. fine clots. some sericite

Kfs: **Sil:** 0 **Tlc:** minor. fine clots

Others : **Chl:** tr. with Tlc and Ms

Notes: not foliated. from a breccia fragment. surrounding matrix is calcite

---

Sample: 37 **Rock type :** Py-Hem-Ab-Tr rock

Field notes: amphibolite contact with Cal vein

Sample location: Overbykollen. 036? contact with Cal vein

Strike: **Geochemical analysis:**

Dip: **Microprobe analysis:**

y: 1%. coarse euhedral grains **Po:** 0 **Ccp:** 0

Ilm: 0 **Hem:** 5% fine laths or plates

Mag: 0 **Gr:** 0

Opaque mineralogy notes:

Plagioclase (Pl) ***General:*** 20%

Alteration : moderate ***extinction angle:*** 30% Ab

Qtz: 5% **Scp:** 0

Amphiboles: 70% Tr **Cal:** possible trace

Bt: 0 **Ms:** 0

Kfs: 0 **Sil:** 0 **Tlc:**

Others : **Chl:**

Notes: not foliated; Pl concentrated in local areas

Sample: 38 **Rock type :** Act-Pl gneiss

Field notes: coarse Amp. w/ Ab matrix, ; patchy white areas

Sample location: Overbykollen, 70m down road

Strike: **Geochemical analysis:**

Dip: **Microprobe analysis:**

y: tr., fine grained **Po:** 0 **Ccp:**

Ilm: tr. med grains **Hem:** tr.

Mag: 0 **Gr:**

Opaque mineralogy notes: some Rt occurs with/ within Ilm

Plagioclase (Pl) ***General:*** coarse-med grained, unconfirmed albitized

Alteration : moderate-strong ***extinction angle:***

Qtz: 0 **Scp:** 0

Amphiboles: 30% Act **Cal:** 0

Bt: 0 **Ms:** 0

Kfs: 0 **Sil:** 0 **Tlc:**

Others : fine veins of Srp **Chl:** minor

Notes: not foliated, patchy areas of Act and others of Pl

Sample: 40 **Rock type :** Act-Ab gneiss

Field notes:

Sample location: Overbykollen on road, 30m nw of 039

Strike: 170 **Geochemical analysis:**

Dip: 72 **Microprobe analysis:**

y: 0 **Po:** 0 **Ccp:** 0

Ilm: 0 **Hem:** tr. fine dissem.

Mag: 0 **Gr:**

Opaque mineralogy notes:

Plagioclase (Pl) ***General:*** 60%,fine grained, unconfirmed albitized

Alteration : light ***extinction angle:*** generally not twinned

Qtz: 0 **Scp:** 0

Amphiboles: 40% fine foliated Act **Cal:**

Bt: 0 **Ms:** 0

Kfs: **Sil:** 0 **Tlc:**

Others : **Chl:**

Notes: generally fine grained and well foliated, a "type one albitite"

Sample: 41 **Rock type :** Hbl-Scp-Ab gneiss

Field notes: med gr fol. Mag .Hb-Ab-gneiss, not layered

Sample location: Overbykollen, 30m nw of 040

Strike: **Geochemical analysis:**

Dip: **Microprobe analysis:**

y: tr. fine partially rimmed by high temp Hem **Po:** tr. in Py **Ccp:** tr. within Py

Ilm: 0 **Hem:** tr.

Mag: 0 **Gr:**

Opaque mineralogy notes: Hem rimming Py

Plagioclase (Pl) ***General:*** 60% fine, not well twinned, possibly Ab

Alteration : very light ***extinction angle:*** 30

Qtz: 0 **Scp:** 10% intergrown with plag

Amphiboles: 30%, fine grained **Cal:**

Bt: 0 **Ms:** 0

Kfs: **Sil:** 0 **Tlc:**

Others : **Chl:**

Notes: fine gneissic layering, section is thick

Sample: 42.1 **Rock type :** proto-amphibolite

Field notes: from roadside blast rubble, 3 rocks a, b,c,

Sample location: Overbykollen road collected with Eion, nw from 041-beyond the intersection

Strike: **Geochemical analysis:** 100, qtz vein m

Dip: **Microprobe analysis:**

y: tr.equant, cubic **Po:** tr. **Ccp:** tr. in Py

Ilm: tr. no exsolution **Hem:**

Mag: 0 **Gr:**

Opaque mineralogy notes: there is a isotropic sulphide that has a pink hue (at the bottom of the slide). Po locally rims Py with Ccp

Plagioclase (Pl) ***General:*** 30%, fine mosaic,

Alteration : patchy, strong ***extinction angle:*** 35,15

Qtz: 0 **Scp:** 0

Amphiboles: 50% **Cal:** 0

Bt: 0 **Ms:** 0

Kfs: **Sil:** 0 **Tlc:**

Others : 0 **Chl:**

Notes:

Sample: 42.2 **Rock type :** proto-amphibolite

Field notes: from roadside blast rubble. 3 rocks a. b.c.

Sample location: Overbykollen road collected with Eion. nw from 041-beyond the intersection

Strike: **Geochemical analysis:** 100. qtz vein m

Dip: **Microprobe analysis:**

y: tr. fine **Po:** Pl. vein Po.Ccp.Py **Ccp:** tr. in vein

Ilm: tr. **Hem:**

Mag: 0 **Gr:**

Opaque mineralogy notes: a 2mm vein of altered Pl with intergrown Py and Po

Plagioclase (Pl) ***General:*** fine mosaic

Alteration : strong ***extinction angle:***

Qtz: 0 **Scp:** 0

Amphiboles: 30% fine aggregate of Hbl **Cal:**

Bt: 0 **Ms:** 0

Kfs: 0 **Sil:** 0 **Tlc:**

Others : 0 **Chl:**

Notes:

Sample: 42.3 **Rock type :** proto-amphibolite

Field notes: from roadside blast rubble

Sample location: Overbykollen road collected with Eion. nw from 041-beyond the intersection

Strike: **Geochemical analysis:**

Dip: **Microprobe analysis:**

y: tr. fine **Po:** 0 **Ccp:**

Ilm: 1%. fine to med. **Hem:** tr. as exsolution in Ilm

Mag: 0 **Gr:**

Opaque mineralogy notes: some very fine Py through some Cam

Plagioclase (Pl) ***General:*** 30%. laths med. grained

Alteration : variable ***extinction angle:*** 40

Qtz: 0 **Scp:** 0

Amphiboles: 60% **Cal:**

Bt: tr. **Ms:** tr. with Ms

Kfs: **Sil:** 0 **Tlc:**

Others : **Chl:**

Notes:

Sample: 43 **Rock type :** equigranular amphibolite

Field notes: from roadside blast rubble , 3 rocks a, b,c,

Sample location: Overbykollen road collected with Eion. nw from 041-beyond the intersection

Strike: **Geochemical analysis:**

Dip: **Microprobe analysis:**

y: tr. fine **Po:** 0 **Ccp:** tr., with Py.<Py

Ilm: tr. fine **Hem:**

Mag: 0 **Gr:**

Opaque mineralogy notes: also discrete Rt?

Plagioclase (Pl) ***General:*** 20% fine grained

Alteration : variable ***extinction angle:***

Qtz: 0 **Scp:** 0

Amphiboles: 80% **Cal:**

Bt: 0 **Ms:** 0

Kfs: **Sil:** 0 **Tlc:**

Others : **Chl:**

Notes: not foliated

Sample: 47 **Rock type :** albitite

Field notes: strongly albitized foliated amphibolite

Sample location: Overbykollen road sw of quarry

Strike: **Geochemical analysis:** 1

Dip: **Microprobe analysis:** y?rt+Pl +ap?

y: fine - tr., altered **Po:** 0 **Ccp:** 0

Ilm: 0 **Hem:** 0

Mag: 0 **Gr:** 0

Opaque mineralogy notes: 3% medium grained foliated aggregates of Rt

Plagioclase (Pl) ***General:*** 60% fine grained, unconfirmed ***albitized*

Alteration : moderate ***extinction angle:*** small

Qtz: 30% fine grained **Scp:** 0

Amphiboles: 5% Tr **Cal:**

Bt: 0 **Ms:** 0

Kfs: possible **Sil:** 0 **Tlc:** 5% with Tr. fine radiating

Others : tr. Ap. **Chl:**

Notes: foliation is variable, med. grained and unfoliated, fine augen Qtz mylonite?

Sample: 48 **Rock type :** granite

Field notes: no description

Sample location: Overbykollen waste pile?

Strike: **Geochemical analysis:** crush

Dip: **Microprobe analysis:** x

y: 0 **Po:** 0 **Ccp:** 0

Ilm: tr. **Hem:**

Mag: 2% **Gr:** 0

Opaque mineralogy notes: medium grained Mag with minor Ilm lamellae

Plagioclase (Pl) ***General:*** 30%

Alteration : 0 ***extinction angle:*** <5

Qtz: 30 **Scp:** 0

Amphiboles: **Cal:** 0

Bt: 5% green, unoriented **Ms:** 0

Kfs: 30% **Sil:** 0 **Tlc:**

Others : **Chl:**

Notes: interlocking medium grained texture, no foliation apparent

---

Sample: 49 **Rock type :** Chl-Ab-Qtz-Bt-Cal

Field notes: no description

Sample location: Overbykollen waste pile?

Strike: **Geochemical analysis:** 1

Dip: **Microprobe analysis:**

y: tr. v.fine equant grains **Po:** 0 **Ccp:** 0

Ilm: tr. **Hem:**

Mag: tr. in relict grains **Gr:** 0

Opaque mineralogy notes: Ilm is altered, as well as minor alteration Hem anround the grains there may be intergrowths

Plagioclase (Pl) ***General:*** possibly but no twinning observed

Alteration : ? ***extinction angle:***

Qtz: approximately 20% **Scp:** possible

Amphiboles: **Cal:** 1% in patches

Bt: tr. fine grained **Ms:** 0

Kfs: ? **Sil:** 0 **Tlc:**

Others : tr. clear, mod to high biref. late? **Chl:** 20 to 50%

Notes: dusty alteration, possibly epidote, throughout

Sample: 50 **Rock type :** metagabbro

Field notes: meta-gabbro? with little alteration

Sample location: south of Overbykollen-from behind houses in Bingås area-see map p.50

Strike: **Geochemical analysis:** 1

Dip: **Microprobe analysis:** amphibole, Pyroxene,

y: trace fine grained **Po:** tr. **Ccp:**

Ilm: tr. **Hem:**

Mag: tr, with Py and Po **Gr:**

Opaque mineralogy notes: much Ilm replaced by a graphic textured Rt?; a possible composite grain of Po, Py and Mag see notes page 83

Plagioclase (Pl) ***General:*** 40%, coarse igneous laths

Alteration : patchy ***extinction angle:*** 30

Qtz: 0 **Scp:** 0

Amphiboles: 50%, typically uralitic hornblende **Cal:** 0

Bt: 0 **Ms:** 0

Kfs: **Sil:** 0 **Tlc:**

Others : corroded Opx, possible trace Ol **Chl:**

Notes: Hbl are cored by relict Opx, igneous textures presserved. Two sections

---

Sample: 51 **Rock type :** scapolized-metagabbro

Field notes: moderate alteration, foliation stronger than PWN 050

Sample location: south of Overbykollen-from behind houses in Bingås area-see map p.50

Strike: **Geochemical analysis:** 1

Dip: **Microprobe analysis:** y

y: trace fine equant or aggregates **Po:** 0 **Ccp:** trace

Ilm: tr. **Hem:** 0

Mag: 0 **Gr:**

Opaque mineralogy notes: trace loose aggregates of fine Rt, Ilm partially replaced by blue mineral with clear internal reflections as in 50 (but not wormy)

Plagioclase (Pl) ***General:*** 30%, laths and finer

Alteration : strong ***extinction angle:*** about 30

Qtz: 0 **Scp:** 20%, medium to coarse grained, w/ Py locally

Amphiboles: 50%, hornblende, half is uralitic **Cal:**

Bt: 5%, med. gr., unoriented, Rt rods; with Ilm **Ms:** tr. see probe results

Kfs: **Sil:** 0 **Tlc:**

Others : Rt **Chl:**

Notes: Hbl are cored by relict Opx, some is Cpx. Py in contact with Scp

Sample: 52 **Rock type :** Act-albitite

Field notes: local foliation defined by reminant mafic mineral

Sample location: south of Overbykollen-from behind houses in Bingås area -see map p.50

Strike: **Geochemical analysis:** 1

Dip: **Microprobe analysis:**

y: 0 **Po:** 0 **Ccp:** 0

Ilm: tr. **Hem:** tr.

Mag: 0 **Gr:**

Opaque mineralogy notes: discrete grains of a blue grey oxide with strong anisotropy are present Hem or Ilm; minor anhedral Ttn and lesser tr. Rt with a ragged habit

Plagioclase (Pl) ***General:*** 80%, variable gr. size, Ab, possibly chessboard texture, (Escher like)

Alteration : light patchy ***extinction angle:***

Qtz: 0 **Scp:** possible based on chem

Amphiboles: 20% medium grained Act, anhedral with Rt **Cal:** 0

Bt: 0 **Ms:** 0

Kfs: 0 **Sil:** 0 **Tlc:** 0

Others : 0 **Chl:** 0

Notes: fine grained unfoliated, no sharp contact with mafics is noted

---

Sample: 53 **Rock type :** metagabbro

Field notes: foliated and layered block, note variable foliation, good photo of source

Sample location: block, from behind houses in Bingås area

Strike: **Geochemical analysis:** 1

Dip: **Microprobe analysis:** y

y: present **Po:** 0 **Ccp:**

Ilm: tr. **Hem:** tr.

Mag: 0 **Gr:**

Opaque mineralogy notes: Ilm may contain 3 mottled phases Ilm, Rt, Hem

Plagioclase (Pl) ***General:*** 20% coarse igeous laths

Alteration : strong, grains porous (turbid) ***extinction angle:***

Qtz: 0 **Scp:** minor ,typical habit and low biref.

Amphiboles: 60% fine uralitic hornblende **Cal:**

Bt: minor, unoriented, fine grained, rutile needles **Ms:** 0

Kfs: **Sil:** 0 **Tlc:**

Others : **Chl:**

Notes: Hbl are cored by relict Opx

Sample: 54 **Rock type :** albitite

Field notes: bleached Amp. w/ some med. gr. veins of Pl. (<2cm) . the fine grained rock appears unfoliated. some type II veins in the area

Sample location: just north of Butjern lake

Strike: 10 **Geochemical analysis:** 1

Dip: 70e **Microprobe analysis:**

y: one oxidized cubic grain **Po:** 0 **Ccp:**

Ilm: 0 **Hem:** tr. minor fine, Ilm lamelae?

Mag: 0 **Gr:** 0

Opaque mineralogy notes: minor trace fine Rt and Ttn, sometimes with Hem, some minor Hem in Bt

Plagioclase (Pl) ***General:*** 50% fine grained, unconfirmed albitized, rounded grains

Alteration : 0 ***extinction angle:***

Qtz: 10% fine equant grains **Scp:** possibly as much as 20%

Amphiboles: 5% anhedral irregular fine Tr-Act **Cal:**

Bt: minor unoriented, fine grained **Ms:** 0

Kfs: **Sil:** 0 **Tlc:** 30% forming fine matrix

Others : **Chl:** minor with Tlc in matrix, unconfirmed

Notes: made up of fine rounded grains of mainly Pl in a matrix of Tlc and Chl, psammite?

Sample: 55 **Rock type :** albitite-quartzite

Field notes: type I alb? with relic mafic rocks through out

Sample location: 93m on traverse east from Butjern lake

Strike: **Geochemical analysis:** 1

Dip: **Microprobe analysis:**

y: 0 **Po:** 0 **Ccp:** 0

Ilm: 0 **Hem:** minor fine grained dissem.

Mag: 0 **Gr:**

Opaque mineralogy notes: Rt and Ttn as trace discrete grains and rarely with Hem

Plagioclase (Pl) ***General:*** 30% fine some local concentrations appear to be Ab as in PWN 052

Alteration : 0 ***extinction angle:*** 20

Qtz: 60% **Scp:** 0

Amphiboles: **Cal:** 0

Bt: 0 **Ms:** minor fine grained clots

Kfs: **Sil:** 0 **Tlc:** tr. often with Ms

Others : **Chl:**

Notes: Ab enriched quartzite

Sample: 56 **Rock type :** albitite

Field notes: foliated type I Ab fine grained, foliation defined by 0.5 cm Qtz veins, notice north arrow on sample when horizontal

Sample location: 150m on traverse east from Butjern lake

Strike: 10 **Geochemical analysis:** 1

Dip: 90 **Microprobe analysis:** yes (lost) Hem w/Ti,Tur, Tc, Cal

y: present **Po:** 0 **Ccp:**

Ilm: 0 **Hem:** 2%, dissem., fine grained w/ Ti

Mag: 0 **Gr:** 0

Opaque mineralogy notes: minor Ttn and Rt as lamelae and separate grains

Plagioclase (Pl) ***General:*** 1mm and 0.1mm mosaic like grains, chessboard texture

Alteration : unaltered ***extinction angle:*** 20

Qtz: 10% in 0.5 cm veins **Scp:** 0

Amphiboles: minor 0.1mm equant Act **Cal:** tr.(pure)

Bt: 0 **Ms:** minor, med. grained unoriented

Kfs: **Sil:** 0 **Tlc:** 5%, in generally medium graned clots

Others : **Chl:** trace, with Tlc

Notes: possibly the most Hem other than in samples from Overbykollen

---

Sample: 57 **Rock type :** Na-enriched amphibolite

Field notes: Amphibolite pos. weak albitization, fol. not layered

Sample location: 178m on traverse east from Butjern lake

Strike: **Geochemical analysis:** 1

Dip: **Microprobe analysis:**

y: 0 **Po:** 0 **Ccp:** 0

Ilm: tr. fine -med. often connected with Hem **Hem:** 2% Hem fine gr

Mag: 0 **Gr:**

Opaque mineralogy notes: Ilm, Hem mainly in Hbl; occasionally Ilm rims a grain and replaces Hbl in skelaton like texture. no Rt or Ttn observed

Plagioclase (Pl) ***General:*** possibly 70% Ab, though scapolite appears to have replaced most

Alteration : moderate ***extinction angle:***

Qtz: 0 **Scp:** 30-60% fine in aggregates replacing Pl

Amphiboles: 30%, Hbl, some cores appear to have Opx **Cal:** 0

Bt: tr. fine grained unfoliated **Ms:** 0

Kfs: 0 **Sil:** 0 **Tlc:**

Others : **Chl:**

Notes:

Sample: 58 **Rock type :** Qtz-Pl-Bt gneiss

Field notes: Bt-Qtz schist and unfoliated coarse Ab-Qtz (vein), this is the vein

Sample location: 210m east from Butjern L.

Strike: **Geochemical analysis:**

Dip: **Microprobe analysis:**

y: 0 **Po:** 0 **Ccp:** 0

Ilm: 0 **Hem:** 0

Mag: 0 **Gr:** 0

Opaque mineralogy notes: no opaques

Plagioclase (Pl) ***General:*** 20%, local, coarse

Alteration : strong, epidote like ***extinction angle:***

Qtz: 70%, coarse, foliated **Scp:** 0

Amphiboles: **Cal:** 0

Bt: 5% foliated, elongate **Ms:** 0

Kfs: one fine grain, with Pl **Sil:** 0 **Tlc:**

Others : Rt? **Chl:**

Notes: half of the section is a Bt-Qtz-schist (060), while half is a type two Ab vein (059)

Sample: 59 **Rock type :** Ab-Qtz-Kfs-Bt gneiss

Field notes: Ab- Qtz vein type 2- for whole rock.

Sample location: 210m east from Butjern L.

Strike: **Geochemical analysis:**

Dip: **Microprobe analysis:**

y: **Po:** 0 **Ccp:**

Ilm: 0 **Hem:**

Mag: 0 **Gr:**

Opaque mineralogy notes: no opaques

Plagioclase (Pl) ***General:*** 70% coarse equant Ab

Alteration : light patchy ***extinction angle:*** 20

Qtz: 30%, coarse looks deformed **Scp:** 0

Amphiboles: **Cal:**

Bt: minor isn clots especially with quartz **Ms:** 0

Kfs: trace fine grained **Sil:** 0 **Tlc:**

Others : **Chl:**

Notes: this vein material also seen in half of 058, the Qtz and Bt are likely from wall rocks

Sample: 60 **Rock type :** Qtz-Bt Schist

Field notes: Bt-Qtz-schist

Sample location: 210m on traverse east from Butjern lake

Strike: **Geochemical analysis:** 1

Dip: **Microprobe analysis:**

y: **Po:** 0 **Ccp:**

Ilm: 0 **Hem:**

Mag: 0 **Gr:** 0

Opaque mineralogy notes: no opaques

Plagioclase (Pl): ***General:*** 30% fine-med. grained equant and dissem

Alteration : light patchy ***extinction angle:*** 5; zoned low in centre

Qtz: 60%, med grained, foliated **Scp:** 0

Amphiboles: **Cal:**

Bt: 8% fine, foliated, slight green hue **Ms:** 0

Kfs: tr. fine grains **Sil:** 0 **Tlc:** 0

Others : **Chl:** 0

Notes: this rock also seen on one half of PWN058, generally fine - med. grained

---

Sample: 61 **Rock type :** equigranular amphibolite

Field notes: meta sed, shearing, on the other side of of anticline from mine?

Sample location: 310m on traverse east from Butjern lake

Strike: **Geochemical analysis:** 1

Dip: **Microprobe analysis:**

y: tr. about 0.2mm **Po:** 0 **Ccp:** <Py, with Py

Ilm: tr., fine- med. gr. along foliation **Hem:**

Mag: tr. exsolution in Ilm, with Py **Gr:**

Opaque mineralogy notes: 5% Mag in Ilm, usually as thin lamellae; Mag attached to Py as irregular grains, locally surrounding Py, some patchy alteration of Ilm with white internal reflections

Plagioclase (Pl): ***General:*** med grained recrystallized,

Alteration : local strong sericitic alt. ***extinction angle:*** 35-60

Qtz: 0 **Scp:** 0

Amphiboles: 80 med grained **Cal:**

Bt: minor coarse late unfoliated Bt **Ms:** 0

Kfs: **Sil:** 0 **Tlc:**

Others : **Chl:** tr. interlayered in Bt

Notes: several photos, probably good, r3:1-5?, 13

Sample: 62 **Rock type :** equigranular amphibolite

Field notes: from an interlayered unit with seds that is about 5m wide

Sample location: 310m on traverse east from Butjern lake

Strike: **Geochemical analysis:** 100

Dip: **Microprobe analysis:**

y: fine - tr. **Po:** 0 **Ccp:**

Ilm: directly replaced, now Rt, Hem, Ttn? **Hem:** dominant oxide

Mag: 0 **Gr:** 0

Opaque mineralogy notes: most Ilm has been replaced possibly late

Plagioclase (Pl) ***General:*** fine grained, usually not twinned

Alteration : unaltered ***extinction angle:***

Qtz: possibly **Scp:** minor

Amphiboles: >20% **Cal:**

Bt: <10%, fine foliated with gneissocity **Ms:** 0

Kfs: minor **Sil:** 0 **Tlc:** minor along thin wispy veins?, also as a matrix in some areas

Others : minor usually with Tlc

Notes: one area has 20% Tlc in matrix. Tlc may be an alteration of Pl.

Sample: 63 **Rock type :** microcline pegmatite

Field notes: graphic Qtz parallel to the foliation

Sample location: 380m on traverse east from Butjern lake

Strike: **Geochemical analysis:** 1

Dip: **Microprobe analysis:**

y: 0 **Po:** 0 **Ccp:** 0

Ilm: 0 **Hem:** 0

Mag: 0 **Gr:** 0

Opaque mineralogy notes: no opaques

Plagioclase (Pl) ***General:*** coarse rounded equant grains

Alteration : generally light ***extinction angle:*** 33-10, Ab

Qtz: 20%, fine, bulk of interstitial to Ab grains **Scp:** 0

Amphiboles: **Cal:** 0

Bt: 0 **Ms:** unoriented fine grains

Kfs: tr.between larger Pl. **Sil:** 0 **Tlc:**

Others : **Chl:** trace fine-med strong green colour

Notes:

Sample: 64 **Rock type :** Qtz-Ab-Ms-Tur-Sil gneiss

Field notes: cut parallel double dotted line which is horizontal, note felsic clasts with quartz, fldspr and Act in matrix

Sample location: 380m on traverse east from Butjern lake

Strike: **Geochemical analysis:** 100

Dip: **Microprobe analysis:** ? nov 93

y: 0 **Po:** 0 **Ccp:** 0

Ilm: 0 **Hem:** 0

Mag: 0 **Gr:**

Opaque mineralogy notes: 1% fine dissem Rt?

Plagioclase (Pl): ***General:*** 30% equant med. grains, dominate a 2mm vein along foliation

Alteration : light ***extinction angle:*** close to zero

Qtz: 60%, fine **Scp:** 0

Amphiboles: **Cal:** 0

Bt: 0 **Ms:** 10% fine - med in equil. w/ Sil

Kfs: 0 **Sil:** 15%, clusters of rods **Tlc:**

Others : tr. fine Cld **Chl:**

Notes: Sil and Ms are not foliated, but part of a strong banding

Sample: 65 **Rock type :** Na-enriched-proto-amphibolit

Field notes: amp with fine veins 10% up to 1cm roughly parallel fol.

Sample location: 410m on traverse east from Butjern lake

Strike: **Geochemical analysis:**

Dip: **Microprobe analysis:**

y: 0 **Po:** 0 **Ccp:** 0

Ilm: 1%, fine grains rimmed by Ttn, exsol.of Hem and Rt **Hem:** in Ilm (45%), lamellae

Mag: tr. in a separate grain **Gr:** 0

Opaque mineralogy notes: Ttn rims Hem-Ilm-Rt, not Mag

Plagioclase (Pl): ***General:*** 60%, fine mosaic, not often twinned

Alteration : light patchy ***extinction angle:*** 20, little twinning

Qtz: 0 **Scp:** minor possible

Amphiboles: 20% Act? inhomogenious distribution **Cal:** 0

Bt: 0 **Ms:** 0

Kfs: possibly about 10% **Sil:** 0 **Tlc:**

Others : ?,Rt, Ttn **Chl:**

Notes:

Sample: 66 **Rock type :** Na-enriched-proto-amphibolit

Field notes: bleached amphibolite with a type 2 vein

Sample location: 410m on traverse east from Butjern lake

Strike: **Geochemical analysis:** 1

Dip: **Microprobe analysis:**

y: 0 **Po:** 0 **Ccp:** 0

Ilm: 0 **Hem:** tr. possible

Mag: tr. possible **Gr:** 0

Opaque mineralogy notes: fine dissem Rt

Plagioclase (Pl) ***General:*** 30%, fine-med. grained roughly equant

Alteration : some is intense ***extinction angle:*** small

Qtz: <5% **Scp:** 0

Amphiboles: 50% Tr? (low biref.) **Cal:** tr. as 1mm veins

Bt: tr. fine-med. grains, not foliated **Ms:** 0

Kfs: **Sil:** 0 **Tlc:**

Others : minor Rt and Ttn **Chl:** minor fine grained

Notes: section is too thin

Sample: 67 **Rock type :** scapolitized proto-amphibolite

Field notes: amp. 3m from and peg. vein

Sample location: 410m on traverse east from Butjern lake

Strike: **Geochemical analysis:** 1

Dip: **Microprobe analysis:** Hbl. Opx.

y: tr. fine (0.1mm) **Po:** 0 **Ccp:** 0

Ilm: tr. fine-med **Hem:** as thin lamelae in Ilm(10%)

Mag: as irregular blebs in Py **Gr:**

Opaque mineralogy notes:

Plagioclase (Pl) ***General:*** 0

Alteration : 0 ***extinction angle:***

Qtz: 0 **Scp:** 30% see probe data, low biref.

Amphiboles: 60% fine gr. (not uralitic) with relict opx in cores **Cal:**

Bt: tr. fine unoriented sheets **Ms:** 0

Kfs: 0 **Sil:** 0 **Tlc:**

Others : **Chl:**

Notes: check probe data for Pl

Sample: 68 **Rock type :** Na enriched gneissic amphibo

Field notes: weakly alter magnetic Amp. cross cut by vein < .5cm wide (Py bearing, med-fine Ab minor Amp. cross cutting fol.)

Sample location: Svarzvelt area traverse around separate pit, map page 6

Strike: **Geochemical analysis:** I

Dip: **Microprobe analysis:**

y: tr. fine irregular **Po:** 0 **Ccp:** tr. with Py,<Py

Ilm: minor, no exsolution **Hem:** local tr.

Mag: tr., marginal to and through Py **Gr:**

Opaque mineralogy notes:

Plagioclase (Pl) ***General:*** 60%

Alteration : some strongly alt.: epidote? ***extinction angle:*** 20

Qtz: 0 **Scp:** 0

Amphiboles: 40% Hbl possible tr. Act **Cal:** 0

Bt: 0 **Ms:** 0

Kfs: 0 **Sil:** 0 **Tlc:**

Others : possible Cld **Chl:**

Notes: amp are cored by textures of Px; Hem, Act or Cld, and strong Pl alt retrograde

---

Sample: 69 **Rock type :** Na-enriched-gneissic amphibo

Field notes: gradational contact with 068, alt is more pervasive, possible Qtzite within?, see map p6

Sample location: Svarzvelt area traverse around separate pit, 30m west of 068

Strike: **Geochemical analysis:** I

Dip: **Microprobe analysis:**

y: 0 **Po:** 0 **Ccp:** 0

Ilm: 0 **Hem:** tr., local aggregates, platty-no rim

Mag: 0 **Gr:**

Opaque mineralogy notes: tr. Rt, always surounded by Ttn (3%), irregular

Plagioclase (Pl) ***General:*** 40% fine-med. grained, equant mosaic,

Alteration : very light ***extinction angle:*** twinning not observed

Qtz: 0 **Scp:** some present (S in whole rockchem)

Amphiboles: 50% fine-med grained Hbl **Cal:**

Bt: 0 **Ms:** 0

Kfs: **Sil:** 0 **Tlc:**

Others : 2% Ttn, Rt (see above) **Chl:**

Notes: some areas of coarser Pl?,

Sample: 70 **Rock type :** Act-Qtz-Ab gneiss

Field notes: more strongly bleached than 069

Sample location: Svarzvelt area traverse around separate pit, 40 m west of 069

Strike: **Geochemical analysis:** 1

Dip: **Microprobe analysis:**

y: 0 **Po:** 0 **Ccp:** 0

Ilm: tr. dissem very fine portions are Rt **Hem:** tr.dissem. very fine

Mag: 0 **Gr:**

Opaque mineralogy notes:

Plagioclase (Pl) ***General:*** 30% generally coarser than the quartz, often not twinned

Alteration : light ***extinction angle:***

Qtz: 30% fine grains from clastics? **Scp:** possibly present

Amphiboles: 20% Act fine discrete grains **Cal:** 0

Bt: 0 **Ms:** minor fine grains

Kfs: **Sil:** 0 **Tlc:**

Others : 0 **Chl:** 0

Notes:

Sample: 71 **Rock type :** Act-Ab-Qtz-Ep-Py gneiss

Field notes:

Sample location: Svarzvelt area traverse around separate pit, 3 samples from waste rock pile

Strike: **Geochemical analysis:** 1

Dip: **Microprobe analysis:** Py,Ccp.

y: 3%, fine but in aggregates **Po:** 0 **Ccp:** tr. with Py

Ilm: 0 **Hem:** 0

Mag: 0 **Gr:**

Opaque mineralogy notes: probe found trace Co in Py, no oxides

Plagioclase (Pl) ***General:*** 20% fine light alteration

Alteration : 0 ***extinction angle:***

Qtz: 5-10% fine equant grains often grouped **Scp:** 0

Amphiboles: 70% coarse stuby clear Cam.(Hbl probed) **Cal:** 0

Bt: 0 **Ms:** 0

Kfs: 3% or less **Sil:** 0 **Tlc:** 0

Others : 10% Ep med. grained **Chl:** 0

Notes: not foliated, Py is often with, and at equilibrium with Ep

Sample: 72.1 **Rock type :** Qtz-Pl-Tur-Ms-Chl-Gr-Py gne

Field notes: footwall Ms-quartzite schist

Sample location: Svarzvelt area traverse around separate pit. 2 samples from immediatly around the mine. S and E side

Strike: **Geochemical analysis:**

Dip: **Microprobe analysis:**

y: 2% .2-1mm. sub. to anhedral **Po:** 0 **Ccp:** 0

Ilm: 0 **Hem:** 0

Mag: 0 **Gr:** tr.

Opaque mineralogy notes: tr. Rt as 0.7mm equant grains

Plagioclase (Pl) ***General:*** 40% strongly altered med grained interstitial appearing

Alteration : strong ***extinction angle:***

Qtz: 50%. with irregular sutures **Scp:** 0

Amphiboles: **Cal:** 0

Bt: 0 **Ms:** tr. fine w/ Chl?. weak pleoch.

Kfs: **Sil:** 0 **Tlc:**

Others : 10% 0.5 mm equant Tur grains. disseminated **Chl:** minor. sometimes with graphite

Notes: also 71.2: Gr 1mm very thin. bent but generally foliated

---

Sample: 73.1 **Rock type :** Ab-Qtz-Chl-Rt-Gr-Bt-Ms-Tur

Field notes: 3 samples:large (meta)quartzite from immediate H-wall. fol Amp from 10m unit with little alb-cut by tvne 2 alb.. &Gneiss 30m from pit

Sample location: Svarzvelt area traverse around separate pit. 3 samples from the west side

Strike: **Geochemical analysis:** 1

Dip: **Microprobe analysis:**

y: tr. most fine. subhedral cubic **Po:** 0 **Ccp:** tr. alone or in Py

Ilm: 0 **Hem:**

Mag: 0 **Gr:** tr.

Opaque mineralogy notes: tr. 0.02mm Rt grains. tr. Ttn

Plagioclase (Pl) ***General:*** 70% fine equant and interstitial

Alteration : some is strongly altered. chessb ***extinction angle:***

Qtz: 20% fine round equant **Scp:** 0

Amphiboles: **Cal:** one med. grain

Bt: minor. fine elongated foliated **Ms:** <Bt. foliated. fine

Kfs: **Sil:** 0 **Tlc:** unclear

Others : minor local bands of Tur fine equant. Gr **Chl:** minor. foliated. fine may interfinger with Bt

Notes: micas and Gr well foliated. banding of Bt and Tur: Gr is thin 0.5mm long bent foliated

Sample: 73.2 **Rock type :** amphibolite

Field notes: foliated Amp from a 10m wide unit, foliation is somewhat variable with little albitization

Sample location: Svarzvelt area traverse around separate pit, 3 samples from the west side

Strike: **Geochemical analysis:**

Dip: **Microprobe analysis:**

y: fine - tr., alt Hem at margin **Po:** 0 **Ccp:** tr. discrete grains

Ilm: 1% med. grained with some spotty alt. to Rt **Hem:** 0

Mag: 0 **Gr:** 0

Opaque mineralogy notes:

Plagioclase (Pl) ***General:*** 30% fine-med. equant interstitial to Hbl

Alteration : all strongly altered ***extinction angle:***

Qtz: 0 **Scp:** 0

Amphiboles: 60% blocky fresh med. gr. **Cal:** 0

Bt: 5% med. Bt, foliated **Ms:** 0

Kfs: **Sil:** 0 **Tlc:**

Others : tr. Ep replacing Bt, thin med relief clear mineral in Bt **Chl:**

Notes:

Sample: 76 **Rock type :** Na-enriched amphibolite gnei

Field notes: seds affected by Ab, relic layering? photos 31,32 hammer at sample location

Sample location: Embretfoss, 20 cm from sharp contact with mafics

Strike: **Geochemical analysis:**

Dip: **Microprobe analysis:**

y: 0 **Po:** 0 **Ccp:** 0

Ilm: 0 **Hem:** 0

Mag: 0 **Gr:** 0

Opaque mineralogy notes: tr fine equant Rt and Ttn

Plagioclase (Pl) ***General:*** 70% fine matts (chessboard?) to med. grains

Alteration : 0 ***extinction angle:*** 10

Qtz: 0 **Scp:** 0

Amphiboles: 30% Act fine - med. bands of discrete grains **Cal:** 0, in hand sample?

Bt: 0 **Ms:** 0

Kfs: **Sil:** 0 **Tlc:**

Others : tr. Ep **Chl:**

Notes: bands of Act define fol.

Sample: 80.1 **Rock type :** Ab-Qtz-Act-Ilm-Chl gneiss

Field notes: part of seds unit encountered near the beginning of the traverse? no specific notes

Sample location: from a traverse SW of Søndregrube

Strike: **Geochemical analysis:**

Dip: **Microprobe analysis:**

y: 0 **Po:** 0 **Ccp:** 0

Ilm: 3%, dissem, no exsol. **Hem:** 0

Mag: 0 **Gr:** 0

Opaque mineralogy notes: only fine irregular Ilm

Plagioclase (Pl): ***General:*** 60% fine grained and med-coarse grained, probably Ab

Alteration : light patchy ***extinction angle:*** 30, twinning is variable

Qtz: 40% some >2mm most equant, 0.3mm **Scp:** 0

Amphiboles: minor clots and discrete fine grains of Act **Cal:**

Bt: 0 **Ms:** 0

Kfs: possible minor **Sil:** 0 **Tlc:**

Others : **Chl:** minor isolated fine grains

Notes:

Sample: 80.2 **Rock type :** proto-amphibolite

Field notes: from the dominate amphibolite unit

Sample location: from a traverse SW of Søndregrube marked as 80b

Strike: **Geochemical analysis:**

Dip: **Microprobe analysis:**

y: **Po:** 0 **Ccp:**

Ilm: tr. fine irregular, with rare patches of Rt **Hem:**

Mag: 0 **Gr:** 0

Opaque mineralogy notes: Ilm may have a skelatal habit especially within Hbl grains

Plagioclase (Pl): ***General:*** 30% most fine and equant, a few grains are med. turbid laths

Alteration : fine grains are not altered ***extinction angle:*** 25 for coarse grains

Qtz: 0 **Scp:** 0

Amphiboles: 70% fine and equant, some coarse and porous **Cal:** 0

Bt: tr. fine unfol. **Ms:** 0

Kfs: 0 **Sil:** 0 **Tlc:**

Others : 1% white nonreflective opaque grains likely Ap **Chl:**

Notes: slide is unfoliated, no Px observed

Sample: 87.1 **Rock type :** magnesite-serpentinite rock

Field notes: all serpentenized to some extent, e.g. slickensides. Mag within magnesite, the bright green material

Sample location: Magnesite quarry, from immediate area

Strike: **Geochemical analysis:** 100

Dip: **Microprobe analysis:** x-ray analysis of whole rock powder, major serpentin

y: 0 **Po:** 0 **Ccp:** 0

Ilm: possible, unusual **Hem:** 0

Mag: ? **Gr:** 0

Opaque mineralogy notes: 10% (1)blue grey and anisotropic probably not magnetic; (2) magnetic pink brown anisotropic as 30% patchy irregular network in I

Plagioclase (Pl) ***General:*** 0

Alteration : 0 ***extinction angle:***

Qtz: 0 **Scp:** 0

Amphiboles: **Cal:** 20% Mgs see notes

Bt: 0 **Ms:** 0

Kfs: 0 **Sil:** 0 **Tlc:** trace fine fibres

Others : Srp 80%, fine felt habit **Chl:**

Notes: Mgs local coarse and fine dissem

Sample: 87.2 **Rock type :** magnesite-serpentinite rock

Field notes: all serpentenized to some extent, e.g. slickensides. Mag within magnesite, the darker material

Sample location: Magnesite quarry, from immediate area

Strike: **Geochemical analysis:** 100

Dip: **Microprobe analysis:**

y: **Po:** 0 **Ccp:**

Ilm: tr. **Hem:**

Mag: 0 **Gr:**

Opaque mineralogy notes: 1% blue grey and anisotropic probably not magnetic; slight patchy exsolution of pink brown anisotropic, sample is not magnetic; dissem fine grained

Plagioclase (Pl) ***General:*** 0

Alteration : 0 ***extinction angle:*** 0

Qtz: 0 **Scp:** 0

Amphiboles: **Cal:** 0

Bt: 0 **Ms:** 0

Kfs: 0 **Sil:** 0 **Tlc:** 60% fine to med, not foliated

Others : 30% fine aggregates of Srp **Chl:**

Notes:

Sample: 88 **Rock type :** equigranular Qtz-diorite

Field notes: alb1 vein 10 cm wide, oriented at 120 degrees, diffuse amphibolite boundaries to vein, ? from the bluff above an to the SE of the quarry

Sample location: Magnesite quarry, on o/c SE and above quarry

Strike: **Geochemical analysis:** 100?

Dip: **Microprobe analysis:**

y: 0 **Po:** 0 **Ccp:** 0

Ilm: tr. fine equant dissem. **Hem:** 0

Mag: 0 **Gr:**

Opaque mineralogy notes: not magnetic, but v. fine grained

Plagioclase (Pl) ***General:*** 30% fine equant

Alteration : 0 ***extinction angle:*** 35

Qtz: 30% fine roughly equant **Scp:** 0

Amphiboles: 20% fine-med. irregular **Cal:** 0

Bt: minor fine unoriented **Ms:** 0

Kfs: possible **Sil:** 0 **Tlc:**

Others : **Chl:**

Notes: probably a rock of igneous origin

Sample: 90 **Rock type :** equigranular amphibolite

Field notes: 10 m from vein, overall little alt on this outcrop

Sample location: Magnesite quarry, on o/c SE and above quarry

Strike: **Geochemical analysis:** 100

Dip: **Microprobe analysis:** y

y: 0 **Po:** 0 **Ccp:** 0

Ilm: tr. fine irregular **Hem:** 0

Mag: 0 **Gr:**

Opaque mineralogy notes:

Plagioclase (Pl) ***General:*** 10% med relic turbid laths, 40% fine equant grains

Alteration : 0 ***extinction angle:***

Qtz: 0 **Scp:** 0

Amphiboles: 40% fine-med. some rims have a blue tint **Cal:**

Bt: 5% fine unfoliated, needles of rutile within **Ms:** 0

Kfs: **Sil:** 0 **Tlc:**

Others : tr. fine round opaque Ap **Chl:**

Notes:

Sample: 91 **Rock type :** proto-amphibolite

Field notes: Pl rich vein 30cm wide.

Sample location: Gamphue quarry on next ridge (at 300deg.)

Strike: **Geochemical analysis:**

Dip: **Microprobe analysis:**

y: tr. fine equant grains, Hem alt **Po:** 0 **Ccp:**

Ilm: tr. very fine blebs **Hem:**

Mag: 0 **Gr:**

Opaque mineralogy notes:

Plagioclase (Pl) ***General:*** medium grained laths

Alteration : light ***extinction angle:*** 30-40 (intermediate)

Qtz: 0 **Scp:** 0

Amphiboles: 30% as coarse aggregates of fine zones **Cal:**

Bt: v **Ms:** 0

Kfs: **Sil:** 0 **Tlc:** 0

Others : minor low relief min.in patches and network; tr. Cpx? **Chl:** 0

Notes: note possible pressence of Cpx, possibly as much as 10%, section is thick

---

Sample: 92 **Rock type :** Na enriched gneissic amphibo

Field notes: foliated mafic gneiss with a fine Pl matrix, coarse amphibole, country rock for the next 3 samples, unit 100m across strike

Sample location: Gamphue quarry on next ridge? (at 300deg.)

Strike: 14 **Geochemical analysis:** 100

Dip: 85e **Microprobe analysis:**

y: 0 **Po:** 0 **Ccp:** 0

Ilm: tr., fine grains **Hem:** 0

Mag: tr. possible **Gr:** 0

Opaque mineralogy notes:

Plagioclase (Pl) ***General:*** possibly 40% but likely scapolite

Alteration : 0 ***extinction angle:***

Qtz: 0 **Scp:** 40% med-fine grains and aggregates

Amphiboles: 60% coarse aggregates of fine Hbl **Cal:** present

Bt: 0 **Ms:** 0

Kfs: **Sil:** 0 **Tlc:**

Others : tr. Ep .3mm grains with Scp **Chl:** late 0.3mm vein ntework

Notes: section is too thick

Sample: 96 **Rock type :** Bt-Scp-Pl-Hem-Chl gneiss

Field notes: foliated amphibolite, nodular gneiss in many ways similar to pwn 092. 1cm Hbl clots in Pl matrix.unit 10m wide

Sample location: map p.14.on hill 100m nw of Søndregrube

Strike: 180 **Geochemical analysis:** 100

Dip: 85w **Microprobe analysis:**

y: present **Po:** 0 **Ccp:** tr.

Ilm: tr in composite grains, see below **Hem:** minor in composite grains

Mag: tr. very fine and discrete **Gr:** 0

Opaque mineralogy notes: 5% 4mm long composite grains some in sectors all dominated by Hem with lesser lenses and lamelae of Ilm

Plagioclase (Pl) ***General:*** minor fine grained, may have been sedimentary

Alteration : unaltered ***extinction angle:***

Qtz: not identified **Scp:** 10% fine-med. fine inclusions of Bt

Amphiboles: tr. **Cal:**

Bt: 30% fine foliated, concentrated around **Ms:** minor, fine, weak green colour

Kfs: 0 **Sil:** 0 **Tlc:**

Others : Scp **Chl:** tr. with Bt

Notes:

Sample: 97 **Rock type :** Qtz-Ab-Ms-Bt gneiss

Field notes: fine fol. somewhat weathered, strongly alb. HS shows layering, bedded sediment?

Sample location: map p.14.on hill 160m nw of Søndregrube

Strike: **Geochemical analysis:** 100, no vein in

Dip: **Microprobe analysis:**

y: 0 **Po:** 0 **Ccp:** 0

Ilm: 0 **Hem:** 0

Mag: 0 **Gr:**

Opaque mineralogy notes:

Plagioclase (Pl) ***General:*** about 20%, 0.2 mm

Alteration : unaltered ***extinction angle:***

Qtz: 60%, fine grained; 6mm vein **Scp:** 0

Amphiboles: **Cal:**

Bt: trace fine thin grains foliated, green tint **Ms:** tr. fine, slight green colour

Kfs: minor, fine irregular **Sil:** 0 **Tlc:**

Others : **Chl:**

Notes:

Sample: 98 **Rock type :** metasediment?

Field notes: fol. med. alb. with ? of Act

Sample location: map p.14,on hill 160m nw of Søndregrube, 30 cm across strike west from 097

Strike: **Geochemical analysis:** 100

Dip: **Microprobe analysis:**

y: **Po:** 0 **Ccp:**

Ilm: 0 **Hem:**

Mag: 0 **Gr:**

Opaque mineralogy notes:

Plagioclase (Pl) ***General:***

Alteration : 0 ***extinction angle:***

Qtz: 0 **Scp:** 0

Amphiboles: **Cal:**

Bt: 0 **Ms:** 0

Kfs: **Sil:** 0 **Tlc:**

Others : **Chl:**

Notes: no section present

Sample: 99 **Rock type :** Na-enriched amphibolite

Field notes:

Sample location: map p.14,on hill 160m nw of Søndregrube, 30 cm across strike west from 98

Strike: 7 **Geochemical analysis:** 100

Dip: 20e **Microprobe analysis:**

y: tr., 0.08mm w/ Hem rims **Po:** 0 **Ccp:** <Py, with Py

Ilm: minor fine rounded grains **Hem:** 20% of Ilm grains

Mag: tr. occuring w/ Py, see photos **Gr:** 0

Opaque mineralogy notes: Py is weakly anisotropic,Hem in Ilm

Plagioclase (Pl) ***General:*** 50%, fine grained, unconfirmed albitized, some coarse laths, altered cores

Alteration : strong only in coarse Pl ***extinction angle:*** 10 (for fine grained)

Qtz: 0 **Scp:** 0

Amphiboles: 40% fine and evenly distributed **Cal:** 0

Bt: tr. in med-coarse aggregates, unfoliated **Ms:** 0

Kfs: 0 **Sil:** 0 **Tlc:**

Others : 0 **Chl:**

Notes:

Sample: 100 **Rock type :** scapolitized amphibolite

Field notes: fine amp, not visibly altered , but only about 1-3m from another albitite vein

Sample location: map p.14,on hill 160m nw of Søndregrube, 15m of last o/c

Strike: **Geochemical analysis:** 100

Dip: **Microprobe analysis:**

y: tr. fine **Po:** possible **Ccp:**

Ilm: 2% fine dissem (associated with exsolved Hem) **Hem:** 10% of Ilm grains

Mag: tr. discrete with Ilm, or with Py **Gr:** 0

Opaque mineralogy notes: Hem in Ilm

Plagioclase (Pl) ***General:*** 0

Alteration : ***extinction angle:***

Qtz: 0 **Scp:** 60% med-fine grains

Amphiboles: 40% fine, in aggregates **Cal:**

Bt: tr. 0.05mm **Ms:** 0

Kfs: 0 **Sil:** 0 **Tlc:**

Others : 0 **Chl:**

Notes:

Sample: 102.1 **Rock type :** equigranular amphibolite

Field notes: fine gr

Sample location: map p.14,on hill NW of Søndregrube, farther south on the last few samples

Strike: **Geochemical analysis:** wr

Dip: **Microprobe analysis:**

y: 1 0.05mm grain **Po:** 0 **Ccp:** 0

Ilm: 1-3% fine with exsolution of Hem and other **Hem:** tr. exsolution in Ilm

Mag: 0 **Gr:** 0

Opaque mineralogy notes: darker exsolution from Ilm may be Ttn or an alteration product

Plagioclase (Pl) ***General:*** 40% fine grained, unconfirmed albitized

Alteration : light patchy local sericitic alt. ***extinction angle:*** 5

Qtz: 0 **Scp:** possible

Amphiboles: 60% fine-med not aggregated **Cal:** 0

Bt: minor unfoliated med. grained **Ms:** 0

Kfs: ? **Sil:** 0 **Tlc:**

Others : **Chl:**

Notes:

Sample: 103 **Rock type :** equigranular amphibolite

Field notes: like 102 slightly more Bt

Sample location: map p.14.on hill nw of Søndregrube. 2m west of 102 towards seds. 50 cm from vein

Strike: **Geochemical analysis:** 100

Dip: **Microprobe analysis:**

y: tr 0.5mm grains **Po:** 0 **Ccp:**

Ilm: tr. fine and equant, minor exsolution of alt? **Hem:** tr.

Mag: tr. w/ Py and discrete grains **Gr:** 0

Opaque mineralogy notes: Ilm has exsolution of a dark mineral, alteration product(?), tr. dissem Rt

Plagioclase (Pl) ***General:*** fine grained mosaic habit

Alteration : strong ***extinction angle:***

Qtz: 0 **Scp:** 0

Amphiboles: 70% fine-med. equgranular, even distribution **Cal:**

Bt: <10% **Ms:** 0

Kfs: 0 **Sil:** 0 **Tlc:**

Others : tr. anhedral corroded grains of Cpx **Chl:** tr. fine can occur with Pl

Notes: oxides are altered as is Pl

Sample: 105 **Rock type :** equigranular amphibolite

Field notes: amp just west of zone of bleaching. 15 cm from contact with sed unit

Sample location: 2-4

Strike: **Geochemical analysis:**

Dip: **Microprobe analysis:** 100

y: 1 0.05mm grain **Po:** 0 **Ccp:** 0

Ilm: 5% fine equant, exsol of alt and tr. Hem **Hem:** tr. exsolution in Ilm

Mag: 0 **Gr:**

Opaque mineralogy notes:

Plagioclase (Pl) ***General:*** minor, 0.2mm equant grains, not obviously corroded by Scp

Alteration : light ***extinction angle:***

Qtz: 0 **Scp:** 30% 2nd order biref. equant 0.2mm

Amphiboles: 60% fine Hbl **Cal:** 0

Bt: 0 **Ms:** 0

Kfs: 0 **Sil:** 0 **Tlc:**

Others : **Chl:** minor in thick grains with variable pleochroism, pennite

Notes: equigranular unfoliated texture

Sample: 110 **Rock type :** albitite

Field notes: 3m section of fol. Pl generally fine grained but with about 30% veins usually 1mm, .lenses of coarse segregations, the coarse piece is an e.g. of the area, see also notes.

Sample location: on dirt road south from mine, 100m south of magnesite quarry road

Strike: **Geochemical analysis:**

Dip: **Microprobe analysis:**

y: 0 **Po:** 0 **Ccp:** 0

Ilm: 0 **Hem:** 0

Mag: 0 **Gr:** 0

Opaque mineralogy notes: 2% 0.3 mm dissem Rt

Plagioclase (Pl) ***General:*** 90% coarse grained, Ab, chessboard?

Alteration : unaltered ***extinction angle:*** 25

Qtz: 0 **Scp:** 0

Amphiboles: 10% 0.2mm euhedral Act as inclusions in Pl **Cal:**

Bt: minor 0.3 mm grains inclusions in Pl **Ms:** 0

Kfs: **Sil:** 0 **Tlc:**

Others : Rt **Chl:**

Notes: not foliated

Sample: 111 **Rock type :** albitite

Field notes: mafic lenses in a felsic matrix

Sample location: Overbykollen on skidder road, about 50 m nnw of quarry

Strike: **Geochemical analysis:** 1

Dip: **Microprobe analysis:**

y: 0 **Po:** 0 **Ccp:** 0

Ilm: 0 **Hem:** 0

Mag: 0 **Gr:** 0

Opaque mineralogy notes: no opaques

Plagioclase (Pl) ***General:*** 80% fine grained, Ab with a felty texture and little twinning

Alteration : moderate turbid ***extinction angle:***

Qtz: <5%, if present **Scp:** 0

Amphiboles: 10% med blocky skeletal grains of Act **Cal:** tr discrete grains

Bt: 0 **Ms:** 0

Kfs: **Sil:** 0 **Tlc:**

Others : minor Ttn or zircon **Chl:** minor radiating fine cluster in Act rich area

Notes: the felty texure and the habit of the Act compared to 110

Sample: 113 **Rock type :** albitite

Field notes: bleached zone with at least one indistinct Pl vein.

Sample location: Overbykollen on skidder road, about 50 m nnw of quarry, 85-200 cm SE of 111

Strike: 10 **Geochemical analysis:** 1

Dip: 90 **Microprobe analysis:**

y: tr. anhedral fine equant **Po:** 0 **Ccp:**

Ilm: 0 **Hem:** 0

Mag: one fine broken grain **Gr:** 0

Opaque mineralogy notes: Py is rimmed with shallow alteration Hem; Ttn? and Rt in trace amounts fine grained and associated with above

Plagioclase (Pl) ***General:*** fine grained, Ab, fine to med. mosaic to felty

Alteration : moderate, turbid ***extinction angle:*** 26

Qtz: 0 **Scp:** 0

Amphiboles: possible trace Act **Cal:** fine to med. grains

Bt: 0 **Ms:** 0

Kfs: **Sil:** 0 **Tlc:**

Others : **Chl:** 5% in veins and isolated

Notes: Cal may be in veins in hand sample ,fine dissem chl. in Pl,some high relief, high biref, colourles diamond shaped grains

---

Sample: 114 **Rock type :** gneissic amphibolite

Field notes: less altered mafics, but this one is approaching a zone of bleaching again

Sample location: Overbykollen on skidder road, about 50 m nnw of quarry,170 cm SE of 113

Strike: **Geochemical analysis:** 1

Dip: **Microprobe analysis:**

y: tr. fine some with minor Mag **Po:** 0 **Ccp:**

Ilm: 3%, in thin broken bands about 1cm along fol. **Hem:**

Mag: tr. with Py **Gr:** 0

Opaque mineralogy notes: Ilm has a "galvanized" texture but it is completely opaque and no internal reflections, fine Ilm throughout coarse Hbl grain

Plagioclase (Pl) ***General:*** coarse grained, unconfirmed albitized, some coarse laths

Alteration : moderate, generally turbid ***extinction angle:*** 20

Qtz: probable minor fine grains **Scp:** 0

Amphiboles: 20%, mainly fine but aggregated into wispy bands **Cal:** tr. in 1mm vein

Bt: 0 **Ms:** 0

Kfs: 0 **Sil:** 0 **Tlc:**

Others : **Chl:**

Notes: Cal. only noted in thinsec. maybe another carb. alteration of Pl is odd

Sample: 118.1 **Rock type :** proto-amphibolite

Field notes: unfoliated block from slope beside a cliff, with brown weathering pits

Sample location: at Knatten, from slope, near bridge

Strike: **Geochemical analysis:** 1

Dip: **Microprobe analysis:** y

y: tr. fine, associated with Mag: **Po:** 0 **Ccp:** tr. with Py

Ilm: 1% with Hem and Mag **Hem:** exsolution from Ilm

Mag: 0 **Gr:** 0

Opaque mineralogy notes: Ilm grains with fine exsolution lamelae of Hem and lesser lamelae and blebs of Mag

Plagioclase (Pl) ***General:*** med grained laths, unconfirmed albitized

Alteration : moderate. ***extinction angle:*** 30

Qtz: 0 **Scp:** 0

Amphiboles: 40%, not uralitic **Cal:** 0

Bt: 0 **Ms:** 0

Kfs: 0 **Sil:** 0 **Tlc:**

Others : 0 **Chl:**

Notes: microstructure is similar to 118.2, except that this one has no relic Opx

---

Sample: 118.2 **Rock type :** metagabbro

Field notes: unfoliated with brown weathering pits

Sample location: at Knatten, from slope near bridge

Strike: **Geochemical analysis:** 1

Dip: **Microprobe analysis:**

y: tr. fine, associated with Mag: **Po:** possible **Ccp:** tr with Py

Ilm: 1% with Hem and Mag **Hem:** exsolution from Ilm

Mag: tr?, with Py and exsolution from Ilm **Gr:** 0

Opaque mineralogy notes: Ilm grains with fine exsolution lamelae of Hem and lesser lamelae and blebs of Mag

Plagioclase (Pl) ***General:*** med. grained, unconfirmed albitized

Alteration : moderate, patchy ***extinction angle:*** 35-rim,58-core

Qtz: 0 **Scp:** 0

Amphiboles: 40%, not uralitic **Cal:** 0

Bt: 0 **Ms:** 0

Kfs: 0 **Sil:** 0 **Tlc:**

Others : 0 **Chl:**

Notes: there appears to be Opx presserved with Cam around it

Sample: 119 **Rock type :** gneissic amphibolite

Field notes: 2 pieces one with rare subhorizontal felsic vein (3cm) and a comparable mafic vein in second sample. see fig. in notes

Sample location: knatten bridge 100m south

Strike: **Geochemical analysis:** 1

Dip: **Microprobe analysis:**

y: tr. fine may follow Pl, Gr. **Po:** 0 **Ccp:** tr. in Py

Ilm: tr. fine, some in Grt **Hem:** 0

Mag: 0 **Gr:** 0

Opaque mineralogy notes:

Plagioclase (Pl) ***General:*** fine grained equant, good triple junctions

Alteration : unaltered ***extinction angle:*** 35

Qtz: 0 **Scp:** 0

Amphiboles: 60% med. equant **Cal:** 0

Bt: 0 **Ms:** 0

Kfs: 0 **Sil:** 0 **Tlc:**

Others : Grt: 5% subhedral 3mm grains **Chl:**

Notes:

Sample: 120 **Rock type :** metagabbro

Field notes: coarse amphibolite

Sample location: Road cut at Knatten , about 200 m south of the bridge across the Snarum Selva river

Strike: **Geochemical analysis:** 1

Dip: **Microprobe analysis:** Ilm, rt,calcite, epidote.

y: tr. fine blebs **Po:** tr. very tiny hex. grain. **Ccp:** tr.

Ilm: tr.very fine discrete grains **Hem:** 0

Mag: 0 **Gr:**

Opaque mineralogy notes: some Py is rimmed by thin alteration Hem; Po contains a Pn flame, Ccp on margin of grain

Plagioclase (Pl) ***General:*** 40%, coarse igneous laths

Alteration : light patchy ***extinction angle:*** 30-rim,59-core

Qtz: 0 **Scp:** 0

Amphiboles: 40%, hornblende some is uralitic **Cal:** tr.

Bt: 0 **Ms:** 0

Kfs: **Sil:** 0 **Tlc:**

Others : Grt, Srp, tr. Ep **Chl:**

Notes: Cam are cored by relict Px

Sample: 121 **Rock type :** gneissic amphibolite

Field notes: med grained foliated amphibolite with local veins of Py. gneissic segregations produce something similar to "dalmation texture" . Pypiece occures mainly on one horizon

Sample location: about 400 m south of 120 on road

Strike: **Geochemical analysis:** 1

Dip: **Microprobe analysis:**

y: tr. fine, shattered texture **Po:** 0 **Ccp:**

Ilm: 2%, in fine to coarse patches esp. in Hbl **Hem:** 0

Mag: 0 **Gr:** 0

Opaque mineralogy notes: Py with network of alt Hem through it

Plagioclase (Pl) ***General:*** 50% fine mosaic

Alteration : local strong patches ***extinction angle:*** 40

Qtz: possible **Scp:** 0

Amphiboles: 50%, medium and equant **Cal:** 0

Bt: tr. fine grains mainly in the Hbl **Ms:** 0

Kfs: 0 **Sil:** 0 **Tlc:** 0

Others : minor Ap **Chl:** 0

Notes: hetrogenious sample half only Hbl, half mainly Pl.

Sample: 122 **Rock type :** gneissic amphibolite

Field notes:

Sample location:

Strike: **Geochemical analysis:** 1

Dip: **Microprobe analysis:**

y: **Po:** 0 **Ccp:**

Ilm: 0 **Hem:**

Mag: 0 **Gr:**

Opaque mineralogy notes:

Plagioclase (Pl) ***General:***

Alteration : 0 ***extinction angle:***

Qtz: 0 **Scp:** 0

Amphiboles: **Cal:**

Bt: 0 **Ms:** 0

Kfs: **Sil:** 0 **Tlc:**

Others : **Chl:**

Notes:

Sample: 91030 **Rock type :** equigranular amphibolite

Field notes:

Sample location:

Strike: **Geochemical analysis:** No

Dip: **Microprobe analysis:**

y: **Po:** 0 **Ccp:**

Ilm: 0 **Hem:**

Mag: 0 **Gr:**

Opaque mineralogy notes:

Plagioclase (Pl) ***General:***

Alteration : ***extinction angle:***

Qtz: **Scp:**

Amphiboles: **Cal:**

Bt: **Ms:**

Kfs: **Sil:** **Tlc:**

Others : **Chl:**

Notes:

Sample: 91034 **Rock type :** proto-amphibolite

Field notes: I think that Eion gave me some notes

Sample location:

Strike: **Geochemical analysis:** No

Dip: **Microprobe analysis:** yes

y: fine - tr. **Po:** 0 **Ccp:** tr.

Ilm: 0 **Hem:**

Mag: 0 **Gr:** 0

Opaque mineralogy notes:

Plagioclase (Pl) ***General:*** coarse grained, unconfirmed

Alteration : sericte in laths ***extinction angle:*** 30.10

Qtz: 0 **Scp:** 0

Amphiboles: >20% **Cal:**

Bt: 0 **Ms:** 0

Kfs: **Sil:** 0 **Tlc:**

Others : Grt,?,Chl **Chl:**

Notes:

APPENDIX 2 MICROPROBE RESULTS

Microprobe data were collected as described in Chapter 3 (Methods). The results are presented in the following tables. Mineral formulas are calculated using a computer program entitled "MR" by J. Pringle of the Geological Survey of Canada in Ottawa. Amphiboles formulas are calculated using an Excel™ spreadsheet template ("Probe-amph") written by an anonymous author, the results generally agree with those of the MR program. The Proportions of ferric and ferrous iron are calculations from the "Probe-amph" template based on stoichiometric considerations. this method is not very accurate (Peter Jones, pers. comm. 1994).

THE RESULT TABLES, IN ORDER, COVER THE FOLLOWING MINERALS.

Oxides:

- hematite
- ilmenite
- rutile
- magnetite

Sulphides

- pyrite
- pyrrhotite
- siegenite
- pentlandite (the exact structure is unknown for this fine intergrowth)
- coboltite

Silicates

- orthopyroxene
- plagioclase
- scapolite
- K-feldspar
- talc
- chlorite
- muscovite
- biotite
- xenotime
- monazite
- apatite
- amphiboles

*Total FeO expressed as FeO

HEMATITE

Sample	PWN118.1					PWN053
Target	y118111 POINT	y118311 POINT	y118512 POINT	y118514 POINT	y118515 RASTER	X53123 POINT
Fe_2O_3	103.23	102.43	86.82	103.02	63.56	97.89
TiO_2	1.19	0.00	14.24	0.22	40.99	6.87
Al_2O_3	0.60	0.00	0.32	0.33	0.21	0.00
V_2O_3	0.31	0.00	0.47	0.21	0.00	0.00
Cr_2O_3	0.00	0.00	0.00	0.25	0.00	0.00
TOTAL	105.33	102.43	101.85	104.03	104.76	104.76
FORMULA (BASIS 3 OXYGENS)						
Fe^{+3}	1.946	2.000	1.626	1.975	1.073	1.829
Ti	0.022	0.000	0.267	0.004	0.691	0.128
Al	0.018	0.000	0.009	0.010	0.006	0.000
V	0.006	0.000	0.009	0.004	0.000	0.000
Cr	0.000	0.000	0.000	0.005	0.000	0.000
TOTAL	1.992	2.000	1.911	1.998	1.770	1.957

Sample	PWN067					
Target	X67113 POINT	X67114 POINT	X67212 POINT	X67221 RASTER	X67222 POINT	X67223 RASTER
Fe_2O_3	86.64	86.85	93.37	59.07	85.03	55.82
TiO_2	13.26	13.59	0.00	43.47	13.30	46.50
Al_2O_3	0.00	0.23	0.84	0.00	0.29	0.23
V_2O_3	0.45	0.49	0.00	0.00	0.55	0.00
Cr_2O_3	0.14	0.00	0.00	0.00	0.17	0.00
TOTAL	100.49	101.16	94.21	102.54	99.34	102.55
FORMULA (BASIS 3 OXYGENS)						
Fe^{+3}	1.651	1.641	1.972	1.010	1.636	0.945
Ti	0.253	0.257	0.000	0.743	0.256	0.787
Al	0.000	0.007	0.028	0.000	0.009	0.006
V	0.009	0.010	0.000	0.000	0.011	0.000
Cr	0.003	0.000	0.000	0.000	0.004	0.000
TOTAL	1.916	1.915	2.000	1.753	1.916	1.738

ILMENITE

Sample	PWN053			
Target	X5312IL	X53121I	L X53122I	L X53124
MgO	0.65	0.52	0.64	0.00
MnO	0.78	0.71	0.77	0.62
FeO	41.93	41.84	41.60	45.41
CaO	0.00	0.00	0.00	0.00
Fe_2O_3	8.11	8.03	8.24	0.00
Cr_2O_3	0.00	0.00	0.00	0.00
SiO_2	0.00	0.18	0.00	0.00
Al_2O_3	0.00	0.00	0.21	0.00
TiO_2	48.80	48.05	48.46	52.16
TOTAL (wt.%)	100.27	99.33	99.92	98.19
FORMULA (BASIS 6 OXYGENS)				
Mg	0.049	0.039	0.048	0.000
Mn	0.033	0.030	0.033	0.027
Fe^{+2}	1.764	1.778	1.755	1.948
Ca	0.000	0.000	0.000	0.000
SUBTOTAL	1.846	1.847	1.836	1.975
Fe^{+3}	0.307	0.307	0.313	0.000
Cr	0.000	0.000	0.000	0.000
Si	0.000	0.009	0.000	0.000
Al	0.000	0.000	0.012	0.000
Ti	1.846	1.837	1.839	2.012
TOTAL	2.153	2.153	2.164	2.012

Sample	PWN067			
Target	X67111	X67112	X67115	X67116
MnO	0.41	0.54	0.00	0.37
FeO	41.71	42.07	20.08	37.41
CaO	0.00	0.00	0.00	0.00
Fe_2O_3	10.16	8.85	56.33	18.73
Cr_2O_3	0.00	0.14	0.00	0.00
Al_2O_3	0.00	0.00	0.21	0.00
TiO_2	46.78	47.43	22.35	41.99
TOTAL (wt.%)	99.06	99.03	98.97	98.50
FORMULA (BASIS 6 OXYGENS)				
Mn	0.018	0.023	0.000	0.016
Fe^{+2}	1.788	1.802	0.881	1.620
Ca	0.000	0.000	0.000	0.000
SUBTOTAL	1.806	1.825	0.881	1.636
Fe^{+3}	0.392	0.341	2.224	0.730
Cr	0.000	0.006	0.000	0.000
Al	0.000	0.000	0.013	0.000
Ti	1.803	1.827	0.882	1.635
TOTAL	2.195	2.174	3.119	2.365

RUTILE

Sample	PWN053
Target	X53125
TiO_2	97.56
FeO	1.47
TOTAL (wt.%)	99.03
FORMULA (BASIS 2 OXYGENS)	
Ti	0.992
Fe	0.017
TOTAL	1.009

MAGNETITE

Sample	PWN087.1			
Target	MT87.1	HM87.1	MT87. 2	HM87.2
SiO_2	0.27	0.22	0.18	0
Al_2O_3	0.37	0	0.21	0.28
TiO_2	2.01	1.6	2.72	2.13
Cr_2O_3	0	0	0.12	0
V_2O_3	0	0	0	0.13
Fe_2O_3	62.19	65.91	61.25	65.63
FeO	31.84	30.41	32.17	32.7
MgO	0.31	1.34	0.51	0.4
MnO	0.13	0.25	0	0.21
TOTAL (wt.%)	97.12	99.73	97.16	101.48
Formula (Basis 4 Oxygens)				
Si	0.011	0.008	0.007	0.000
Al	0.017	0.000	0.010	0.012
Ti	0.060	0.046	0.080	0.060
Cr	0.000	0.000	0.004	0.000
V	0.000	0.000	0.000	0.004
Fe^{+3}	1.842	1.892	1.812	1.863
	1.930	1.946	1.913	1.940
Fe^{+2}	1.048	0.970	1.058	1.032
Mg	0.018	0.076	0.030	0.022
Mn	0.004	0.008	0.000	0.007
Ni	0.000	0.000	0.000	0.000
TOTAL	1.070	1.054	1.088	1.061

All sulphide formula calculations based on 1 atom

PYRITE

Probe Results	Sample	PWN010		PWN012	PWN025	PWN071	
	Target	z1051py	z1062	z1241	z2511	z7111	z7121py
Weight Percent	Fe	42.59	46.40	46.31	46.92	45.60	43.17
	Pb	0.00	0.00	0.00	0.00	0.00	0.00
	Zn	0.00	0.00	0.00	0.00	0.00	0.00
	Ni	0.00	0.00	0.00	0.00	0.65	0.00
	Co	2.97	0.00	0.00	0.00	0.00	2.22
	Sb	0.00	0.00	0.00	0.00	0.00	0.00
	S	52.08	53.72	53.82	54.44	53.80	52.85
	As	2.30	0.00	0.00	0.00	0.00	0.00
	TOTAL	99.94	100.12	100.13	101.36	100.05	98.24
Formula Calculation							
Mole Percent	Fe	0.31	0.33	0.33	0.33	0.33	0.31
	Pb	0.00	0.00	0.00	0.00	0.00	0.00
	Zn	0.00	0.00	0.00	0.00	0.00	0.00
	Ni	0.00	0.00	0.00	0.00	0.00	0.00
	Co	0.02	0.00	0.00	0.00	0.00	0.02
	Sb	0.00	0.00	0.00	0.00	0.00	0.00
	TOTAL a	0.33	0.33	0.33	0.33	0.33	0.33
	S	0.66	0.67	0.67	0.67	0.67	0.67
	As	0.01	0.00	0.00	0.00	0.00	0.00
	TOTAL b	0.67	0.67	0.67	0.67	0.67	0.67

PYRRHOTITE

Probe Results	Sample	PWN012	PWN025
	Target	z1231	z2521
Weight Percent	Fe	57.91	58.92
	Ni	0.66	0.89
	Co	0.52	0.43
	Mn	0.00	0.00
	Cu	0.00	0.00
	S	38.49	39.97
	TOTAL	97.58	100.21
Formula Calculation			
Mole Percent	Fe	0.46	0.45
	Ni	0.01	0.01
	Co	0.00	0.00
	TOTAL a	0.47	0.46
	S	0.53	0.54
	TOTAL b	0.53	0.54

SIEGENITE

Sample	PWN010
Target	z1041
Co	39.16
Ni	14.60
Cu	1.21
Fe	2.98
S	41.71
TOTAL	99.66
Co	0.29
Ni	0.11
Cu	0.01
Fe	0.02
TOTAL a	0.43
S	0.57
TOTAL b	0.57

PENTLANDITE?

Probe Results	Sample	PWN042.1	
	Target	Pn42B1.1	Pn42B1.2
Weight Percent	S	32.65	37.46
	Fe	24.47	25.24
	Cu	0.00	0.00
	Ni	41.00	25.73
	Co	0.00	0.00
	Total	98.12	88.43
Formula Calculation			
Mole Percent	Fe	0.20	0.22
	Cu	0.00	0.00
	Ni	0.32	0.21
	Co	0.00	0.00
	TOTAL a	0.53	0.43
	S	0.47	0.57
	TOTAL b	0.47	0.57

COBALTITE

Sample	PWN010		
Target	z1021	z1031	1061.00
Co	32.03	33.02	32.30
As	41.62	42.13	42.33
Fe	3.74	3.74	3.44
Ni	1.36	1.36	1.30
Cu	0.00	0.00	0.00
S	21.24	21.24	21.16
Total	99.99	101.49	100.53
Co	0.29	0.30	0.30
As	0.30	0.30	0.30
Fe	0.04	0.04	0.03
Ni	0.01	0.01	0.01
Cu	0.00	0.00	0.00
	0.64	0.65	0.65
S	0.36	0.35	0.36
	0.36	0.35	0.36

ORTHOPYROXENE

Sample	PWN053				
Target	X53132	X53133	X53134	X53212	X53214
SiO_2	52.36	51.83	50.80	51.81	52.10
Al_2O_3	3.49	2.82	4.56	4.41	3.36
Fe_2O_3	1.53	2.37	3.36	2.19	1.85
MgO	26.58	26.52	26.19	26.19	26.47
FeO	14.92	14.29	13.63	14.84	14.71
MnO	0.36	0.29	0.21	0.31	0.30
CaO	0.00	0.11	0.11	0.09	0.15
TOTAL	99.24	98.23	98.86	99.84	98.94

ORTHOPYROXENE

Sample	PWN120	
Target	PX120.1	PX120.2
SiO_2	53.67	53.52
Al_2O_3	2.53	1.66
* FeO	9.56	18.31
MgO	21.28	25.03
MnO	0.00	0.37
CaO	0.09	0.13
TOTAL	87.13	99.02

PLAGIOCLASE

Sample	PWN055					PWN051	PWN052
Target	PL055.1	PL055.2	PL055.3	PL055.4	PL055.5	PL051.1	PL0521.2
SiO_2	68.07	68.06	67.90	67.27	67.22	52.89	51.86
Al_2O_3	19.52	19.26	19.58	19.13	19.20	29.41	29.73
CaO	0.42	0.24	0.44	0.39	0.37	12.69	13.19
Na_2O	11.34	11.51	11.54	11.28	11.49	4.79	4.34
K_2O	0.06	0.05	0.05	0.02	0.03	0.00	0.00
* FeO	0.04	0.16	0.15	0.04	0.06	0.03	0.13
TOTAL	99.45	99.28	99.66	98.13	98.37	99.81	99.25

PLAGIOCLASE

Sample	PWN047					
Target	PL47.1	PL47.2	PL47.3	PL47.4	PL47.5	Y47.3
SiO_2	68.83	69.41	68.93	67.97	68.69	64.97
Al_2O_3	19.36	19.41	19.44	19.88	19.42	21.10
CaO	0.25	0.18	0.30	0.50	0.21	0.61
Na_2O	11.36	11.40	11.51	11.13	11.27	9.73
K_2O	0.17	0.15	0.16	0.19	0.19	1.40
FeO	0.08	0.05	0.00	0.07	0.10	0.23
TOTAL	100.05	100.60	100.34	99.74	99.88	98.04

SCAPOLITE

Sample	PWN057		PWN051		PWN067
Target	SC57.1	SC57.2	SCO51.1	SCO51.2	SC67.1
SiO_2	54.29	54.37	54.88	55.34	53.72
Al_2O_3	22.94	22.99	23.91	23.61	22.77
TiO_2	0.06	0.04	0.04	0.03	0.00
* FeO	0.10	0.00	0.04	0.09	0.04
MgO	0.21	0.13	0.19	0.04	0.10
CaO	8.26	8.56	8.75	7.93	8.12
Na_2O	8.55	8.51	8.66	8.88	8.19
K_2O	0.47	0.48	0.27	0.34	0.54
$S0_3$	0.44	0.57	0.13	0.18	0.34
Cl	2.97	2.85	3.20	3.34	2.98
H_2O	0.00	0.00	0.00	0.00	0.00
TOTAL	98.29	98.50	100.07	99.78	96.80
TOTAL-0	97.62	97.86	99.35	99.03	96.13

TALC

Sample	PWN055		PWN056
Target	TC055.1	TC055.2	TC56.1
SiO_2	61.92	61.36	61.51
Al_2O_3	1.41	0.80	1.02
TiO_2	0.16	0.00	0.03
* FeO	0.72	1.45	1.99
MnO	0.01	0.01	0.00
Cr_2O_3	0.00	0.00	0.00
MgO	30.53	29.95	28.80
CaO	0.00	0.00	0.05
K_2O	0.17	0.15	0.16
TOTAL	94.92	93.72	93.56

CHLORITE

Sample	PWN055	PWN047
Target	Y055.1	CL47.1
SiO_2	32.92	29.25
Al_2O_3	17.49	20.10
TiO_2	0.00	0.00
* FeO	4.00	17.48
MnO	0.00	0.00
MgO	33.23	22.05
CaO	0.02	0.08
K_2O	0.01	0.05
TOTAL	87.67	89.01

MUSCOVITE

Sample	PWN012		PWN047
Target	z1261	z1262	MS47.1
SiO_2	47.89	47.92	47.21
Al_2O_3	35.82	37.00	33.57
TiO_2	0.00	0.69	0.00
* FeO	0.62	0.16	0.91
MgO	1.92	1.60	1.52
CaO	0.25	0.00	0.04
Na_2O	0.00	0.68	0.34
K_2O	10.68	11.29	10.55
Cl	0.00	0.00	0.06
TOTAL	97.18	99.34	94.20
TOTAL-0	97.18	99.34	94.19

K-FELDSPAR

Sample	PWN009
Target	z0924
SiO_2	47.27
Al_2O_3	28.91
Na_2O	5.74
CAO	0.35
K_2O	7.62
* FeO	1.18
TOTAL	91.07

BIOTITE

Sample	PWN009	
Target	z0913	z0914
SiO_2	39.43	39.08
Al_2O_3	19.30	19.12
Fe_2O_3	5.19	5.41
Cr_2O_3	0.00	0.00
TiO_2	2.03	2.52
FeO	2.91	2.92
MnO	0.00	0.00
MgO	18.64	18.13
CaO	0.00	0.00
Na_2O	0.59	0.00
K_2O	10.13	10.30
TOTAL	98.22	97.48

BIOTITE

Sample	PWN057		PWN067
Target	BT57.1	BT57.2	BT67.1
SiO_2	37.04	36.63	36.49
Al_2O_3	16.95	17.20	14.91
Cr_2O_3	0.00	0.00	0.00
TiO_2	1.68	1.64	3.27
* FeO	9.11	10.01	14.61
MnO	0.00	0.00	0.00
MgO	20.67	21.24	15.05
CaO	0.11	0.28	0.05
Na_2O	0.68	0.84	0.71
K_2O	8.43	7.54	9.38
Cl	0.28	0.25	0.97
TOTAL	94.95	95.63	95.44
TOTAL-0	94.89	95.57	95.22

XENOTIME **MONAZITE**

Sample	PWN009		
Target	z0921	z0922	z0923
Y_2O_3	42.08	42.42	4.66
La_2O_3	0.00	0.00	9.77
Ce_2O_3	0.00	0.00	19.89
Pr_2O_3	0.00	0.00	2.49
Nd_2O_3	0.58	0.44	9.73
Sm_2O_3	0.69	0.54	2.41
Gd_2O_3	1.98	2.34	2.28
Tb_2O_3	0.00	0.70	0.00
Dy_2O_3	5.21	5.06	1.05
Er_2O_3	3.93	3.86	0.49
Yb_2O_3	3.70	4.01	0.00
ThO_2	0.80	0.72	13.12
SrO	1.57	1.32	0.66
UO_2	2.80	3.61	2.32
* FeO	0.00	0.00	0.22
P_2O_5	34.48	35.05	30.64
SiO_2	0.66	0.63	0.95
CaO	0.19	0.15	3.06
TOTAL	98.67	100.85	103.74

APATITE

Sample	PWN118.1	PWN090	PWN009	
Target	y118411	y90111	z0911	z0912
CaO	56.25	55.49	54.35	54.36
* FeO	0.18	0.00	0.00	0.00
MnO	0.00	0.00	0.00	0.00
SrO	0.00	0.00	0.40	0.36
P_2O_5	41.90	42.07	42.76	42.40
SiO_2	0.38	0.00	0.55	0.59
CO_2	0.00	0.00	0.00	0.00
F	0.00	0.00	0.00	0.00
Cl	1.04	0.00	0.21	0.46
TOTAL	99.75	97.56	98.27	98.17
TOTAL-0	99.52	97.56	98.22	98.07

AMPHIBOLES

METAGABBROIC ROCKS

	PWN050									PWN053		PWN120
	AM501.3	AM501.4	AM501.5	AM501.7	AM501.8	AM501.9	AM501.10	AM501.11	AM501.12	X53131	X53221	AM120.1
SiO_2	40.13	40.61	40.38	39.24	41.38	41.32	40.37	40.45	40.21	38.88	39.28	41.69
TiO_2	0.94	1.06	0.74	0.98	0.81	0.24	0.97	0.92	0.91	0.89	0.76	0.36
Al_2O_3	17.87	17.97	18.07	18.11	16.60	17.79	17.99	18.44	18.49	15.48	17.06	16.86
Cr_2O_3	0.00	0.00	0.00	0.00	0.00	0.00	0.00	0.00	0.00	0.00	0.00	0.00
Fe_2O_3	6.86	6.76	8.02	7.28	10.21	14.27	5.95	7.55	7.71	10.83	8.17	7.12
FeO	6.97	6.30	6.09	6.29	3.23	0.00	7.20	5.16	5.34	4.56	5.82	5.08
MnO	0.09	0.07	0.02	0.04	0.03	0.09	0.04	0.09	0.07	0.16	0.18	0.00
MgO	10.89	11.24	10.71	10.65	12.61	12.89	10.86	11.38	11.23	11.36	11.15	12.50
CaO	11.32	11.13	11.09	10.85	10.93	9.52	11.07	11.14	11.09	10.65	10.91	11.07
Na_2O	2.32	2.40	2.04	2.35	2.39	2.58	2.48	2.21	2.27	2.33	2.55	2.62
K_2O	0.45	0.40	0.41	0.59	0.28	0.31	0.43	0.38	0.42	0.59	0.56	0.49
Cl	1.80	1.67	1.70	1.97	1.51	1.66	1.68	1.56	1.69	2.03	1.60	1.48
H_2O	1.60	1.65	1.63	1.53	1.71	1.70	1.63	1.68	1.64	1.49	1.62	1.70
O=F,Cl	0.41	0.38	0.38	0.44	0.34	0.37	0.38	0.35	0.38	0.46	0.36	0.33
Total	100.83	100.89	100.51	99.43	101.35	101.99	100.28	100.64	100.69	98.79	99.29	100.64
No. of O	23	23	23	23	23	23	23	23	23	23	23	23
Structural formulae												
Si	5.85	5.88	5.88	5.80	5.93	5.84	5.90	5.85	5.82	5.82	5.82	6.02
Al^{IV}	2.15	2.12	2.12	2.20	2.07	2.16	2.10	2.15	2.18	2.18	2.18	1.98
Al^{VI}	0.92	0.95	0.97	0.95	0.73	0.80	0.99	0.99	0.98	0.55	0.80	0.88
Ti	0.10	0.12	0.08	0.11	0.09	0.03	0.11	0.10	0.10	0.10	0.08	0.04
Cr	0.00	0.00	0.00	0.00	0.00	0.00	0.00	0.00	0.00	0.00	0.00	0.00
Fe^{3+}	0.75	0.74	0.88	0.81	1.10	1.52	0.65	0.82	0.84	1.22	0.91	0.77
Fe^{2+}	0.85	0.76	0.74	0.78	0.39	0.00	0.88	0.62	0.65	0.57	0.72	0.61
Mn	0.01	0.01	0.00	0.01	0.00	0.01	0.00	0.01	0.01	0.02	0.02	0.00
Mg	2.37	2.43	2.32	2.35	2.69	2.72	2.36	2.45	2.42	2.54	2.46	2.69
Ca	1.77	1.73	1.73	1.72	1.68	1.44	1.73	1.73	1.72	1.71	1.73	1.71
Na	0.66	0.67	0.58	0.67	0.66	0.71	0.70	0.62	0.64	0.68	0.73	0.73
K	0.08	0.07	0.08	0.11	0.05	0.06	0.08	0.07	0.08	0.11	0.11	0.09
Cl	0.44	0.41	0.42	0.49	0.37	0.40	0.42	0.38	0.41	0.52	0.40	0.36
OH^*	1.56	1.59	1.58	1.51	1.63	1.60	1.58	1.62	1.59	1.48	1.60	1.64
Total	17.51	17.47	17.38	17.50	17.39	17.28	17.51	17.41	17.44	17.50	17.57	17.54
Amphibole	Ca	Ca	Ca	Ca	Ca	Ca	Ca	Ca	Ca	Ca	Ca	Ca
Amphibole names	ferrian-pargasite	ferrian-tschermakite	ferri-tschermakite	ferri-subcalcic pargasite	ferrian-tschermakite	magnesio-hastingsite	ferrian-pargasite					
	tschermakite	ferrian-pargasite	ferrian-tschermakite	ferri-tschermakite								

AMPHIBOLES

METAGABBROS, cont.

	PWN051						Munz and Morvik, 1991		**AMPHIBOLITES** PWN67			PWN118 1
	AM051.1	AM051.2	AM051.3	AM051.4	AM051.5	AM051.6	IA-29B	IA-6	AM67.1	AM67.2	AM67.3	y118211
SiO_2	43.00	43.19	43.31	44.26	44.57	43.20	40.46	40.78	39.94	40.16	40.44	38.88
TiO_2	0.59	0.66	0.60	0.24	0.29	0.29	0.36	0.76	1.31	1.31	1.25	0.89
Al_2O_3	15.56	15.21	16.77	18.09	18.11	18.26	16.13	14.49	13.58	13.05	13.52	15.48
Cr_2O_3	0.00	0.00	0.00	0.00	0.00	0.00	0.00	0.00	0.00	0.00	0.00	0.00
Fe_2O_3	11.18	11.05	12.81	0.79	0.40	1.33	4.85	5.48	8.95	6.22	6.19	10.83
FeO	0.86	0.70	0.00	12.87	12.87	12.61	7.22	8.05	9.04	10.82	11.46	4.56
MnO	0.06	0.00	0.13	0.26	0.24	0.24	0.05	0.05	0.00	0.00	0.04	0.16
MgO	14.02	14.30	15.72	20.17	20.37	19.21	12.57	12.57	10.63	10.28	10.19	11.36
CaO	10.66	10.64	7.73	0.58	0.62	1.28	11.54	11.54	10.71	10.76	11.19	10.65
Na_2O	2.29	2.29	2.14	2.26	2.25	2.20	3.08	3.08	2.71	2.62	2.54	2.33
K_2O	0.32	0.33	0.32	0.04	0.06	0.15	0.69	0.69	0.91	0.92	0.98	0.59
Cl	0.89	0.88	0.76	0.14	0.13	0.33	0.00	0.00	1.53	1.44	1.52	2.03
H_2O	1.89	1.89	1.97	2.12	2.13	2.05	2.03	2.03	1.62	1.61	1.62	1.49
O=F,Cl	0.20	0.20	0.17	0.03	0.03	0.07	0.00	0.00	0.34	0.32	0.34	0.46
Total	101.12	100.94	102.09	101.79	102.02	101.08	98.98	99.52	100.58	98.87	100.59	98.79
No. of O	23	23	23	23	23	23	23	23	23	23	23	23
Structural formulae												
Si	6.08	6.11	6.01	6.15	6.17	6.07	5.96	6.02	5.96	6.10	6.06	5.82
Al^{IV}	1.92	1.89	1.99	1.85	1.83	1.93	2.04	1.98	2.04	1.90	1.94	2.18
Al^{VI}	0.68	0.65	0.75	1.11	1.12	1.10	0.76	0.54	0.35	0.44	0.44	0.55
Ti	0.06	0.07	0.06	0.03	0.03	0.03	0.04	0.08	0.15	0.15	0.14	0.10
Cr	0.00	0.00	0.00	0.00	0.00	0.00	0.00	0.00	0.00	0.00	0.00	0.00
Fe^{3+}	1.19	1.18	1.34	0.08	0.04	0.14	0.54	0.61	1.01	0.71	0.70	1.22
Fe^{2+}	0.10	0.08	0.00	1.49	1.49	1.48	0.89	0.99	1.13	1.37	1.44	0.57
Mn	0.01	0.00	0.02	0.03	0.03	0.03	0.01	0.01	0.00	0.00	0.01	0.02
Mg	2.96	3.02	3.25	4.18	4.20	4.03	2.76	2.77	2.37	2.33	2.28	2.54
Ca	1.62	1.61	1.15	0.09	0.09	0.19	1.82	1.83	1.71	1.75	1.80	1.71
Na	0.63	0.63	0.58	0.61	0.60	0.60	0.88	0.88	0.78	0.77	0.74	0.68
K	0.06	0.06	0.06	0.01	0.01	0.03	0.13	0.13	0.17	0.18	0.19	0.11
Cl	0.21	0.21	0.18	0.03	0.03	0.08	0.00	0.00	0.39	0.37	0.39	0.52
OH^*	1.79	1.79	1.82	1.97	1.97	1.92	2.00	2.00	1.61	1.63	1.61	1.48
Total	17.30	17.30	17.20	17.62	17.61	17.63	17.83	17.84	17.67	17.70	17.72	17.50
Amphibole	Ca	Ca	Ca	---Fe-Mg-Mn----			Ca	Ca	Ca	Ca	Ca	Ca
Amphibole names	ferri-chermakite	ferri-tschermakite	ferri-subcalcic tschermakite	gedrite	gedrite	gedrite	pargasite	magnesio-hastingsite	magnesian hastingsite	magnesian hastingsite	magnesian hastingsite	ferri-tschermakite

	Na ENRICHED AMPHIBOLITES							ALBITITES			
	PWN057						PWN071	PWN052			
	AM57.1	AM57.2	AM57.3	AM57.4	AM57.5	AM57.6	z7141	AM52.1	AM52.2	AM52.3	AM52.4
SiO_2	41.21	42.34	41.24	41.77	41.15	41.70	39.28	54.71	54.01	56.08	53.48
TiO_2	1.90	1.37	1.78	1.44	1.84	1.48	0.76	0.01	0.35	0.12	0.36
Al_2O_3	13.44	12.96	13.53	13.09	12.87	12.57	17.06	0.79	2.67	0.55	3.63
Cr_2O_3	0.00	0.00	0.00	0.00	0.00	0.00	0.00	0.06	0.25	0.11	0.21
Fe_2O_3	6.74	6.71	6.77	5.99	7.24	8.06	8.17	2.93	3.14	1.39	6.62
FeO	6.53	6.49	6.22	6.96	5.88	4.91	5.82	8.66	4.03	6.04	0.00
MnO	0.00	0.00	0.00	0.00	0.00	0.00	0.18	0.00	0.00	0.00	0.00
MgO	13.60	13.98	13.59	13.72	13.75	14.21	11.15	17.46	19.91	20.22	21.27
CaO	11.52	11.91	11.53	11.83	11.52	11.51	10.91	12.41	12.65	13.10	11.10
Na_2O	2.76	2.45	2.62	2.53	2.46	2.40	2.55	0.46	0.81	0.54	1.16
K_2O	0.91	0.84	0.83	0.88	0.87	0.84	0.56	0.13	0.15	0.05	0.21
Cl	1.16	0.94	1.17	0.94	1.02	1.09	1.60	0.00	0.06	0.00	0.07
H_2O	1.77	1.84	1.76	1.82	1.78	1.78	1.62	2.10	2.13	2.15	2.15
O=F,Cl	0.26	0.21	0.26	0.21	0.23	0.25	0.36	0.00	0.01	0.00	0.02
Total	101.34	101.62	100.77	100.75	100.15	100.30	99.29	99.73	100.14	100.35	100.25
No. of O	23	23	23	23	23	23	23	23	23	23	23
Structural formulae											
Si	6.00	6.12	6.02	6.10	6.04	6.09	5.82	7.80	7.55	7.83	7.39
Al^{IV}	2.00	1.88	1.98	1.90	1.96	1.91	2.18	0.13	0.44	0.09	0.59
Al^{VI}	0.30	0.33	0.35	0.35	0.27	0.26	0.80	0.00	0.00	0.00	0.00
Ti	0.21	0.15	0.20	0.16	0.20	0.16	0.08	0.00	0.04	0.01	0.04
Cr	0.01	0.00	0.00	0.00	0.00	0.00	0.00	0.01	0.03	0.01	0.02
Fe^{3+}	0.74	0.73	0.74	0.66	0.80	0.89	0.91	0.31	0.33	0.15	0.69
Fe^{2+}	0.79	0.78	0.76	0.85	0.72	0.60	0.72	1.03	0.47	0.71	0.00
Mn	0.00	0.00	0.00	0.00	0.00	0.00	0.02	0.00	0.00	0.00	0.00
Mg	2.95	3.01	2.96	2.99	3.01	3.09	2.46	3.71	4.15	4.21	4.38
Ca	1.80	1.84	1.80	1.85	1.81	1.80	1.73	1.90	1.89	1.96	1.64
Na	0.78	0.69	0.74	0.72	0.70	0.68	0.73	0.13	0.22	0.15	0.31
K	0.17	0.15	0.15	0.16	0.16	0.16	0.11	0.02	0.03	0.01	0.04
Cl	0.29	0.23	0.29	0.23	0.25	0.27	0.40	0.00	0.01	0.00	0.02
OH^*	1.71	1.77	1.71	1.77	1.75	1.73	1.60	2.00	1.99	2.00	1.98
Total	17.74	17.69	17.70	17.73	17.67	17.64	17.57	17.05	17.14	17.11	17.10
Amphibole	Ca	Ca	Ca	Ca	Ca	Ca	Ca	Ca	Ca	Ca	Ca
Amphibole names	magnesio-hastingsite	magnesio-hastingsit	magnesio-hastingsite	magnesio-hastingsit	magnesio-hastingsite	magnesio-hastingsite	magnesio-hastingsite	actinolite	actinolite	tremolitic hornblende	

APPENDIX 3. MAJOR AND TRACE ELEMENT WHOLE ROCK DATA

Becquerel Laboratories Inc. supplied the following information about acceptance criteria for results. The controls must fall within ±2.5 standard deviations of the mean for acceptance. This means that 100% variation is acceptable within 5 times the detection limit and 20% variation is acceptable up to 50 times the detection limit and 10% variation is acceptable above that. On the following page a table describing the precision of the major/trace element analyses done at the Geological Survey of Canada is included. this information was supplied by the laboratory.

The REE analyzed by INAA and ICP-MS methods produced similar values for each method. these unused INAA results are not reproduced in this thesis. The equivalent range and overall slope of the REE in Figure 4.16 for both methods suggests this similarity. The more jagged nature of the INAA plot show that there is somewhat less accuracy with this method. Some of the elements (e.g. Eu) are below detection limit with the INAA procedure for many samples and the 1 ppm increments for numbers just above the detection limit produce poor precision.

Blind duplicate analyses of samples PWN 025, PWN 026, PWN 87.2 and PWN 102 are included in the following list of analyses and are marked as PWN 025.5, PWN 026.6, PWN 87.5 and PWN 102.5 respectively.

ESTIMATE OF VALIDITY OF RESULTS FOR MAJOR AND TRACE ELEMENTS ANALYZED BY THE GEOLOGICAL SURVEY OF CANADA AS SUPPLIED BY THE G.S.C. LABORATORY

Element	± (ABSOLUTE	+	RELATIVE)
SiO_2	± (0.5	+	1% of concentration)
TiO_2	± (0.02	+	1% of concentration)
Al_2O_3	± (0.2	+	1% of concentration)
Fe_2O_3 (total)	± (0.06	+	1% of concentration)
MnO	± (0.01	+	2% of concentration)
MgO	± (0.04	+	1% of concentration)
CaO	± (0.01	+	1% of concentration)
Na_2O	± (0.03	+	1% of concentration)
K_2O	± (0.05	+	1% of concentration)
P_2O_5	± (0.01	+	1% of concentration)
FeO	± (0.2	+	5% of concentration)
H_2O (total)	± (0.1	+	3% of concentration)
CO_2	± (0.01	+	3% of concentration)
S (total)	± (0.02	+	5% of concentration)
Ag	± (2	+	10% of concentration)
Ba	± (30	+	10% of concentration)
Be	± (0.5	+	5% of concentration)
Co	± (5	+	5% of concentration)
Cr	± (10	+	5% of concentration)
Cu	± (10	+	5% of concentration)
La	± (10	+	5% of concentration)
Nb	± (10	+	10% of concentration)
Ni	± (10	+	5% of concentration)
Pb	± (20	+	10% of concentration)
Rb	± (10	+	2% of concentration)
Sc	± (0.5	+	5% of concentration)
Sr	± (20	+	10% of concentration)
V	± (5	+	5% of concentration)
Y	± (5	+	5% of concentration)
Yb	± (0.5	+	5% of concentration)
Zn	± (5	+	5% of concentration)
Zr	± (10	+	10% of concentration)

SAMPLE	Rock type	SiO_2 %	TiO_2 %	Al_2O_3 %	Fe_2O_3 %	FeO %	MnO %	MgO %	CaO %	Na_2O %	K_2O %	P_2O_5 %	H_2O^{total} %	CO_2= %	C %	CO_2^{total} %	S ppm	Cl ppm	LOI %	Total %
PWN 50	metagabbro	45 2	0 80	20 0	1 6	7 4	0 15	9 22	9 90	2 5	0 64	0 09	1 5			<0 1	339	7070		99 7
PWN 51	scapolized-metagabbro	45 2	0 58	20 5	1 6	6 0	0 09	9 26	9 90	2 7	1 1	0 07	2 0			0 1	318	6564		99 8
PWN 53	metagabbro	44 7	0 91	18 5	2 8	7 4	0 12	10 10	9 07	3 0	1 04	0 13	1 4			0 1	420	9244		100 2
PWN 120	metagabbro	46 4	0 82	20 0	2 0	7 2	0 16	8 23	10 10	2 9	0 37	0 11	1 1	1 1	0 1		574	5970		101 2
PWN 42 1	proto-amphibolite	45 9	1 51	17 7	2 5	8 8	0 11	7 75	9 43	3 5	0 39	0 3	1 8			<0 1	784	2166		100 0
PWN 42 2	proto-amphibolite	44 7	1 54	16 9	2 6	9 9	0 11	8 56	9 70	2 9	0 49	0 1	1 7			<0 1	476	4132		99 7
PWN 42 3	proto-amphibolite	46 1	1 52	18 1	2 2	8 5	0 10	7 53	9 49	3 2	0 69	0 2	1 8			<0 1	1180	2854		99 8
PWN 100	scapolitized amphibolite	44 1	2 62	14 7	6 4	7 8	0 07	6 43	9 25	4 7	0 76	0 4	0 9			<0 1	791	19000		100 1
PWN 118 1	proto-amphibolite	48 1	1 99	17 5	4 4	8 6	0 19	5 94	9 25	3 1	0 41	0 26	0 5	0 5	0 1		936	1867		101 1
PWN 118 2	proto-amphibolite	47 1	2 02	17 1	4 1	8 7	0 16	5 65	9 10	3 7	0 5	0 26	0 7	0 7	0 1		964	6472		100 6
PWN 1	amphibolite	46 8	4 12	16 6	2 9	9 1	0 11	5 07	8 44	3 7	0 93	0 87	1 2			<0 1	785	3332		100 3
PWN 18	Bt-Hbl-Ccp amphibolite	38 4	2 44	14 8	3 9	14 6	0 08	9 90	2 05	0 5	5 17	0 3	5 6			0 2	4777	2252		98 6
PWN 19	Bt-Hbl-Qtz-Czo-Chl gneissic	47 2	2 20	16 4	1 7	9 6	0 04	8 51	2 30	1 9	5 83	0 2	2 8			<0 1	2989	2924		99 3
PWN 21	amphibolite	50 3	2 60	14 0	2 2	12 3	0 07	5 69	2 63	2 1	5 15	0 3	1 8			<0 1	2100	5045		99 9
PWN 23	amphibolite	44 6	2 05	15 8	2 8	11 6	0 11	7 24	9 50	2 0	2 02	0 3	1 9			0 1	1435	6087		100 8
PWN 61	equigranular amphibolite	46 6	1 57	16 8	3 4	8 8	0 12	7 76	9 60	2 8	0 88	0 13	1 4			<0 1	856	4088		100 4
PWN 67	scapolitized proto-amphibolite	44 1	2 15	15 5	4 1	9 1	0 08	6 93	9 29	4 4	0 81	0 22	0 6			<0 1	1003	20000		99 4
PWN 90	equigranular amphibolite	46 0	1 86	15 8	3 6	9 7	0 21	6 83	9 21	3 7	0 59	0 2	1 3			<0 1	188	4958		99 5
PWN 102 1	equigranular amphibolite	46 2	2 42	15 4	4 5	8 7	0 08	6 46	8 57	4 0	1	0 36	1 2			<0 1	312	4819		99 4
PWN 102 5	*duplicate of PWN 102 1*	47 4	2 35	15 2	4 4	8 4	0 09	6 20	8 51	4 0	0 84	0 34	1 1			0 1	625	4278		99 4
PWN 103	equigranular amphibolite	46 0	2 57	15 2	4 4	8 7	0 09	6 65	8 22	3 9	1 18	0 4	1 5			<0 1	590	4421		99 3
PWN 105	equigranular amphibolite	45 9	2 64	14 9	3 8	8 5	0 08	6 28	9 90	3 5	0 81	0 4	1 3			0 2	1303	7384		99 1
PWN 115	amphibolite	48 2	2 00	16 7	2 9	5 3	0 07	4 87	10 30	5 5	0 5	0 19	0 7	0 7	0 1		421	18000		99 9
PWN 2	Hbl-Bt gneissic amphibolite	46 2	2 34	17 5	3 1	8 3	0 08	4 92	8 90	4 0	0 73	0 3	1 2			<0 1	3751	5387		98 5
PWN 17	gneissic amphibolite	44 5	1 99	17 0	3 3	8 9	0 12	7 78	7 75	3 1	1 62	0 2	2 3			0 2	598	4446		99 3
PWN 114	gneissic amphibolite	45 4	3 03	16 9	4 4	8 7	0 06	5 34	6 94	4 4	0 8	0 5	1 9	1 9	0 1		871	4133		100 9
PWN 119	gneissic amphibolite	48 1	1 64	19 1	1 9	7 5	0 07	6 01	9 90	3 7	0 33	0 18	0 8	0 8	0 1		930	2536		100 5
PWN 121	gneissic amphibolite	49 5	0 90	17 3	2 6	7 2	0 05	6 73	8 89	4 5	0 65	0 16	1 1	1 1	0 1		643	2640		101 1
PWN 122	gneissic amphibolite	44 7	1 16	17 1	3 0	9 9	0 14	7 58	9 09	3 1	0 55	0 08	2 0	2 0	0 1		319	4848		101 0
PWN 20 1	Hbl-Bt-Ab amphibolite	71 0	0 12	15 6			0 01	0 44	2 53	5 2	1 59		0 7	0 1	0 1		1047	585		97 6
PWN 20 2	Hbl-Bt-Ab amphibolite?	52 9	0 98	13 5	3 6	9 9	0 09	4 84	6 74	2 5	2 24	0 1	1 8	0 1	0 1		2508	5984		100 2
PWN 38	Act-Pl gneiss	45 3	0 63	19 3	1 9	7 2	0 06	8 27	9 90	2 8	0 9	0 1	2 3			<0 1	537	4664		99 2
PWN 40	Act-Ab gneiss	63 7	0 76	9 7	2 2	2 7	0 02	9 09	5 00	5 5	0 06	0 2	1 1			0 1	<50	289		100 2
PWN 41	Hbl-Scp-Ab gneiss	49 0	2 00	17 9	3 0	8 0	0 12	3 62	10 10	3 8	0 82	0 2	0 7			<0 1	967	>10000		99 4
PWN 57	Na-enriched amphibolite	44 5	1 45	16 1	8 4	4 4	0 03	8 33	9 32	4 9	0 65	0 13	1 0			0 1	622	>10000		99 4
PWN 65	Na-enriched-proto-amphibolite	57 6	3 52	13 2	2 0	2 8	0 01	4 90	7 42	6 5	0 23	0 64	0 7			0 1	60	755		99 7
PWN 66	Na-enriched-proto-amphibolite	64 6	0 90	11 1	0 9	2 2	0 02	5 10	5 79	5 7	0 08	0 28	1 1	1 8	0 1		56	385		99 7
PWN 68	Na enriched gneissic amphibolite	46 7	2 19	17 1	4 4	8 6	0 05	4 50	8 15	4 7	0 66	0 22	1 6	0 3	0 1		846	5186		99 9
PWN 69	Na-enriched-gneissic amphibolite	51 3	4 19	13 8	1 2	3 0	0 02	6 27	12 10	5 2	0 22	0 44	0 6			0 1	181	6528		99 1
PWN 92	Na enriched gneissic amphibolite	46 7	1 44	16 8	3 4	5 2	0 03	7 83	9 50	5 1	0 6	0 1	1 6	0 3	0 1		240	14000		100 1
PWN 99	Na-enriched amphibolite	47 7	2 60	14 7	5 2	8 7	0 12	5 45	8 14	4 7	0 93	0 6	0 8			<0 1	322	6692		100 3
PWN 15	Bt-Ms quartzite	95 0	0 12	1 9			<0 01	1 10	0 10	0 0	0 33	0 1	0 7			0 1	513	205		99 5
PWN 60	Qtz-Bt Schist	78 7	0 50	8 9	0 4	1 4	0 01	3 61	1 03	1 9	2 12	0 03	0 7			<0 1	<50	392		99 3
PWN 96	Bt-Scp-Pl-Hem-Chl gneiss	45 8	2 68	16 8	7 5	6 5	0 02	4 97	3 79	5 4	3 38	0 7	1 5			<0 1	954	>10000		99 1
PWN 98	metasediment?	74 0	0 14	7 1	0 4	1 7	0 03	4 70	6 15	2 2	1 26		0 8	<0 1	0 1		92	3106		98 9
PWN 5	Qtz-Ms-sulphide schist	88 3	0 19	2 0			<0 01	1 82	0 13	0 1	0 56					<0 1	16700	211	1 8	94 8
PWN 9	albitized Qtz-Bt-Kfs-Ms-Chl schist	81 0	0 79	9 8			<0 01	0 82	0 06	0 8	2 44		0 9			<0 1	5853	124		97 2
PWN 10	Qtz-Ms-Sil quartzite	81 5	0 73	7 9			<0 01	1 75	0 08	0 7	3 28		1 1			<0 1	3948	132		97 4
PWN 12	Ms-Sil-Tur-Bt gneiss	73 2	1 34	10 1			<0 01	2 22	0 01	0 2	2 34					<0 1	30100	163	3 9	92 4
PWN 14	Qtz-Bt-Ms-Sil? schist	80 9	0 68	9 8	0 6	1 1	<0 01	1 68	0 01	0 3	2 72	0 1	1 0	<0 1	0 1		4779	292		99 5
PWN 22	Ms-Tur-Sil quartzite	82 9	0 57	8 8	<0 2	1 4	<0 01	1 71	0 64	0 5	1 69	0 1	0 8	<0 1	0 3		3382	259		99 8
PWN 4	Pl-Kfs-Qtz vein	58 2	1 80	16 2			0 01	3 88	4 04	3 2	2 51	0 5				<0 1	12200	1332	1 6	91 7
PWN 7	Qtz-Bt-Ms-Gr-Rt schist	55 7	1 74	15 7			0 01	3 72	3 94	3 0	2 42	0 5		<0 1	0 8		37300	266	5	91 3
PWN 31	Cal-Ab rock	44 4	0 44	8 7	20 2	1 7	0 02	2 72	9 21	5 1	<0 05	0 1	0 6	5 8	0 1		2191	308		99 3
PWN 35	Qtz-Ab-Act?-Ms-Cal-Chl breccia	73 5	0 55	5 8	5 6	1 1	0 01	3 80	3 04	3 2	<0 05	0 1	0 8	0 8	0 1		185	258		98 4
PWN 47	albitite	57 6	2 56	22 1	<0 2	0 7	<0 01	0 91	4 37	7 4	1 64	0 06	1 9			<0 1	<0 02			99 2
PWN 52	Act-albitite	55 2	1 51	11 6	6 9	3 0	0 02	9 04	4 04	5 6	0 18	0 21	2 5	<0 1	0 2		72	477		100 1
PWN 54	albitite	62 9	1 03	10 6	2 5	3 0	0 02	10 90	1 84	3 9	0 38	0 07	2 9			0 1	62	298		100 2
PWN 56	albitite	67 1	0 88	9 2	7 8	0 7	<0 01	6 69	0 27	4 9	<0 05	0 04	1 1			0 1	<50	217		98 8

SAMPLE	Rock type	SiO_2	TiO_2	Al_2O_3	Fe_2O_3	FeO	MnO	MgO	CaO	Na_2O	K_2O	P_2O_5	H_2O^{total}	CO_2=	C	CO_2^{total}	S	Cl	LOI	Total
		%	%	%	%	%	%	%	%	%	%	%	%	%	%	%	ppm	ppm	%	%
PWN 64	Qtz-Ab-Ms-Tur-Sil gneiss	73 3	1 51	8 3	<0 2	1 7	0 01	7 28	0 76	4 4	<0 05	0 23	0 9			<0 1	<50	176		98 4
PWN 70	Act-Qtz-Ab gneiss	75 6	0 61	7 8	1 8	1 1	<0 01	4 25	2 66	4 5	0 07	0 1	0 5	0 5	0 1		62	323		99 6
PWN 97	Qtz-Ab-Ms-Bt gneiss	76 4	0 45	9 8	0 6	1 5	0 02	2 89	1 21	3 5	0 81	0 1	1 5			0 1	<50	165		98 9
PWN 101	Albitite	75 4	1 25	7 9	<0 2	1 1	0 01	2 62	5 05	4 4	0 15	0 1	0 3			0 1	<50	428		98 4
PWN 110	albitite	66 0	1 96	16 3	0 3	0 6	0 01	2 10	1 84	8 9	0 49	0 19	0 2	0 2	0 1		71	303		99 2
PWN 111	albitite	60 3	0 39	17 7	0 5	2 0	0 02	3 52	2 74	9 0	0 26	0 03	1 6	1 6	0 1		225	462		99 8
PWN 113	albitite	58 8	2 42	17 8	1 0	2 2	0 01	2 19	2 50	8 9	0 25	0 31	1 6	1 6	0 1		1155	366		99 8
PWN 28	Ab-Cal-Act-Chl rock	42 7	0 76	12 0	1 0	3 8	0 01	4 73	15 30	5 5	0 11	0 1	2 1	10 3	0 1		2704	512		98 8
PWN 37	Py-Hem-Ab-Tr rock	54 0	0 50	10 0	12 0	2 4	0 02	7 19	4 42	5 2	<0 05	0 1	1 8	1 0	0 1		2961	175		99 0
PWN 55	albitite-quartzite	72 4	0 93	8 2	2 9	0 8	0 01	2 43	3 27	4 3	0 17	0 35	0 8	1 8	0 1		85	230		98 5
PWN 73 1	Ab-Qtz-Chl-Rt-Gr-Bt-Ms-Tur-Cal schist	62 4	0 87	17 4			0 01	2 07	1 69	6 0	2 03	0 35				1 2	116d	460	1 4	94 2
PWN 80	Ab-Qtz-Act-Ilm-Chl gneiss	45 7	1 72	16 5	3 6	9 1	0 13	7 22	9 50	3 3	0 52	0 1	1 5			0 2	117	5008		99 6
PWN 16 1	Chl-Py-Oam?-Mag vein	33 2	1 19	14 4			0 04	5 35	6 80	2 1	1 31	1 8		<0 1	0 1		20300	1148	5 5	68 4
PWN 24	Bt vein + quarztite?	78 0	0 35	9 9	<0 2	1 3	0 01	1 40	1 87	2 1	1 65	0 1	1 0	0 3	0 1		255	285		98 1
PWN 25	Pl-Qtz-Bt-Tur-Sil-Py-Gr schist	49 1	0 62	8 9			0 02	4 29	1 91	0 9	1 65	0 5		<0 1	3 0		103000	50	11 5	81 1
PWN 25 5	*duplicate of PWN 25*	44 9	0 83	11 9			0 02	6 48	2 61	1 2	3 04	0 7		<0 1	2 7		72700	845	9 5	81 8
PWN 71	Act-Ab-Qtz-Ep-Py gneiss	64 1	0 36	8 8			0 04	7 41	6 06	3 8	0 27	0 19				0 2	14800	380	1 9	92 7
PWN 72 1	Qtz-Pl-Tur-Ms-Chl-Gr-Py gneiss	62 4	0 91	12 8			<0 01	3 70	1 05	3 5	0 6	0 55		<0 1	4 1		21800	169	7 7	91 8
PWN 63	microcline pegmatite	74 8	0 03	14 9	<0 2	0 3	<0 01	0 11	1 03	5 6	2 87	0 03	0 1			0 1	50	183		99 9
PWN 3	Pl-rich vein	72 2	0 36	13 9	0 3	1 6	<0 01	0 79	3 45	3 9	0 75	0 1	0 3			<0 1	3817	529		98 1
PWN 13 1	Oam-Ms-Crd rock	62 7	0 78	9 5	9 5	0 9	0 01	9 19	1 69	3 7	0 15		1 3			0 1	<50	296		99 5
PWN 26	Hbl-Ep-Mgs amphibolite	41 1	0 96	12 0			0 07	10 00	10 10	2 5	1 44	0 2		0 3	0 1		13400	5924	1 5	80 7
PWN 26 5	*duplicate of PWN 26*	41 1	0 98	12 1			0 07	9 90	9 80	2 5	1 4	0 1		0 3	0 9		15000	5576	1 9	81 2
PWN 87 1	magnesite-serpentinite rock	33 3	0 13	0 3	7 4	0 9	0 02	40 30	0 26	0 0	<0 05	0 2	11 6	2 2	0 8		265	906		97 5
PWN 87 2	magnesite-serpentinite rock	49 1	0 16	0 9	6 7	0 4	0 01	33 80	0 08	0 0	0 06	0	7 7			<0 1	59	273		99 0
PWN 87 5	*duplicate of PWN 87 2*	49 7	0 11	1 2	4 7	0 4	0 01	34 30	0 09	0 0	0 16	0	7 9			<0 1	126	397		98 6
PWN 104	Pl-rich felsics	79 9	0 25	8 6	0 2	1 5	0 01	1 79	1 61	2 7	0 51	0 1	1 1			0 2	<50	630		98 5
PWN 32	coarse Cal vein	44 8	0 51	18 2	1 6	5 4	0 02	8 37	4 87	4 4	1 98	0 1	4 8	3 3	0 1		1150	273		98 6
PWN 48	granite	67 8	0 78	12 4	2 2	4 2	0 10	0 40	2 36	3 2	4 09	0 1	0 5			<0 1	<50	160		98 1
PWN 49	Chl-Ab-Qtz-Bt-Cal	45 0	1 09	17 4	3 6	6 5	0 02	7 59	8 38	4 6	1 3	0 14	2 8	1 5	0 1		310	9218		101 0
PWN 88	equigranular Qtz-diorite	66 3	1 00	14 0	1 1	3 4	0 05	2 43	5 59	3 7	0 23	0 3	0 6			<0 1	70	2167		98 9

SAMPLE	Ag	As	Au	Ba	Be	Br	Cd	Co	Cr	Cs	Cu	F	Ga	Hf	In	Ir	Mo	Nb	Ni	Pb	Rb	Sb	Sc	Se	Sn	Sr	Ta
	ppm	ppm	ppb	ppm	ppm	ppm	ppm	ppm	ppm	ppm	ppm	ppm	ppm	ppm	ppm	ppb	ppm	ppm	ppm	ppm	ppm	ppm	ppm	ppm	ppm	ppm	ppm
PWN 50	<0 1	1 4	0 2	200	<0 5	10 0	<5	73	59	1	22	131	15	1 8	0 1	<50	0 34	1 3	210	1 5	23	0 2	13 0	<5	<100	390	0 8
PWN 51	<0 1	0 7	1 1	110	<0 5	10 0	<5	69	42	0 89	16	120	14	2 2	0 08	<50	0 3	0 89	220	1 1	30	0 1	9 1	<5	<100	330	0 6
PWN 53	<0 1	0 7	0 7	200	<0 5	13 0	<5	68	35	1 3	10	199	14	2 4	<0 05	<50	0 25	1 8	220	1 2	32	0 2	12 0	<5	<100	290	1
PWN 120	<0 1	0 8	1 03	110	<0 5	23 0	<5	61	56	0 5	40	156	15	2 3	0 11	<50	0 37	1 3	150	2 2	9 7	<0 1	9 4	<5	<100	320	0 5
PWN 42 1	0 2	<0 5	0 2	80	0 7	0 9	<5	65	46	0 24	17	268	16	2 9	0 06	<50	0 25	2 6	140	1 3	12	<0 1	18 0	<5	<100	340	0 4
PWN 42 2	<2	<0 5	<2	90	0 7	0 7	<5	74	48	<0 5	16	320		3		<50	<1	12	140		21	<0 1	19 0	<5	<100	220	0 6
PWN 42 3	<2	<0 5	<2	120	0 7	1 3	<5	66	42	0 8	27	261		3		<50	<1	<10	140		37	<0 1	16 0	<5	<100	340	<0 5
PWN 100	<2	1 9	0 3	130	1 3	119 0	<5	70	72	2	18	560		5		<50	<1	15	97		17	0 2	31 0	<5	<100	140	0 8
PWN 118 1	<2	0 6	<2	160	0 9	40 0	<5	60	56	0 6	50	327		3		<50	<1	<10	69		13	<0 1	25 0	<5	<100	330	0 6
PWN 118 2	<0 1	0 7	0 4	120	0 9	5 1	<5	53	59	0 55	34	302	20	3 8	0 14	<50	0 44	3 8	60	<1	5 9	<0 1	24 0	<5	<100	300	0 6
PWN 1	<2	1 9	<2	360	1 7	2 0	<5	65	130	<0 5	47	662		11		<50	<1	10	46		30	0 2	36 8	<5	<100	420	1 2
PWN 18	<2	15 0	1100	370	0 8	1 1	<5	140	75	5 6	5300	867		4		<50	<1	<10	130		260	0 1	28 0	<5	<100	46	0 5
PWN 19	<2	6 4	<2	230	1 5	<0 5	<5	120	110	6 9	230	1083		4		<50	<1	<10	87		310	0 1	34 0	<5	<100	110	<0 5
PWN 21	<2	53 2	60	560	1 1	<0 5	<5	77	94	7 6	1300	804		6		<50	<1	<10	37		320	<0 1	31 0	<5	<100	120	<0 5
PWN 23	<2	22 0	<2	120	1 4	1 0	<5	96	94	1	210	442		4		<50	<1	10	91		61	0 1	34 0	<5	<100	110	0 7
PWN 61	<2	1 2	<2	70	0 6	1 8	<5	61	88	<0 5	49	216		2		<50	<1	<10	100		25	0 2	31 0	<5	<100	160	<0 5
PWN 67	<0 1	0 5	<2	110	0 9	96 3	<5	74	100	0 62	20	304	20	4 8	0 09	<50	0 2	3 5	97	<1	9 1	<0 1	31 0	<5	<100	190	0 7
PWN 90	<2	<0 5	<2	140	1	1 8	<5	57	93	<0 5	20	451		5		<50	<1	<10	82		18	<0 1	26 0	<5	<100	310	0 6
PWN 102 1	<2	<0 5	3 1	180	1 1	0 9	<5	67	82	<0 5	33	416		5		<50	<1	14	86		32	<0 1	26 0	<5	<100	220	0 6
PWN 102 5	<2	<0 5	<2	120	1 1	1 1	<5	71	80	<0 5	72	289		5		<50	<1	<10	83		28	0 2	26 0	<5	<100	210	0 8
PWN 103	<2	0 7	<2	80	1 2	0 9	<5	70	86	<0 5	38	463		6		<50	<1	11	92		39	0 2	29 0	<5	<100	220	0 6
PWN 105	<2	<0 5	<2	100	1 3	81 2	<5	62	66	2 1	<10	621		6		<50	<1	13	68		20	<0 1	31 0	<5	<100	180	0 9
PWN 115	<2	1 7	<2	170	1 1	112 0	<5	44	140	2 2	<10	331		3		<50	<1	14	51		19	0 2	36 0	<5	<100	240	1 1
PWN 2	<2	2 0	<2	120	2 1	33 0	<5	85	33	<0 5	330	545		5		<50	<1	10	89		14	0 2	12 0	<5	<100	440	0 8
PWN 17	<2	<0 5	<2	230	1	1 9	<5	66	91	1	17	383		4		<50	<1	11	140		72	<0 1	24 0	<5	<100	300	<0 5
PWN 114	<2	0 5	<2	120	1 1	1 1	<5	65	100	1 2	26	470		6		<50	<1	<10	71		31	0 1	18 0	<5	<100	260	0 8
PWN 119	<0 1	<0 5	0 2	110	0 6	1 8	<5	53	56	0 09	38	195	17	3 1	0 06	<50	0 36	2 7	64	1 5	4 7	<0 1	22 0	<5	<100	370	0 4
PWN 121	<0 1	<0 5	0 1	<30	0 6	0 6	<5	63	60	0 15	14	313	18	2 8	0 13	<50	<0 2	1 5	87	<1	11	0 1	15 0	<5	<100	200	0 5
PWN 122	<0 1	<0 5	0 2	130	0 6	1 8	<5	61	72	0 45	15	207	20	2 1	0 07	<50	<0 2	2 3	100	2 1	12	<0 1	14 0	<5	<100	250	0 5
PWN 20 1	<2	35 0	4	260	4 4	2 0	<5	35	<10	0 8	100	113		1		<50	1	<10	<10		77	<0 1	2 4	<5	<100	360	0 9
PWN 20 2	<2	70 1	25	310	3 7	3 1	<5	57	32	3 2	1200	434		5		<50	<1	<10	30		79	0 2	36 0	<5	<100	130	3 1
PWN 38	<2	0 6	0 3	90	<0 5	2 5	<5	56	150	0 8	12	156		1		<50	<1	<10	130		37	<0 1	11 0	<5	<100	230	<0 5
PWN 40	<2	0 6	<2	30	1 5	0 7	<5	25	41	<0 5	69	612		8		<50	<1	16	73		<10	1 2	8 7	<5	<100	26	1 3
PWN 41	<2	1 5	<2	260	1 1	39 0	<5	57	67	<0 5	120	334		5		<50	<1	13	41		20	0 2	27 0	<5	<100	340	1
PWN 57	<2	0 9	<2	80	0 5	71 5	<5	58	92	5 6	<10	347		2		<50	<1	<10	98		16	<0 1	29 0	<5	<100	93	0 8
PWN 65			0 4	120	2 4			53	10		<10	477						16	29		19		45 0			170	
PWN 66	<2	<0 5	<2	70	1 4	1 0	<5	32	42	<0 5	<10	846		8		<50	<1	21	33		14	0 1	16 0	<5	<100	100	1 6
PWN 68	<2	0 7	2	70	0 9	4 4	<5	59	72	<0 5	66	380		4		<50	<1	<10	70		17	0 5	32 0	<5	<100	210	0 7
PWN 69	<2	2 3	<2	60	1 1	66 7	<5	35	45	<0 5	10	354		6		<50	<1	<10	41		12	0 2	59 0	<5	<100	210	0 9
PWN 92	<2	1 2	<2	60	0 9	93 7	<5	52	150	7 6	<10	455		2		<50	<1	12	81		10	0 2	22 0	<5	<100	110	<0 5
PWN 99	<2	0 9	0 4	180	1 3	<0 5	<5	62	60	<0 5	25	736		7		<50	<1	15	74		20	<0 1	31 0	<5	<100	160	0 8
PWN 15	<2	1000 0	<4	50	<0 5	4 8	<5	700	<10	<0 5	19	112		6		<50	<5	10	33		20	<0 3	2 0	<5	<100	<20	1 2
PWN 60	<2	<0 5	<2	50	1 3	0 8	<5	55	28	1 2	<10	484		14		<50	<1	18	14		99	0 2	5 6	<5	<100	72	1 5
PWN 96	<2	2 3	<2	420	1 3	90 6	<5	47	30	6 2	10	752		5		<50	<1	17	30		130	<0 1	22 0	<5	<100	210	0 9
PWN 98	<2	<0 5	0 7	190	1 2	39 0	<5	44	14	16	<10	167		3		<50	<1	<10	22		76	0 1	4 7	<5	<100	86	1 2
PWN 5	<2	61 6	18	40	0 5	2 2	<5	130	19	0 5	11000	123		19		<50	4	<10	57		28	0 5	2 9	<5	<100	<20	0 8

SAMPLE	Ag	As	Au	Ba	Be	Br	Cd	Co	Cr	Cs	Cu	F	Ga	Hf	In	Ir	Mo	Nb	Ni	Pb	Rb	Sb	Sc	Se	Sn	Sr	Ta
	ppm	ppm	ppb	ppm	ppm	ppm	ppm	ppm	ppm	ppm	ppm	ppm	ppm	ppm	ppm	ppb	ppm	ppm	ppm	ppm	ppm	ppm	ppm	ppm	ppm	ppm	ppm
PWN 9	<2	2600	42	180	1 2	<7 9	<5	930	26	2 4	1400	178		18		<50	<8	15	61		73	<1 1	6 3	<5	<210	21	0 7
PWN 10	<2	845 0	11	210	<0 5	3 3	<5	700	27	1 7	690	265		15		<50	2	<10	43		80	<0 3	8 3	<5	<100	25	1 4
PWN 12	<2	103 0	8	90	1 5	1 3	<5	370	42	0 8	970	284		24		<50	3	23	190		62	0 7	10 0	<5	<100	<20	2 7
PWN 14	<2	35 0	2	160	0 9	1 1	<5	51	25	2 3	910	273		17		<50	<1	<10	31		70	<0 1	7 1	<5	<100	22	1 4
PWN 22	<2	404 0	29	100	0 9	2 3	<5	200	24	1 2	2400	266		16		<50	2	14	27		54	<0 1	6 4	<5	<100	64	1 4
PWN 4	<2	0 9	3	460	3 2	1 6	<5	80	30	1 5	480	601		11		<50	1	11	41		76	<0 1	19 0	<5	<100	360	1
PWN 7	<2	17 0	5	430	0 9	0 8	<5	79	42	3 6	500	924		11		<50	1	12	26		68	0 4	12 0	<5	<100	340	1 4
PWN 31	<2	0 6	<2	<30	1 9	0 6	<5	45	35	<0 5	<10	295		5		<50	<1	<10	94		10	<0 1	14 0	<5	<100	38	0 8
PWN 35	<2	0 6	<2	<30	1 5	1 0	<5	41	26	<0 5	<10	417		6		<50	<1	<10	31		12	<0 1	10 0	<5	<100	<20	1
PWN 47	<2	<0 5	<2	65	3 7	0 8	<5	31	86	0 8	<10	113		4		<50	<1	16	<10		90	0 7	3 2	<5	<100	210	1 2
PWN 52	<0 1	<0 5	0 3	80	3 6	1 9	<5	36	87	5 2	<10	608	13	6	0 07	<50	<0 2	6 6	73	<1	15	0 4	35 0	<5	<100	<20	0 7
PWN 54	<2	0 9	<2	70	1 4	0 7	<5	41	46	1 5	<10	419		6		<50	<1	16	60		24	0 4	16 0	<5	<100	87	1 2
PWN 56	<2	<0 5	<2	50	0 8	0 7	<5	25	52	<0 5	<10	317		7		<50	<1	13	20		<10	2 3	14 0	<5	<100	42	1 2
PWN 64				50	1 1			56	71		<10	119						23	27		<10		10 0			51	
PWN 70	<2	<0 5	<2	<30	1 7	1 2	<5	62	29	<0 5	<10	440		6		<50	<1	15	28		10	0 2	8 4	<5	<100	<20	2 1
PWN 97	<2	<0 5	<2	100	0 6	0 7	<5	68	31	<0 5	<10	294		20		<50	1	18	14		39	<0 1	4 5	<5	<100	53	2 2
PWN 101	<2	1 6	<2	60	0 7	2 3	<5	81	33	<0 5	<10	104		12		<50	1	21	14		<10	<0 1	4 6	<5	<100	39	2 3
PWN 110	<2	15 0	<2	60	11	1 0	<5	33	24	<0 5	<10	763		8		<50	<1	41	17		17	0 6	11 0	<5	<100	220	3 5
PWN 111	<0 1	0 7	<2	30	1 8	3 6	<5	26	36	0 46	97	220	11	1 5	0 07	<50	<0 2	1 5	49	2 7	5 1	0 1	10 0	<5	<100	53	0 5
PWN 113	<2	0 6	0 4	70	1 8	2 1	<5	100	120	0 7	<10	450		3		<50	<1	11	29		14	0 2	15 0	<5	<100	31	0 6
PWN 28	<2	1 8	0 6	40	2 8	2 2	<5	64	68	0 6	<10	330		2		<50	<1	11	97		12	0 2	20 0	<5	<100	50	<0 5
PWN 37	<2	1 6	<2	30	2 9	1 0	<5	100	33	<0 5	<10	643		4		<50	<1	13	65		14	<0 1	40 0	<5	<100	<20	<0 5
PWN 55	<2	4 9	<2	60	1 1	1 6	<5	65	40	2 6	61	454		9		<50	<1	16	<10		22	4 6	7 6	<5	<100	39	2 3
PWN 73 1	<2	81 1	30	40	1 9	1 6	<5	87	29	0 7	500	583		7		<50	<1		36			<0 1	10 0	<5	<100	47	1 8
PWN 80	<2	<0 5	<2	80	1 2	1 3	<5	60	110	<0 5	21	345		3		<50	<1	<10	99		17	<0 1	25 0	<5	<100	280	0 6
PWN 16 1	<2	17 0	11	180	1	0 9	<5	230	29	1 8	64	515		1		<50	<1	<10	120		71	0 8	9 5	<5	<100	390	<0 5
PWN 24	<2	135 0	7	120	3 3	2 2	<5	91	16	1 5	220	181		8		<50	4	15	16		75	0 1	5 5	<5	<100	130	1 3
PWN 25	<2	15 0	8	80	3 2	<0 5	<5	550	33	2	3400	440		5		<50	44		820			<0 1	11 0	5	<100	31	1 1
PWN 25 5	<2	146 0	7	90	3 2	<0 5	<5	380	49	1 9	1600	1221		5		<50	40		590			<0 1	12 0	<5	<100	34	1 3
PWN 71	<2	600 0	56	40	1 2	<3 7	<5	520	20	<0 5	4500	362		5		<50	2	<10	150		12	0 2	13 0	<5	<100	39	1 6
PWN 72 1				30	2 1			160	53		90	848						23	230		23		14 0			<20	
PWN 63	<2	<0 5	<2	110	5 6	1 1	<5	68	<10	0 7	<10	112		10		<50	<1	22	<10		140	<0 1	4 0	<5	<100	78	3 4
PWN 3	<2	0 6	<2	180	4 2	5 6	<5	42	<10	<0 5	180	123		18		<50	<1	<10	10		25	<0 1	6 1	<5	<100	510	1 7
PWN 13 1	<2	<0 5	<2	40	0 9	1 4	<5	26	170	<0 5	<10	196		7		<50	<1	17	21		15	0 3	12 0	<5	<100	170	0 8
PWN 26	<2	12 0	7	180	1 3	1 1	<5	140	91	1 6	410	548		1		<50	<1	<10	240		28	0 2	28 0	<5	<100	96	<0 5
PWN 26 5	<2	13 0	12	150	1 2	9	<5	140	96	2 1	290	519		2		<50	<1	14	260		32	0 2	27 0	<5	<100	130	<0 5
PWN 87 1	<2	80 5	<2	30	<0 5	5 4	<5	8	12	<0 5	<10	287		<1		<50	<1	13	25		13	1 6	5 9	<5	<100	<20	<0 5
PWN 87 2	<2	8 9	2	30	0 7	2 1	<5	8	13	<0 5	<10	262		2		<50	<1	10	17		14	0 4	7 7	<5	<100	<20	<0 5
PWN 87 5	<2	8 4	<2	40	1 1	1 8	<5	8	12	0 8	<10	319		1		<50	<1	11	18		30	0 4	7 1	<5	<100	<20	<0 5
PWN 104	<2	<0 5	<2	60	0 7	4 9	<5	27	<10	<0 5	<10	174		10		<50	<1	16	<10		28	<0 1	1 9	<5	<100	73	1 3
PWN 32	<2	<0 5	3	180	1 8	1 7	<5	36	41	0 8	<10	542		1		<50	<1	<10	130		85	0 2	8 8	<5	<100	66	<0 5
PWN 48	<2	<0 5	<2	620	3 4	<0 5	<5	27	<10	2 3	<10	708		18		<50	<1	18	<10		160	<0 1	9 5	<5	<100	110	2 1
PWN 49	<2	<0 5	<2	120	0 7	29 0	<5	48	120	8 8	<10	449		1		<50	<1	12	140		58	0 1	24 0	<5	<100	160	0 7
PWN 88	<2	0 6	2	80	1 3	5 5	<5	46	15	<0 5	17	137		24		<50	<1	<10	50		10	<0 1	12 0	<5	<100	380	0 9

SAMPLE	Te	Th	Tl	U	V	W	Y	Zn	Zr	La	Ce	Pr	Nd	Sm	Eu	Gd	Tb	Dy	Ho	Er	Tm	Yb	Lu
	ppm	ppm	ppm	ppm	ppm	ppm	ppm	ppm	ppm	ppm	ppm	ppm	ppm	ppm	ppm	ppm	ppm	ppm	ppm	ppm	ppm	ppm	ppm
PWN 50	<10	0 24	0 15	0 13	60	100	11	47	74	2 8	7 8	1 1	5 9	1 8	0 82	2 1	0 34	1 9	0 39	1	0 18	1 1	0 17
PWN 51	<10	0 23	0 17	0 25	40	85	7 9	28	94	2 2	6	0 82	4 6	1 3	0 77	1 6	0 26	1 5	0 29	0 8	0 14	0 84	0 14
PWN 53	<10	0 34	0 17	0 31	64	77	15	34	98	3 8	11	1 5	8 3	2 3	1 1	2 9	0 48	2 8	0 56	1 5	0 25	1 5	0 24
PWN 120	<10	0 27	0 08	0 17	69	86	14	60	130	3 4	8 5	1 2	6 5	1 9	0 89	2 5	0 45	2 5	0 51	1 4	0 24	1 5	0 23
PWN 42 1	<10	0 48	0 11	0 3	120	53	24	17	110	7	19	2 6	14	3 9	1 6	4 6	0 76	4 3	0 88	2 4	0 4	2 4	0 36
PWN 42 2	<10	0 4		0 3	120	113	24	14	97	7	13			5 3	2		0 8					2 1	0 4
PWN 42 3	<10	0 5		0 3	120	86	22	23	110	6	14			4 4	2		0 7					1 9	0 4
PWN 100	<10	1 4		0 6	270	66	54	30	210	13	31			9	3		1 6					4 8	1 4
PWN 118 1	<10	0 4		0 2	170	82	30	110	140	8	13			4 4	2		0 9					2 4	0 5
PWN 118 2	<10	0 69	0 04	0 3	160	63	31	70	160	8 5	23	3 2	18	4 8	1 8	6 1	0 98	5 7	1 2	3 1	0 52	3 1	0 51
PWN 1	<10	0 8		1 3	170	80	42	28	430	29	53			30	3		1 5					5	0 8
PWN 18	<10	0 5		1 3	240	16	22	110	190	14	18			5 5	1		0 7					2	0 5
PWN 19	<10	2 4		1 6	230	29	15	25	130	91	150			12 4	1		0 9					1 1	0 3
PWN 21	<10	1 5		2 6	240	57	22	39	240	11	18			3 7	<1		0 7					2	0 4
PWN 23	<10	0 6		1 2	230	70	36	32	130	11	18			7 5	3		1 3					3 6	0 8
PWN 61	<10	0 3		0 5	200	76	29	12	80	5	8			3 4	1		0 9					2 2	0 4
PWN 67	<10	0 76	0 03	0 48	210	130	32	20	190	8 9	31	3 4	18	5 1	1 9	6 4	1 1	5 9	1 2	3 4	0 57	3 4	0 51
PWN 90	<10	1 1		0 5	150	50	32	56	160	11	23			7 4	2		1 1					2 8	0 7
PWN 102 1	<10	1 4		0 7	210	47	36	14	210	15	27			7 6	2		1 3					5	0 8
PWN 102 5	<10	3 2		0 8	200	75	36	25	210	16	34			8 1	2		1 2					4	0 7
PWN 103	<10	1 4		0 8	230	62	43	15	220	22	49			10	3		1 5					3 8	1 1
PWN 105	<10	0 9		0 8	240	107	43	11	210	18	38			9 3	2		1 3					4	1
PWN 115	<10	1 4		1 3	240	89	32	37	140	19	34			5 3	2		0 9					2 9	0 5
PWN 2	<10	0 3		0 8	130	79	39	34	110	26	46			12 7	4		1 7					4	0 7
PWN 17	<10	0 4		0 7	160	30	24	15	120	10	17			5 1	2		0 9					2 4	0 6
PWN 114	<10	0 4		0 4	220	54	30	7	250	12	17			4 7	1		0 9					2 5	0 5
PWN 119	<10	0 7	0 04	0 2	140	51	23	39	97	5 6	14	1 9	11	3 3	1 2	4 3	0 72	4 3	0 86	2 5	0 38	2 4	0 37
PWN 121	<10	0 47	0 05	0 6	120	47	28	6	97	11	23	2 7	14	4 2	1 9	5 7	0 97	5 6	1 1	3 1	0 49	3	0 43
PWN 122	<10	0 39	0 09	0 31	130	49	28	42	48	5 3	16	2 4	14	4 1	1 7	5 7	0 96	5 5	1 1	3 1	0 52	3 1	0 48
PWN 20 1	<10	0 5		0 5	11	236	5	<5	15	4	<5			1 1	1		<0 5					0 6	<0 2
PWN 20 2	<10	0 6		1 2	200	76	78	29	76	8	17			10	3		2 3					8 2	1 9
PWN 38	<10	0 01		<0 2	61	42	9	<5	33	2	5			2	<1		<0 5					0 6	<0 2
PWN 40	<10	8 3		1	30	70	22	6	280	1	<5			1 8	<1		0 6					2 6	0 5
PWN 41	<10	2 2		0 6	230	96	31	46	170	17	32			6 2	1		1 1					3	0 7
PWN 57	<10	0 3		0 1	190	99	25	<5	73	5	8			3 1	2		0 8					1 9	0 5
PWN 65					150		90	6	560													8 2	
PWN 66	<10	3 1		2 3	130	133	70	<5	330	8	27			6 7	2		1 7					7 7	1 1
PWN 68	<10	0 7		0 3	240	82	37	10	140	10	17			4 9	2		1					3	0 6
PWN 69	<10	3 3		17	430	67	140	6	260	120	220			27 3	7		4 3					13	0 8
PWN 92	<10	0 7		0 3	180	58	39	12	72	9	23			8	2		1 4					3 6	0 8
PWN 99	<10	1 8		0 9	200	63	48	20	270	21	39			11 1	3		1 8					4 3	1
PWN 15	<21	3 7		1 9	5	497	10	<5	130	2	<5			0 6	<1		<0 5					1	0 5
PWN 60	<10	11		1 1	47	387	24	<5	550	30	47			4 4	1		0 6					2 5	0 4
PWN 96	<10	1 8		0 8	230	53	40	<5	210	47	86			15 4	4		1 8					2 6	0 7
PWN 98	<10	3 8		0 6	64	301	21	12	130	4	8			2 8	<1		0 6					2 3	0 7
PWN 5	<10	9 4		21 4	20	296	13	33	590	12	18			3 5	<1		<0 5					1 9	<0 2

SAMPLE	Te	Th	Tl	U	V	W	Y	Zn	Zr	La	Ce	Pr	Nd	Sm	Eu	Gd	Tb	Dy	Ho	Er	Tm	Yb	Lu
	ppm	ppm	ppm	ppm	ppm	ppm	ppm	ppm	ppm	ppm	ppm	ppm	ppm	ppm	ppm	ppm	ppm	ppm	ppm	ppm	ppm	ppm	ppm
PWN 9	<37	10 0		6 4	35	316	39	<5	510	10	18			3 4	<1		<0 5					4 2	<1 3
PWN 10	<10	8 1		4	35	200	20	<5	490	12	12			2 9	<1		<0 5					2 2	0 5
PWN 12	<10	5 8		5 6	47	238	11	7	760	15	24			2 8	<1		<0 5					1 7	0 3
PWN 14	<10	14 0		5 1	28	232	37	<5	570	30	55			8 3	<1		1 2					3 9	0 6
PWN 22	<10	7 4		3 5	28	287	29	7	580	8	14			2 8	<1		0 5					3 4	0 5
PWN 4	<10	5 2		3 2	98	76	29	13	440	52	82			9 3	2		1 1					2 7	0 5
PWN 7	<10	16 0		3 4	72	128	26	<5	410	39	73			8 9	1		1					1 9	0 6
PWN 31	<10	5 3		0 7	150	50	12	<5	180	3	<5			1 3	<1		<0 5					0 7	0 3
PWN 35	<10	4 1		0 9	81	184	16	8	200	2	9			3 3	1		0 6					1 5	0 4
PWN 47	<10	1 3		1 8	110	112	5	<5	190	15	19			1 7	<1		<0 5					<1	<0 2
PWN 52	<10	2 2	0 04	2 4	200	65	29	14	250	12	34	4 8	24	5 4	1 8	5 8	0 92	5 2	1 1	3	0 53	3 2	0 51
PWN 54	<10	2 6		0 6	46	135	13	12	240	2	<5			1 3	<1		<0 5					1 4	0 3
PWN 56	<10	3 9		0 4	68	181	11	5	290	4	<5			0 6	<1		<0 5					0 8	<0 2
PWN 64					27		18	5	570													1 5	
PWN 70	<10	4 3		0 7	45	401	34	5	230	2	9			4 1	1		1					3 5	0 6
PWN 97	<10	9 4		1 6	11	548	14	12	630	3	<5			1	<1		<0 5					2 2	0 6
PWN 101	<10	5 6		2 9	47	571	22	<5	430	10	28			5 2	1		0 7					2 5	0 4
PWN 110	<10	1 6		3 9	44	173	24	<5	430	15	30			3 5	<1		0 8					2 9	<0 2
PWN 111	<10	0 14	0 03	0 54	56	41	10	16	64	8 1	15	1 8	7 1	1 5	0 49	1 7	0 29	1 6	0 34	0 97	0 16	1 1	0 16
PWN 113	<10	0 1		2 5	130	83	38	<5	130	15	37			6 9	3		1 4					3 2	<0 2
PWN 28	<10	2		0 8	98	8	26	<5	53	365	571			11 4	1		0 9					5 5	0 9
PWN 37	<10	3 1		0 7	150	41	15	<5	120	1	<5			2 4	<1		<0 5					1 4	0 4
PWN 55	<10	7 3		0 3	16	462	29	12	360	12	25			3 2	1		0 6					2 3	0 6
PWN 73 1	<10	7		3 1	46	177	34	6	280	34	60			6 1	<1		1					3 4	0 3
PWN 80	<10	0 6		0 5	160	46	34	13	110	6	19			6 6	2		1 4					3	0 9
PWN 16 1	<10	1 2		1 1	110	32	21	18	21	47	76			8	3		1					1	0 3
PWN 24	<10	12 0		23 5	22	228	11	6	270	9	19			3	<1		<0 5					1 6	<0 2
PWN 25	<10	5 4		7 5	440	107	46	11	210	23	39			7 8	<1		1 2					3	0 7
PWN 25 5	<10	3 6		6 6	550	86	80	5	210	28	38			10	<1		1 9					6	1 2
PWN 71	<10	3 1		2 9	91	251	23	14	240	15	19			2 5	<1		<0 5					2 6	0 3
PWN 72 1					160		31	<5	370													2 8	
PWN 63	11	14		8 1	<5	462	92	<5	100	16	28			6 1	<1		1 8					11	1 4
PWN 3	<10	12 0		6	7	192	28	<5	550	42	64			7 4	3		0 8					3 4	0 7
PWN 13 1	<10	0 5		0 2	<5	129	<5	<5	270	<10	<5			0 1	<1		<0 5					<0 5	<0 2
PWN 26	<10	1 2		0 7	360	32	30	17	51	22	42			10	4		1 5					2 6	0 7
PWN 26 5	<10	1 0		0 7	360	77	29	15	59	19	34			9 2	4		1 2					2 5	0 6
PWN 87 1	<10	0 01		0 4	13	2	<5	13	13	<2	<5			0 05	<1		<0 5					<0 5	<0 2
PWN 87 2	<10	0 01		0 9	11	3	<5	6	72	<2	<5			0 05	<1		<0 5					<0 5	<0 2
PWN 87 5	<10	<0 2		0 5	9	5	<5	9	65	<2	<5			<0 1	<1		<0 5					<0 5	<0 2
PWN 104	<10	6 2		1 2	8	340	10	<5	320	6	13			2 5	<1		<0 5					1 2	0 5
PWN 32	<10	0 4		0 7	91	8	15	8	19	120	200			4 9	<1		0 6					1 5	0 4
PWN 48	<10	14		4 8	<5	138	83	100	620	61	110			17 9	3		2 6					8 8	2
PWN 49	<10	0 5		0 2	150	39	19	13	75	12	20			2 9	1		0 6					1 7	0 4
PWN 88	<10	3		1 4	48	197	26	6	750	5	13			3 3	<1		0 6					3 4	0 8

TEST TARGET (QA-3)

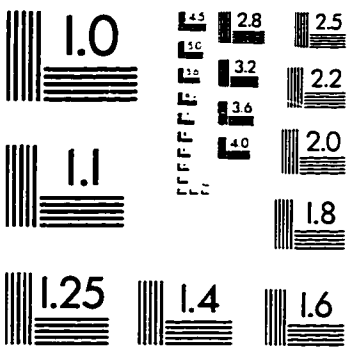

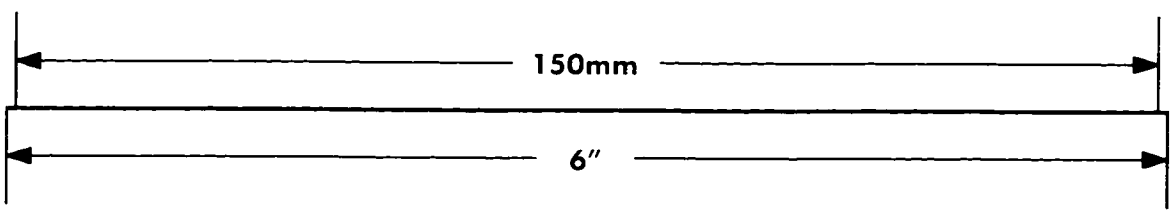

APPLIED IMAGE, Inc
1653 East Main Street
Rochester, NY 14609 USA
Phone: 716/482-0300
Fax: 716/288-5989